THE TRANSPASSIVE BEHAVIOUR OF THE ANODIC FILM ON Fe-Cr ALLOYS

by

CHARLES HENRY LLEWELYN TONKINSON
B.Sc (Hons) (Natal)

Submitted in partial fulfilment of
the requirements for the degree of
Master of Science
in the Department of Chemistry
University of Natal

Durban
1993

PREFACE

The experimental work described in this thesis was carried out in the Department of Chemistry, University of Natal, Durban, under the supervision of Professor H.C. Brookes.

These studies represent original work by the author and have not been submitted in any form to another University. Where use was made of work of others, it has been duly acknowledged in the text.

DECLARATION

I hereby certify that this research is the result of my own investigation, which has not already been accepted in any substance for any degree, and is not concurrently submitted in candidature for any other degree.

Signed : 

C.H.L. Tonkinson
B.Sc (Hons) (Natal)

I hereby certify that the above statement is correct.

Signed : 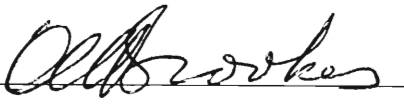

Professor H.C. Brookes
Ph.D. (Cape Town)
Professor of Inorganic Chemistry
University of Natal
Durban

Department of Chemistry
University of Natal
Durban
1993

ACKNOWLEDGEMENTS

I would like to thank the following :

- Professor H.C. Brookes for his guidance, suggestions, his confidence in me and the assistance he has given .
- Mr Dave Balson for his much needed technical assistance.
- Miss Fiona Graham for the many brainstorming discussions, the guidance with the experimental side and the high good humour displayed under duress of acute badgering.
- The South African Corrosion Institute for the bursary in 1992.
- Professor J.W. Bayles, for the help he gave and time he gave up to do it.
- My father, for his financial assistance and encouragement.
- My mother, for her encouragement and because she'll be so proud she'll try to read the whole thesis.
- I particularly wish to thank my wife, Bronwen, because she kept (and keeps) me laughing, happy, whole and far too well fed. I also thank her for the patience and interest she maintained during the many discussions of my research with her.

DEDICATION

I would like to dedicate this, my first tome, to my wife, Bronwen, who by now, due to a much appreciated talent for listening to me, probably knows more about the subject of this study than I do.

ABSTRACT

This work was undertaken to investigate the transpassive behaviour of the anodic film on two Fe-Cr alloys, namely Fe18Cr and Fe18Cr2Mo in acidic aqueous media in the pH range 0.5 to 3.8. Two electrochemical techniques were used, namely cyclic voltammetry and chronoamperometry. The two primary experimental variables in the cyclic voltammetric experiments were pH and sweep rate (2 - 800 mV/s). The main variables in the chronoamperometric experiments were the size of the potential step, the number of potential steps and the starting and ending potentials. Secondary experimental variables were temperature (25, 90°C), rotation rate (0, 150 rad/s), and the artificial addition of cations (Fe^{2+}, Fe^{3+} and Cr^{3+}) to some of the solutions.

A voltammetric anodic peak, referred to as peak A, occurs in the transpassive region of the above Fe-Cr alloys, followed by a region of secondary passivity and then oxygen evolution. It was this peak that was investigated by cyclic voltammetric methods. The peak A current response was independent of rotation rate at pH 3.8 but was dependent on rotation rate at pH 0.5 with solutions of intermediate pH showing a gradual change in rotation rate dependence. This indicated a predominantly solid state process in less acidic solutions (pH 2.4 & 3.8) whereas in strongly acidic solutions (pH 0.5) the action of ions in solution must contribute significantly towards peak A processes.

A method was developed to correct the peak A current response for the current due to oxygen evolution. The results of this method indirectly confirmed the hypothesis that more than one oxidation process contributes to the peak A current response.

A diagnostic plot for diffusion control was applied to the peak height of peak A. The diagnostic involves plotting the peak height over the square root of the sweep rate versus the square root of the sweep rate. A process under diffusion control would give a horizontal line for this diagnostic plot. At pH 0.5 and at slow sweep rates (less than or equal to 60 mV/s) the diagnostic plot gave a positive deviation from the horizontal and this deviation was enhanced as the temperature was increased. As the pH was increased (towards pH 3.8), the deviation from the horizontal at slow sweep rates gradually became negative and this deviation was again enhanced when the temperature was increased. This phenomenon is explained in terms of the role of the hydronium ion.

From the addition of Fe^{2+}, Fe^{3+}, and Cr^{3+} to pH 0.5 and pH 3.8 solutions it was noted that ferrous ions increased the peak A current response more than chromic ions of the same concentration. Ferric ions slightly decreased the peak A current response. Based on these results, reports in the literature, and the apparent role of the hydronium ion, a partial scheme was proposed in order to explain the role of Fe and Cr, from the alloy substrate, in the anodic film in the transpassive region.

In chronoamperometric experiments, stepping to the transpassive region confirmed the phenomenon of the rising transient. A quantitative nucleation model - which was based on previous models from the literature - was generated. The model was successfully fitted to two rising transients, one from the pH 3.8, and the other from the pH 0.5 solution. The model also allows for the presence of a pre-existent layer at

the starting potential of a chronoamperometric experiment after the electrochemical cleaning procedure. The model incorporates both diffusion controlled and charge transfer controlled steps. A key concept in the model is that of nucleation and "slow death" of corrosion pits growing into the electrode. "Death" of a pit occurs when it is covered by a nucleating and or growing passivating film.

The rising transients were only obtained on Fe-Cr alloys (with one exception) when stepping to the transpassive region and also only in solutions where peak A was obtained in a cyclic voltammetric experiment. The exception to this was that in the pH 0.5 solution and at 90°C, rising transients were obtained when stepping to the passive region. This did not occur at 25°C. Rising transients were also obtained on pure iron when stepping to the passive region.

In addition to the rising transient, a reverse rising transient was discovered. This reverse rising transient (which generated a cathodic current) was obtained when stepping the potential cathodically from the transpassive region. It was shown that the occurrence of the reverse rising transient was dependent on the presence of a stable, transpassive anodic film before the potential step. One indirect result from the discovery of the reverse rising transient was that it indicates that secondary passivity exists at least 200 mV into the oxygen evolution region.

TABLE OF CONTENTS

LIST OF SYMBOLS

ELECTROCHEMICAL CONVENTION:

- Potentials more oxidising than a saturated sulphate electrode (SSE) are positive.
  $E_{SSE,\,mV} = E_{NHE,mV} - 642mV$ at 25°C.
- Currents at an electrode corresponding to a net oxidation are positive.

Some of the symbols which are used only once are not defined here, but are adequately defined in the text.

Roman Symbols

Symbol	Description	First page of use	Units
A	Area of electrode	4	cm^2
A_k	Nucleation rate constant	32	$cm^{-2}\ s^{-1}$
A_k'	Rate of conversion of an active site into a nucleus	22	s^{-1}
C_1	Concentration of species 1	3	mol cm^{-3}
$C^*_{H_2O}$	Bulk concentration of pure water	9	0.0556 mol cm^{-3}
c_k	Kink error constant	68	-
D_1	Diffusion coefficient of species 1	3	$cm^2\ s^{-1}$
E'	Applied potential	8	mV
Ea	Activation energy	77	kJ mol^{-1}
Ea,pA	Apparent activation energy for peak A processes	77	kJ mol^{-1}
E_1'	Initial potential in a potential step experiment	21	V
E_2'	Final potential in a single step experiment Intermediate potential in a double step experiment	21	V
E_3'	Final potential in a double step experiment	66	V
E_1	Starting potential in a voltammetric experiment	11	V
E_2	Minimum potential in a voltammetric experiment	11	V
E_3	Maximum potential in a voltammetric experiment	11	V
E_{corr}	Corrosion potential	16	V
E_{csp}	Critical secondary passivation potential	16	V
E_{Flade}	Flade potential	16	V
E^o	Standard potential	14	V
E_{pA}	Potential at which peak A occurs	53	V
E_{pa}	Potential of an anodic voltammetric peak	11	V
E_{pc}	Potential of a cathodic voltammetric peak	11	V
E_{pp}	Primary passivation potential	16	V
E_{pr}	Prepassive potential	35	V
E_{stop}	Potential where a voltammogram is halted so that a relaxation current can be obtained	17	V

Symbol	Description	First page of use	Units
E_{tr}	Transpassive potential	16	V
F	Faraday constant	3	96485 C mol^{-1}
h	Thickness of a monolayer of film	24	cm
I	Current density	8	mA cm^{-2}
i	Current	4	mA
I_a	Anodic current density	7	mA
Ic	Cathodic current density	7	mA
I_{cr}	Critical current density	16	mA cm^{-2}
I_e	Experimental (as opposed to theoretical) current density	131	mA cm^{-2}
$I_{l,a}$	Limiting anodic current density	8	mA cm^{-2}
$i_{l,a}$	Limiting anodic current	5	mA
I_{lev}	Steady state (levelling out) current density of a rising transient	23	mA cm^{-2}
I_{max}	Peak current density of a rising transient	23	mA cm^{-2}
I_{min}	Current density of the local minimum in the chronoamperogram of a rising transient	23	mA cm^{-2}
I_o	Exchange current density	7	mA
I_p'	Passive current density	16	mA cm^{-2}
I_{pA}	Current density of peak A	53	mA cm^{-2}
I_{pa}	Current density of an anodic voltammetric peak	11	mA cm^{-2}
i_{pa}	Current of an anodic voltammetric peak	11	mA
I_{pc}	Current density of a cathodic voltammetric peak	11	mA cm^{-2}
i_{pc}	Current of a cathodic voltammetric peak	11	mA
I_t	Theoretical (as opposed to experimental) current density	131	mA cm^{-2}
$J_1(x)$	Flux of species 1 at a distance x (cm) from the electrode surface	3	mol s^{-1} cm^{-2}
k	Rate of incorporation of atoms at the periphery of a 2-D growth centre	24	cm^2 s^{-1}
k'	Growth rate constant parallel to electrode (horizontal rate constant)	32	cm^2 s^{-1}
k''	Growth rate constant perpendicular to electrode (vertical rate constant)	32	cm^2 s^{-1}
k_b	Backward rate constant	7	s^{-1}
k_f	Forward rate constant	5	s^{-1}
l	Limiting height at which growth of nuclei stops	32	cm
M_1	Molar mass of the passive film	12	g mol^{-1}
n	No. of electrons in an electron transfer reaction	3	dimensionless

Symbol	Description	First page of use	Units
N_o	Number density of active sites	22	cm^{-2}
pK_a	Negative logarithm of the acid dissociation constant	58	-
P_i	Parameter used in simplification of nucleation equations. i = 1 to 9 in the nucleation model	28	variable
R	The gas constant	3	8.314 J K^{-1} mol^{-1}
r	Rate of reaction	4	mol cm^{-2} s^{-1}
r_1	Radius of a disc electrode	5	cm
R_o	Resistance of the solution external to the film	12	Ω cm^{-2}
T	Temperature	3	K or °C
t	Time	18	s
t_{max}	Time at which I_{max} occurs	23	s
t_{min}	Time at which I_{min} occurs	23	s
$V_M^{\chi'}$	Notation for a (metal) cation vacancy carrying a negative charge of magnitude χ	42	-
$V_O^{\cdot\cdot}$	Notation for an (oxygen) anion vacancy containing a double positive charge	42	-
v(x)	Velocity of species 1 along the x axis	3	cm s^{-1}
z_1	Charge of species 1	3	C

Greek symbols

Symbol	Description	First page of use	Units
ω	Rotation rate	5	rad s^{-1}
α	Anodic transfer coefficient	7	-
α_O	Anodic transfer coefficient for oxygen evolution	9	-
η	Overpotential	7	V
σ	Standard deviation	69	-
ν	Sweep rate	11	mV s^{-1}
ρ	Density	12	g cm^{-3}
κ	Specific conductivity	12	S cm^{-1}
δ''	Fitting parameter	131	dimensionless
δ_f	Normalised fitting parameter	131	dimensionless
δ_O	Nernst diffusion layer thickness	4	cm
δ_{pass}	Thickness of the passive film	12	cm
υ_k	Kinematic viscosity	5	cm^2 s^{-1}
θ_m	Degree of coverage of the electrode	12	dimensionless

LIST OF ABBREVIATIONS

Abbreviation	Meaning	First page of use
AES	**A**uger **E**lectron **S**pectrocopy	10
APC	**A**nodic **P**olarisation **C**urve	16
CE	A mechanism where a **C**hemical reaction precedes an **E**lectron transfer.	12
CV	**C**yclic **V**oltammetry	2
E	A mechanism involving only an **E**lectron transfer	12
EA	A mechanism where an **E**lectron transfer precedes an **A**dsorption reaction	12
EC	An **E**lectron transfer precedes a **C**hemical reaction	12
EC_{cat}	An **E**lectron transfer precedes a **cat**alytic **C**hemical reaction	12
$EC_{complex}$	A one step process where a metal atom dissolves and **complex**es with an anion of the electrolyte	12
ECE	**E**lectron transfer reactions precede and follow a **C**hemical reaction	12
EDAX	Scanning electron microscopy with **E**nergy **D**ispersive **X**-ray **A**nalysis	47
EIS	**E**lectrochemical **I**mpedance **S**pectroscopy	39
Irrev	**Irrev**ersible	12
IRS	**I**nfra**r**ed **S**pectroscopy	47
NHE	**N**ormal **H**ydrogen **E**lectrode	51
PDM	**P**oint **D**efect **M**odel	42
PMR	**P**otential **M**odulated **R**eflectance Spectroscopy	36
Quasirev	**Quasirev**ersible	12
RDE	**R**otating **D**isk **E**lectrode	4
rds	**r**ate **d**etermining **s**tep	24
Rev	**Rev**ersible	12
RHEED	**R**eflection **H**igh **E**nergy **E**lectron **D**iffraction	47
RRDE	**R**otating **R**ing **D**isk **E**lectrode	39
SALI	**S**urface **A**nalysis by **L**aser **I**onisation	45
SCE	**S**aturated **C**alomel **E**lectrode (+ 244mV against NHE)	35
SEM	**S**canning **E**lectron **M**icroscopy	25
SIMS	**S**econdary **I**on **M**ass **S**pectroscopy	10
SSE	**S**aturated **S**ulphate **E**lectrode (+ 642mV against NHE)	36
SVIM	**S**olute **V**acancy **I**nteraction **M**odel	42
XES	**X**-ray **E**lectron **S**pectroscopy	38
XPS	**X**-ray **P**hotoelectron **S**pectroscopy	10

Alloy abbreviations

The table below gives the percentage composition of alloys referred to in the thesis that are named according to a numerical abbreviation. The major constituent element is, of course, Fe. Of the alloys mentioned in the table only 444 was used in experiments (Fe18Cr was also used). More detailed compositions of 444 and Fe18Cr are given in the experimental chapter.

Alloy	Cr	Ni	C	Mo	First page of use
304	18 - 20	8 - 10.5	0.08	-	48
304L	18 - 20	8 - 12	0.03	-	49
316	16 - 18	10 - 14	0.08	2.0 - 3.0	compare to 316L
316L	16 - 18	10 - 14	0.03	2.0 - 3.0	48
430	17	0.1	0.09	-	16
444	17.4	0.3	0.003	1.8	2

LIST OF FIGURES

LIST OF TABLES

CHAPTER 1

1. INTRODUCTION

This work has focused on the investigation of the transpassive behaviour of two Fe-Cr alloys (Fe18Cr and Fe18Cr2Mo) in acidic aqueous media. The passive region of Fe-Cr alloys has been well investigated, but little appears in the literature about the transpassive region. Previous research in this laboratory has resulted in the discovery of two important characteristics of the transpassive region:

(1) A transpassive peak, referred to as peak A occurs in the transpassive region, followed by a region of secondary passivity (*cf* fig 3.9) [1,2,3]. Peak A is considered to be the current response resulting from a partial oxidation and or dissolution of the passive film, followed by the formation of a secondary "passive" film. The secondary "passive" film is probably porous and does not contain the barrier layer of a true passive film. Some questions which have arisen concerning peak A and the region of secondary passivity include:

- What oxidation steps contribute to the peak A current response ? In particular, is the oxidation of Fe species or the oxidation of Cr species primarily responsible ?
- To what extent does the passive film break up or dissolve at peak A potentials ?
- Does oxygen evolution interfere with peak A processes ?
- Does secondary passivity extend into the oxygen evolution region ?
- Does the secondary "passive" film occur by a solid-state or a dissolution-precipitation process ?
- Are the processes contributing to peak A activation or diffusion controlled ?

A common diagnostic for establishing diffusion control is the plot of the peak height (I_p) divided by the root of the sweep rate ($\nu^{1/2}$) versus $\nu^{1/2}$. If the plot yields a horizontal line, then the system is diffusion limited. The validity of this diagnostic to the above system will be established later (*cf* section 2.3.1). One of the main aims of the thesis is to use diffusion diagnostic plots (and other appropriate techniques) obtained from a range of voltammetric conditions to explain questions regarding peak A. In particular, are peak A processes activation or diffusion controlled ? Another important technique, used in differentiating solid-state from dissolution-precipitation processes, involves observing the fluctuation of the current response as a function of rotation rate of a rotating disk electrode.

(2) When stepping from noble (~ -1.0V vs. SSE) or passive potentials to the transpassive region, and in particular, the region of secondary passivity, chronoamperometric rising transients are obtained. Since a rising transient is diagnostic of a nucleation process, this indicates that the growth of the secondary "passive" film occurs by a nucleation process. As yet, nucleation theory has not been adequately developed to quantitatively describe this rising transient. The rising part of the transient is attributed to a temporary increase of the area of the surface through which the current flows. It is not known whether this surface area increase is due to direct pitting of the electrode, pitting of a pre-existent film (e.g. the passive film) or whether it is due to the formation and initial growth of metal

oxide nuclei. Furthermore there is disagreement as to whether the relevant metal oxides are semiconductors [4,5] or insulators [6,7]. However, in this study, a **quantitative** model for the rising transient on Fe-Cr alloys is developed which includes the effects of a possible pre-existent film, charge transfer controlled pitting of the electrode and diffusion controlled growth of metal oxide nuclei. The model is based upon the concept of the "slow death" of nuclei. This is just an extension of the concept of "sudden death" of nuclei which was suggested by Abyaneh and Fleischmann [8].

One question which is pertinent for interpretation of results from chromoamperometric experiments (and in the nucleation model) is:
Does a pre-existent film form at the starting or "noble" potential of a chronoamperometric experiment ? In order to provide an indication to the answer to this question a previously developed scratch technique was used [9].

A useful and relatively simple method in determining how the Fe and Cr species are involved in transpassive behaviour of the anodic film is to artificially add cationic species of Fe and Cr to the solution. Thus voltammetric and chronoamperometric experiments can be performed where Fe(II), Fe(III) and Cr(III) are (separately) artificially added to the base solutions and the results can then be compared with corresponding results where these cations were not added to the base solution.

It is suggested that a key concept in understanding peak A processes in acidic aqueous solutions lies in the role of the hydronium ion. A premise involving the hydronium ion which the results of this thesis widely support is the following:

An acid solution will resist any reaction process that results in an overall increase in the acidity of the solution in the region of the electrode.

One application of the acid premise is that it can be used to resolve the apparent contradiction amongst those who consider the peak A current response to be due to the oxidation and dissolution of chromium species as Cr(VI) [10-13] and those who consider it largely to be due to the oxidation and dissolution of iron species as Fe(III) [1,14], and in some cases, Fe(VI) [15]. The last case involves a mild steel electrode in basic carbonate solutions.

The thesis therefore concentrates on the two predominant transpassive phenomena - peak A and the rising transient - in order to obtain more information on the transpassive (and secondary passive) behaviour of Fe-Cr alloys. As corrosion in a number of industrialised countries is alleged to cost 3-5% of the gross national product [16], sufficient incentive is provided for the continued study of this relatively new area.

To summarise, in this investigation two electrochemical techniques, namely cyclic voltammetry (CV) and chronoamperometry have been used, together with an on-line computerised data-acquisition system to investigate the transpassive behaviour of two Fe-Cr alloys, namely Fe18Cr and Fe18Cr2Mo (444). The transpassive behaviour of the anodic film of these alloys was in investigated as a function of pH (0.5 - 3.8), temperature (25, 90°C), sweep rate (in CV, 2 - 800 mV/s), and rotation rate (0, 150 rad/s).

CHAPTER 2

2. THEORETICAL BACKGROUND

The following is a selective summary of the theory of the methods and arguments used. Numerical curve fitting and correction techniques that were applied are also described.

2.1. Mass transfer

Consider the simple electrode reaction

$$O + ne^- \rightleftharpoons R \tag{2.1}$$

where the species O and R may be in solution, adsorbed on the electrode, or may be electrode material and n is the integer number of electrons transferred in the reaction. If the electron transfer is fast compared with the processes of mass transfer, then the reaction is mass transfer controlled. Homogenous reactions can then be regarded as being in electrochemical equilibrium and the surface concentrations of the species involved in the faradaic processes are related to the potential by means of an equation of the Nernst type. Such electrode reactions are called reversible or Nernstian.

Mass transfer can take place in three modes:

- Migration of charged particles under the influence of an electrical field. This is usually negligible compared to the next two modes of mass transport for an electrode reaction of type (2.1). However, for a solid state reaction, where a metal oxide film exists between the electrode and the solution, the electrode processes might very well be limited by the migration of ions through the film under the influence of a potential dependent electric field between the electrode and the solution.
- Diffusion of molecules and or ions in a gradient of chemical potential.
- Convection of molecules and or ions due to stirring, agitation or hydrodynamic transport such as is created by a rotating electrode.

One dimensional mass transfer to an electrode along the x axis is given by the Nernst - Planck equation

$$J_1(x) = -D_1 \frac{\partial C_1(x)}{\partial x} - \frac{z_1 F}{RT} D_1 C_1(x) \frac{\partial E(x)}{\partial x} + C_1(x) v_1(x) \tag{2.2}$$

where $J_1(x)$ (units of mol s^{-1} cm^{-2}) is the flux of species 1 at a distance x (in cm) from the surface, D_1 (units of cm^2/s) is the diffusion coefficient of species 1, $\frac{\partial C_1(x)}{\partial x}$ is the concentration gradient at distance x, $\frac{\partial E(x)}{\partial x}$ is the potential gradient, z_1 is the charge in Coulombs, C_1 the concentration of species 1 in mol/cm^3, and $v(x)$ is the velocity of the solution along the axis in cm/s. F, R and T are the Faraday constant, the gas constant and the temperature (in Kelvin) respectively. The terms on the right hand side of the equation relate to the mass transfer caused by diffusion, migration and convection respectively. Neglecting migration and in the absence of convection, the mass transfer rate of species O for reaction (2.1), r_O in mol/cm^2, is proportional to the concentration gradient of O at the surface of the electrode

$$r_O(x=0) \propto \left(\frac{\partial C_O}{\partial x}\right)_{x=0} \tag{2.3}$$

Here C_O is the concentration of the species O. Upon integration and some approximation, (2.3) gives

$$r = m_O [\, C_O(x=0) - C_O^* \,] \tag{2.4}$$

where r is the rate of reaction in mol cm^{-2} s^{-1}, C_O^* is the bulk concentration of O and $C_O(x=0)$ is the concentration of O at the electrode. m_O (units cm/s) is the mass transfer coefficient, where $m_O = \frac{D_O}{\delta_O}$. δ_O is the thickness of the Nernst diffusion layer in cm. The Nernst diffusion layer approximation assumes that $\frac{\partial C_O}{\partial x}$ is constant from $x = 0$ to the first point ($x = \delta_O$) at which $C_O = C_O^*$. i.e.

$$\frac{\partial C_O}{\partial x} = \frac{C_O(x=0) - C_O^*}{\delta_O} \tag{2.5}$$

The rate of the reaction, r, is related to the current by

$$r = \frac{i}{nFA} \tag{2.6}$$

A is the area of the electrode in cm^2 and i is the current in mA. It is acceptable, at certain rotation rates (*cf* equation (2.10)), to regard that part of the solution in which there is a concentration gradient as not subject to convection [17]. The assumption is made that the Nernst diffusion layer is of negligible thickness compared with the Prandtl hydrodynamic layer. It is important to note that as the rotation rate of a rotating disk electrode (RDE) increases, the Nernst diffusion layer thickness will decrease (*cf* equation (2.9)).

2.1.1. The rotating disk electrode

The rotating disk electrode provides a situation where the mass transfer for a system involving equation (2.1) - and other reaction types - is defined. For reaction (2.1), the diffusion limited anodic current, $i_{l,a}$, at a RDE is given by the Levich equation [18]

$$i_{l,a} = 0.620nFAD_O^{2/3}\omega^{1/2}\upsilon_k^{-1/6}C_O^* \tag{2.7}$$

Here υ_k is the kinematic viscosity of the solution in cm^2/s and ω is the rotation rate in rad/s. The main implication is that $i_{l,a}$ is proportional to $\omega^{1/2}$ and C_O^*.

From equations (2.4) and (2.6)

$$i_{l,a} = nFA\frac{D_O}{\delta_O}C_O^* \tag{2.8}$$

and therefore, when combining equations (2.7) and (2.8) for a RDE

$$\delta_O = 1.61D_O^{1/3}\omega^{-1/2}\upsilon_k^{1/6} \tag{2.9}$$

The important point here is that the Nernst diffusion layer thickness is proportional to $\omega^{-1/2}$ for a diffusion limited case. If $k_f\frac{\delta_O}{D_O} << 1$, where k_f is the rate constant for the forward direction of reaction (2.1) in s^{-1}, then the reaction is kinetically limited and $i_{l,a}$ is independent of $\omega^{1/2}$. If, however, $k_f\frac{\delta_O}{D_O} >> 1$, then the reaction is diffusion limited.

The range over which the rotation rate can be changed (and therefore the range for which the Nernst diffusion layer approximation is valid) in water at 25°C is given by

$$10\frac{\upsilon_k}{r_1^2} < \omega < 2\times10^5\frac{\upsilon_k}{r_1^2} \tag{2.10}$$

where r_1 is the radius of the disk in cm. At ω less than the lower theoretical limit, the hydrodynamic boundary thickness becomes too large, and at ω greater than the larger theoretical limit, turbulent flow commences.

Using RDE, Armstrong *et al* derived criteria for distinguishing between dissolution - precipitation mechanisms and solid state mechanisms of corrosion in parallel with metal dissolution [19,20,21]. The criteria derived for a RDE under potentiostatic control are as follows:

(a) For irreversible metal dissolution:

(i) The steady state i - E curve will be independent of rotation rate for a solid state mechanism.

(ii) Rotation rate dependence will be found for the dissolution - precipitation mechanism, since by increasing the rotation rate the surface concentration of metal cations will be decreased. This happens because as the rotation rate increases the Nernst diffusion layer thickness decreases (this was shown for a simpler electrochemical system - *cf* equations (2.1) and (2.9). The smaller the value of δ_O, the larger the concentration gradient for active species (*cf* equation (2.5)).

(b) For reversible metal dissolution the i - E curve is rotation rate dependent for both the solid state and dissolution - precipitation mechanisms.

2.2. Charge transfer and the Butler-Volmer equation

As before, consider the simple electrodic reaction

$$O + ne^- \underset{k_b}{\overset{k_f}{\rightleftharpoons}} R \tag{2.11}$$

where the electron transfer is slow compared to the processes of mass transfer, and hence the rate of the forward (k_f) and backward (k_b) reactions (in s^{-1}) must be taken into account. Here O and R are assumed to be in solution. Under the condition of kinetic control when the respective surface and bulk concentrations of O and R do not appreciably differ, and in the absence of adsorption, the Butler - Volmer equation may be derived [22]

$$I = I_o\left[\exp\left(\frac{\alpha nF\eta}{RT}\right) - \exp\left(-\frac{(1-\alpha)nF\eta}{RT}\right)\right] \tag{2.12}$$

where I_o is the exchange current density, α is the anodic transfer coefficient and η is the overpotential in V. The first exponential term refers to the anodic (I_a) contribution to the overall current density and the second refers to the cathodic (I_c) contribution to the overall current density where $I = I_a + I_c$. When the surface and bulk concentrations of the respective species are not similar, then the following form of equation (2.12) applies

$$I = I_o\left[\frac{C_R(x=0)}{C_R^*}\exp\left(\frac{\alpha nF\eta}{RT}\right) - \frac{C_O(x=0)}{C_O^*}\exp\left(-\frac{(1-\alpha)nF\eta}{RT}\right)\right] \tag{2.13}$$

When η is small (η < 10 mV), then the Taylor expansion approximation ($\exp(x) \approx 1+x, \quad x<<1$) can be applied to the Butler - Volmer equation to give

$$I = I_o\frac{nF\eta}{RT} \tag{2.14}$$

As the (positive) value of η increases, the second exponential term in equation (2.12) diminishes towards zero and (2.12) simplifies to (for η > ~ 50 mV)

$$\ln I = \ln I_o + \frac{\alpha nF\eta}{RT} \tag{2.15}$$

This means that only the anodic current density contributes to the overall current density at large positive overpotentials.

2.2.1. Charge transfer and mass transport

Consider the case of an irreversible oxidation reaction

$$R \xrightarrow{k_f} O + ne^- \tag{2.16}$$

If the reaction is under mixed kinetic and mass transport control, then an i - E curve will have three distinctive regions:

(a) At low currents, the reaction will be kinetically controlled and the current will be independent of rotation rate.

(b) At intermediate currents, the reaction will be partially kinetically controlled and partially mass transport controlled.

(c) When the applied potential is large a limiting current plateau ($i_{l,a}$) - which is dependent on rotation rate - will occur as a result of total mass transport control.

Combining the required variations of equations (2.8,13,15) and expressing the current as current density leads to [23]

$$\ln\left(\frac{I I_{l,a}}{I_{l,a} - I}\right) = c' + \ln C_R^* + \frac{\alpha n F E'}{RT} \tag{2.17}$$

where I and $I_{l,a}$ are the overall and limiting anodic current density (in mA/cm^2) respectively, c' is a constant and E' is the applied potential in mV.

A more mathematically "pure" form of equation (2.17) would be

$$\ln\left(\frac{I I_{l,a}}{I_{l,a} - I} \Big/ \text{mA cm}^{-2}\right) = c' + \ln\left(\frac{C_R^*}{\text{mol cm}^{-3}}\right) + \frac{\alpha n F E'}{RT} \tag{2.17a}$$

Equation (2.17a) would satisfy the condition that only the logarithm of a dimensionless number may be taken. The convention in this thesis is that an equation containing logarithmic terms is written in the "brief" form (e.g. equation (2.17)) and it is assumed that the "pure" form (e.g. equation (2.17a)) is implied.

2.2.2. The oxygen evolution correction

The oxygen evolution reaction is

$$2H_2O \rightarrow O_2 \uparrow + 4H^+ + 4e^- \tag{2.18}$$

For this reaction, R in equation (2.16) becomes H_2O. Two simplifying steps can be taken:

(a) $C^*_{H_2O}$ is constant in aqueous solution. Therefore a constant c'' can be defined as

$$c'' = c' + \ln C^*_{H_2O} \tag{2.19}$$

(b) Since $I_{l,a}$ is very large for oxygen evolution, it is easy to limit an experiment such that $I << I_{l,a}$. Then the left hand side of equation (2.17) is simplified

$$\frac{I I_{l.a}}{I_{l,a} - I} \approx \frac{I I_{l.a}}{I_{l,a}} = I \tag{2.20}$$

Substituting equations (2.18,20) into (2.17) gives

$$\ln I = c'' + \frac{\alpha_O nFE'}{RT} \tag{2.21}$$

which is simply equation (2.15) in another form. α_O is the anodic transfer coefficient for oxygen evolution.

Ideally, c'' and $\frac{\alpha_O nF}{RT}$ can be obtained respectively from the intercept and slope of a Tafel plot of equation (2.21).

Oxygen evolution may interfere with the current responses due to anodic processes on stainless steels in at least three ways:

(a) The $4e^-$ on the right hand side of equation (2.18) will add a background current which may add to peak A, provided that oxygen evolution coincides appreciably with peak A processes in the potential region of peak A.

(b) The $4H^+$ may contribute towards dissolution of the anodic film. For example

$$Fe_2O_3 + 6H^+ \rightleftharpoons 2Fe^{3+} + 3H_2O$$

However, at acidic pH's (such as the range used in this study - pH 0.5 - 3.8) it is unlikely that the $4H^+$ would significantly increase the acidity of the solution adjacent to the electrode.

(c) The O_2 may oxidise cations in the anodic film which are not yet in their highest oxidation state. However, it is not unlikely that at the onset of oxygen evolution, all ions will have already been oxidised to their highest stable oxidation state.

If two assumptions are made, then an oxygen correction can be performed on voltammograms where there is an oxygen evolution interference with peak A:

(a) The first assumption is that the initial exponential rise in current after the secondary passive region is due to oxygen evolution only. i.e. the secondary passive region extends into oxygen evolution for some duration before the breakdown of the secondary passive film contributes to the current. Datta *et al* have shown (using AES and XPS) that on iron in basic nitrate solutions, the secondary passive layer that is found in these solutions extends well into the oxygen evolution region before it begins to dissolve [24]. Also, chronoamperometric studies have indicated that the film formed on stepping to the oxygen evolution region is stable (*cf* section 7.1, fig. 7.4). The assumption is therefore reasonable and if it is valid, then equation (2.21) can be used, together with a suitable experimental technique (*cf* section 2.3.4), to fit an empirical equation to the experimental oxygen evolution data. The peak A current response can then be corrected for current produced by oxygen evolution by means of the empirical equation.

(b) The second assumption is that the first interfering effect of oxygen evolution (positive current error) is large compared with the other two. i.e. oxygen evolution does not significantly affect the chemistry of the anodic film. This assumption follows from the first assumption as if the secondary passive film is stable, then it is not likely that it is being dissolved by the production of excess acid or that it is being oxidised by the evolved oxygen. In support of this assumption, mention can be made of a study that was performed on anodically formed passive films formed on a Fe25Cr alloy in 0.1M H_2SO_4. The experiment involved exposing the passive film to an atmosphere enriched in the isotope $^{18}O_2$. Using SIMS profiling, it was shown that anodically formed passive films are not further oxidised on exposure to air [25]. Thus it is also unlikely that oxygen affects the chemistry of the secondary passive film on Fe18Cr.

There are some other factors complicating the second assumption including:

- If the secondary passive film is very porous, oxygen may diffuse through pores to the electrode surface.
- Oxygen may even extend passivity by blocking pores or forming an adsorbed layer on the surface of the anodic film.

However, it is certain that the "true" transpassive current response - that current in the transpassive region produced due to processes not involving O_2 or the oxidation of H_2O - will lie somewhere between the experimentally recorded voltammogram and the voltammogram corrected for oxygen evolution according to equation (2.21).

2.3. Cyclic Voltammetry

This technique involves varying the potential of a system in a triangular fashion at a known time rate whilst monitoring the current response. The adjustable variables are the initial potential, E_1 , the minimum potential, E_2 , the maximum potential, E_3 (all of these in V), and the sweep rate, ν, in mV/s. In cyclic voltammetry (CV), a reversible or quasi - reversible system such as

$$R \rightleftharpoons O + ne^- \tag{2.22}$$

will produce cathodic current peak (i_{pc}) on the reverse sweep as well as the initial anodic peak (i_{pa}) on the forward sweep. An irreversible system such as

$$R \rightarrow O + ne^-$$

will not produce a cathodic current peak on the reverse sweep. For various types of reactions (e.g. reversible, quasi-reversible, irreversible, adsorption, catalytic) general solutions to the equations and diagnostic criteria for the cyclic voltammograms, based on the anodic and cathodic peak potentials (E_{pa}, E_{pc}) and the current densities (I_{pa}, I_{pc}), have been obtained and a good summary can be found in reference [28]. For example, for reaction (2.22) it can be shown that for planar diffusion [26,27,28]

$$I_p = 0.4463nF\left(\frac{nF}{RT}\right)^{1/2} C_R^* D^{1/2} \nu^{1/2} \tag{2.23}$$

where, as before, I_p is in mA/cm^2, C_R^* is in mol/cm^3, D is in cm^2/s and ν is in mV/s. This equation is known as the Randles-Sevcik equation and is one of the most fundamental in the theory of CV. A more detailed treatment of the catalytic mechanism will be given later (Section 2.3.2).

2.3.1. The diffusion diagnostic

The common factor to all diffusion controlled processes that are investigated with CV is that the peak height (I_p) of the peak of interest is proportional to the root of the sweep rate. Therefore a diagnostic plot of $I_p/\nu^{1/2}$ versus $\nu^{1/2}$ will produce a horizontal line if the process is diffusion controlled. Table 2.1 summarises the range of applicability of this diagnostic.

Müller originally developed the pore resistance theory for the passive film [29]. The reaction equation is

$$M + nA^- \rightarrow MA_n + ne^-$$

The film is envisaged to nucleate at certain points and then to spread laterally across the surface until only a small fraction of the initial area remains uncovered. The area available for dissolution therefore decreases with time until ultimately the rate of the reaction is limited by the resistance of the solution in the pores of the passive film. Macdonald [30] and Calandra *et al* [31, 32] separately derived the solutions for i_p and E_p for this system

$$i_p = \left(\frac{nF\rho\kappa}{M_1}\right)^{1/2} A(1-\theta_m)\,\nu^{1/2} \tag{2.24}$$

$$E_p = \left(\frac{nF\rho\kappa}{M_1}\right)^{1/2}\left[\frac{\delta_{pass}}{\kappa} + R_o A(1-\theta_m)\right]v^{1/2} \qquad (2.25)$$

where ρ is the density of the passive film in g/cm^3, κ is the specific conductivity of the electrolyte solution (in S/cm) in the pores, M_1 is the molar mass of the passive film in g/mole, A is the surface area of the electrode in cm^2, θ_m is the degree of coverage of the electrode by the passive film at E_p, δ_{pass} is the thickness of the passive film in cm and R_o is the resistance of the solution external to the film in Ω/cm^2. A linear plot of $E_p/v^{1/2}$ vs. $v^{1/2}$ would also be a diagnostic for this mechanism.

Mechanisms not involving formation of a metal oxide film adjacent to the electrode					
	Irrev / Quasirev / Rev		Insoluble / soluble[a]		
Mechanism	E	C / A	Reactant	Product	Reference
CE	rev	rev	soluble	soluble	33
CE	irrev	rev	soluble	soluble	33
EC	rev	rev	soluble	soluble	33
EC	rev	irrev	soluble	soluble	33
EC	quasirev	irrev	insoluble[b]	soluble	34
EC_{cat}	rev	irrev	soluble	soluble	33
EC_{cat}	irrev	irrev	soluble	soluble	33
ECE	rev - rev	irrev	soluble	soluble	35
ECE	irrev - rev	irrev	soluble	soluble	35
ECE	rev - irrev	irrev	soluble	soluble	35
ECE	irrev - irrev	irrev	soluble	soluble	35
EA	rev	rev	soluble	adsorbed	36
E	rev	-	soluble	insoluble[b]	37
$EC_{complex}$	one step irreversible		insoluble	soluble	38
Mechanisms involving formation of a metal oxide film adjacent to the electrode					
			Insoluble / soluble[a]		
Mechanism			Reactant	Product	Reference
Charge transfer followed by deposition of product. An electrodeposition mechanism			soluble	insoluble	39, 40, 41
Dissolution of the electrode followed by deposition and passive layer formation. Resistance of the solution in the pores of the passive film is rate determining.			insoluble	insoluble	30, 31, 32
An extension of the above where the conducting layer may increase in thickness.			insoluble	insoluble	42

Table 2.1: Table summarising the mechanisms for which the $Ip/v^{1/2}$ versus $v^{1/2}$ diffusion diagnostic is valid.

a This refers to the solubility of species in the phase adjacent to the electrode

b These species are in their amalgamated form

The abbreviations used in table 2.1 are as follows:

- "E" refers to a charge transfer step
- "C" refers to a chemical reaction
- "A" refers to an adsorption step
- "C_{cat}" refers to a catalytic chemical reaction
- "$EC_{complex}$" refers to the one step process where a metal atom in the electrode is oxidised, dissolves, and then complexes with an anion of the electrolyte according to

$$M + A^{-m} \rightarrow [MA]^{n-m} + ne^{-}$$

where M is the metal and A^{-m} is the anion of the electrolyte.

Considering the general applicability of this diffusion diagnostic and the fact that it is also valid for a theoretical type of passive film, it is not unreasonable to assume that it would also be valid for anodic films on stainless steels. Some comments need to be made, however:

- If a horizontal line is obtained then it could indicate a diffusion limiting step either in the solution adjacent to the film or within the film itself. The diagnostic plot cannot be used to distinguish between a dissolution-precipitation or a solid-state diffusion controlled process. For example, the solid-state point defect model considers the diffusivity of cation vacancies within the passive film (*cf* section 3.2). In order to distinguish between a solid-state or a dissolution-precipitation processs, a RDE must be used (*cf* page 5).
- It is quite likely that more than one oxidation process contributes to the current response on stainless steels and this is so particularly in the transpassive region. The possibility that one oxidation step is slow (i.e. kinetically limited) at, say, fast sweep rates may explain a positive deviation from the horizontal in the diagnostic plot at slow sweep rates. However, if both (or all) oxidation steps are diffusion limited, then the diagnostic plot will still produce a horizontal line.

2.3.2. The voltammogram of a catalytic process

The catalytic process is of interest because:

- A diagnostic for the process is that $I_p/v^{1/2}$ decreases as v increases. This result was obtained in some of the results of this thesis (*cf* fig. 5.11, for example).
- In conditions of low pH and low sweep rate and some cyclic voltammograms bear a marked resemblance to the theoretical voltammogram "c" in fig. 2.1. i.e. as the sweep rate decreases, the peak changes to a plateau and the reverse sweep superimposes on the forward sweep.

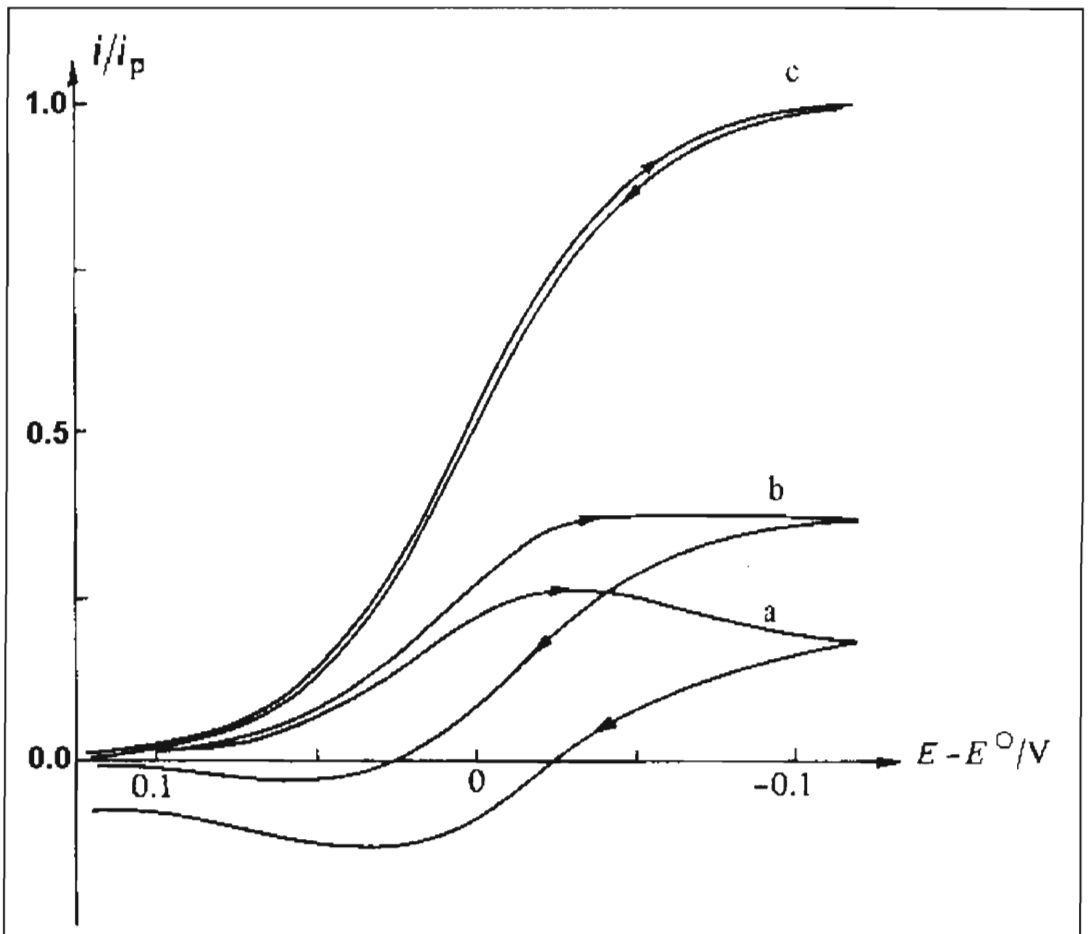

Fig. 2.1: Theoretical cyclic voltammograms for the catalytic mechanism [28]. The current is normalised with respect to the peak current of the largest peak. The curves are for the values of λ (a) 0.04, (b) 0.4, (c) 3.16. E^o is the standard potential in V.

Consider the following two reactions [28,33]

$$R \rightleftharpoons O + ne^-$$

$$O + X \xrightarrow{k_f} R + Y$$

The preceding two reactions describe a catalytic EC mechanism with a reversible electron transfer step and an irreversible chemical reaction. The case of an irreversible charge transfer has also been considered [33], and the results are similar, but with the curves in fig. 2.1 flatter and more spread out on the potential axis. If $C_X^* >> C_R^*$ then it can be assumed that the concentration of X remains unchanged throughout the experiment, and the chemical reaction can be treated as pseudo first order. Under pseudo first order conditions and when ν is large or k_f is small, the chemical reaction has no effect and reversible behaviour is observed. But for larger values of k_f, or as ν is decreased there is effectively more reactant (R) regenerated and therefore I_{pa} values are higher than would be predicted from the Randles-Sevcik equation (equation (2.23)). The $I_p/\nu^{1/2}$ values increase with decreasing sweep rate and the peak becomes less pronounced. In the limit the peak disappears altogether and is replaced by a sweep rate independent plateau. This is shown in fig. 2.1 where normalised theoretical cyclic voltammograms are plotted for several values of λ, defined by

$$\lambda = \frac{k_f C_X^*}{\nu}\left(\frac{RT}{nF}\right) \tag{2.26}$$

For the purposes of this study it is important to note that $\lambda \propto T/\nu$. The current density of the plateau is given by

$$I_{l,a} = nFC_R^*\left(Dk_f C_X^*\right)^{1/2} \tag{2.27}$$

2.3.3. Anodic Polarisation Curves

Slow linear sweep voltammograms, or anodic polarisation curves (APC's[a]) are valuable for determining the corrosion properties of metals [43,44]. The success of linear sweep voltammetry has resulted in its inclusion as the ASTM Recommended Practice G5 used for determining critical potentials. The potentiostatic or potentiodynamic tests involve the slow (0.1 - 2.0 mV/s) linear increase of potential while the current density is recorded, usually on a logarithmic scale. The potentials which define passive and non-passive regions can then conveniently be determined.

The voltammogram usually taken as standard is that of 430 stainless steel in 0.5M H_2SO_4 solution. A schematic based on this voltammogram is given in fig. 2.2.

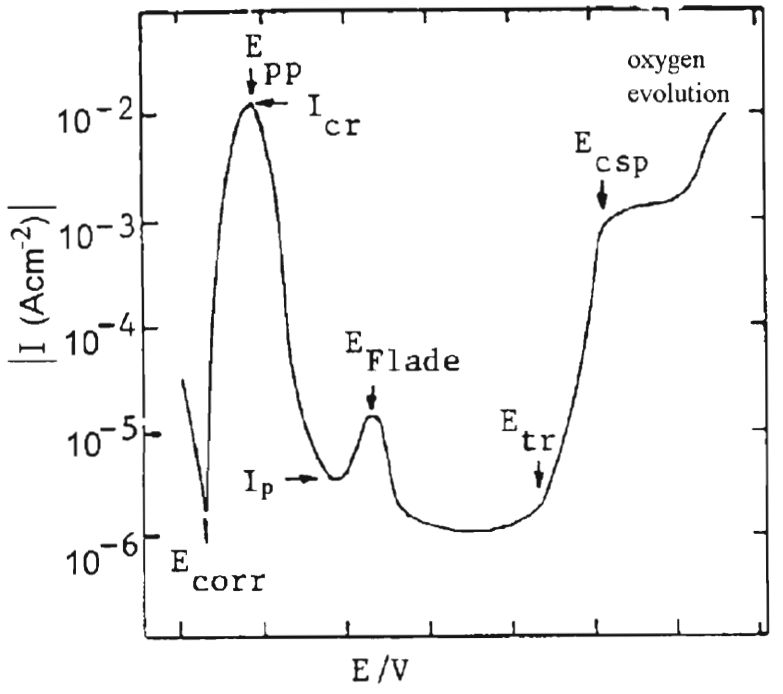

Fig. 2.2: Schematic APC of a stainless steel based on the APC (0.17 mV/s) of 430 stainless steel in 0.5 M sulphuric acid at 25°C [44].

E_{corr} : Corrosion potential
E_{pp} : Primary passivation potential
E_{Flade} : Flade potential
E_{tr} : Transpassive potential
E_{csp} : Critical secondary passivation potential
I_{cr} : Critical current density
I_p' : Passive current density

As the potential is increased from the corrosion potential (E_{corr}) so the measured current density increases to a maximum at the critical current density (I_{cr}), obtained at the primary passivation potential (E_{pp}). For $E > E_{pp}$ the electrode undergoes the active-passive transition and the current decreases until the passive current density (I_p') is reached. The passive region extends from the Flade potential (E_{Flade}) to the transpassive potential, E_{tr}. A secondary active region, where the current once again increases, extends until the critical secondary passivation potential. After E_{csp}, the current levels out (or may even decrease) to the secondary passivation current until the secondary passive region is obscured by the onset of oxygen evolution.

---

[a] APC's are sometimes referred to as "steady state" linear sweep voltammograms. In this thesis "steady state" may also refer to a cyclic voltammogram that superimposes upon itself.

2.3.4. The potential stop technique

If a reaction occurs at a potential close to that for another reaction then the current densities are additive and the recorded curve is the sum of the individual curves. These can be separated by using the decay current of the first reaction as the base line for the second reaction [45]. For a system with interfering processes, the base line for the second process can be established by stopping the sweep (at E_{stop}) before the second wave begins and recording the i - t curve on an oscilloscope or Y - t recorder. Then the sweep with both peaks is obtained and a subtraction of the two cycles (fig. 2.3) should give the current density for the second reaction. This is referred to as the potential stop technique and should not be confused with chronoamperometric "potential step" terminology.

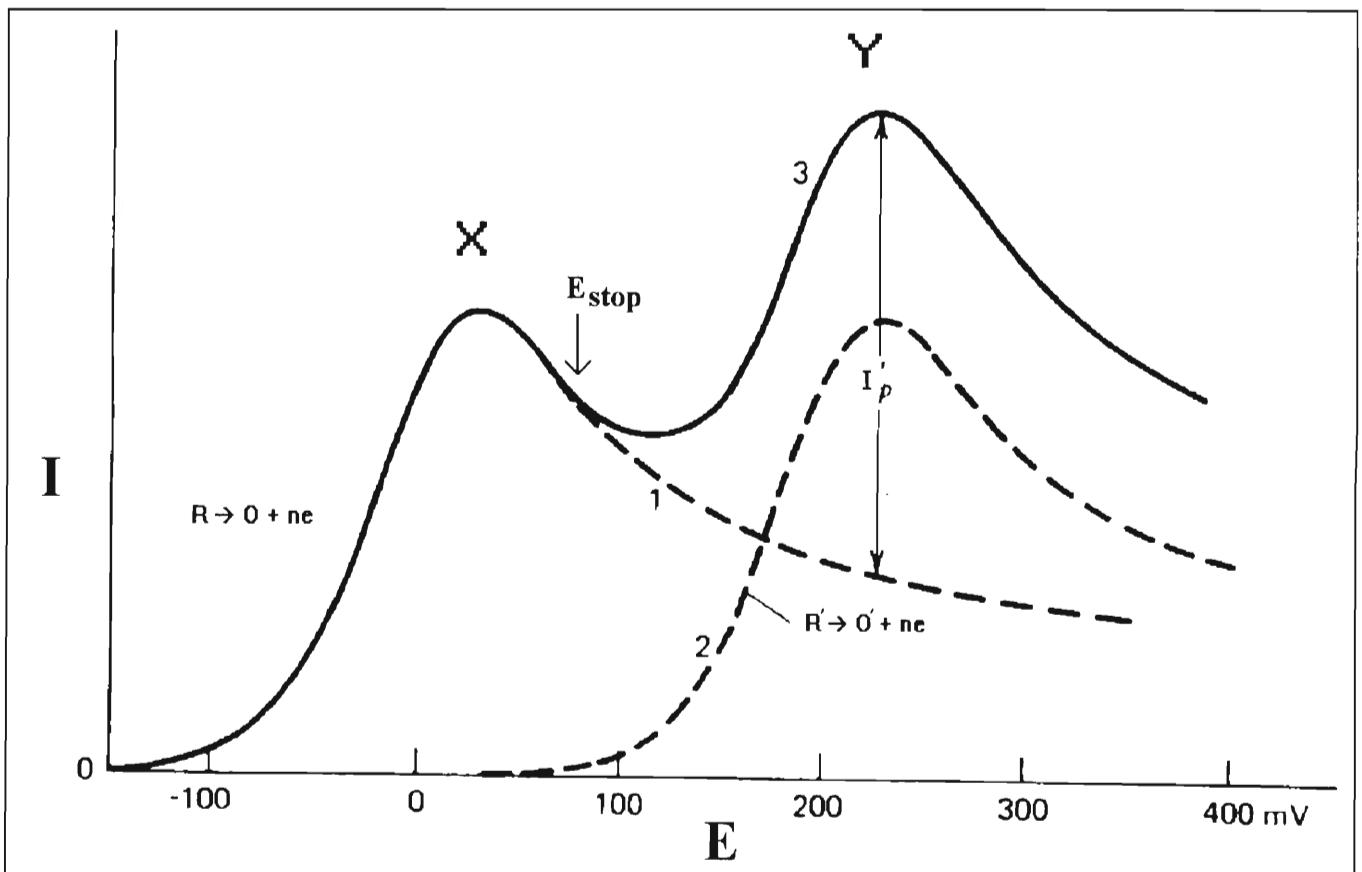

Fig. 2.3: Voltammograms when only (1) R → O + ne⁻ occurs (2) R' → O' + n'e⁻ alone (3) both reactions [45].

2.3.5. Simulation of voltammetric curves

Ramamurthy and Rangarajan have applied a Guassian quadrature analysis to the simulation of the voltammetric curve for a simple reversible charge transfer reaction

$$O + ne^- \rightleftharpoons R$$

taking place at a plane boundary [46]. The boundary value problem for the case of semi-infinite linear diffusion of O and R under the set of boundary conditions given in reference [33] needs the evaluation of the integral $\oint$ defined as

$$\oint = \int_0^{at} \frac{\exp(\ln \gamma\theta - Z)}{\left[1+\exp(\ln \gamma\theta - Z)\right]^2} \frac{dZ}{\sqrt{at-Z}} \tag{2.28}$$

where $a = nF\nu/RT$, t is the time in seconds, $\gamma = \sqrt{D_O/D_R}$ and $\theta = \exp\left[(nF/RT)(E_1 - E^o)\right]$, where E_1 is the initial potential and E^o is the standard potential in V. The non dimensional current $\chi(at)$, is related to the actual current $i(t)$ by

$$i(t) = nFAC_O^* \sqrt{\pi D_O a}\, \chi(at) \tag{2.29}$$

and analysis [46] leads to an expression for $\chi(at)$ as

$$\sqrt{\pi}\chi(at) = \frac{\oint}{\pi} + \frac{1}{\sqrt{\pi a t}}\left[\frac{1}{1+\exp(\ln \gamma\theta)}\right] \tag{2.30}$$

In what follows $\ln \gamma\theta$ is denoted as μ.

The guassian quadrature method of interest is

$$\int_a^b f(x)dx = (b-a)\sum_{i=1}^{2n+1} V_i f\left[a+(b-a)X_i\right] \tag{2.31}$$

where the weights V_i's, and the nodes X_i's are tabulated in reference [46] for n = 10. Application of this method to equation (2.28) gives [46]

$$\int_0^{at} \frac{\exp[\mu - Z]}{\left[1+\exp(\mu - Z)\right]^2} \frac{dZ}{at - Z} = \sqrt{at} \sum_{i=1}^{2n+1} V_i \frac{\exp\left[\mu - at\left(1 - X_i^2\right)\right]}{\left[1+\exp\left(\mu - at\left(1 - X_i^2\right)\right)\right]^2} \tag{2.32}$$

A simple program was written by the author to combine equations (2.30) and (2.32) and generate figures 2.4 and 2.5. As recommended [46], the choice $\ln \gamma\theta = 10$ was made for the purpose of calculations. Fig. 2.4 shows two voltammetric curves generated using this method. Voltammogram Y was specifically adjusted so that its peak height was half that of voltammogram X and so that its peak potential was positive of X. Fig. 2.5 shows in the one case, the vector sum of X and Y, and in the other case the effect on the vector sum of X and Y of stopping the sweep rate and holding the potential at E_{stop} whilst continuing to record the relaxing current as an i - t curve on the i - E axes. Fig. 2.5 shows how an experimental "kink" may be obtained when using the potential stop method. If voltammograms X and Y combine to form what looks like a voltammogram due to a single process, and the experimentalist desires to separate the combined voltammogram from another interfering process positive to it (such as oxygen evolution), then this "kink" may be obtained. The potential stop kink phenomenon is then a clear indication that there is more than one charge transfer process contributing to what appears to be a single voltammetric curve.

An example of a practical situation is when the two electron transfer reaction is Fe(0) $\rightarrow$ Fe(II), the one electron transfer reaction is Fe(II) $\rightarrow$ Fe(III) and they combine to form peak A[a]. Under certain conditions oxygen evolution interferes with peak A and in these cases it would be desirable to correct peak A for the oxygen evolution current response. Conditions would then be chosen such that oxygen evolution is reasonably well separated from peak A and the potential stop technique would then be applied to peak A. The residual peak A current can then be subtracted from the oxygen evolution current to obtain the true oxygen evolution current. This current can then be fitted to equation (2.21) by Tafel plots or an iterative non-linear regression technique. This will give an equation for the current due to oxygen evolution only. This equation can then be used to correct peak A for oxygen evolution.

One way of avoiding the kink phenomenon and hence the error in the residual current is to position E_{stop} such that it is positive of the peak potential of voltammogram Y in fig. 2.4. However, it might not be possible to stop the sweep rate at a potential positive to E_{pA} as oxygen evolution is then evident. In fig. 2.5 it can be seen that the discrepancy in current between the potential stop voltammogram and the normal voltammogram gradually decreases as the potential increases positively after E_{stop}. Therefore, provided that an analysis is done only on the oxygen evolution current which is a reasonable positive potential increment away from E_{stop}, the error in the residual current can be neglected.

---

[a] Cr(III) $\rightarrow$ Cr(VI) is also believed to contribute to the peak A current response [10-13]. However, for the sake of simplicity, this possible charge transfer is not included in the discussion. It would also be possible (and probably more likely) to obtain the kink effect when three charge transfers are involved in producing an overall single current peak.

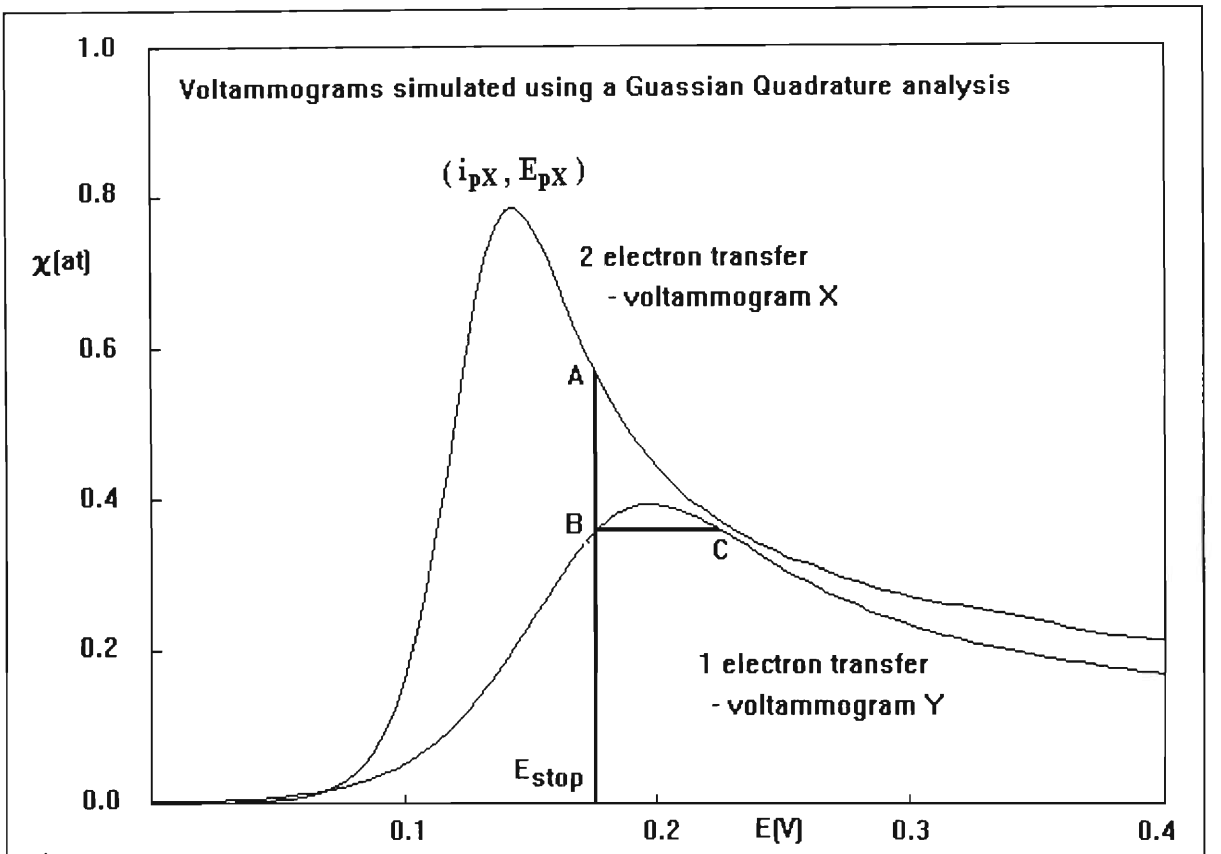

Fig. 2.4: Voltammograms simulated from a Gaussian Quadrature analysis. χ(at) is itself normalised with respect to the peak height of the voltammogram obtained from the addition of X and Y. The 1 electron transfer voltammogram has been adjusted so that its peak height is half that of the two electron transfer voltammogram and so that its peak potential is positive of that of X. "A" and "B" show a likely position where the potential would be held constant (at E_{stop}) in a potential stop experiment . "C" shows the position from which the current contribution of Y would relax after the potential has been held constant.

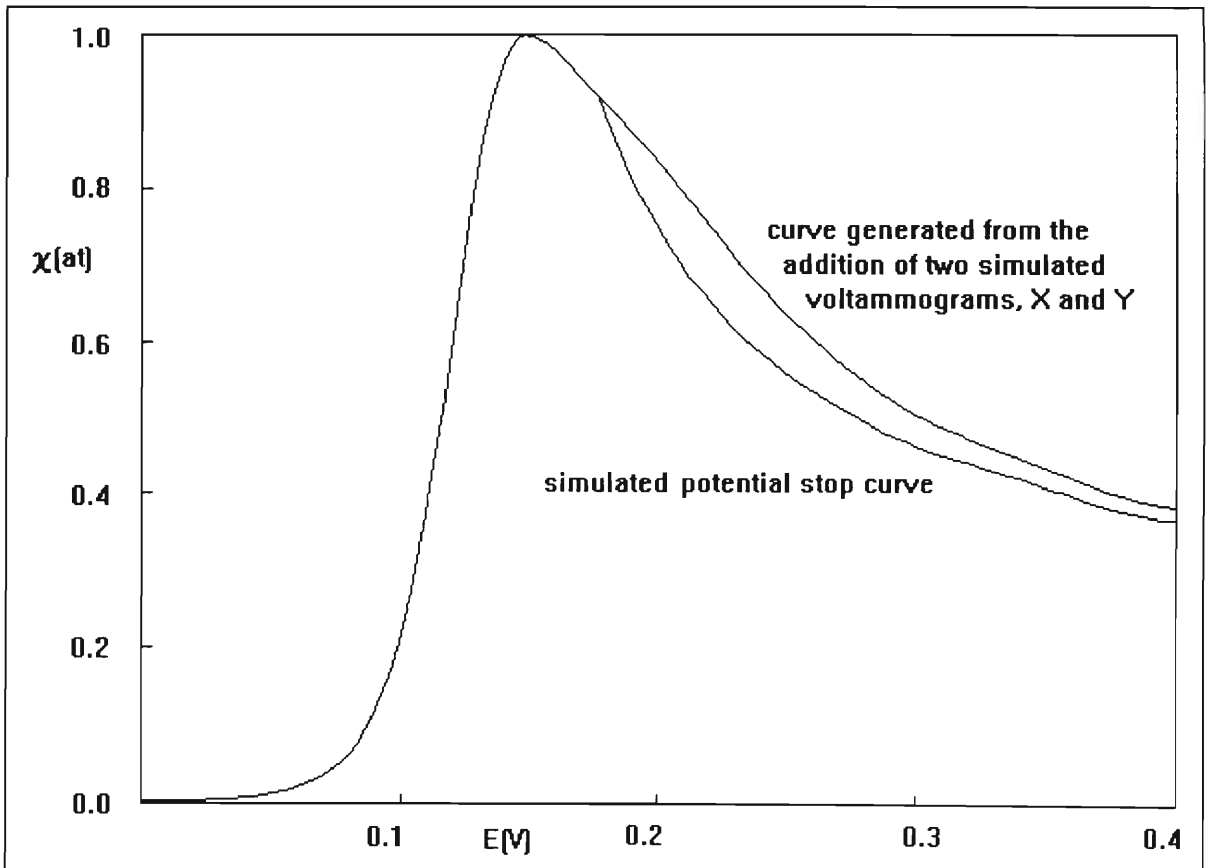

Fig. 2.5: The upper voltammogram shows the result of the vector addition of X and Y from fig. 2.4. The lower curve shows the kink arising from the vector addition of X and Y when the potential has been held constant at E_{stop}.

2.4. Chronoamperometry

Chronoamperometry is a controlled potential technique involving the application of a potential step perturbation to an electrode and monitoring the subsequent current response of the electrode. The basics of this technque are discussed for a reduction reaction

$$O + ne^- \xrightarrow{k_f} R, \quad \text{or} \quad O + ne^- \rightleftharpoons R$$

where O and R are soluble. The initial potential, E_1', is generally chosen such that no reaction occurs at the electrode at that potential i.e no current is flowing at E_1'. At time $t = 0$, the potential is instantaneously changed to E_2', which, if it is a sufficiently large overpotential for the reaction such that the reduction of O will occur at a diffusion controlled rate, then Ficks second law may be solved to give at a planar electrode and in the reversible case the Cottrell equation [47,48]

$$|I| = \frac{nFD^{1/2}C_O^*}{\pi^{1/2}t^{1/2}} \tag{2.33}$$

In the irreversible case [47]

$$|I| = nFk_fC_O^*\left(\frac{1-2k_ft^{1/2}}{\pi^{1/2}t^{1/2}}\right) \tag{2.34}$$

where t is the time after the potential step in seconds. Equations describing I - t curves for other systems have been obtained and are well documented [48,49].

There are certain experimental limitations which will affect I - t behaviour in chronoamperometric experiments:

(a) Instrumental limitations.
  (i) The actual current maximum is dependent on the output characteristics of the potentiostat
  (ii) The vertical amplifier of the oscilloscope or other recording device may require time to recover, before accurate readings are displayed, if overdriven.

(b) Limitations imposed by uncompensated resistance, R_u, and double layer capacitance, C_d.
  (i) During a potential step a non-faradaic current will flow, due to the charging of the electrical double layer, and will decay exponentially with a time constant R_uC_d.

(c) Limitations due to convection.
  (i) At longer times, dependent on the experimental arrangement, the build-up of concentration gradients cause convective disruption of the diffusion layer usually resulting in current densities larger than those predicted by the Cottrell equation.

2.4.1. Nucleation and growth of anodic oxide films

One type of dissolution - precipitation mechanism which has found particular application in the formation of anodic films on stainless steels (particularly with the discovery of a rising transient obtained when stepping to transpassive potentials), is that of nucleation [50,51,52]. Hence it is desirable to summarise the theory available on nucleation, and in particular, nucleation resulting in the growth of anodic films. Unfortunately, only the case of electrocrystallisation of metals (metal depositing onto an electrode surface from a solution already containing that metal cation) has been considered in any detail in the literature. However, the source of metal cations for the nucleation and growth of anodic films on stainless steels must be the electrode itself.

In the early stages of nucleation and growth of an anodic film (where the source of metal cations is the electrode) a thin (one to several monolayers) continuous layer of essentially insulating material is formed. Further growth of the film might only be posssible with the migration of ionic species. This would only occur in the presence of large electric fields, of the order of 10^6 V/cm. Thus while the equations describing the electrocrystallisation of metals can be used to describe the nucleation and initial stages of growth of anodic films, it is unlikely that they could be used to describe the subsequent film growth, due to the differences in the growth mechanism. In contrast, the growth of metals by electrocrystallisation is controlled by the diffusion of metal ions from the solution to the metal surface.

The early stages of anodic film formation are invariably associated with two or three dimensional nucleation reactions the rate of which, and hence the number of nuclei per unit area, are strongly potential dependent. If a specific number of active sites are formed immediately after the imposition of the potential step, then the nucleation rate is instantaneous but if nucleation and growth occur simultaneously then it is progressive [53].

It should be mentioned, however, that the progressive and instantaneous cases of nucleation are merely limiting cases of the general nucleation law

$$N = N_o\left[1-\exp\left(-A_k' t\right)\right] \tag{2.35}$$

where N is the number density of actual growing centres whereas N_o is the number density of active sites available for nucleation (both in cm^{-2}). A_k' is the rate of conversion of an active site into a nucleus in s^{-1}. Instantaneous nucleation is the limiting case when $A_k' \rightarrow \infty$ and equation (2.35) becomes $N = N_o$. Progressive nucleation is the limiting case when $A_k' \rightarrow 0$ and equation (2.35) then becomes $N = N_o A_k' t$.

In what follows, three main theoretical types of nucleation and their applicability to the case of the rising transient obtained when stepping to the transpassive region of Fe-Cr alloys will be discussed. For the purposes of comparison, a schematic of a typical case of such a rising transient is presented in fig. 2.6 and some of the terms which characterise the rising transient are defined in the schematic.

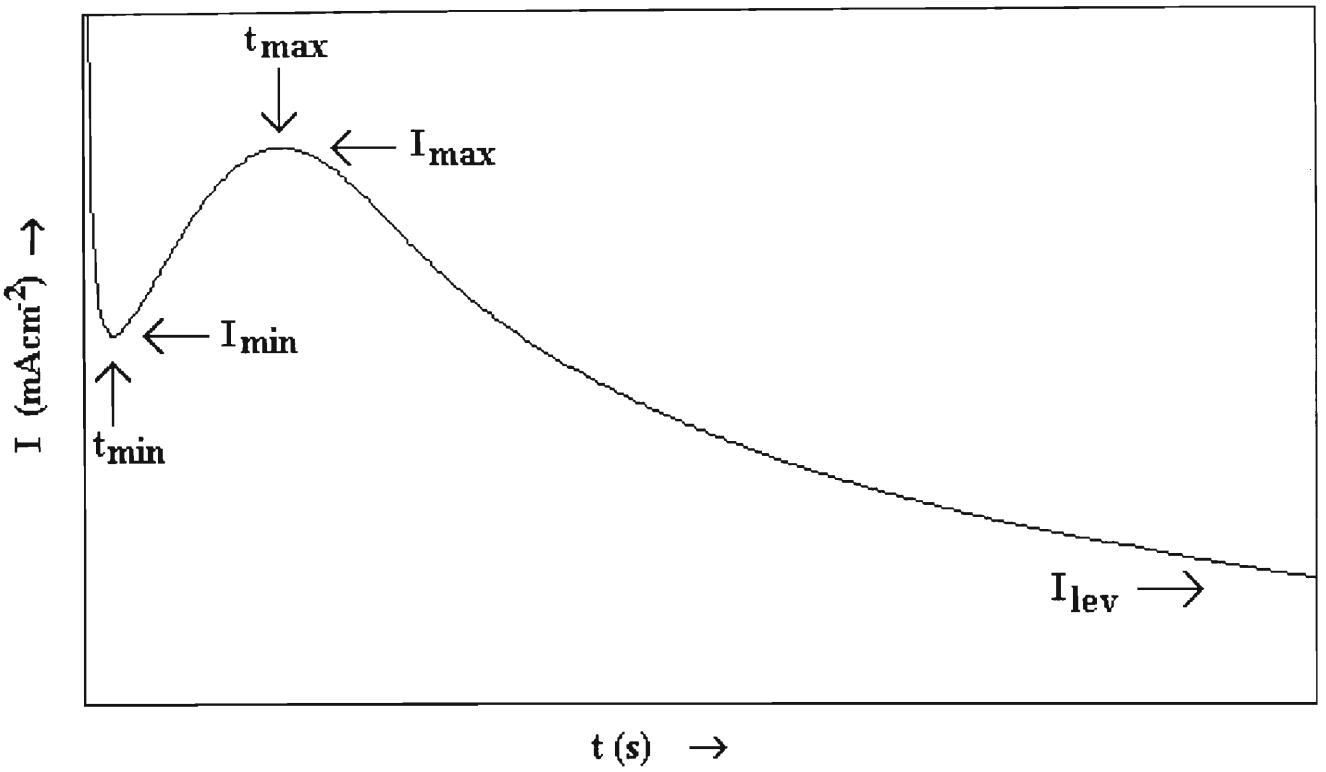

Fig. 2.6: Schematic of a typical rising transient obtained from a potential step to the transpassive region on a Fe-Cr alloy. The terms I_{max}, t_{max}, I_{min}, t_{min} and I_{lev} are defined.

One ratio term which is particularly important in the characterisation of rising transients on Fe-Cr alloys is defined as I_{max} / I_{lev}. This ratio may vary widely in value and none of the available nucleation models can allow for this variation. The smaller the value of I_{lev}, the better the electrode surface has been passivated. The ratio I_{min} / I_{lev} is also of importance as it is usually significantly larger than one. On the other hand, depending on experimental conditions, the ratio I_{max} / I_{min} may be equal to one. This might happen in the case when t_{max} is very short.

2.4.1.1. *Two dimensional nucleation*

It has been shown that the current density associated with the two dimensional growth of an isolated disc-shaped growth site is given (for instantaneous nucleation) by [53,54]

$$I = \frac{2N_o \pi nF k^2 hM}{\rho} t \tag{2.36}$$

The equivalent equation for progressive nucleation is

$$I = \frac{2A_k' N_o \pi nF k^2 hM}{\rho} t^2 \tag{2.37}$$

where N_o is the number of sites where nucleation can occur in cm^{-2}, k is the rate of incorporation of atoms or molecules at the extending periphery of the growth centre in mol cm^{-2} s^{-1}, h is the thickness of a monolayer of film in cm, M is the molar mass of the film in g/mole, ρ is the density of the film. The rds (rate determining step) is assumed to be the incorporation of adsorbed particles at the expanding periphery of the centres.

Equations (2.36,37) are only valid as long as the growing sites do not overlap. While this is true in the early stages of film growth, in the latter stages the boundaries of the expanding centres impinge on one another, reducing the area available for further nucleation and growth. This aspect of growth is known as the "overlap problem" and has been treated theoretically by Fleischmann, Bewick and Thirsk [55,56] by applying the Avrami theorem and introducing the notation that the actual area covered by the film, S (cm^2), is related to the extended area, S_{ex}, by the expression

$$S = 1 - \exp(-S_{ex}) \tag{2.38}$$

Incorporation of this correction into equations (2.36,37) results in the following expression for instantaneous nucleation [54]

$$I = \frac{2N_o \pi nF k^2 hMt}{\rho} \exp\left(-\frac{\pi N_o M^2 k^2 t^2}{\rho^2}\right) \tag{2.39}$$

The equivalent expression for progressive nucleation is

$$I = \frac{A_k' N_o \pi nF k^2 hMt^2}{\rho} \exp\left(-\frac{\pi A_k' N_o M^2 k^2 t^3}{3\rho^2}\right) \tag{2.40}$$

The effect of the exponential term introduced by the Avrami theorem is to introduce a maximum into the transient after which the current density diminishes towards zero. These two equations can be reduced to a more convenient form by using the co-ordinates of their respective maxima (I_{max},t_{max}) to obtain expressions in terms of reduced variables. For instantaneous nucleation [54]

$$\frac{I}{I_{max}} = \frac{t}{t_{max}} \exp\left(-\frac{\left(t^2 - t_{max}^2\right)}{2t_{max}^2} \right) \tag{2.41}$$

The equivalent expression for progressive nucleation is

$$\frac{I}{I_{max}} = \frac{t^2}{t_{max}^2} \exp\left(-\frac{2\left(t^3 - t_{max}^3\right)}{3t_{max}^3} \right) \tag{2.42}$$

Equations (2.41,42) were computed (from a program written by the author) to give fig. 2.7

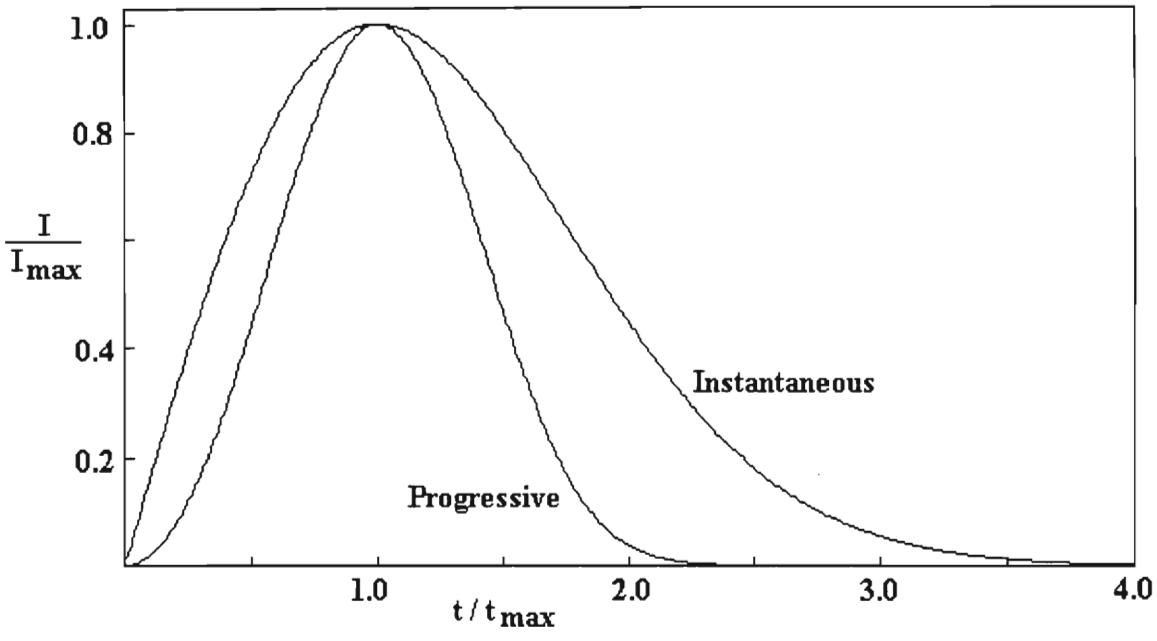

Fig. 2.7: Plots of dimensionless variables for two dimensional instantaneous and progressive nucleation.

There are a number of reasons why this model, although suitable for introducing nucleation theory, cannot be used with Fe-Cr alloys:

- Scanning electron micrograph (SEM) studies of the anodic film formed by potential steps to the transpassive region on Fe-Cr alloys has a definite three dimensional structure [52].
- The model does not allow for the initial falling current density shown in the schematic in fig. 2.6, which is characterised by the co-ordinate pair (t_{min}, I_{min}).
- As t increases, the current density for progressive and instantaneous nucleation (in the model) diminishes towards zero, but as fig. 2.6 shows, the rising transients on Fe-Cr alloys only diminish towards a constant value, I_{lev}.
- This model assumes that the source of metal cations is the solution and not the electrode. i.e. The model applies to an inert electrode where predissolved ions are deposited onto the electrode surface.

2.4.1.2. *Three dimensional hemispherical nucleation*

It has been shown that the current density associated with a three dimensional hemispherical and diffusion controlled growth site (for instantaneous nucleation) is [57,58]

$$I = \frac{nF\pi\left(2DC^*\right)^{3/2} M^{1/2} N_o t^{1/2}}{\rho^{1/2}} \tag{2.43}$$

The equivalent expression for progressive nucleation is

$$I = \frac{4nF\pi\left(DC^*\right)^{3/2} M^{1/2} A_k' N_o t^{3/2}}{3\rho^{1/2}} \tag{2.44}$$

Approximate treatments have been attempted to take into account the overlap between the diffusion fields of a random array of growing centres [59,60]. For instantaneous nucleation

$$I = \frac{nFD^{1/2}C^*}{\pi^{1/2} t^{1/2}}\left[1 - \exp\left(-\frac{\pi^{3/2} M^{1/2} C^{*1/2} N_o D t}{\rho^{1/2}}\right)\right] \tag{2.45}$$

The equivalent expression for progressive nucleation is

$$I = \frac{nFD^{1/2}C^*}{\pi^{1/2} t^{1/2}}\left[1 - \exp\left(-\frac{4\sqrt{2}\,\pi^{3/2} M^{1/2} C^{*1/2} A_k' N_o D t^2}{3\rho^{1/2}}\right)\right] \tag{2.46}$$

These equations have also been reduced in terms of I_{max}, t_{max} to give (for instantaneous nucleation) [59]

$$\frac{I^2}{I_{\max}^2} = \frac{1.9542}{t/t_{\max}}\left\{1 - \exp\left[-1.2564\left(\frac{t}{t_{\max}}\right)^2\right]\right\} \tag{2.47}$$

The equivalent expression for progressive nucleation is

$$\frac{I^2}{I_{\max}^2} = \frac{1.2254}{t/t_{\max}}\left\{1 - \exp\left[-2.3367\left(\frac{t}{t_{\max}}\right)^2\right]\right\}^2 \tag{2.48}$$

A program was written to generate plots of equations (2.47,48) in terms of the dimensionless variables, I/I_{max} and t/t_{max} and it is shown in fig. 2.8.

It has also been shown that the progressive and instantaneous forms of nucleation are merely limiting situations and a general equation has been derived for diffusion controlled nucleation with hemispherical nuclei by Scharifker and Mostany [60]

$$I = \frac{nFD^{1/2}C^*}{\pi^{1/2}t^{1/2}}\left[1 - \exp\left\{-\pi k''' N_o D\left(t - \left[\frac{1-\exp\{-A'_k t\}}{A'_k}\right]\right)\right\}\right] \qquad (2.49)$$

where k''' is the dimensionless constant $\left(8\pi C^* M/\rho\right)^{1/2}$. Instantaneous nucleation is the limiting case when the dimensionless parameter $\alpha' = \pi k' N_o D/A'_k$ tends towards zero, and progressive nucleation is the special case when $\alpha' \to \infty$. Equation (2.49) has been reduced to a general non dimensional form [65]

$$I = \frac{1}{\alpha'\left(A'_k t\right)^{1/2}}\left\{1 - \exp\left[-\alpha'\left(A'_k t - 1 + \exp\{-A'_k t\}\right)\right]\right\} \qquad (2.50)$$

A program was written (by the author) to generate normalised I - t curves by means of equation (2.50) and the results for various values of α' (except for the limiting cases where equations (2.47,48) were used) are shown in fig. 2.8.

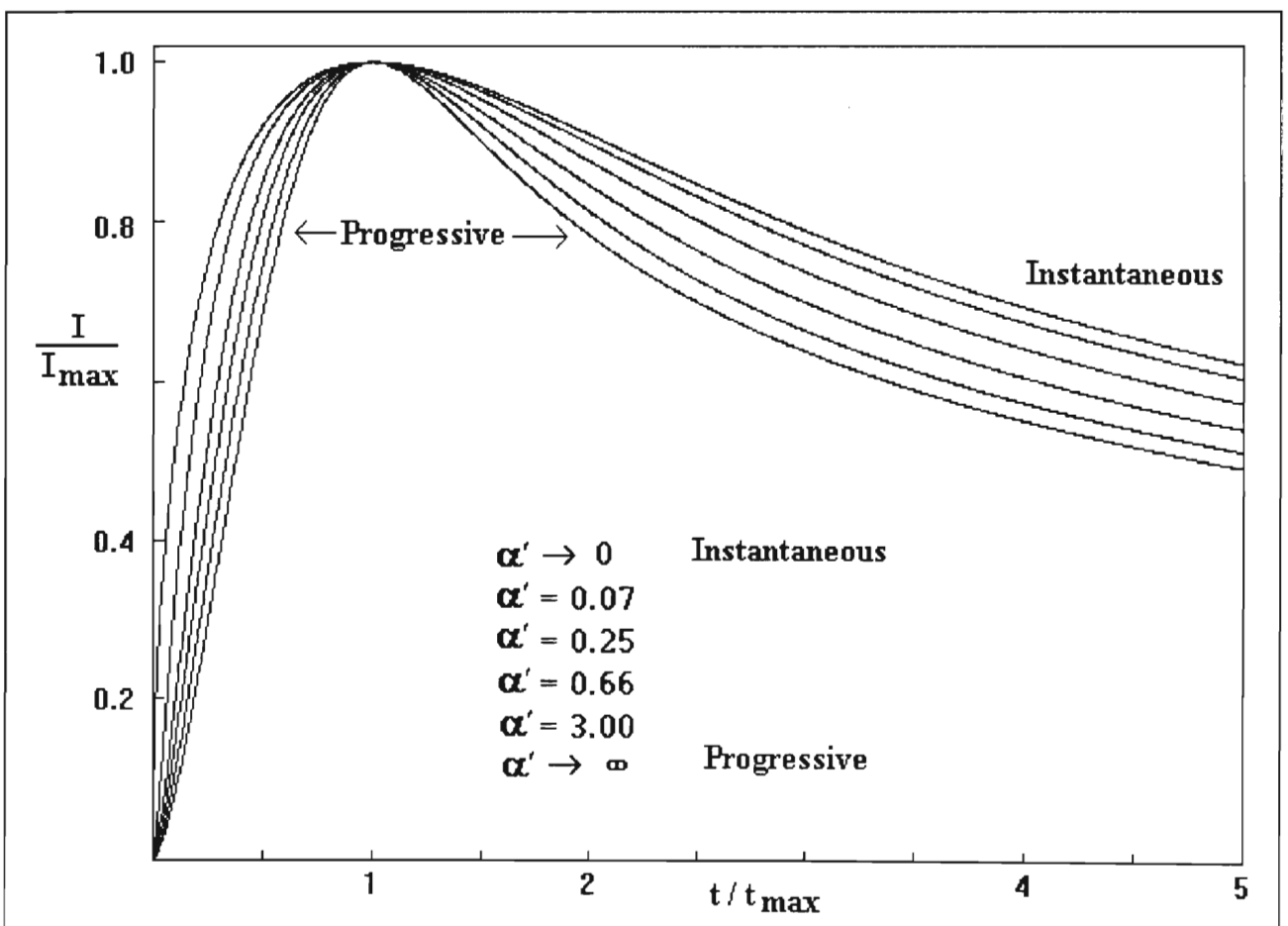

Fig. 2.8: Plot of the two limiting and some intermediate cases of three dimensional, hemispherical, diffusion controlled nucleation in terms of the dimensionless parameter, α'.

The disadvantages of this model are:

- It does not allow for the initial falling current density shown in the schematic in fig. 2.6, which is characterised by the co-ordinate pair (t_{min}, I_{min}).
- It assumes that the source of metal cations is the solution and not the electrode.
- It does not allow for a large range in the ratio I_{lev} / I_{max}. For $t / t_{max} = 5$, this ratio is 0.63 and 0.50 for the instantaneous and progressive cases respectively. However, the value of I_{lev} / I_{max} for rising transients on Fe-Cr alloys may easily be above 0.63 or below 0.50, depending on the experimental conditions.

However, the following variation of this model is far more useable, and was used as a component of the nucleation model proposed in chapter 8.

The case where the formation of a basal layer precedes nucleation

One of the most promising, and one of the most recent models of three dimensional nucleation (also involving hemispherical nuclei forming and growing under diffusion control) was proposed by Alonso *et al* [61]. Their work involved the anodic Ag_2O film formed on polycrystalline silver electrodes in alkaline solutions.

The first major advantage of the theory is that the electrode is in this case the source of the metal cations. The second advantage arises out of their suggestion that a thin basal layer (of silver oxide) forms on the electrode before the onset of nucleation. The rate of nucleation must then be controlled by the diffusion of Ag^+ cations through the primary basal layer (and later on, through the growing secondary layer as well) as evidenced by the fact that the rising transient current density was independent of rotation rate [61]. The theory has been based on equation (2.49) and in essence only one term has been added to account for the formation of the basal layer. The formation of the basal layer was found to give a diffusion controlled current density of the usual form, $I \propto t^{-1/2}$. The inclusion of the term for the primary basal layer therefore gives an initial falling current, before the transient rises, as required by the schematic in fig. 2.6. The proposed equation is [61]

$$I = \frac{P_4}{t^{1/2}} + \frac{P_1}{t^{1/2}}\left\{1 - \exp\left[-P_2 t + \frac{P_2}{P_3}\left(1 - \exp\{-P_3 t\}\right)\right]\right\} \qquad (2.51)$$

where $P_4 = nFD^{1/2}C^*/\pi^{1/2}$, $P_1 = nFD'^{1/2}C'^*/\pi^{1/2}$, $P_2 = k'''N_o \pi D$ and $P_3 = A'_k$.

D and D', and C^* and C'^* are the diffusion coefficients and the bulk concentrations of the species involved in the electroformation of the primary and secondary oxide layers, respectively. Only the secondary oxide layer grows by nucleation. A program was written (by the author for this thesis) to calculate the effects each of the four parameters (P_i's) has on the rising transient. Figures 2.9,12,10,11

show the results and table 2.2 summarises the effects of the P_i's on the rising transient in terms of the parameters t_{max}, I_{max}, t_{min}, I_{min} and I_{lev} as defined in fig. 2.6.

	Theoretical meaning of parameter	I_{max}	t_{max}	I_{min}	t_{min}	I_{lev}
P_1	$nFD'^{1/2}C'^{*}/\pi^{1/2}$	↑	↑	↑	-	↑
P_2	$k'N_o\pi D$	↑	↓	↑	↓	×
P_3	A_k'	↑	↓	↑	↓	×
P_4	$nFD^{1/2}C^{*}/\pi^{1/2}$	↑	-	↑	↑	↑

Table 2.2: Table of the effect of the P_i's from equation (2.51) on the parameters of a rising transient as defined in fig. 2.6. The symbols in the table refer to the effect that **increasing** the value of P_i (while all other $P_{j,\ j\neq i}$ are held constant) on the rising transient parameters as follows:

↑ and ↑ refer respectively to a large and small increase in the rising transient parameter.

↓ and ↓ refer respectively to a large and small decrease in the rising transient parameter.

"-" means there was a negligible effect and "×" means there was no effect at all.

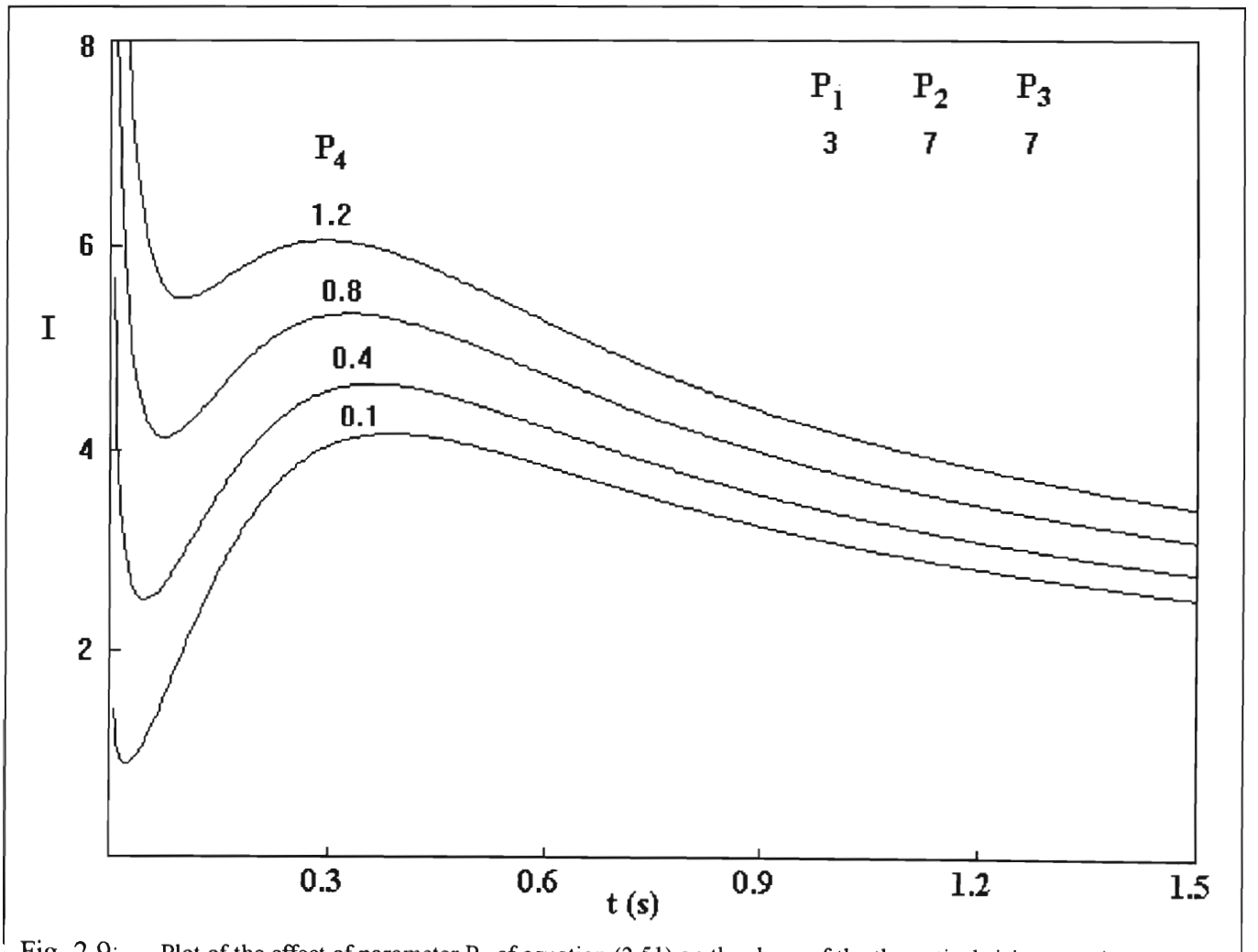

Fig. 2.9: Plot of the effect of parameter P_4 of equation (2.51) on the shape of the theoretical rising transient.

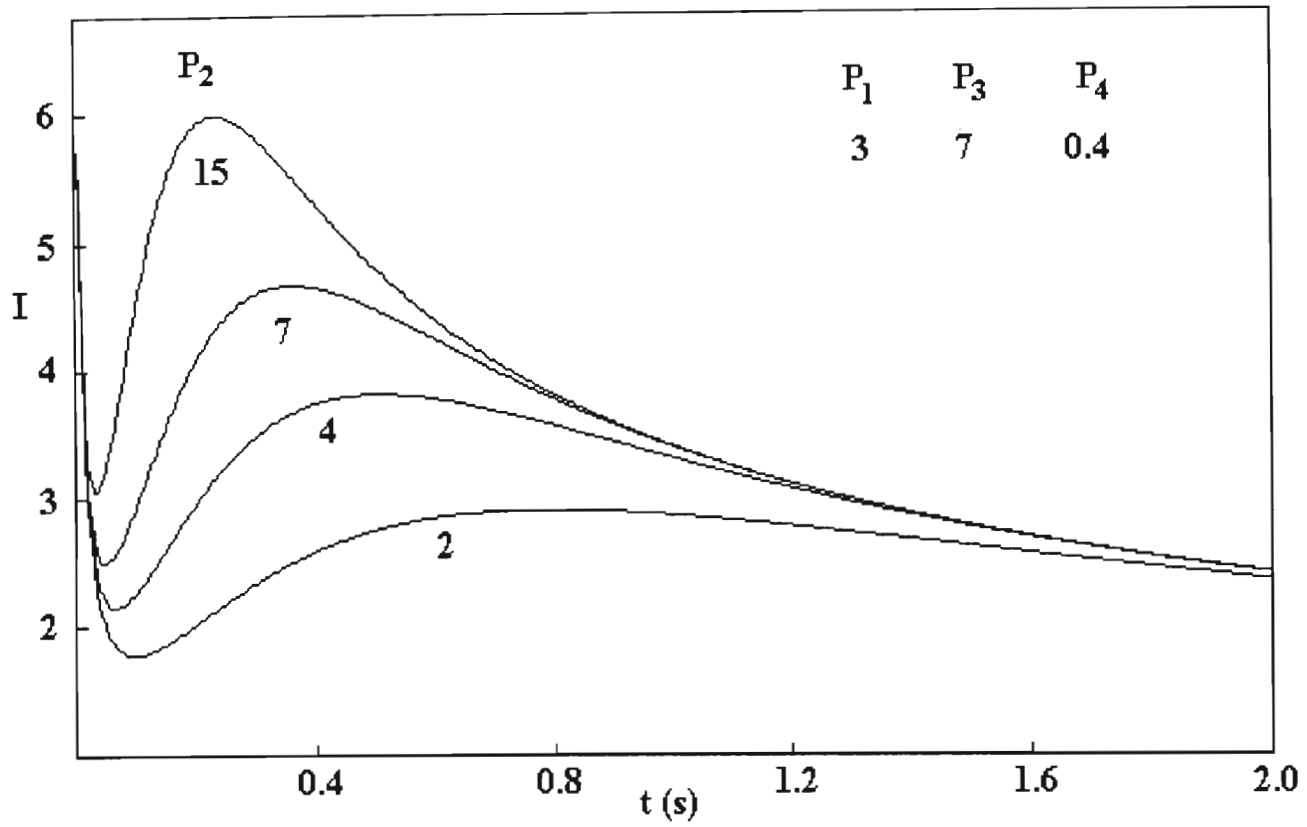

Fig. 2.10: Plot of the effect of parameter P_2 of equation (2.51) on the shape of the theoretical rising transient.

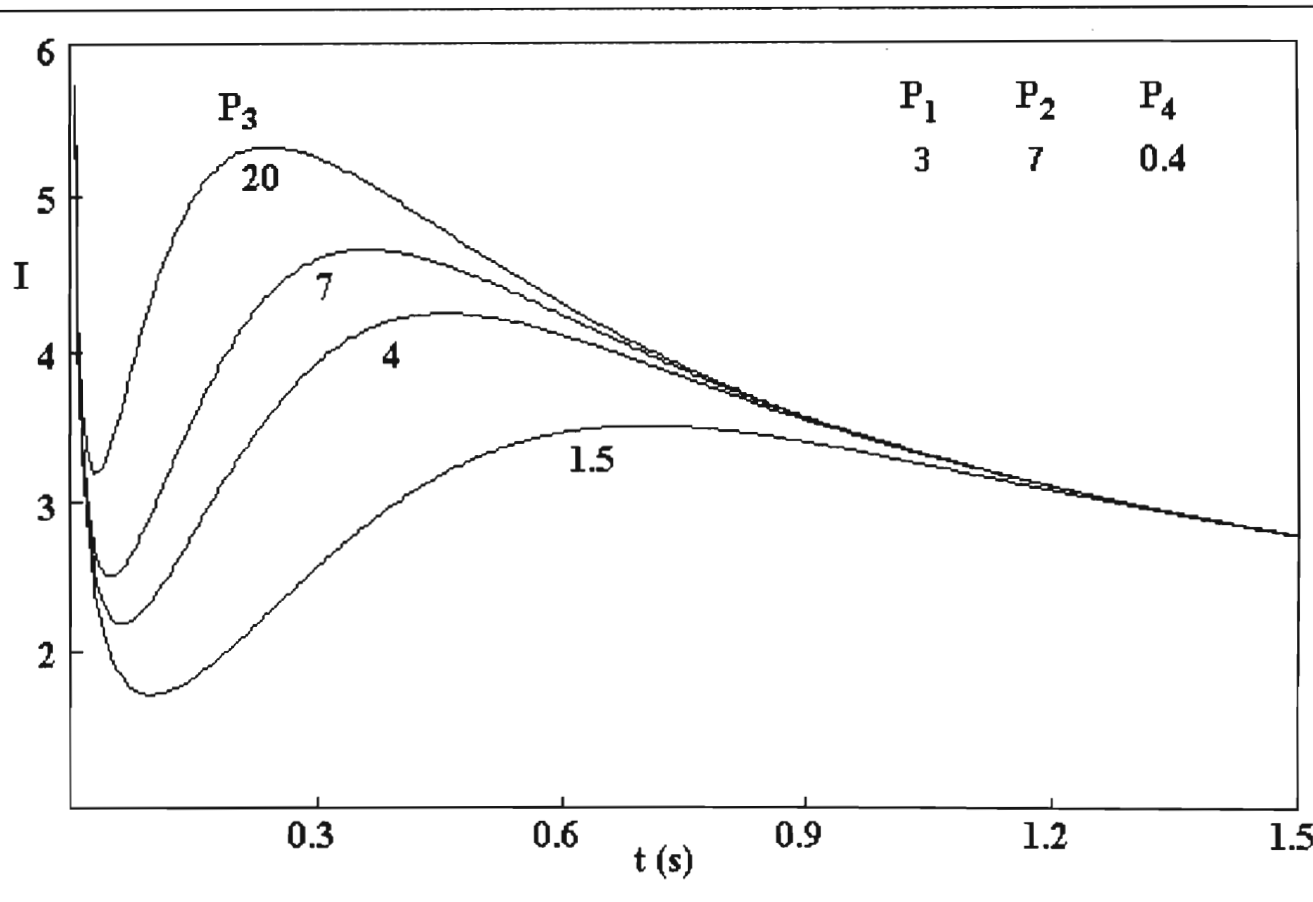

Fig. 2.11: Plot of the effect of parameter P_3 of equation (2.51) on the shape of the theoretical rising transient.

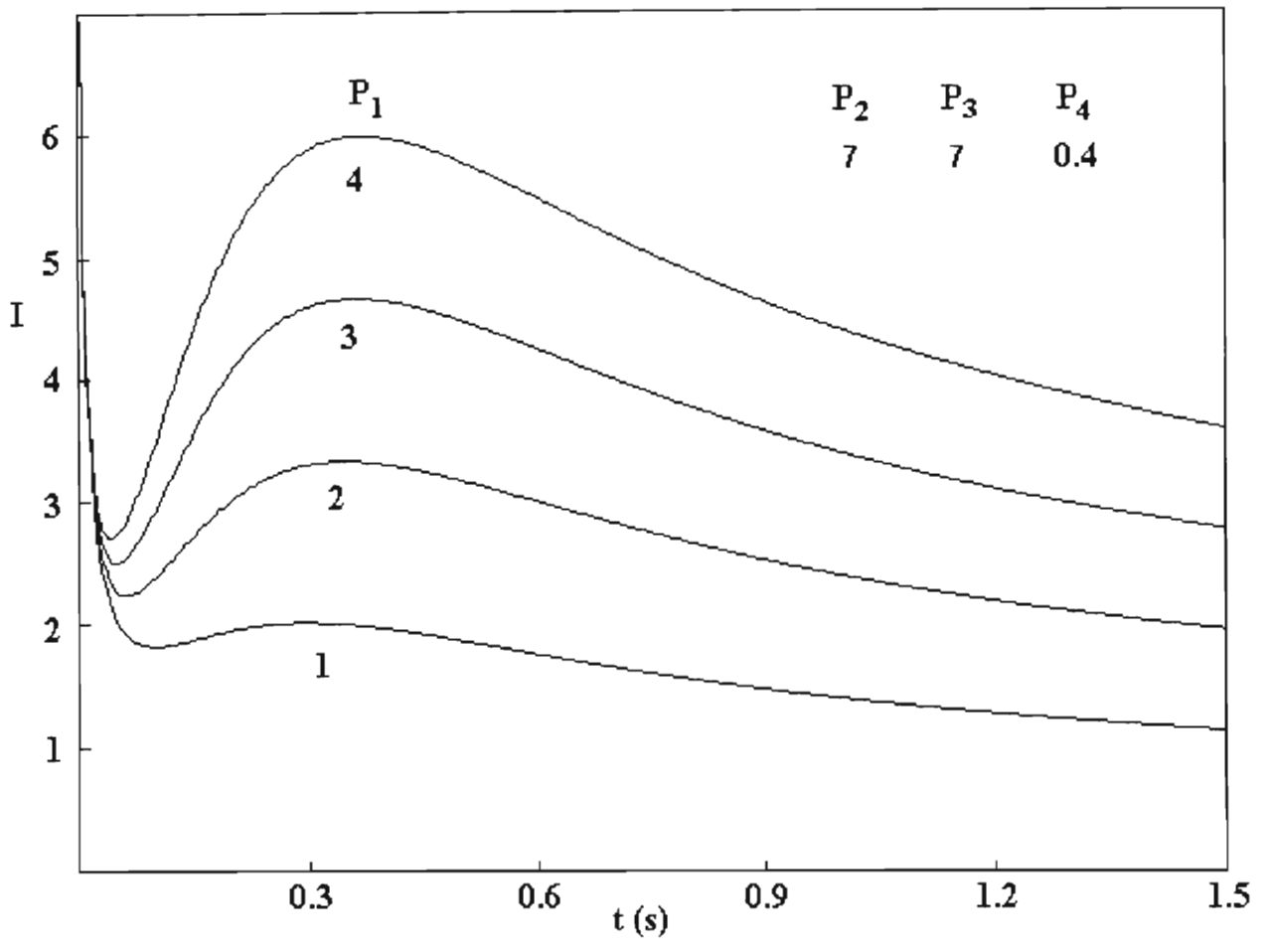

Fig. 2.12: Plot of the effect of parameter P_1 of equation (2.51) on the shape of the theoretical rising transient.

Further comments on this model include:

- Although the model allows for an initial falling current, it does not allow for the double layer charging current. Since rising transients on Fe-Cr alloys have a t_{max} value of 60 ms or less (for pH < 1), this interfering effect can be important.
- The model does not consider the possibility of kinetic control by charge transfer, for example.
- A hemispherical nucleus must make contact with a surface at an angle of ninety degrees. This is costly, and therefore unlikely, in terms of energy requirements [62,63].
- Since the model is based on that of Scharifker and Mostany, it will also be limited in its range of values of I_{max} / I_{lev}. The additional term in this model will only slightly increase this range.

2.4.1.3. *Three dimensional nucleation as right circular cones*

The other major three dimensional form of a nucleus that has been considered is the right circular cone. This model has only been treated for the limiting case of charge transfer. There is one important difference between this and the hemispherical model. A hemisphere has only one rate constant describing its growth as it grows equally in the parallel and perpendicular directions. However, a right circular cone has two rate constants - one describing the growth parallel to, and the other describing the growth perpendicular to the electrode. The general expression for a charge transfer controlled cone nucleation is [8]

$$I = nFk''\left\{1-\exp\left[-\frac{\pi M^2 k'^2 A_k}{A_k'\rho^2}\left(t^2-\frac{2t}{A_k'}+\frac{2}{A_k'^2}-\frac{2}{A_k'^2}\exp-A_k't\right)\right]\right\} \qquad (2.52)$$

Where k' and k'' are the growth rate constants in the directions parallel and perpendicular to the electrode surface respectively (in mol cm^{-2} s^{-1}) and A_k is the nucleation rate constant (in cm^{-2} s^{-1}) defined as $A_k = A_k' N_o$. For instantaneous nucleation the above equation simplifies to [64]

$$I = nFk''\left\{1-\exp\left(-\frac{\pi M^2 k'^2 N_o t^2}{\rho^2}\right)\right\} \qquad (2.53)$$

The equivalent expression for progressive nucleation is

$$I = nFk''\left\{1-\exp\left(-\frac{\pi M^2 k'^2 A_k' t^3}{3\rho^2}\right)\right\} \qquad (2.54)$$

These equations give a transient which increases rapidly to a constant current density plateau. Since the current density does not decrease to form a peak, the model, as it is, cannot be used to fit curves to most rising transient data as there is usually a peak followed by some sort of a current density decrease. In order to resolve this problem, Abyaneh and Fleischmann developed the concept of the "death" of nuclei. This simply means that once a nucleus reaches a certain, predefined perpendicular distance from the electrode surface, it will stop growing i.e. experience "death". Thus when the time is defined by $u < \rho l/Mk''$, where l is the limiting height at which the outward growth of centres into the solution stops (in cm), then the current density is given by equation (2.52). When $u \geq \rho l/Mk''$, then the current density (which is given in the instantaneous form for the sake of simplicity) is given by [8]

$$I = nFk''\left\{\exp\left(-\frac{\pi M^2 k'^2 N_o (t-u)^2}{\rho^2}\right)-\exp\left(-\frac{\pi M^2 k'^2 N_o t^2}{\rho^2}\right)\right\} \qquad (2.55)$$

and the general and progressive forms also follow [8]. The effect of this change is that a peak now appears in the transient, but the current density approaches zero with increasing time instead of attaining a desired steady current density. Further amendments were made to overcome this difficulty, including the "rebirth"

of new nuclei on top of the "dead" ones and the consideration of simultaneous two and three dimensional nucleation [8]. These discussions are not relevant here. A new concept, developed by the author for this thesis, referred to as "slow death" of nuclei will be defined later (*cf* section 8.1) and is based on this theory of the "death" of nuclei .

2.4.1.5. Other models and comments on nucleation

Other nucleation models

In order to overcome the difficulty associated with the ninety degree contact angle of hemispheres, Abyaneh developed a spherical cap model [62] and later a model based on hemispheroidal nuclei [63] (a shape produced by the rotation of a quarter ellipse around one axis). The contact angle can be varied in both of these models. One useful conclusion he made was that the current is not proportional to the surface area (at least in his models) but is rather proportional to the change of volume of the nuclei with time.

Sluyters-Rehbach *et al* [65] have improved and developed the mathematics involved with the overlap of growing hemispherical nuclei, but the resulting transients are very similar to those of Scharifker and Mostany [60]. Abyaneh has also developed the theory for the overlap of hemispherical nuclei, but he has considered the case of charge transfer control [66]. It is interesting to note that for short times he found that, for instantaneous nucleation, $I \propto t^2$ and for progressive nucleation, $I \propto t^3$. These results are the same as the short time approximations for charge transfer controlled right circular cone growth. The general equations that Abyaneh developed for charge transfer controlled growth of hemispheres are rather complex and will not be dealt with here.

Obretenov has shown (by using a Monte Carlo simulation) how a transient with oscillating peaks and minima may be obtained if the transient is considered to be the sum of the transients obtained from the formation of consecutive layers by polynuclear nucleation [67]. Bosco and Rangarajan have also reported a slight oscillatory behaviour of the current in their analysis of progressive, diffusion controlled, hemispherical nuclei [68], but this result has been criticised by Abyaneh and Halvorsen [69].

General comments on nucleation

Table 2.3 summarises the time dependency of the rising part (short times) of rising transients for the various mechanisms. Note that the diagnostics which apply for hemispheres also apply for spherical caps and hemispheroids.

Plots of I vs. t^x, where x = 1/2, 1, 3/2, 2 or 3 could be diagnostic for the mechanism involved. However, these plots have not been used in this study for the following reasons:

- The current density at short times may have interference from the double layer charging current or from an initial, diffusion controlled dissolution current which decays with the root of time (*cf* section 8.2).
- The diagnostics are somewhat ambiguous (*cf* table 2.3).
- More than one process may be contributing to the initial rising current on rising transients from Fe-Cr alloys.
- The diagnostics only consider limiting situations. It would be possible to have mixed diffusion and charge transfer control or an intermediate state between instantaneous and progressive nucleation, for example.

$I \propto ?$	**Shape of nuclei**	**rds**	**progressive/instantaneous**
$t^{1/2}$	hemisphere	diffusion	instantaneous
t	2-D disc	incorporation of adsorbed particles	instantaneous
$t^{3/2}$	hemisphere	diffusion	progressive
t^2	hemisphere	charge transfer	instantaneous
t^2	2-D disc	incorporation of adsorbed particles	progressive
t^2	right circular cone	charge transfer	instantaneous
t^3	hemisphere	charge transfer	progressive
t^3	right circular cone	charge transfer	progressive

Table 2.3: Time dependence of the rising part of the rising current transient (i.e. during nucleation) for various nucleation mechanisms.

CHAPTER 3

3. LITERATURE REVIEW

A review of the passivity and transpassivity of relevant elements and stainless steels, as well as models of passivity and passivity breakdown, follows. A summary of relevant work performed in this laboratory is also given. Since this study did not include an investigation of chloride-induced pitting or of the effect of the chloride ion it is not reviewed here in detail, but an excellent review and study on pitting (on Fe-Cr alloys) is presented elsewhere [70].

3.1. Electrochemical behaviour of pure metals

When Cr and other alloying elements are added to iron, the corrosion resistance of the resulting stainless steel is greatly improved compared to that of iron itself. It is therefore useful to review the electrochemistry of the relevant metals (Fe, Cr, Mo).

3.1.1. Iron

The anodic polarisation curves for iron in a strongly acidic [71] and a weakly acidic [72] solution are given in figures (3.1) and (3.2) respectively. The predominant feature of the strong acid (1M H_2SO_4) APC is the single oxidation peak in the active region. In the weaker acid, however, (pH = 7.0, $[CH_3COO^-]$=1M) there are two peaks in the active region, characterised by the potentials E_{pr} (the potential of the prepasssive peak) and E_{pp} (the potential of the primary passivation peak). Qualitatively, this corresponds to the separation of the two charge transfer steps $Fe \rightarrow Fe(II)$ and $Fe(II) \rightarrow Fe(III)$ into two peaks. Except for the additional potential, E_{pr}, the characteristic potentials (E_{pp}, E_{Flade}, E_{tr} etc.) and the characteristic current density values (I_{cr}, I_p') for the APC's of Fe, Cr and Fe-Cr alloys have all been previously defined from the standard APC of 430 stainless steel in 0.5M H_2SO_4 (fig. 2.1). A number of models have been proposed for the (active) dissolution of iron in weakly acidic media, most notably those of Lorbeer and Lorenz [73,74], Keddam *et al.* [75], Bockris *et al.* [76], Epelboin *et al.* [77] and Takahashi *et al.* [72].

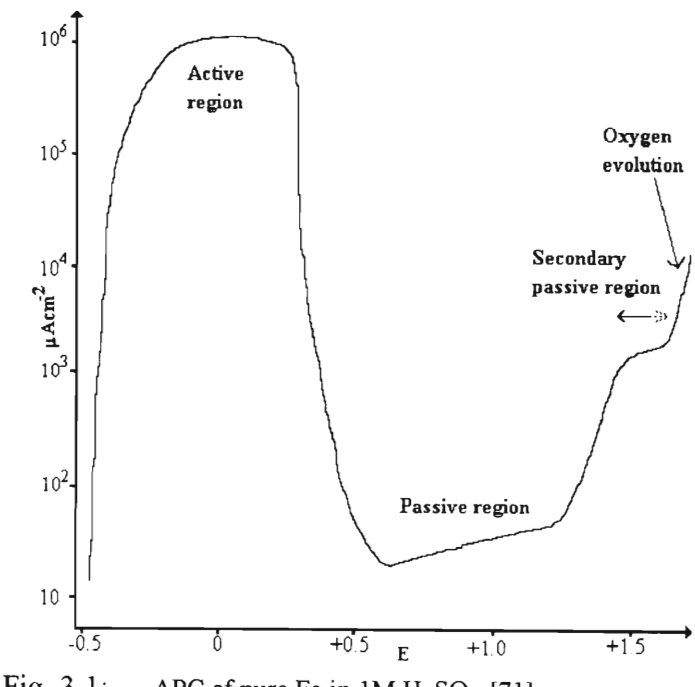

Fig. 3.1: APC of pure Fe in 1M H_2SO_4 [71].
Sweep rate = 1mV/s. Rotation rate = 100 rad/s.
Temperature = 25°C. Potential is versus the saturated calomel electrode (SCE).

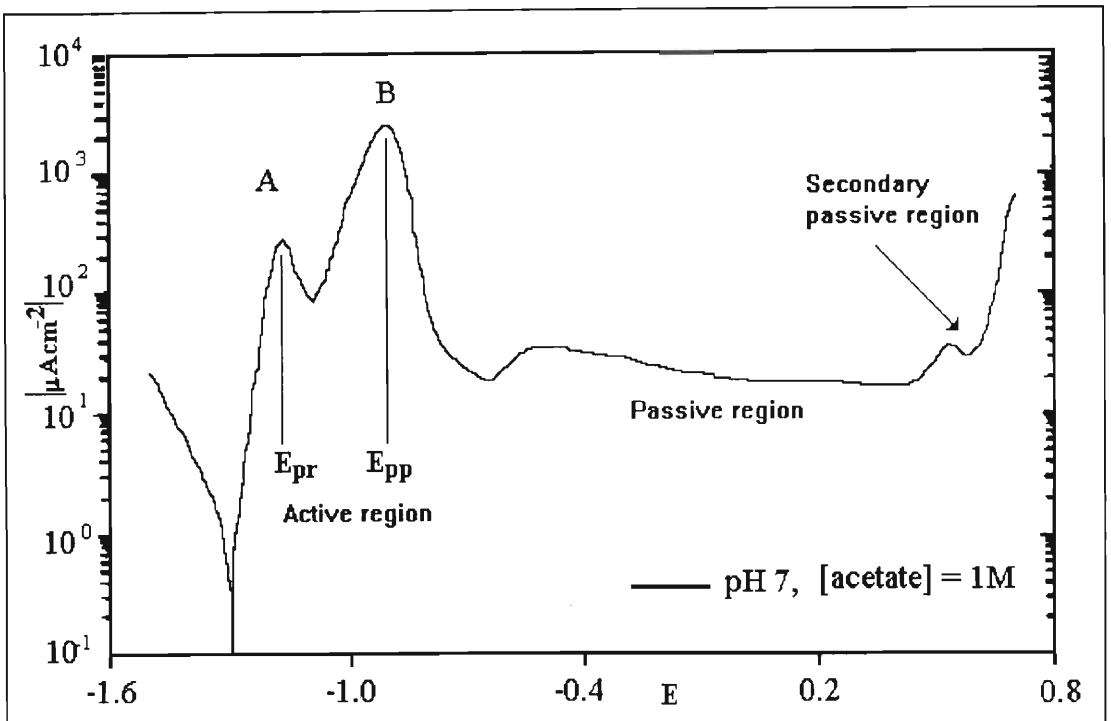

Fig. 3.2: Anodic quasi-polarisation curve for pure iron in a pH 7.0 acetate buffer solution ($[CH_3COO^-]$=1M) [72]. Sweep rate = 5mV/s. The potential is versus the saturated sulphate electrode (SSE).

The above mentioned mechanisms for the (active region) dissolution and passivation of iron in weakly acidic solutions will not be discussed in detail here, but the common points of the mechanisms can be summarised and contrasted to the corresponding mechanisms in strong acids as follows:

(1) The active region in weak acids contains two peaks and hence at least two reaction pathways are given:
   (a) A pathway involving the oxidation of Fe to some Fe(II) species (adsorbed or soluble).
   (b) A pathway involving the oxidation of an adsorbed Fe(II) species to Fe(III) species (adsorbed or soluble).

   These pathways involve irreversible oxidation steps which are rate determining.

(2) The main dissolution product of the first peak of the active region is Fe^{2+}. The main dissolution product of the second peak and that of the passive region is Fe^{3+}. In contrast, the primary dissolution product of iron electrodes in strongly acidic solutions in the active region (one anodic peak) is considered to be Fe^{2+} [78,79]. In strong acids Fe(II) species are oxidised to Fe(III) species in the prepassive range (the active-passive transition between E_{pp} and E_{Flade}) but these Fe(III) species are passivating and are not lost to the solution [79,80].

(3) The adsorbed species are usually $(FeOH)_{ads}$, $(Fe(OH)_2)_{ads}$ and $(Fe(OH)_3)_{ads}$. It has also been proposed that these species inhibit the dissolution reaction [81]. The anion in the adsorbed species may in some cases also be the anion of the supporting electrolyte [72].

(4) The passive film consists of Fe_2O_3, Fe_3O_4 and iron oxyhydroxides. It may also contain the anion of the supporting electrolyte. In more acidic solutions, potential modulated reflectance spectroscopy (PMR) studies have indicated that Fe(II) species are present in the passive film at all passive region potentials, including up to the beginning of oxygen evolution [82].

In strongly acidic sulphate solutions, Russell and Newman considered the formation of a porous salt film on the electrode [83]. They found that the high rate of iron dissolution causes the solution to become supersaturated in ferrous sulphate, and when the surface concentration reaches a critical value (1.8 times saturated concentration), ferrous sulphate crystals precipitate. Continued precipitation results in the growth of a porous ferrous sulphate film on the surface. This porous film is considered to be a prepassive film by Pintauro and Roy, who measured its thickness as between 12 - 39 μm [84]. During the existence of the prepassive film, the mass transfer of cations therein is considered to be rate determining. Riggs, using x-ray diffraction, found ferrous and ferric sulphates in the passive film formed from sulphuric acid solutions [85]. Hence the behaviour of the electrode and passive film can easily be influenced by the composition of an electrolyte, as well as its pH.

To account for the large increase in active region current response with decrease in pH, catalytic mechanisms have been proposed. In particular, one mechanism has been suggested which shows the dissolution of iron (in the active range) to be catalytic with respect to $(Fe(OH))_{ads}$ and H^+ [79,80]. It is also noted that the role of H^+ is directly in dissolution of already oxidised Fe species. The dissolution reaction which is common to most proposed mechanisms (weak and strong acid) is

$$FeOH^+ + H^+ \rightleftharpoons Fe^{2+}_{aq} + H_2O$$

Similarly, Fe(III) species may dissolve according to

$$Fe(OH)^+_2 + 2H^+ \rightleftharpoons Fe^{3+}_{aq} + 2H_2O$$

In short, H^+ is responsible for the removal of protective adsorbed hydroxyl species (which would otherwise eventually form the passivating Fe_2O_3 and Fe_3O_4) into the solution. Therefore as the pH is decreased, this effect is increased, and the active region current response may increase.

The transpassive dissolution of the passive film on iron has not been well investigated, mainly because it is often masked by oxygen evolution. However, figures (3.1) and (3.2) both show a region of initial passive film breakdown and then secondary passivity before masking by oxygen evolution. However, in strong acid solutions, the secondary passive region has not always been found [fig. 3 of 11], so its existence is debatable. Graham, however, has also observed a secondary passive region on iron, this time in 0.1M H_2SO_4 [86]. In weakly acidic and basic solutions, the secondary passive region is well established [15,72,87,88-90] and in basic carbonate solutions (on mild steel) a

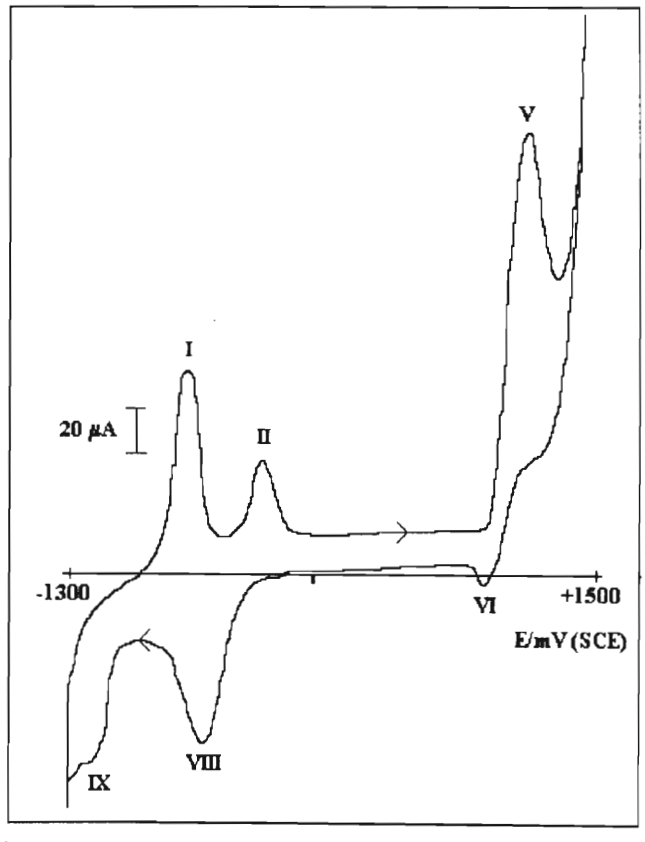

Fig. 3.3: Cyclic voltammogram for mild steel in 600 ppm carbonate / bicarbonate solution [15]. Sweep rate = 50mV/s; pH = 10.05. The potential is versus the SCE.

voltammetric peak very similar to the peak A found on Fe-Cr alloys has been reported [15,87]. The peak V shown in fig. 3.3 is that peak, and its kinetics are attributed to at least three processes:

- Charge transfer under resistive control (the oxidation of Fe(III) to Fe(VI) species such as FeO_4^{2-}).
- A coupled chemical reaction.
- Diffusion of electroactive species.

The Fe(VI) species are stabilised in solutions of high basicity [91], and it is possible that these species are also stabilised by complexing with anions of the electrolyte such as carbonate and acetate. Therefore in acetate buffer solutions of sufficiently high pH, a voltammogram similar to that in fig. 3.3 might be expected.

3.1.2. Chromium

Fig. 3.4 shows a typical APC for chromium in strongly acidic solutions [92]. Chromium dissolves as Cr(II) and Cr(III) in the active region, as Cr(III) in the passive region and as Cr(VI) in the transpassive region (as CrO_4^{2-} and $HCrO_4^-$, pH depending) [93]. In the active and passive regions the dissolution of chromium was found to be independent of pH [94,95]. In contrast to this, Shlepakov *et al*, using ESCA (electron spectroscopy for chemical analysis) studies of chromium surfaces after potentiostatic polarisation in sulphuric acid solutions, (pH between 0.3 and 3.0) showed that the acidity of the electrolytes had a marked effect on the passive film [96,97]. An increase in pH lowered the anodic current density in the passive and active regions. This is not surprising if H^+ is considered as the active agent involved in the dissolution of cationic species.

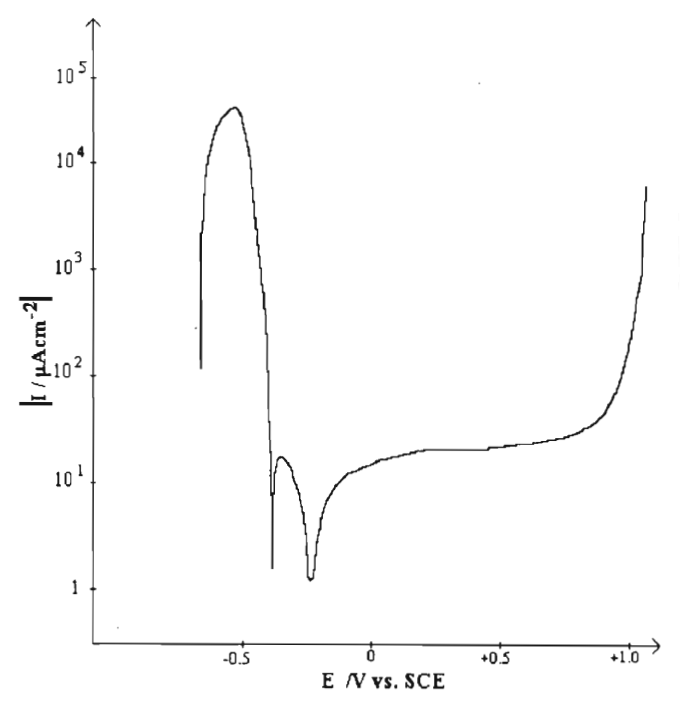

Fig. 3.4: APC of pure chromium in 1M H_2SO_4 [92]. Sweep rate = 1mV/s. Rotation rate = 100 rad/s.

CrOOH and Cr_2O_3 were found to be present in the oxide film in the passive region. In the transpassive region chromium has a thin layer of oxide on its surface, the mean valency of which was found to be a function of the electrode potential [95].

The discovery by XES (x-ray electron spectroscopy) of the hydride CrH was used to explain the apparent disappearance of the active-dissolution region at pH > 3 [98]. The chromium was considered to have been passivated by the formation of a Cr_2O_3 film (which was plated on the chromium over the stable passive range) as a surface phase through the oxidation of CrH by the following reaction:

$$2CrH + 3H_2O \rightarrow Cr_2O_3 + 8H^+ + 8e^-$$

Later, Shlepakov and Sukhotin showed that a maximum current density was observed for the active-passive transition [99]. The film thickness on Chromium (in 0.5M H_2SO_4) was examined (by XES) and was found to be a maximum at 1.2V vs. SCE. On moving into the transpassive region the film thickness dropped sharply and a decrease in the ratio of Cr(VI) / Cr(III) in the film was found, which indicated dissolution of Cr(VI) species in the transpassive region [98]. Armstrong *et al.*, using electrochemical impedance spectroscopy (EIS) also found the presence of a thin oxide film in the transpassive region, which dissolved as Cr(VI) [20,21]

Using a rotating ring disk electrode (RRDE), Haupt and Strehblow showed that the part of the corrosion passivation currents on Chromium (in 0.5M H_2SO_4) due to dissolution of Cr cations (in particular, Cr^{3+}) was far less than 10% [100]. This means that the processes occurring before the transpassive region are probably mostly in the solid state.

Transpassive dissolution takes place at potentials more negative than the oxygen evolution reaction (in contrast to Fe), and hence oxygen evolution is not observed on chromium. The mechanism of transpassive dissolution of chromium is pH dependant [95,101] and is considered to be related to the hydroxyl ion concentration with other anions having no influence on the mechanism.

3.1.3. Molybdenum

The role of Molybdenum in Fe-Cr alloys is not well understood, particularly as the electrochemical behaviour of the pure metal appears to be unrelated to the corrosion resistance (in particular, resistance to pitting) it imparts when added to stainless steels in small quantities (1-2 weight %). Its electrochemical behaviour as the pure metal is also complicated by the dependence of its oxidation state (III - VI) on the supporting anion and the pH, for example. The chemistry of molybdenum in these oxidation states is wide, as it has a tendency to enter into complexation and self-polymerisation reactions.

The APC for molybdenum in sulphuric acid solutions shows two active-passive regions (between the corrosion potentials of -0.262 and 0.126V and between the passivation potentials of -0.205 and -0.0505V vs. SCE) and the usual transpassive region. The two active regions were attributed to the oxidation of Mo to Mo(IV) and the oxidation of Mo(IV) to Mo(VI) respectively [102]. Hull found that molybdenum dissolved quantitatively as Mo(VI) [103]. Hull [103] and Wikstrom *et al.* [102] proposed that the rate determining step in the overall dissolution process was the transition from the IV to the VI oxidation state.

There is no agreement in the literature on the composition of the passive film on Mo nor on whether Mo is resistant to Cl^- attack [104,105] or not [106].

3.2. Theories of passivity and passivity breakdown

Some of the more widely accepted models of passivity and passivity breakdown are presented. Those models which describe passivity breakdown predominantly in terms of the action of the chloride ion (such as ion exchange processes, the hydrated polymeric oxide model and adsorption displacement models) are omitted as they are not relevant to this work. Note that the term "enrichment" refers to an increase in weight percent of a metal (cation) in an anodic film relative to its weight percent in the base alloy.

Pore resistance theory

This theory involves a two stage process with an initial random spread of a solid layer of low conductivity at constant thickness across the electrode surface until only small pores remain, followed by an increase in the thickness of the layer with pore areas remaining constant [44,45].

Dissolution - precipitation mechanism

Anodic metal dissolution followed by precipitation of dissolved (and sometimes supersaturated) metal ions leads to a passivating oxide or insoluble salt film [19,83,107].

Solid state mechanism

Anions, which may be derived from the electrolyte, react with the metal directly to form a passivating film [108]. This process can occur in parallel with metal dissolution in the active region and during the onset of passivity. The bipolar and point defect models are both different versions of the solid state mechanism.

Chemico-mechanical models

A number of versions of these models for breakdown of passivity have been proposed [109,110,111], but the most relevant to this work is that of Sato [112,113]. He has suggested that high electric fields (such as those experienced at large positive potentials) could lead to mechanical rupture of thin films by electrostriction processes exceeding the compressive fracture strengths of the film. Sato has defined a critical film breakdown potential above which breakthrough pores are formed in the film. This critical potential is made more negative (less noble) by the lowering of the surface tension of the film by, for example, adsorption of anions such as chloride onto the film. The critical potential also marks the beginning of electrochemical instability of the film and transpassive dissolution will take place at potentials positive to it.

The other models generally involve the surface tension reduction and consequent rupture of films due to electrostatic repulsive forces between adsorbed chloride ions, thus exposing small regions of the bare metal surface to the electrolyte.

Localised acidification

This model proposes that passive film breakdown initiates as a result of the localised acidification that takes place at the passive film - solution interface. This localised acidification causes local dissolution and also hinders reformation of the passive film. In a strong acid, the following three general reactions have been proposed [114]

$$M \rightleftharpoons M^{n+} + ne^- \tag{3.1}$$

This would be followed by

$$M^{n+} + nH_2O \rightleftharpoons M(OH)_n + nH^+ \tag{3.2}$$

At potentials below a critical potential only the following reaction will occur

$$M + nH_2O \rightleftharpoons M(OH)_n + nH^+ + ne^- \tag{3.3}$$

Thus as long as the potential is below this critical potential, the metal will repassivate. If the potential is above the critical potential, however, then the acidity produced at a localised site by reaction (3.3) will create conditions for reaction (3.1). Reaction (3.1) followed by reaction (3.2) will maintain localised acidity at a metal surface.

If this is a valid model, then one might expect that rotating the electrode would provide a means of removing some of the local acidity (since rotating the electrode makes the Nernst diffusion layer narrower which in turn results in an increase of removal of ions (in this case H^+) by diffusion along the increased concentration gradient to the bulk solution). Therefore increasing the rotation rate of the electrode should decrease the current density at potentials positive of the critical potential if this model is valid (*cf* section 6.3.2.1).

Bipolar mechanism

Clayton *et al.* developed this model for Fe-Cr-Ni stainless steels [115,116]. The model assumes that the inner barrier layer (which is enriched in a mixed phase of CrO_3 and Cr_2O_3) is an anion selective layer (this means that the hydrated metal oxides in the layer have a positive fixed charge) and that the iron oxide enriched outer layer is cation selective (hydrated metal oxides have a fixed negative charge). This arrangement of charge within the film causes the migration of H^+ (from the inner layer) to the solution, causing the chromium oxides to become dehydrated, and the migration of O^{2-} (from deprotonated OH^-) towards the alloy surface. The dehydration of the inner layer results in it becoming glassy and therefore resistant to penetration by damaging anions.

Relevant to the formation of the bipolar layer is that both hydrated Fe(III) and Cr(III) oxides were found to be anion selective in the presence of monovalent anions whereas they were found to be cation selective in the presence of multivalent anions. The bipolarity is then explained by the observation that CrO_4^{2-} was found in the transition between the two layers (by variable angle XPS [115]). This is a divalent anion and thus causes the Fe(III) oxides to be cation selective. The favourable effect of small additions of Mo on the corrosion resistance of these alloys is attributed to the solid state production of MoO_4^{2-} in the

outer Fe-rich layer (also found with variable angle XPS [116]), which enhances the cation selectiveness of that layer. This in turn enhances the bipolarity of the film and thus the eventual glassiness of the chromium rich barrier layer. It was argued that both CrO_4^{2-} and MoO_4^{2-} form in the solid state by dehydration of Cr(III) and Mo(IV) oxides respectively. The coexistence of CrO_3 and Cr_2O_3 in the inner barrier layer was attributed to their highly similar free enthalpies of formation (-141 and -136 k cal mol^{-1} respectively).

At transpassive potentials the disappearance of CrO_4^{2-} from the film was noted, while the inner layer became more enriched in CrO_3 and Cr_2O_3.

Point defect model

Macdonald has developed the point defect model (PDM) [12,117-120] to account for steady state passive films [117,118] and the breakdown of passive films due to pitting and also due to transpassive dissolution [12]. He has also developed an extension of the PDM, the solute-vacancy interaction model (SVIM), in order to account for the effect of alloying elements [119].

The steady state passive film

Macdonald bases the PDM for steady state passive films on certain experimental facts that he sites, including:

- Passive films form as bilayers, with a highly disordered "barrier" layer adjacent to the metal and an outer film comprised of a precipitated porous phase that may incorporate anions from the solution. Passivity is attributed to the barrier layer.
- Given a constant oxidation state of the cation in the film within the desired potential range, the steady-state thickness of the barrier layer and logarithm of the steady-state current vary linearly with applied voltage.

The principle entities involved in oxide growth in the PDM are point defects; notably cation ($V_M^{\chi'}$) and anion ($V_O^{\cdot\cdot}$) vacancies, in a disordered barrier layer of nominal stoichiometry $MO_{\chi/2}$. Here the "V" refers to a vacancy that may "house" in the first case a cation, M, of charge χ that is generated from a metal atom, m, and in the second case an oxygen anion (subscript O) which is, of course, divalent (superscript "$\cdot\cdot$"). These ion vacancies can also "house" ions of charges which are different to χ or "$\cdot\cdot$". A Mott-Schottky pair reaction will generate vacancies according to

$$Null \rightarrow V_M^{\chi'} + \frac{\chi}{2} V_O^{\cdot\cdot} \tag{3.4}$$

which is why the ion vacancies are also known as Schottky defects.

The PDM has been developed for both of the extreme kinetic cases of interfacial equilibrium and irreversible reaction [117,118]. Fig. 3.5 shows the model for the case of irreversible reaction. In

the figure, M_M is a metal cation in a cation site, O_O is an oxygen anion in an anion site, V_m is a vacancy in the metal phase and the other symbols have already been defined.

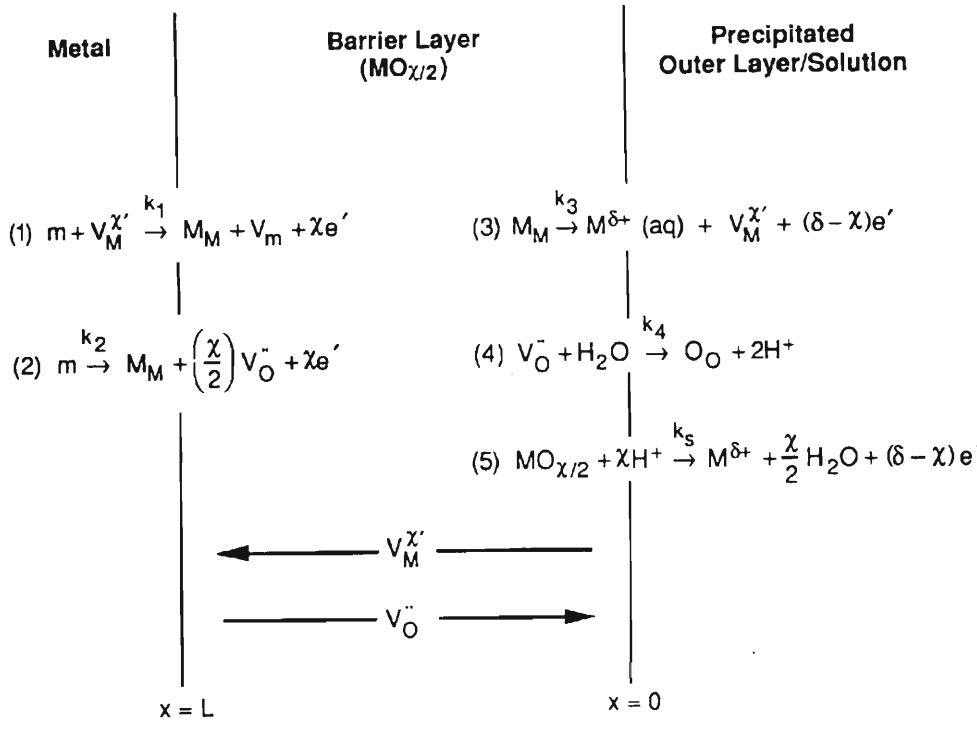

Fig. 3.5: Schematic of physio-chemical processes that occur within a passive film according to the point defect model [12]. (1) to (5) are the five elementary reactions.

Assuming that the transmission of ions through the barrier layer occurs by vacancy motion, Macdonald states that the only possible elementary reactions for vacancy generation and annihilation are the five shown in fig. 3.5. Reactions 1, 3 and 4 conserve the film boundaries (ions are merely moved across the boundaries). Reaction 2 results in the generation of new film. Reaction 5 results in the destruction, by dissolution (which may or may not involve a net transfer of electrons), of the film. Hence reactions 2 and 5 do not conserve the boundaries of the (barrier) film. Therefore, in the steady state (film thickness constant and constant current - but the film as a whole may move relative to a fixed point in space) the rates of reactions 2 and 5 (one film-constructive, one film-destructive) must be equal.

If the base metal and electrolyte are such that the metal cations are transmitted (reaction 3) rather than dissolved from its oxide (reaction 5), then the transmission of cations will be balanced by the inward movement (diffusion) of cation vacancies from the film / solution interface to the metal / film interface where the metal cations are replaced by the annihilation of the cation vacancies (reaction 4). This is the limiting case of cation transmission and in this case the metal grows into the film [117]. If, on the other hand, metal cations are ejected from the film by dissolution of the metal oxide (reaction 5), then the resultant loss of oxygen anions must be balanced by the outward movement of anion vacancies from the metal / film interface so that the oxygen anions may be

replaced by the annihilation of these anion vacancies at the film / solution interface (reaction 1). This is the limiting case of anion transmission and in this case the film grows into the metal.

By expressing the interfacial rate constants as exponential functions of the interfacial potential differences, and by assuming that the potential drop across the film / solution interface varies linearly with applied voltage and pH, Macdonald *et al.* have been able to derive expressions for the steady-state barrier layer thickness and the steady-state current density, I_{ss} [117,118]. The equations are not presented here as it is sufficient to state their qualitatively important predictions:

- The steady state barrier thickness is predicted to increase linearly with the applied voltage and also with increase in pH.
- Provided that either cation vacancies or anion vacancies dominate the barrier layer transport properties, then log I_{ss} will vary linearly with the applied potential.

Passive film breakdown

The PDM has been developed for three types of passivity breakdown, namely pitting corrosion, transpassive dissolution, and erosion-corrosion. Only the second of these is directly relevant to this work, but it is useful to summarise the mechanism for pitting corrosion as well.

Pitting corrosion

Pitting corrosion will occur when an aggressive anion, in particular chloride anions, upon reaching the outer surface of the barrier layer, upsets the balance of ion vacancy regeneration and annihilation. A chloride anion, on approaching the surface of the barrier layer, may interact with it in two ways:

- It can dehydrate and occupy an anion vacancy.
- It can retain its hydration sheath and interact with a surface cation - it would be absorbed at the cation site.

In the first case, the system may react to the loss of anion vacancies by generating more anion (and cation) vacancies by a Mott-Schottky pair reaction (equation (3.4)) and the newly generated anion vacancies may react with additional aggressive anions. The result is an autocatalytic production of cation vacancies. If these cation vacancies cannot be annihilated (at the metal / film interface) at the rate at which they are being produced, then they will coalesce and will form a "bubble" between the metal and the film. The tensile stress on the film and the dissolution of the film at its surface may then cause a rupture at this bubble site.

In the second case, the chloride anion may desorb, taking the associated cation with it (cation extraction). This process may happen when, for example, the cation forms complexes readily with the anion. This cation extraction (coupled with the aggressive anion desorbtion) results in the

generation of an ion vacancy pair. The cation vacancy can then coalesce with the anion vacancy, resulting in the destruction of the (barrier) film at the film / solution interface, or the cation vacancies can submerge and coalesce at the metal / film interface. Since this process results in the regeneration of the aggressive anion, it is also autocatalytic.

Solute vacancy interaction model

The premise of this model, which is an extension of the PDM, is that pairing occurs between highly charged solute (where the term "solute" refers to an alloying element) ions substitutionally present in the barrier layer and mobile cation vacancies. It was shown by SALI (surface analysis by laser ionisation) that alloying elements (in particular, Mo) are segregated into the barrier layer. The degree of segregation increases with increasing charge on the solute. Segregation is believed to occur by a solid-state reaction at the metal / film interface. These highly charged solute ions diminish both the concentration and diffusivities (which are of the order of 10^{-20} cm^2/s) of cation vacancies within the (barrier) film. Thus the ability of these vacancies to coalesce is also diminished.

Transpassive dissolution

In the absence of aggressive anions, and in the particular case of stainless steels, the generation of the "excess" cation vacancies required for coalescence at the metal / film interface is envisaged to occur by the following reaction (*cf* reaction 3, fig. 3.5)

$$Cr_{Cr} + 4H_2O \rightarrow CrO_4^{2-} + V_{Cr}^{3'} + 8H^+ + 3e' \qquad (3.5)$$

in which Cr_{Cr} represents a Cr^{3+} cation in the passive film lattice. The rate of this reaction is a strong function of potential. At sufficiently high (transpassive) potentials the rate of reaction (3.5) is such that reaction 1 of fig. 3.5 cannot annihilate the resulting cation vacancies which then coalesce at the alloy / film interface. In this case, the cohesion is envisaged to happen generally across the surface, so that there is macroscopic decohesion of the barrier film from the metal. Once breakdown has occurred over macroscopic areas the high (mass transport controlled) dissolution rate of the substrate will inhibit the reformation of a barrier layer (hence no true repassivation) although a porous outer layer may form, possibly as a salt film. The formation of this salt film (secondary "passivation") will result in a decrease in current (though not down to the levels experienced in the passive region where the barrier layer existed) due to limiting mass transport through the developing outer layer.

It is noted that this can be viewed as the first published explanation for the peak A phenomenon on Fe-Cr alloys outside of the work produced from the University of Natal - Durban (UND) electrochemistry laboratory.

3.3. Electrochemical behaviour of ferritic stainless steels

Fig. 3.6 shows a schematic diagram of the variation of the APC's as the substrate is changed from Fe to an Fe-Cr alloy to pure Cr in a strong acid. In the active region, as the Cr% is increased the potential and the current maximum of the (main) anodic peak in each case decreases, as does the potential at which passivity commences (E_{Flade}). Similarly the value of the current density in the passive region also decreases as the Cr% of the substrate increases.

The transpassive region of Cr, however, begins significantly before that of Fe, due to the dissolution of the passive film as CrO_4^{2-} [11]. It has been suggested in the literature that the transpassive peak (peak A) is also due (at least initially) to the CrO_4^{2-} dissolution [12] and that the secondary passivation is due to a temporary, porous iron oxide or iron salt film. The onset of oxygen evolution then obscures the secondary passivity on Fe-Cr's and the passive region on Fe. It has not been conclusively established whether iron displays secondary passivity in acidic solutions. Mild steel (slightly impure iron containing no Cr and some trace elements such as carbon and sulphur) has been shown to undergo secondary passivation in basic carbonate solutions [15].

The effect of adding Mo as a minor alloying element would be to significantly reduce the current density of the Fe-Cr alloy in the active, passive, and secondary passive regions. Also the active peak would move slightly negatively and the transpassive peak would move slightly positively (~ 30 mV).

Since most of the work on Fe-Cr alloys has involved the active region and passive film, this will be reviewed first, followed by a summary of the work performed in the transpassive region.

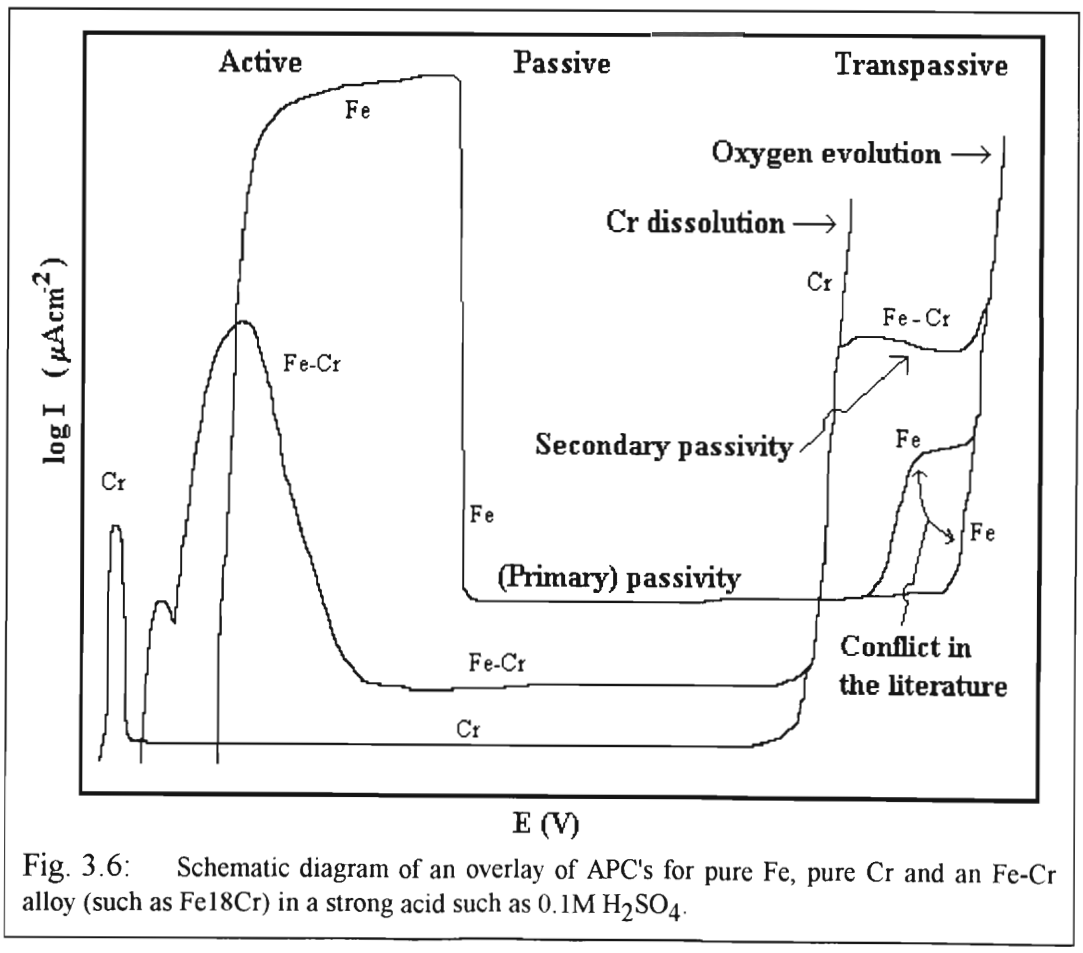

Fig. 3.6: Schematic diagram of an overlay of APC's for pure Fe, pure Cr and an Fe-Cr alloy (such as Fe18Cr) in a strong acid such as 0.1M H_2SO_4.

3.3.1. The passive film

Prior to the advent of surface analytical techniques there was little definitive work on the composition of stainless steel surfaces and their anodic films. Some of the techniques now available include:
Auger electron spectroscopy (AES), ellipsometry, electron spectroscopy for chemical analysis (ESCA), scanning electron spectroscopy (SEM) - with energy dispersive x-ray analysis (EDAX), secondary ion mass spectroscopy (SIMS), x-ray electron spectroscopy (XES), x-ray photoelectron spectroscopy (XPS), reflection high energy electron diffraction (RHEED), infrared spectroscopy (IRS), surface analysis by laser ionisation (SALI) and others. Several books and reviews on these subjects have been published [121,122,123].

It should be mentioned that what has previously been regarded as the passive film is in fact the combination of an inner barrier layer (which is passivating and probably is formed by a solid state process) and an outer, porous layer which is often considered to be precipitated from solution [12,89]. This outer porous layer may be slightly protective, but is not passivating. In this thesis, a passive film will be regarded as any film containing cations of the substrate metal or alloy which imparts some protection to that substrate from its environment. This may be a precipitated porous film (as in secondary passivity [12]) or the combination of the barrier layer and the outer porous layer, as in (primary) passivity. In any case, it should be noted that it is only the barrier layer which imparts significant protection to the subsrate from its environment, and distinction between this layer and the far less protective outer layer will be made where necessary.

With the advent of the abovementioned surface analytical and other techniques the passive film on stainless steels has been well characterised as a thin (10 - 60 Å) amorphous film consisting of both oxides and oxyhydroxides of chromium and iron. However, the composition of the passive film is strongly dependant on the alloy substrate [124]. ESCA analysis of the passive films formed on austenitic and ferritic steels in neutral and acidic aqueous solutions have shown them to probably consist of an inner, chromium rich oxide, Cr_2O_3, and an outer layer of hydroxide containing, Fe^{3+}, Mo^{6+} and Cr^{3+} [124,125]. There is a continuos transition from the oxide to the hydroxide resulting in the characterisation of the film as an oxyhydroxide.

From investigating iron in neutral and acid solutions, it has been reported that differences in the nature of the passive film at the Flade potential (where the film has a polymeric structure) and at the positive limit of the passive region (where the film is a solid phase - possibly Fe_3O_4) exist [126,127]. Similar findings were reported by Frankenthal (for Fe-Cr alloys in 1M H_2SO_4) who found that the passive film at potentials near the Flade potential grows reversibly with a thickness corresponding to less than the equivalent of one oxygen ion per metal surface atom. However, the passive film at the positive limit of the passive region was shown to grow irreversibly to a thickness of 10Å with increasing potential and time [128,129,130].

The presence of oxygen, OH^- and bound water in the passive film has now been well established. Three types of bound water have been considered, viz. M-OH_2, M-OH and M-OOH [131]. Okamoto and

Shibata proposed a model for the structure of the passive film formed on 304 steel. They assumed the films to be amorphous, and the stability thereof was attributed to the ability of the bound water to hydrate and to incorporate cations (which were formed at active sites) into the passive film. By this self-repair mechanism the bound water would inhibit the breakdown of passivity due to chloride ions and it was suggested that chromium enhanced the retention of the bound water [132,133]. The quantity of bound water in the film was found to be potential dependant as at potentials negative of the pitting potential[a] the film was found to contain larger quantities of bound water than those films formed at potentials positive to E_{pit}. This is consistent with the suggestion that bound water inhibits chloride induced pitting. Nielsen and Rhodin showed that the most protective oxide films contained up to 30% bound water [134].

The protective nature of the passive films on Fe-Cr alloys is attributed to hydrated chromium oxyhydroxides (particularly when the weight percentage of chromium in the base alloy is greater than 12.5% [124]). Olefjord, using ESCA, showed that the Cr^{3+} content of the passive film increases with passivation time, with the initial film formed having a high iron content [125,135,136]. Film growth kinetic studies have shown that thickness and structural changes of the passive films on ferritic steels are a direct result of increasing the chromium content of the alloy, thus promoting a more protective structure in a thinner film. The greater protectiveness of the film with increase in Cr% was partially attributed to a gradual change from a crystalline to an amorphous structure as Cr% increases [137]. Investigating the species within the passive film of a Fe19Cr9Ni2.5Mo alloy in 0.1M HCl polarised at a passivating potential, Lu and Clayton reported the presence of Cr_2O_3, CrOOH or $Cr(OH)_3$, CrO_3 and CrO_4^{2-} [138].

Regarding the structure of the oxides within the passive film, an *in situ* x-ray absorption spectroscopy (with fluorescence yield detection) technique has been used to investigate the passive film on Fe and Fe-Cr substrates in borate buffer solution (pH 8.4) [139]. It was found that the film formed on iron consists of FeO_6 octahedra linked together by edges to form what are probably sheets or chains. When iron is alloyed with chromium, it was found that the film became more disordered and the distance between neighbouring iron atoms increased slightly. It was also found that the Cr was incorporated into the passive layer as a phase essentially identical to $Cr(OH)_3$ i.e. CrO_6 octahedra linked by hydrogen bonds into an amorphous phase. The corrosion resistance that chromium imparts to the alloy was attributed to this phase.

It has been well established that with stainless steels iron dissolves preferentially in the active and passive regions [140-144] and that chromium is enriched in the passive film [11,115,140-149], but there is some disagreement as to whether it is enriched in the inner (i.e. close to the alloy / film interface) [115,145,146] or the outer [11,142,143,147-149] region of the passive film. Ramasubramanian *et al.*, using AES for films formed on 316L stainless steel in borate buffer solutions, have shown that at potentials negative to 0.0V (vs. SCE) the film is predominantly chromium oxide. At potentials positive to 0.0V an outer, iron rich oxide film forms, particularly as the potential is made more positive and the passive film thickness increases [145].

---

[a] E_{pit}, or the pitting potential, is defined as the critical potential above which chloride induced pitting may commence.

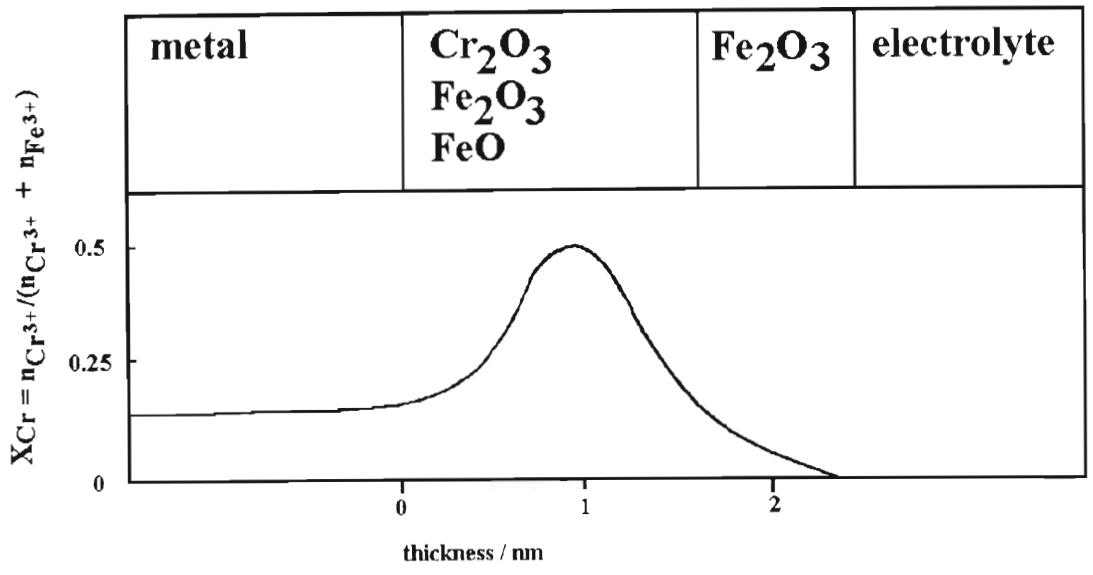

Fig. 3.7: Schematic phase diagram and typical depth profile of an electrochemically formed passive layer on Fe-Cr alloys [146].

Calinski and Strehblow, using ISS on Fe-Cr alloys in 0.5M H_2SO_4, have also found chromium to be enriched in the inner layer, and from their results they have generated the schematic in fig. 3.7 which shows the change in the fraction of Cr^{3+} ions (over the sum of Cr^{3+} + Fe^{3+} ions) in the passive layer with distance [146]. Clayton *et al.* have also found Cr enriched in the inner layer (as Cr_2O_3), using variable angle XPS on 304 stainless steel in 0.5M H_2SO_4, from which they have developed their bipolar model (*cf* page 41) [115].

On Cr enrichment in the outer film, Kirchheim *et al.* have used XPS on films formed on Fe-Cr alloys in 0.5M H_2SO_4 and have found Cr enrichment in the outer region of the passive film [11]. In particular, the outermost 0.1nm of the film was usually most highly enriched in Cr, and also in OH^-, leading to the conclusion that the Cr at the film / solution interface was in the form $Cr(OH)_3$. They also suggest that the mobility of Cr in the film is less than that of Fe. A film was also produced in the secondary passive region (1.5V vs. SHE) and XPS analysis thereof showed that the Cr concentration in the outermost part of the film (the 0.1nm closest to the electrolyte) was reduced by as much as 20% compared to the film produced in the passive region. Also the average Cr concentration in the secondary passive film (for Fe10Cr) was 37% compared to 52% for the passive film. They attribute these results to the preferential dissolution of Chromium as CrO_4^{2-} in the secondary "passive" (transpassive) region [11]. Their conclusions are supported by the results of Strehblow *et al.*, who found that in the transition from the passive to the transpassive region the thickness of the film is decreased by an amount equivalent to about one layer of Cr oxide [13].

Burstein and Marshall attribute their finding of Cr enrichment in the outer region of the passive film (on 304L stainless steel in perchloric acid solutions) to a constructive preferential dissolution of the iron component of the film (they found no direct dissolution from the alloy surface). They measured a diffusion coefficient for the non steady-state diffusion of iron ions through the film at 5×10^{-14} cm^2/s [142]. The diffusion of the iron ions through the oxide lattice is the rate controlling step, and the onset of dissolution of iron ions was suggested to happen at a particular electric field which depends on pH. The effect of Mo in the alloy (a 316L stainless steel) was considered to be the raising of the electric field (compared to

304L) and therefore the onset of constructive dissolution of Fe (and therefore also the onset of passivity) occurs at potentials more negative than those for 304L [143].

For a given bulk alloy chromium content, the addition of molybdenum to the alloy results in higher concentrations of chromium being found in the passive film. This synergistic phenomenon of chromium and molybdenum has been well documented [150,151,152] but is not understood. Contradictory findings as to the absence [153-159] or presence [12,106,125,136,160] of molybdenum oxides within the film have been reported. The concentration and chemical state of molybdenum is potential dependant [125,152,157,161-163]. Under non-potentiostat conditions, at E_{corr} and at potentials in the active region, selective dissolution of iron results in an enrichment of metallic chromium and molybdenum in the outermost alloy layers [125,164,165].

The thickness of the passive film on iron based stainless steels has been studied by several investigators and has been found to be dependant on the potential of formation [102,125,133,152,157,166-169]. Generally, the thickness increases with increase of potential within the passive region. Disagreement exists as to whether increasing the molybdenum content of the alloy increases [102] the thickness of the passive film or not [125].

It appears that the effect of molybdenum is not to be found in its enrichment in the passive film, but rather in changing the kinetics of anodic dissolution and passive film formation of the alloys. Olefjord suggested that the accumulation of the alloying elements, Cr and Mo, in the outermost layers of the alloy during the active dissolution that precedes passivation results in a decrease of the dissolution rate, thus provoking the formation of a passive film [162,165]. In addition Yaniv suggests that molybdenum improves the quality of the bonding at the metal / film interface, thus creating a barrier type oxide [155].

Within the literature, agreement exists as to the presence of anions of the supporting electrolyte within the passive film [170,171,172]. AES analysis of Fe and Fe-Cr alloys in 3M H_2SO_4 revealed that the sulphur concentration was at a maximum at the metal / oxide interface suggesting that sulphate anions penetrate through the passive film [171].

The kinetics of passive film formation may be controlled by electronic or ionic conduction, surface reactions or a combination of all three. Hence the electronic properties of passive films are a significant factor in determining the mechanism of film formation and breakdown. The evolution of oxygen on iron electrodes at high positive potentials, instead of continued film growth, has led workers to suggest that the passive film on iron is an electronic conductor or at least a semiconductor. Delnick and Hackerman [4] and Schmickler [5] both found n-type semiconducting properties for passivated iron surfaces. In contradiction to these results, others consider the passive film, or part thereof, to be an insulator [6,7]. More recently, Paola, using EIS has found n-type semiconducting properties on Fe-Cr-Ni-Mo alloys [173]. Cahan and Chen, in an attempt to reconcile these differences, sought to show that the passive film on iron changes from an insulator to a semiconductor as defects are added or removed [174]. However, the experimental basis for their model has been questioned. Gluszek *et al.*, whilst investigating the electronic properties of passive films reported that increasing the chromium content of the film (with respect to iron) makes the film a p-type semiconductor [175], and Bianchi *et al.* have shown that a p-type semiconducting film makes stainless steels immune to pitting [176].

3.4. Summary of previous work in the transpassive region

There is very little in the literature directly concerning secondary passivity of Fe-Cr alloys. The facts from the relevant publications (outside of those produced out of our UND laboratory) may be summarised as follows:

- Macdonald has explained the secondary passive region in terms of the PDM where the transpassive oxidation of Cr(III) to Cr(VI) (*cf* equation 3.5, page 45) results in an excess of cation vacancies which condense at the alloy / film interface causing breakdown of the passive (barrier) film. The barrier layer does not reform due to the resulting rampant dissolution from the bare alloy surface, but precipitation of a porous iron oxide and or iron salt film does occur. This results in the less protective secondary passivation [12].
- Kirchheim *et al.* consider the breakdown of the passive film to be due to oxidation of Cr_2O_3 to CrO_4^{2-} and have found a decrease in the Cr content in the outermost region of the anodic film in the secondary passive region, compared to the Cr content in the outermost region of the anodic film in the passive region. They conclude that CrO_4^{2-} dissolves preferentially in the transpassive region [11]. Their results are supported by Strehblow *et al.*, who found that the decrease in the thickness of the anodic film over the passive - transpassive transition corresponded to about one monolayer of chromium oxide [13]. Clough and Pinchback have also noted an increase in the Fe concentration of the anodic film on Fe-Ni-Cr alloys at transpassive potentials compared to the concentration of Fe at passive potentials [177].
- Finally, a series of polarisation curves, showing the effect of Cr% on secondary passivity has been published and is shown in fig. 3.8 [10]. The effect of increasing Cr% on secondary passivity is clearly shown to be detrimental, with the Fe-Cr alloy behaving like pure Cr at Cr% $\geq$ 35. This is further evidence towards the suggestion that the dissolution of Cr_2O_3 as CrO_4^{2-} is a primary cause of passive film breakdown. As a result of this work the initial passivity was called chromium passivity and the secondary passivity has been called iron passivity [178].

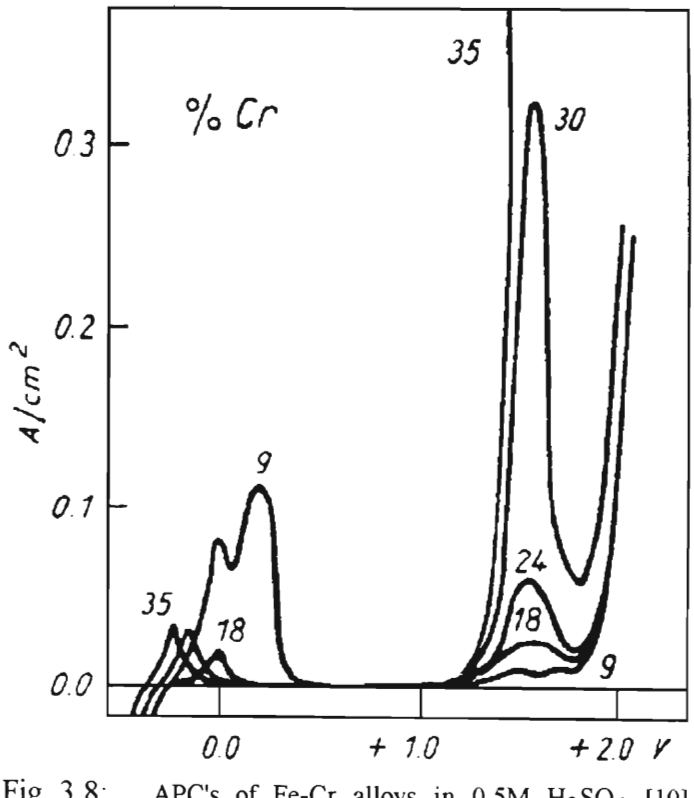

Fig. 3.8: APC's of Fe-Cr alloys in 0.5M H_2SO_4 [10]. Potential is versus NHE.

3.4.1. Peak A

Only one group (outside of those working in the UND laboratory) have performed a systematic voltammetric analysis on a transpassive peak [15,87]. This was, however, for a mild steel in basic carbonate solutions, but the qualitative similarity between their voltammograms and CV's generated in acetate buffer for Fe18Cr is significant. They attribute their transpassive peak to an oxidation of Fe(III) to Fe(VI) where the Fe(VI) is stabilised by bicarbonate ions.

Fig. 3.9 shows a voltammogram at pH 3.8 of peak A and the relevant peaks that have been obtained in voltammetric analyses in this laboratory. The peaks have been labelled according to the system of Graham [1] and McCrindle [3].

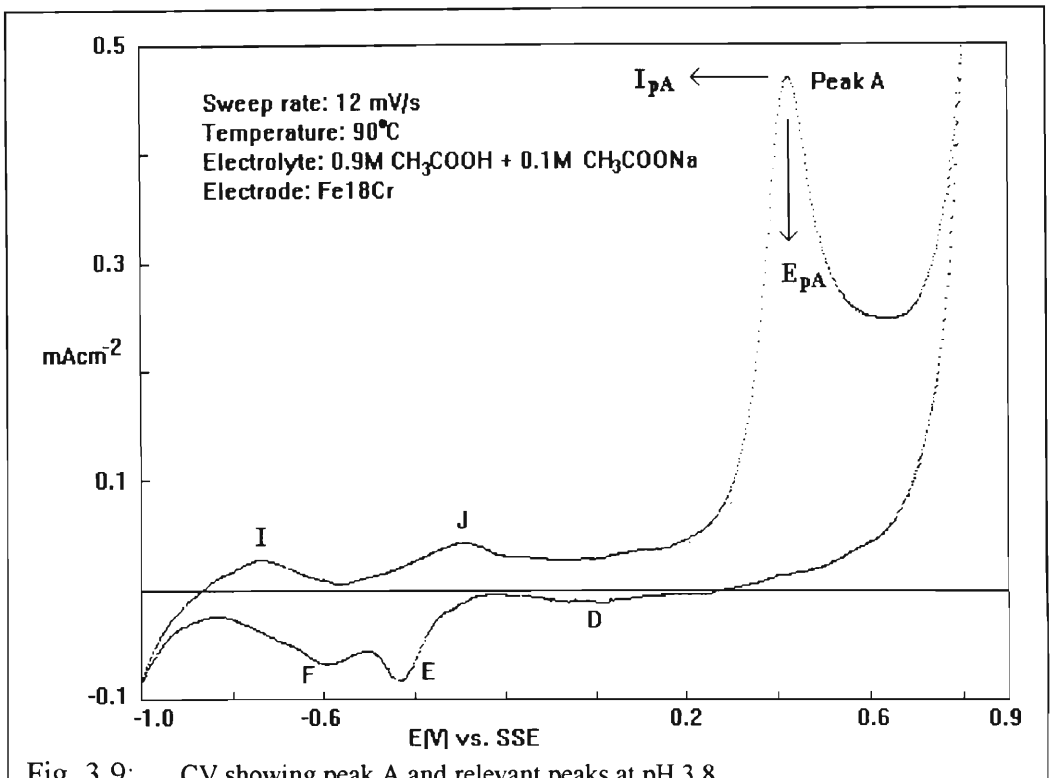

Fig. 3.9: CV showing peak A and relevant peaks at pH 3.8.

A summary of Graham's findings and conclusions from her work on peak A and related peaks in 0.1M H_2SO_4 (on Fe18Cr and Fe18Cr2Mo (444)) follows [1,52]:

- Peak A is dependant on the electrolyte composition. It is only observed if oxidation of the electrode occurs. For example, peak A is not observed in solutions containing only Na_2SO_4 as the electrolyte - this is not sufficiently aggressive to cause oxidation. It was suggested that a minimum H^+ concentration was required for peak A to occur. It was, however, noted that increasing the SO_4^{2-} concentration enhanced secondary passivity, especially in the presence of Cl^-.
- The CV's for Fe18Cr and Fe18Cr2Mo are qualitatively the same.
- The reactions contributing to peak A are irreversible (reduction peaks are roughly an order of magnitude smaller than peak A and are at potentials very negative to that of peak A (*cf* fig.3.9)).
- In the presence of a high Cl^- concentration multiple oxidation peaks are observed, indicating that more than one oxidation process is responsible for peak A.

- The potential at which peak A occurs, E_{pA}, is dependant on the sweep rate. At 25°C (and for 1 - 4000mV/s) the peak height, I_{pA}, is linearly dependant on the root of the sweep rate, $\nu^{1/2}$, (as were the peak heights of peaks D and E) suggesting that the processes occurring at peak A at 25°C in 0.1M H_2SO_4 are diffusion controlled.
- Peak A is dependant on the lower potential limit of the CV. Excluding the reduction peak E from the voltammogram (by moving the negative potential limit positive of the peak potential of peak E) results in a 50% decrease in the magnitude of peak A (for ν = 100mV/s). If peak F is excluded then E_{pA} moves positively and peak E becomes less well defined.
- Only ~20% of the oxidation products of peak A are reduced on the reverse sweep (at peaks D, E and F), thus ~80% of peak A's reaction products either diffuse into solution or are electroinactive.
- Addition of Fe^{2+} to the electrolyte significantly increased peak I_{pA}, while Fe^{3+} additions had very little effect on I_{pA}, but increased E_{pA}.
- From RRDE studies the oxidation of Fe(II) to Fe(III) was shown to occur at the potential of peak A and the reduction of Fe(III) to Fe(II) was shown to occur in the potential region of peak E.
- RRDE studies did not detect chromium species at peak A potentials. Chromium species have been previously detected, but only in the more acidic 1M H_2SO_4 solution [179].
- In 0.1M H_2SO_4 , I_{pA} increases logarithmically with temperature over the temperature range 5 - 80°C, for 5 - 1000mV/s.
- Using coulombic relationships, it was found that the reactions responsible for peaks D and E are predominantly solid state reactions, while reactions involving solution species are responsible for peak F and partly for peak A. The ratio of the charge under peak A (for 444) to the charge in the whole reduction region is almost always greater than one. This ratio increases with decrease in sweep rate and increase in acid concentration.
- The effect of rotating (at 25°C) the electrode on peak A was small, and I_{pA} decreased to a limiting value (at ~200rad/s) as the rotation rate increased. The greatest effect was between 0 and 100 rad/s. The peak height of peak F also decreased with increase in rotation rate and, but peaks D and E were found to be independent of rotation rate. The independence of peaks D and E to rotation rate could mean one, or a combination of, three things:

  (1) Ambrose *et al.* proposed that this independence indicates that the diffusion of species in solution is not the rate determining step for the reaction [180].

  (2) Armstrong uses the independence of peak height to rotation rate as a criterion for the solid state mechanism [19].

  (3) It could mean that the process(es) contributing to these peaks are activation controlled.
- Estimates for the diffusion coefficients of the species involved in reactions responsible for peaks A, D, and E were generated using the equation describing the peak height of a voltammetric peak for an irreversible, diffusion controlled reaction [28]. H^+ was assumed to be the electroactive species. The diffusion coefficient estimates were generated for a number of possibilities, where the transfer coefficient was varied between 0.2 and 0.8 and the number of electrons involved in the overall process was varied between 1 and 6. The range of values of diffusion coefficients found for the peaks (for 444 in 0.1M H_2SO_4 at 25°C) were as follows:

(1) For peak A, 2.5×10^{-5} to 1.8×10^{-7} cm^2/s.

(2) For peak D, 1.0×10^{-7} to 7.1×10^{-10} cm^2/s.

(3) for peak E, 1.2×10^{-7} to 8.2×10^{-10} cm^2/s.

From these and previous results it was concluded that while peaks D and E are due to solid state surface reactions, peak A is due - at least in part - to dissolution reactions of the passive film. The value of diffusion coefficients for diffusion of species in aqueous solutions is of the order of 10^{-5} cm^2/s, whereas the value for a solid state diffusion process is generally not larger than 10^{-8} cm^2/s. It was found that in a solution of lower pH (0.1M $NaHSO_4$), the values of the diffusion coefficients were consistently lower.

McCrindle, in his investigation of 444 in a range of acidic aqueous media made similar observations to those of Graham and also noted the following [3]:

- In acetate buffer solutions (pH $\geq$ 2.45) I_{pA} was independent of rotation rate. In acids of lower pH, he made the same observation as Graham - as the rotation rate increased, I_{pA} decreased to a constant minimum. The decrease in I_{pA}, however, was more marked as acid strength increased.
- Over the range of acids used (pH 0 - 4) and at 25°C, additions of Cr(III) and Cr(VI) to the solutions had no effect on the CV's.
- An experiment was performed where the electrode was held at each of the peak potentials until a steady state was achieved. The electrode was then rotated, and if the current then increased, it would be an indication that ions in solution were contributing to that peak's processes. This was found to be the case for peaks A and F, but not for D and E.
- McCrindle also noted that at lower pH's greater dissolution of the anodic film was likely to occur by reactions such as

$$Fe_2O_3 + 6H^+ \rightarrow 2Fe^{3+} + 3H_2O$$

3.4.2. The rising transient

The rising transient response of Fe18Cr in sulphuric acid solutions was originally discovered by Graham [50,51]. The rising transient only occurs when stepping to transpassive and in particular, peak A and post peak A potentials. The initial potential, E_1', was usually -1.0V vs. SSE. Graham has also reported that I_{max} increases linearly and $\log(t_{max})$ decreases linearly with increase in potential (provided E_1' is constant) as long as the potential to which the electrode is stepped, E_2', is in the transpassive region. It was also noted that the rising transient was only found when the corresponding experimental conditions (electrolyte and electrode) gave a peak A response in the voltammogram. If peak A did not occur in the voltammogram, then neither did the rising transient in the corresponding chronoamperogram. Fig. 3.10 shows the effect of the size of the potential step on the rising transient. It was also found that, for 20 - 80°C, $\log(I_{max})$ increased linearly with temperature.

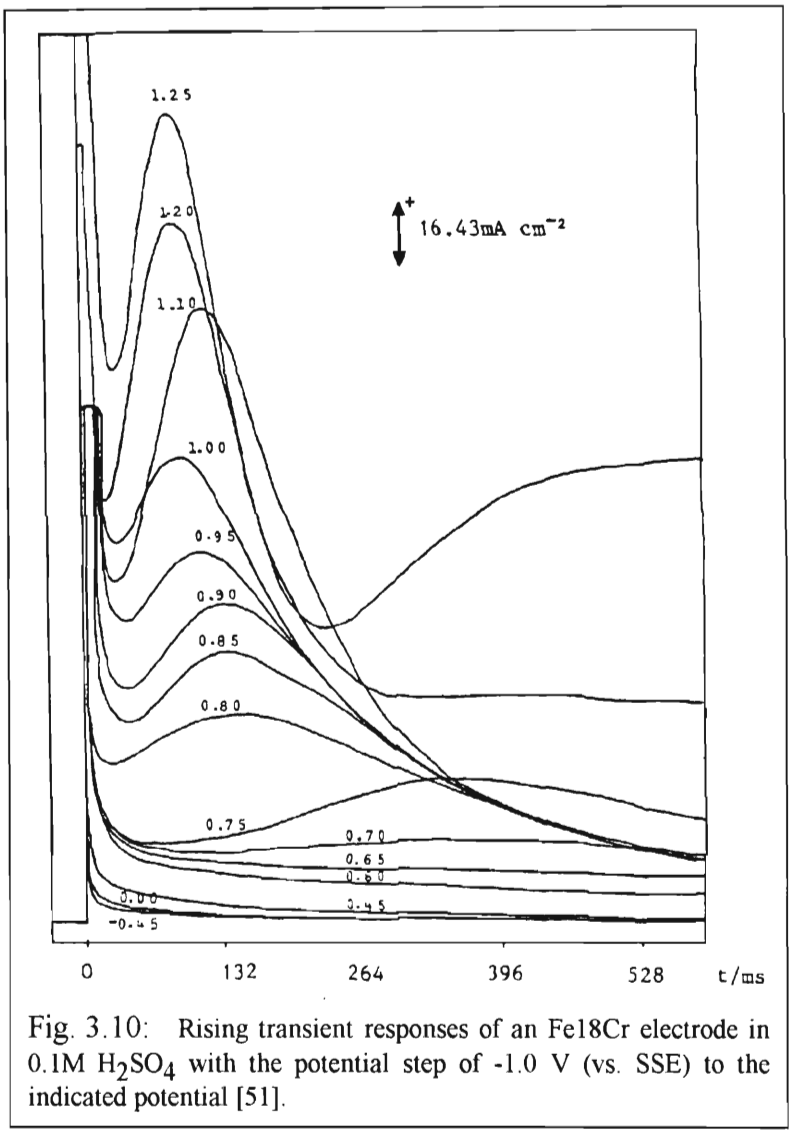

Fig. 3.10: Rising transient responses of an Fe18Cr electrode in 0.1M H_2SO_4 with the potential step of -1.0 V (vs. SSE) to the indicated potential [51].

While rising transients are obtained on Fe-Cr alloys at transpassive potentials, they are found on Fe at passive potentials. The effect of rotation to on the Fe rising transient was to increase I_{max} (with increase in rotation rate) and also to increase I_{lev}, until - at a certain limiting rotation rate - the current density did not decrease again after reaching I_{max} i.e. at a certain maximum limiting rotation rate, $I_{max} = I_{lev}$.

The observation of the above phenomena and the comparison of normalised plots of experimental with theoretical (*cf* section 2.4.1) rising transients has led Graham to propose a qualitative scheme in explanation of the rising transient on Fe and Fe-Cr alloys in acidic media [52]. The following is a summary of that scheme:

Inhomogeneities and surface defects present on the electrode surface result in active sites which will corrode preferentially or at an accelerated rate with respect to the rest of the electrode surface. These sites are analogous to the nucleation sites in electrocrystallisation studies. Imposing a potential step to a suitable potential (transpassive region) on a Fe18Cr based electrode results in transpassive dissolution predominantly at these sites. This results in a localised surface roughening and increase in the electrode

surface area with corresponding increase in current - as is observed subsequent to the decay of the charging current (i.e. after t_{min}). It was assumed that preferential dissolution of Fe[a] occurs transpassively. This has been confirmed in the transpassive region by atomic absorption analysis of the electrolyte near to stationary electrodes (Fe18Cr based) [179]. Accumulation of Fe^{2+} [181,182] (and also possibly Fe^{3+}) will occur in the diffusion layer next to the electrode and in the vicinity of the active sites. This accumulation results in a supersaturation of the dissolving species. Once a certain critical level of supersaturation is reached, at time t_{sat}, where $t_{sat} < t_{max}$, deposition of an anodic surface film will occur. Graham suggests that this precipitation occurs on the active sites, thereby impeding dissolution of the electrode and reducing the available surface area for further dissolution. This results in a decrease in the current which is manifested by the appearance of the maximum I_{max} in the transient.

Once the initial active sites have been passivated, continued deposition and or growth of the surface film on these sites will continue for as long as the required level of supersaturation is maintained. Such continued growth will further reduce the active surface area as manifested by the decrease in current at $t > t_{max}$. As the oxide is porous, dissolution continues through the pores of the oxide. A point is reached at which the rate of dissolution of iron species through the pores is such that a steady state is attained as indicated by the final steady current, I_{lev}. This scheme accounts for Graham's observation (by SEM) that at t_{max} the electrode is not covered entirely by nucleation centres, contrary to that predicted by nucleation studies [54].

The influence of the rotation rate on Fe (I_{max} increases with ω, $I_{lev} = I_{max}$ at high ω) can now be explained. As the rotation rate increases, I_{max} and t_{max} increase due to the longer time required to reach the necessary degree of supersaturation which in turn provides more time for the iron to dissolve prior to the passivation of the active sites. Also, at $t > t_{max}$, and for $\omega > 100$ rad/s, current does not decrease which indicates that the required level of supersaturation cannot be maintained at the electrode surface therefore preventing any further deposition and growth of the surface film.

The above analysis also predicts that as the electrode is stepped to more positive potentials in the transpassive region, supersaturation at the electrode will occur more quickly, due to the enhanced transpassive dissolution of the alloy. This will result in an increase in I_{max} and a decrease in t_{max}. For an increase in temperature, the scheme would predict an increase in the rate of dissolution with the result that I_{max} would increase and t_{max} would decrease with increase in temperature. This was observed experimentally by Graham who found that Arrhenius plots showed a decrease in activation energy (for nucleation of the surface film) with increasing potential step size.

As an alloy becomes more corrosion resistant (e.g. Fe18Cr2Mo instead of Fe18Cr), the transpassive dissolution would be impeded compared to a less corrosion resistant alloy. Supersaturation would therefore take longer and t_{max} increases while I_{max} decreases. Experimental results verified this prediction. The quantitative model proposed in chapter 8 is partially based on Graham's above scheme.

---

a This refers to dissolution from the electrode, rather than dissolution from the anodic film. This would therefore not contradict authors who maintain that Cr species dissolve preferentially from the anodic film in the transpassive region [11,13,177].

CHAPTER 4

4. EXPERIMENTAL

4.1. Samples

The alloys used in this investigation, along with their chemical compositions, are listed in table 4.1.

Alloy	Cr	Mo	V	W	C	Si	Mn	Ni	Nb	P	S	Al
Fe18Cr	18.29	0.011	0.009	N.M.	0.03	0.061	0.023	0.02	-	0.009	0.008	0.026
444	17.39	1.78	0.081	N.M.	0.003	0.17	0.23	0.27	0.28	N.M.	N.M.	N.M.

Table 4.1: The chemical composition of alloys (weight %). N.M. means not measured. "-" means unfound. The balance in both alloys is Fe.

The Fe18Cr alloy was prepared at ISCOR by induction melting (at 1600°C) of the raw materials in an argon atmosphere and then centrifugally casting the alloy in a copper mould. The alloy was then heat treated by placing it in an aluminium oxide crucible and keeping it at 800°C for two hours, after which it was cooled in air. After removal of the oxide the alloy was then cold rolled (deformation approximately 10%).

The 444 alloy was supplied by the Department of Metallurgy, University of the Witwatersrand, who in turn had obtained it from Van Leer & Co. Ltd., (manufactured by the Nippon Steel Company, Japan) in the form of a rolled sheet 0.45mm thick. Since it was a commercial alloy, no preparation details were available. A 99.99% pure Fe rod was used in the preparation of Fe disc electrodes.

4.2. Chemicals

All chemicals were of analytical reagent (AR) quality. Millipore water (18 MΩ cm) was used to make up the solutions. This was obtained from a Milli - Q system, where tap water is passed through a reverse osmosis membrane, an activated carbon cartridge to remove organic impurities, through two ion exchange cartridges to remove dissolved inorganic impurities and finally through a polymeric membrane filter which removes all particles longer than 0.2 μm. Table 4.2 gives the compositions and pH's (at 25°C) of the main solutions that were used.

Solution	pH at 25°C
0.290M $HClO_4$	0.54
0.0590M H_2SO_4	0.93
0.0581M $HClO_4$	1.24
0.020M H_2SO_4 + 0.94M CH_3COOH	1.40
8.71×10^{-3} M $HClO_4$	2.06
1.00M CH_3COOH	2.40
0.90M CH_3COOH + 0.10M CH_3COONa	3.80

Table 4.2: Table of the main solutions used and their pH's at 25°C.

The pH of each solution was checked in the following manner:

- For solutions which, from a simple calculation based on the analytical acid concentration, had a pH of 2 or less, a sample was taken and diluted by a known volume of millipore water such that the calculated pH of the sample should have been exactly 2.0. The pH of the diluted sample was then checked with a pH meter which had been calibrated with pH 2.0 and pH 4.0 buffer solutions. From the discrepancy between the measured pH and the calculated pH, and from the dilution factor, the pH of the original solution could be calculated. Also, for perchloric and sulphuric acid solutions, this method was used to calculate the analytical concentrations of these acids, based on the assumption that all the protons dissociated from the acid in solution. This assumption may not be entirely valid for sulphuric acid, as the second proton does not dissociate entirely ($pK_a \cong 2$). However, this method was used consistently, with the aim that the concentration of the acid that was given should exactly reflect the pH of the solution, as pH was a primary variable in this investigation. The reason that this procedure was used is because pH electrodes tend to be inaccurate at pH's < 2 and are not recommended for pH's < 1. The solutions of higher pH were therefore diluted to a pH where measurement could be done accurately with a pH electrode.
- For solutions with a rough pH between 2 and 4, a sample was measured directly with the calibrated pH meter. For acetate solutions the measured pH's agreed with the pH calculated with the pK_a of acetic acid.

4.3. The cell

A water-jacketed glass cell was used (fig. 4.1) and was connected to a water bath by means of the two horizontal arms on the jacket. This enabled the temperature of the solution to be controlled to ± 0.1°C between 25 and 90°C inclusive. The temperature of the laboratory was maintained at 20°C by efficient air conditioning.

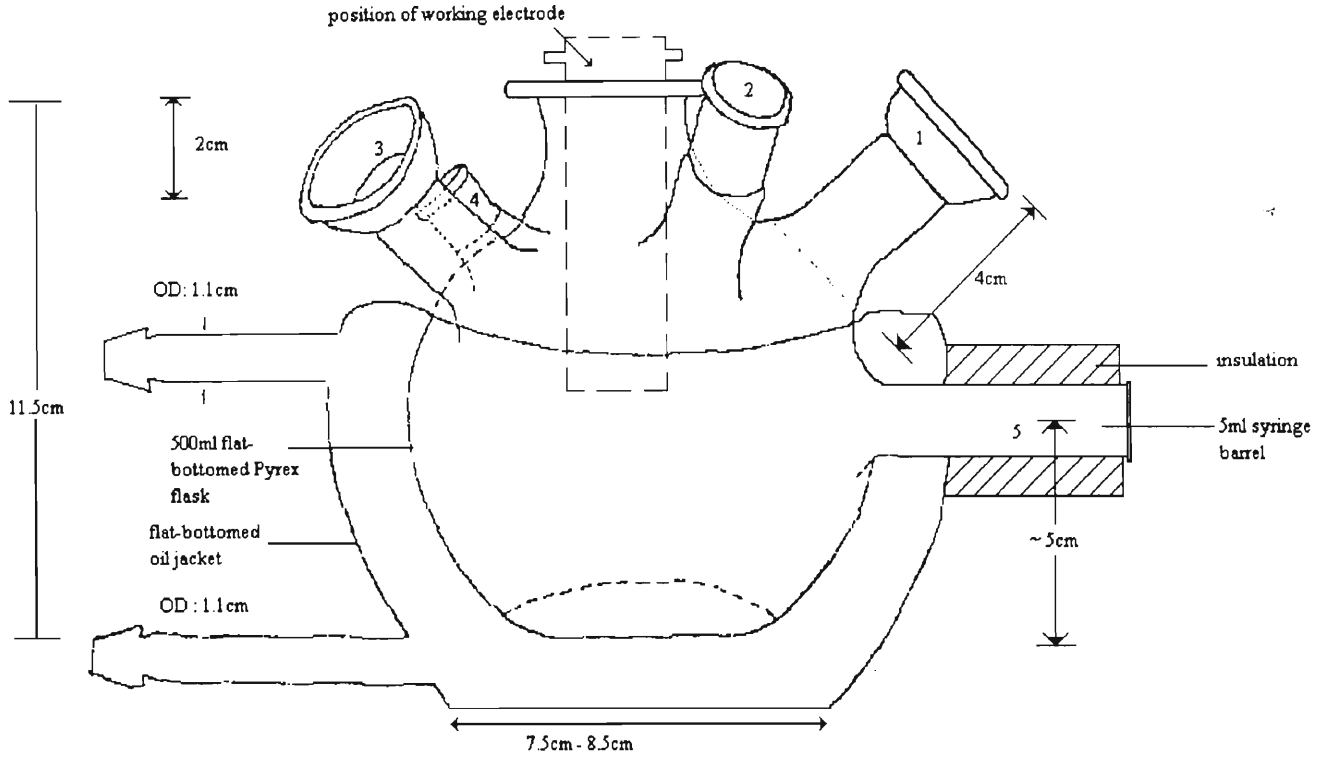

Fig. 4.1: Diagram of the water-jacketed glass cell that was used to control the temperature of solutions.

The items that were inserted into each of the five arms of the cell were as follows :

1. Luggin capillary and reference electrode assembly (fig. 4.2). A mercurous sulphate reference electrode (SSE) was used. The SSE has a potential of +642 mV against the normal hydrogen electrode and a potential of +398 mV against the saturated calomel electrode (SCE). The reference electrode was placed in the reservoir above the luggin capillary. The electrolyte was then drawn up into the reservoir by applying a water pump vacuum to the side arm. This prevented the formation of air bubbles in the capillary. The reference electrode assembly was then connected to the cell by a ball and socket joint and held in position with retaining clamps. This, and the ground glass barrel in which the luggin capillary could be moved up and down (fig. 4.2) facilitated positioning of the luggin capillary tip. The luggin tip was placed directly under the working electrode at a distance of 0.5 - 2.0 mm, depending on the diameter of the luggin tip.
2. A nitrogen bubbler, attached to an oil trap, which was used for deaeration of the solution (fig. 4.3).
3. A counter electrode. A thick platinum wire that was wound into a helix was used.

4. Thermometer / reflux apparatus. Once the temperature of the solution had stabilised, and if the temperature of the solution was such that significant evaporation occurred, the thermometer was removed and the reflux apparatus was inserted into the arm.
5. A scratcher for scratching the electrode surface (only used in the scratch experiment). The scratcher consisted of a diamond set in an annealed brass rod (fig. 4.4) and was made by Graham [183]. The end of the scratcher nearest the diamond was bent such that the culet of the diamond was perpendicular to the electrode surface. The rod was glued (PATTEX super glue) into a glass syringe plunger, and all of the remaining exposed rod was covered in epoxy resin.

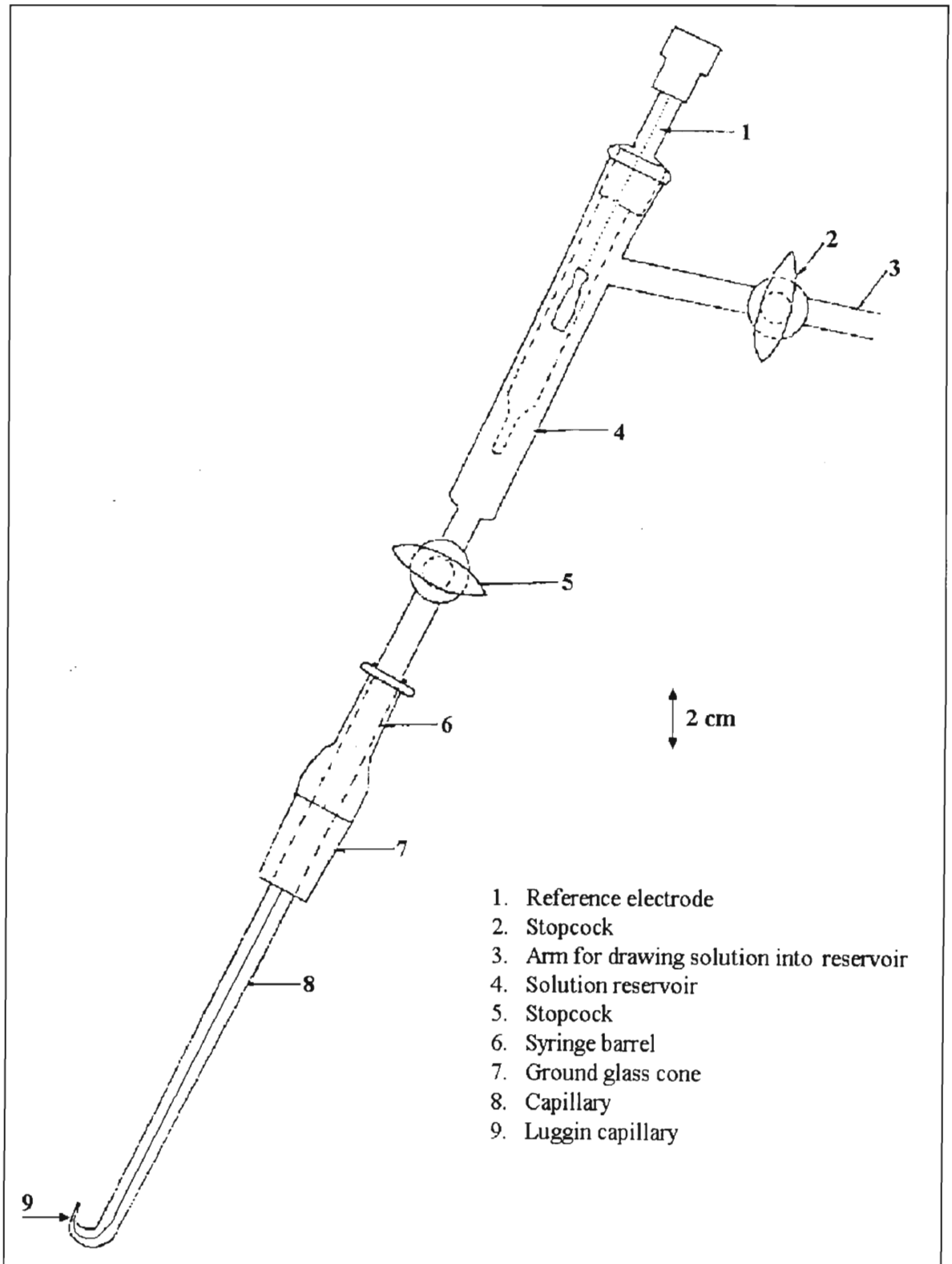

Fig. 4.2 : Diagram of the assembled reference electrode apparatus [183].

When any of the arms were not in use, they were securely stoppered by means of a ground glass plunger, or a rubber bung encased in gladwrap, in order to prevent ingress of atmospheric oxygen or egress of vapourised solution components.

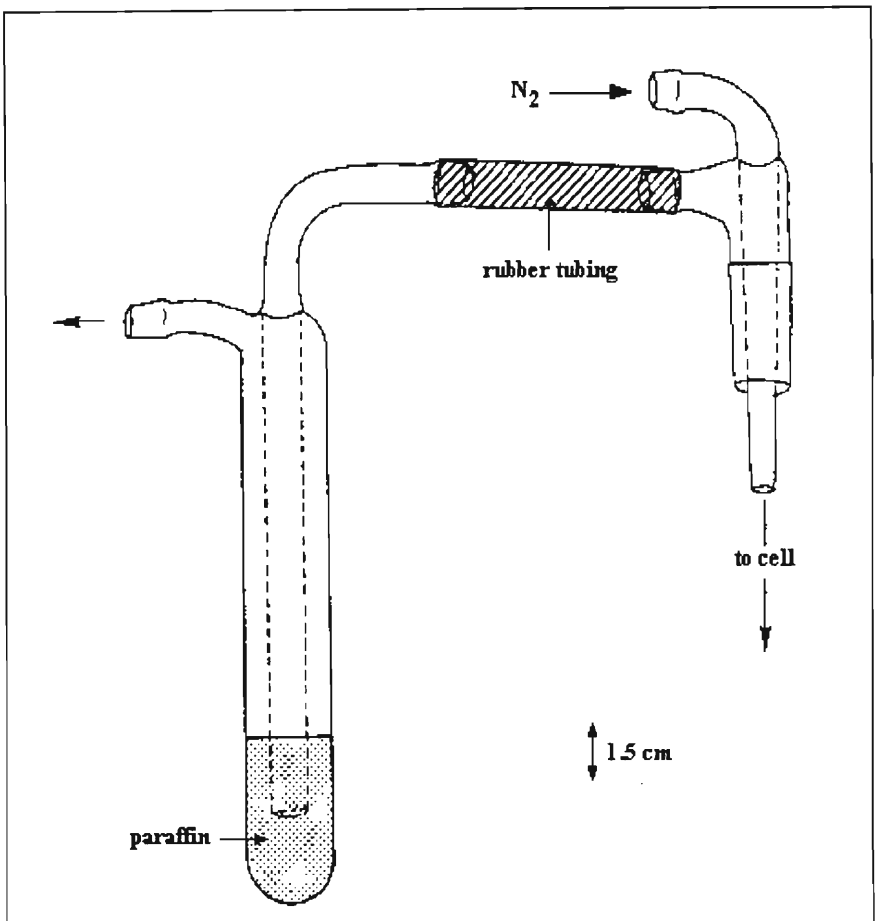

Fig. 4.3: Diagram of an assembled nitrogen bubbler apparatus [183].

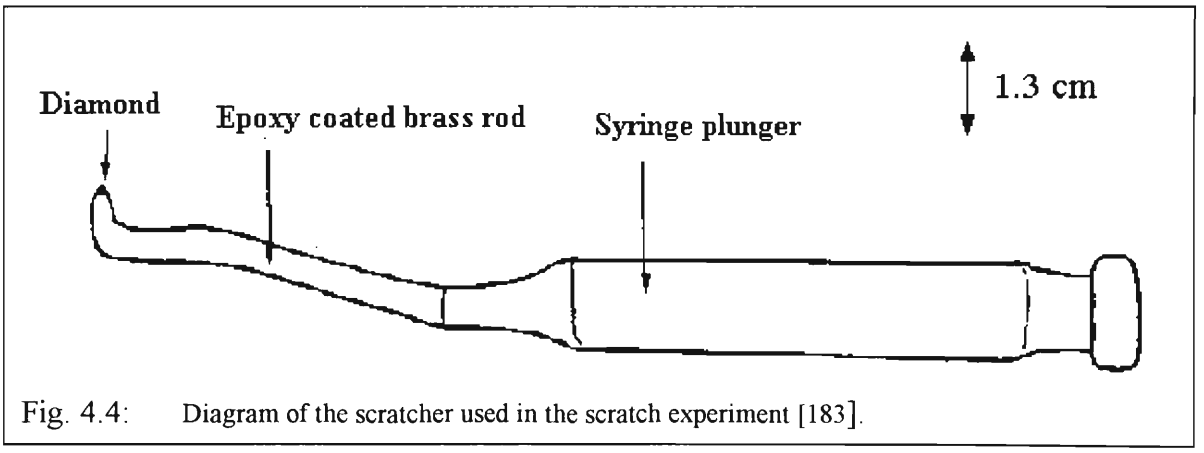

Fig. 4.4: Diagram of the scratcher used in the scratch experiment [183].

4.4. Construction of the working electrode

Fig. 4.5 shows a diagram of an assembled working electrode. A new method of construction has been developed for disk electrodes which minimises the major problem in electrode construction - the formation of bubbles in the resin at the resin-electrode contact on the surface of the electrode. An alloy strip of area ranging from 0.08 to 0.4 cm^2 was ultrasonically cleaned in ethanol and then millipore water before being weakly joined to about 8cm of insulated wire using a silver epoxy (Emerson and Cuming, Belguim) which provided the electrical contact to the electrode.

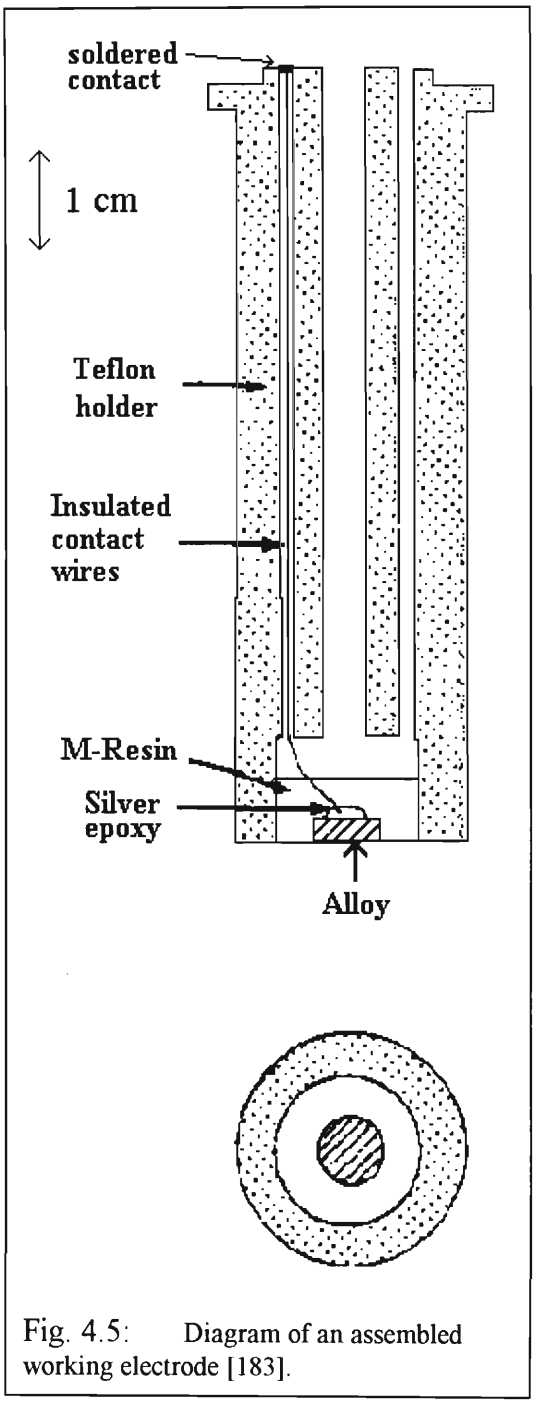

Fig. 4.5: Diagram of an assembled working electrode [183].

The contact between the alloy strip and the far end of the wire was then checked with a SANWA SH-63TR-D11 Multitester. The alloy strip (with the attached insulated wire) was then secured to a double sided adhesive tape on a flat surface. A hollow cylindrical teflon mould was then pressed firmly onto the adhesive tape so that the alloy strip was centred inside it. The mould was then filled with resin (Araldite M-Resin with HY-Hardener) that had been degassed under vacuum at 40°C for five minutes. The resin was then cured in the oven at 100°C for 60 minutes.

After curing, the electrode was removed from the teflon mould and a check for bubbles between the edge of the electrode and the cured resin was performed. If bubbles were found, then the electrode was broken in the vice and the above procedure was repeated. If no bubbles were found, then the cured resin / electrode was sanded along the edges, and then inserted into a teflon holder. The mould was designed so that the resin (which adhered to the alloy strip during curing) would fit snugly inside the teflon holder. The wire attached to the alloy strip was carefully soldered to the teflon holder at its other end (*cf* "soldered contact" label in fig. 4.5) and the soldered contact was then sanded until it was flat. This was found to give the best contact with the rotating electrode unit.

The geometrical area of the exposed section of the alloy strip was found by taking a SEM picture of the strip, drawing an outline of the enlarged picture on graph paper and then counting the squares on the graph paper. Then by using the scale in the photograph, the geometric area was easily calculated. Since roughness factors are not available for Fe-Cr alloys, current densities were obtained from currents using geometric areas only.

4.5. The rotating electrode unit

Controlled rotation of the working electrode was achieved using the rotating electrode unit previously designed and constructed in this laboratory (fig. 4.6), which is a modification of a design used at MINTEK (Council for Mineral Technology). The rotation rate of the driving motor (12V DC.) was controlled by a photocell and a stroboscopic disc device (label 2 in fig. 4.6) controlling a power / amplifier controller. The range of rotation rates available were 40 to 500 rad/s (6.4 to 79.6 Hz). The motor (1) drove the central shaft of the unit (5) which terminated in an externally threaded steel flange, having two spring-loaded brass plungers (9) in a PVC insert for contact with the soldered wires from the disc (and, if desired, a ring) of the working electrode. Two wires (7) soldered to the brass plungers made contact with two silver plated slip rings on the upper part of the unit. External contact was made with the slip rings (3) through carbon-silver brushes (30% Ag, 70% C from Le Carbon, France) mounted on spring loaded brass arms which were in turn mounted on the electrode stand. Ingress of atmospheric oxygen was controlled by means of a non-rotating PVC cylinder (8) which was machined to a minimum clearance with the rotating unit and has a flange, with an O - ring seal, which rested on the flange of the glass jacketed cell.

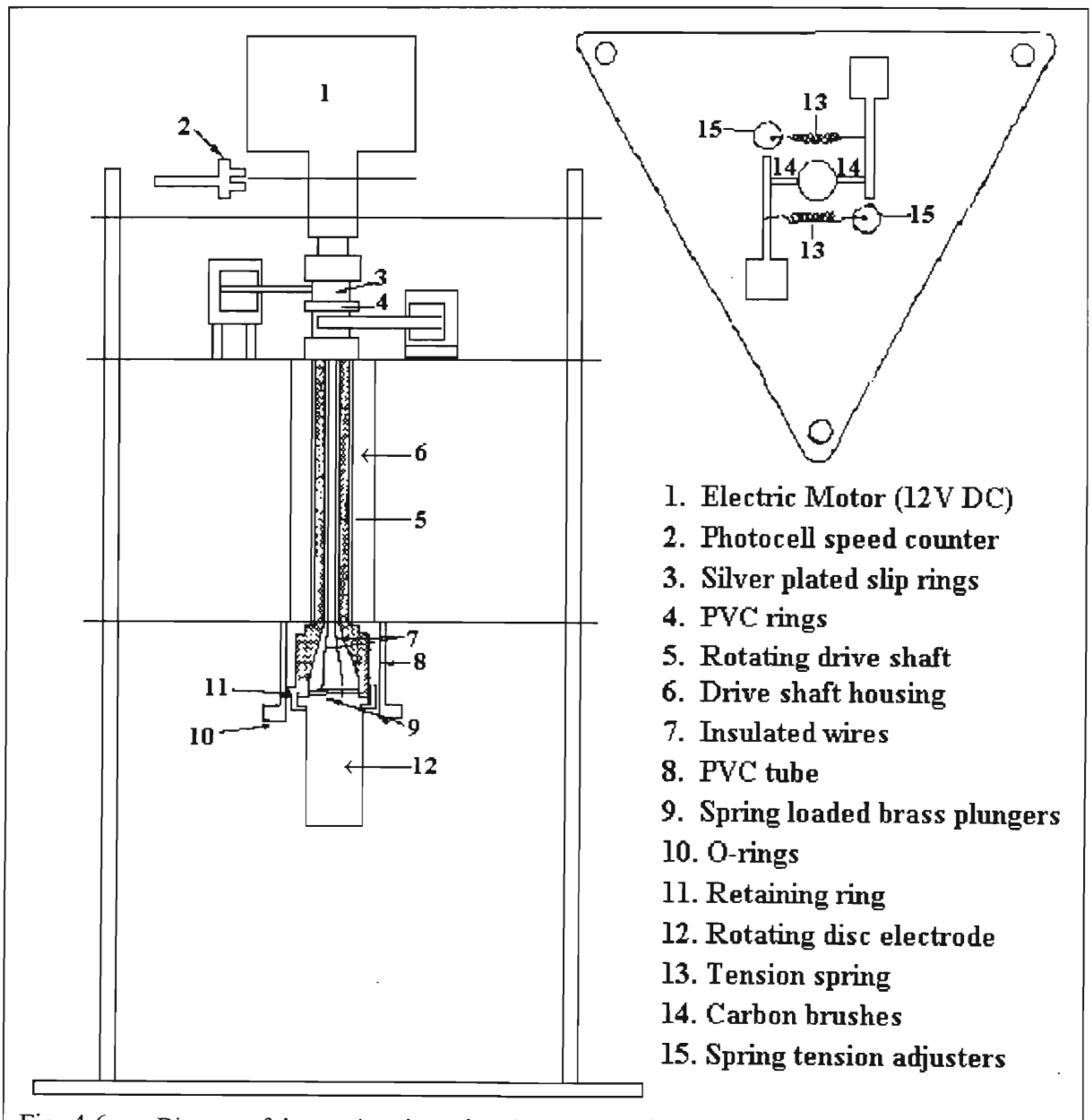

Fig. 4.6: Diagram of the rotating electrode unit, and a top view showing the contacts with the rotating drive shaft [183].

4.6. Instrumentation

A box diagram of the experimental arrangement is shown in fig. 4.7. The potential was controlled with a PAR 173 potentiostat (which was equipped with a linear and logarithmic current to voltage converter, PAR 376) and was programmed by a PAR 175 universal programmer. The reference electrode was connected to the potentiostat through a PAR 178 electrometer probe. A noise filter (PAR 178/41) was connected across the reference and counter electrodes to reduce AC pickup noise. Voltammograms were monitored as current-time and potential-time waveforms (simultaneously) on a NICOLET 3091 twin channel digital oscilloscope. A hard copy of each voltammograms was (usually) simultaneously obtained on a LLOYD PL-3 X-Y recorder. If hard copies of chronoamperograms were required they were sent from the oscilloscope to the X-Y recorder via the pen function of the oscilloscope. A program (COLLVER7.BAS, *cf* Appendix B) was written by the author to collect and store digital data from the oscilloscope via an RS-232 serial interface to a 80-386 computer. The collection program automatically assigned filenames (by incrementing a number) to data files and thus required a minimum of attention from the user between experiments. The data could then be processed and presented graphically (GRAPH.BAS - written by the author, *cf* Appendix B) on the computer screen and on a dot-matrix printer.

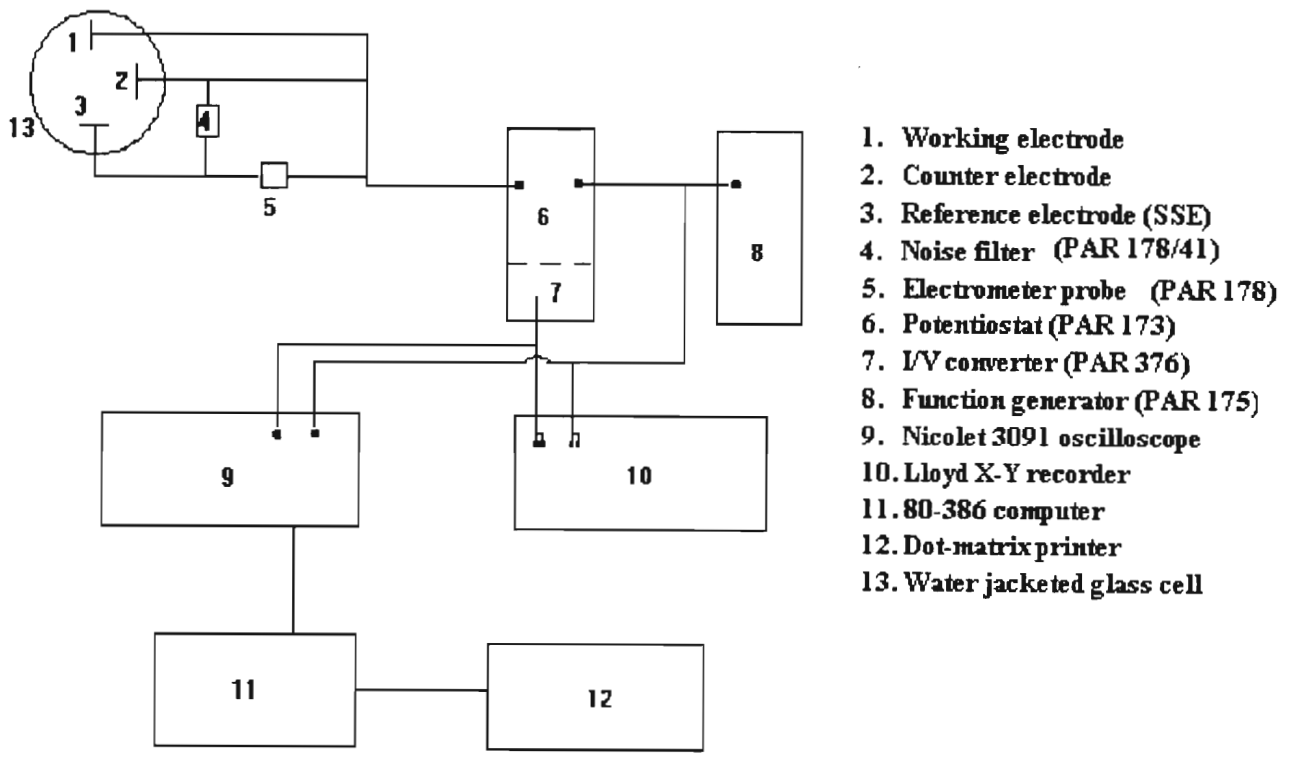

Fig. 4.7: Box diagram of the arrangement of experimental equipment and electrical connections.

4.7. Procedures for electrochemical measurements

4.7.1. Electrode pretreatment

Since electrochemical measurements can be significantly influenced by the pretreatment of the electrode [184], standard pretreatments were developed. The pretreatment can be separated into two stages, namely the pretreatment before and after immersion of the electrode into the electrolyte. The procedure for the pretreatment before immersion was consistent, but the treatment after immersion depended upon the experimental technique and conditions and will be dealt with in subsequent sections.

The pre-immersion pretreatment was as follows:
Using a Struers Planopol-2/PdM-Force polishing system, the electrodes were polished on abrasive paper (SiC) ranging from grade size no. 400 to no. 1200. Fine polishing was done on a MMS / ALHALAP polishing cloth with wet (deionised water) 5μm aluminium oxide powder until no surface scratches could be detected by a ×5 magnifying glass. Some experimentation with finer grades of Al_2O_3 showed that no significant experimental variation, nor any improvement in reproducibility was obtained with the finer grades[a]. The electrode was then ultrasonically degreased in ethanol, followed by deionised and then millipore water. The electrode was then inserted into the rotating electrode stand and the contact between the slip rings (label 3 in fig. 4.6) and the alloy strip of the electrode was checked with the multimeter.

Prior to immersion the solution was deaerated with high purity nitrogen for at least 15 minutes. The electrical connections were then made and the electrode was immersed. The luggin capillary was then positioned so as to minimise resistance errors [185], whilst ensuring that there were no bubbles in the capillary, or adhering to the reference electrode. Bubbles on the surface of the electrode were removed by rotation.

4.7.1.1. *Cyclic voltammetric and anodic polarisation experiments*

The reproducible regime used varied with the temperature of a solution. For CV at lower temperatures, the "switch on" potential was usually -1.0V vs. SSE (this potential which chosen to be slightly cathodic of the corrosion potential and was dependant on the experimental conditions). The electrode was then held at this potential for 30 seconds. A one cycle sweep at 200mV/s was then performed, ending at -1.0V. The electrode was then held at -1.0V for 10s before sweeping at the desired sweep rate. In all cases the **second** cycle was the cycle from which data was taken. This was because over the range of experimental conditions used, if a cyclic voltammogram attained a steady state - a state where further cycles would superimpose - it would do so by the second cycle. All CV's given show the second cycle. For most cyclic voltammograms at higher temperatures, the waiting times at -1.0V were

---

[a] A worhwhile investigation would be to find the simplest possible polishing procedure that would still give reliable and reproducible results over a range of experimental conditions. This need arises because by far the greatest amount of the experimentalist's time (often over half) is spent polishing electrodes.

progressively reduced as the temperature was increased. It was assumed that for the sweep rates used (mostly less than 400 mV/s), the IR drop was negligible. For most experiments, at least two cyclic voltammograms were obtained for each sweep rate, in order to ensure reproducible results.

For CV's in the most corrosive conditions (90°C, pH 0.5), it was not possible to use the previous "switch on" potential as upon the first entry into the active region rampant corrosion of the electrode occurred after which passivity could not be obtained. This was avoided if the "switch on" potential was set in the passive region (0.0 V was used). The potential was held at this value for 20s, and then the first cycle was begun with potential initially sweeping towards the cathodic limit (-1.0V).

APC's were generated at a sweep rate of 2 mV/s after being held at the starting potential (just cathodic of the corrosion potential) usually for 2 minutes.

4.7.1.2. *Chronoamperometric experiments*

For chronoamperometric experiments, the following regime was used:
After immersion, the electrode was rotated at 100 rad/s. The electrode was then held at -1.0V for 10s. The following cycle was then repeated three times, ending at -1.0V:

The electrode was stepped to +1.0V, then held for 2 seconds, then stepped back to -1.0V and held for 2 seconds.

After this the electrode was held at -1.0V for 10s, then stepped to +1.0V for 6 seconds, then back to 1.0V for a further 10s after which the rotation was terminated if the potential step was to occur at 0 rad/s. The electrode was then stepped to the starting potential (E_1') and held for 30s before executing the initial potential step. This "electrochemical cleaning" gave excellent reproducible results.

After the regime and in a one step experiment, the electrode was then stepped to the final potential, E_2'. For a two step experiment, the electrode was first stepped to the intermediate potential, E_2', usually for 1 or 2 seconds, and then to the final potential, E_3'.

4.7.1.3. *Scratch experiment*

This experiment was performed only to determine whether a pre-existent layer exists on the electrode (i.e. a layer which forms after immersion when the electrode is switched on at the supposedly "noble" corrosion potential. This implies that the electrode is not held at any other potential where a film is known to form first, nor is it allowed to reach a rest potential before the switch on potential.). Immediately after immersion (in 0.06M H_2SO_4 at 25°C), the electrode was "switched on" to a potential of -1.0V. The electrode was then rotated at the required rotation rate and was held at -1.0V for 2 minutes in order to reduce any air-formed oxide. The potential was then adjusted to -0.95V (E_{corr}) and was held at that potential for 30s. The culet of the diamond was then lifted (it was moved in one direction only - directly up) and brought into contact with the rotating electrode for the duration of the experiment (4 seconds). The resulting I-t curve was recorded on the oscilloscope. The experiment was repeated for a number of rotation rates.

CHAPTER 5

5. VOLTAMMETRY AT A 444 ELECTRODE IN 0.06M H_2SO_4 SOLUTION

Note that all voltammograms displayed in this chapter were obtained at 0 rad/s. The electrolyte used throughout was 0.0590M H_2SO_4 (pH 0.93).

5.1 Empirical correction for oxygen evolution

The potential stop technique (section 2.3.4) was used to obtain a relaxation current after the peak A current response had been obtained. Ideally, subtracting the relaxation current from the voltammetric current response at potentials positive to the region of secondary passivity should give the current due to oxygen evolution only. Fig. 5.1 shows a typical relaxation curve superimposed upon a normal voltammogram.

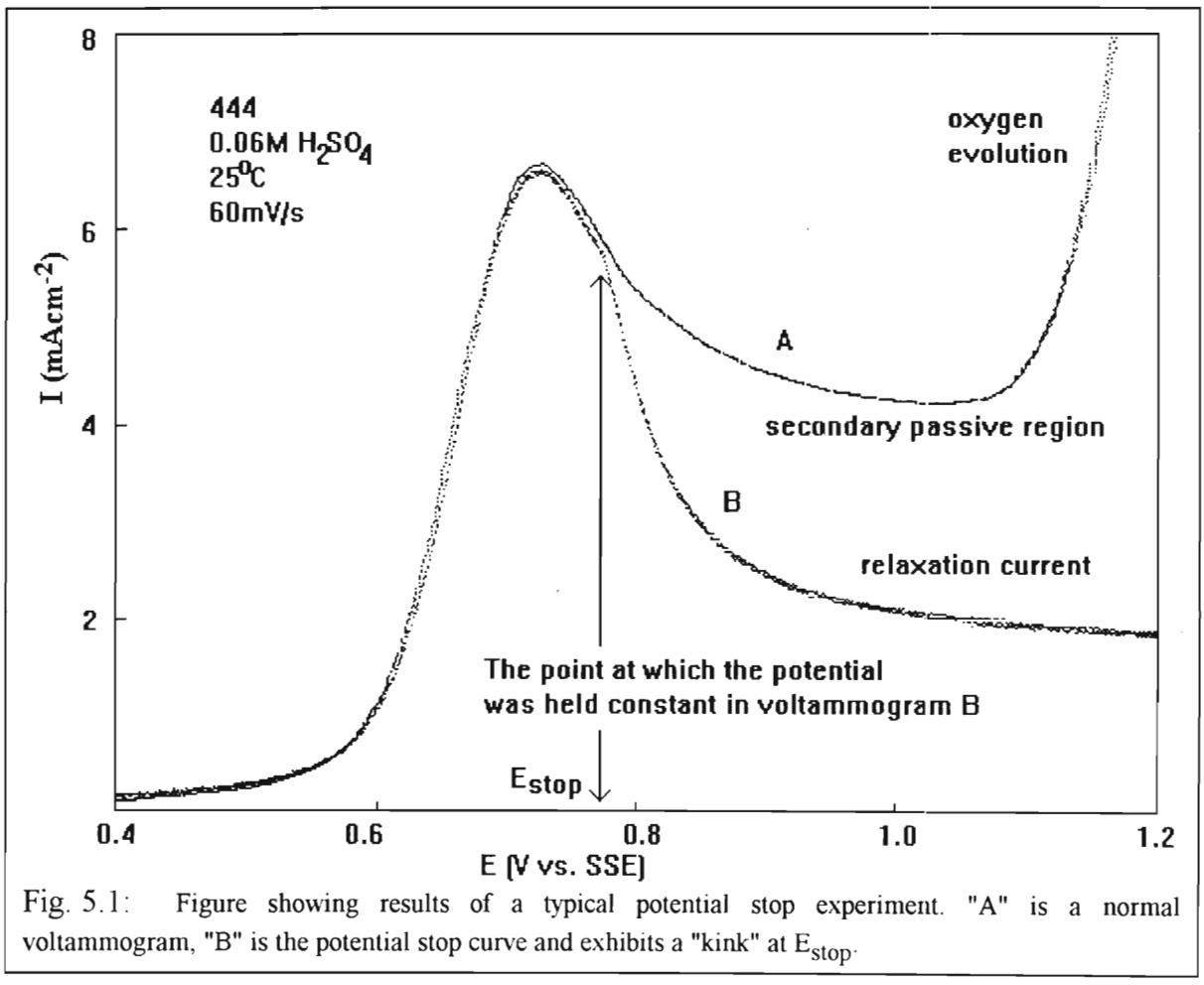

Fig. 5.1: Figure showing results of a typical potential stop experiment. "A" is a normal voltammogram, "B" is the potential stop curve and exhibits a "kink" at E_{stop}.

All the relaxation curves exhibited the "kink" shown in fig. 5.1. The proposed explanation for this kink (as shown by simulation in a simplified situation, *cf* section 2.3.5) is simply that peak A has a number of contributing processes and that E_{stop} always occurs before the peak of at least one of these contributing processes. The "kink", therefore, is indirect evidence towards the fact that there is more then one oxidative

process contributing to peak A. It should be noted that the "kink" occurred even if E_{stop} was situated in the secondary passive region.

In the analyses of potential stop data it was found that the oxygen evolution current was independent of sweep rate, at least between 20 - 400 mV/s over 25 - 80°C, in 0.06M H_2SO_4 and on 444. Fig. 5.2 shows the oxygen evolution curves that were obtained from the subtraction of relaxation currents from voltammetric currents for sweep rates of 20 - 100 mV/s. The 20 mV/s data appeared to give the best average results and numerical analyses were therefore performed on this data only.

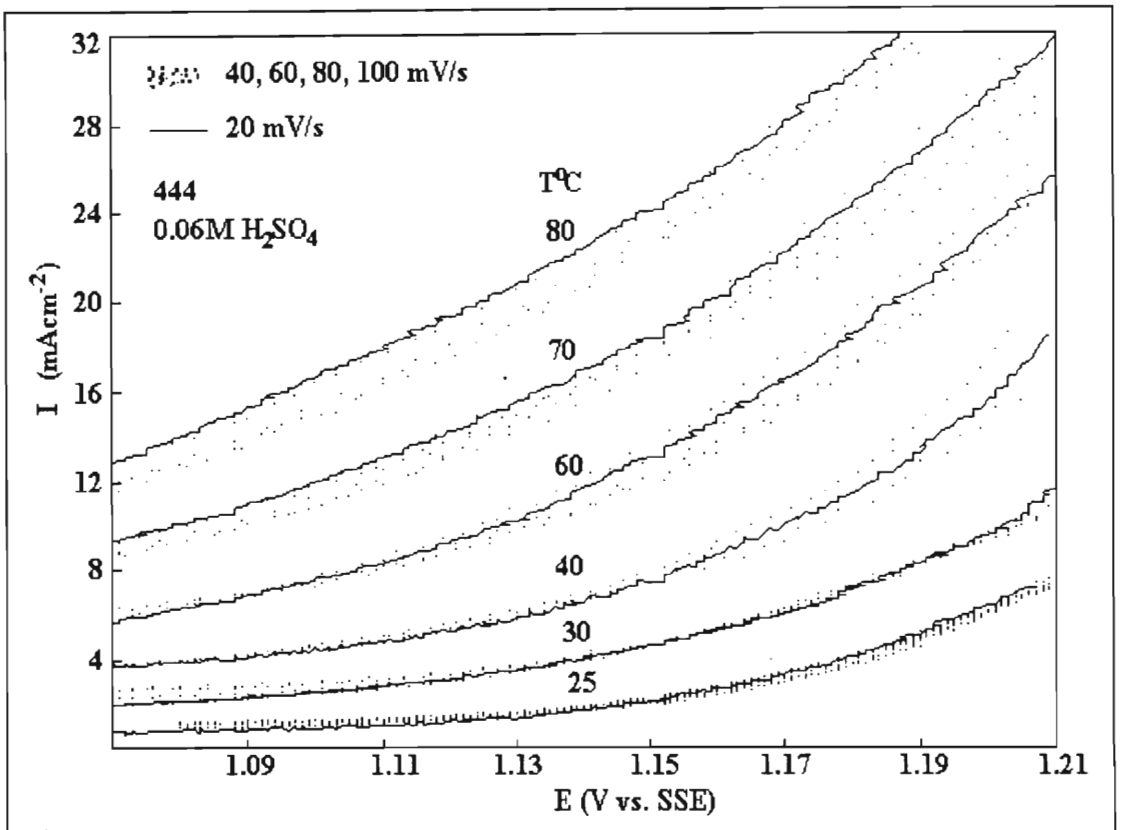

Fig. 5.2: Diagram of the oxygen evolution curves obtained from subtracting relaxation currents from the oxygen evolution portion of CV's. The 20 mV/s data is shown as a solid line.

A simple tafel analysis on each of the six curves in fig. 5.2 did not result in a sufficiently accurate fit to these curves. It was found that by using a non-linear regression routine (with Statgraphics 5.0 software) and by including a "kink error" factor in the equation previously derived, a good fit could be obtained. The equation that was used in the fitting of the data was

$$I = c_k + \exp\left(c'' + \frac{\alpha_o nFE}{RT}\right) \tag{5.1}$$

where c_k is the "kink error" factor. Using the non-linear regression programme, values for c_k, c'' and α_o were obtained for each of the six curves in fig. 5.2. Then using a multiple regression routine (Statgraphics 5.0) empirical formulae for c'' and α_o were found as functions of temperature as follows

$$c'' = -3.120T + 4996 \log T + 321800/T - 12520 \tag{5.2}$$

$$\alpha_o = -3.434 \times 10^{-3} T + 1.118 \log T - 1.58707 \tag{5.3}$$

It has been shown before that the transfer coefficient is not independent of temperature [186]. These results expressed in equation (5.3) agree with that finding, although the change is small (0.11 over 55°C). Values of transfer coefficients for oxygen evolution on Fe-Cr alloys have not previously been published.

Substituting (5.2) and (5.3) into (5.1) and setting $n = 2$ gives

$$I_{O_2} = \exp\left[-3.200T + 4996\ \log T + \frac{3.218\times10^5}{T} - 12520 - 79.70E + \frac{25949(\log T)E}{T} - \frac{36836E}{T}\right] \pm 0.7 \quad (5.4)$$

where I_{O_2} is the current density due to oxygen evolution in $mAcm^{-2}$. Fig. 5.3 shows the fit of this empirical equation (solid line) to the experimental (dotted line) data. Table 5.1 shows the values of c'' and α_o that were obtained from equation (5.4) for the temperatures of interest

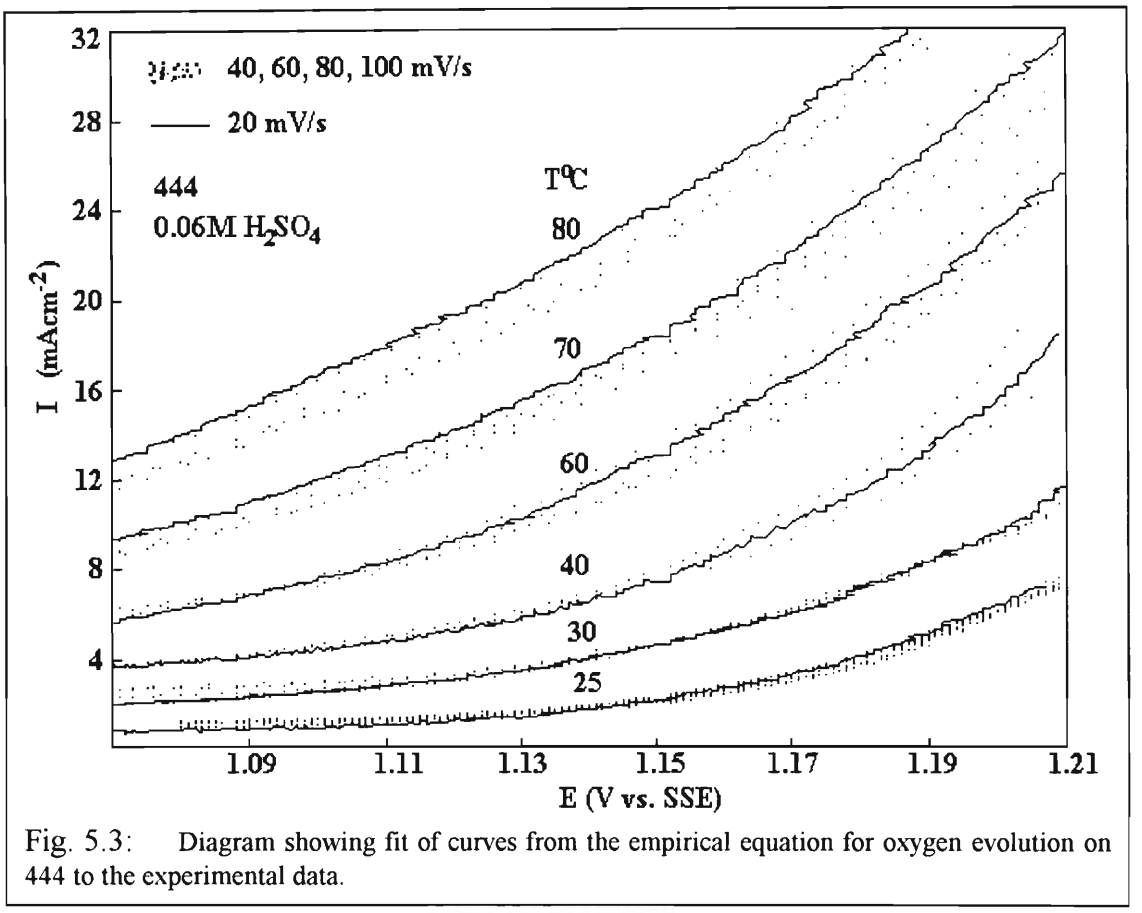

Fig. 5.3: Diagram showing fit of curves from the empirical equation for oxygen evolution on 444 to the experimental data.

T°C	c''	α_o
25	-34.1	0.155
40	-27.3	0.127
50	-22.9	0.108
60	-18.7	0.089
70	-14.6	0.069
80	-10.9	0.048

Table 5.1: Values of the constant, c'', and the anodic transfer coefficient for oxygen evolution on 444 at the indicated temperatures.

Fig. 5.4 shows oxygen evolution curves generated by equation (5.4) extrapolated into the region of peak A. Since (in 0.06M H_2SO_4) the range in E_{pA} is 0.67 to 0.87 V, it is evident from fig. 5.4 that the error imposed by oxygen evolution on I_{pA} is only significant at temperatures greater than 60°C.

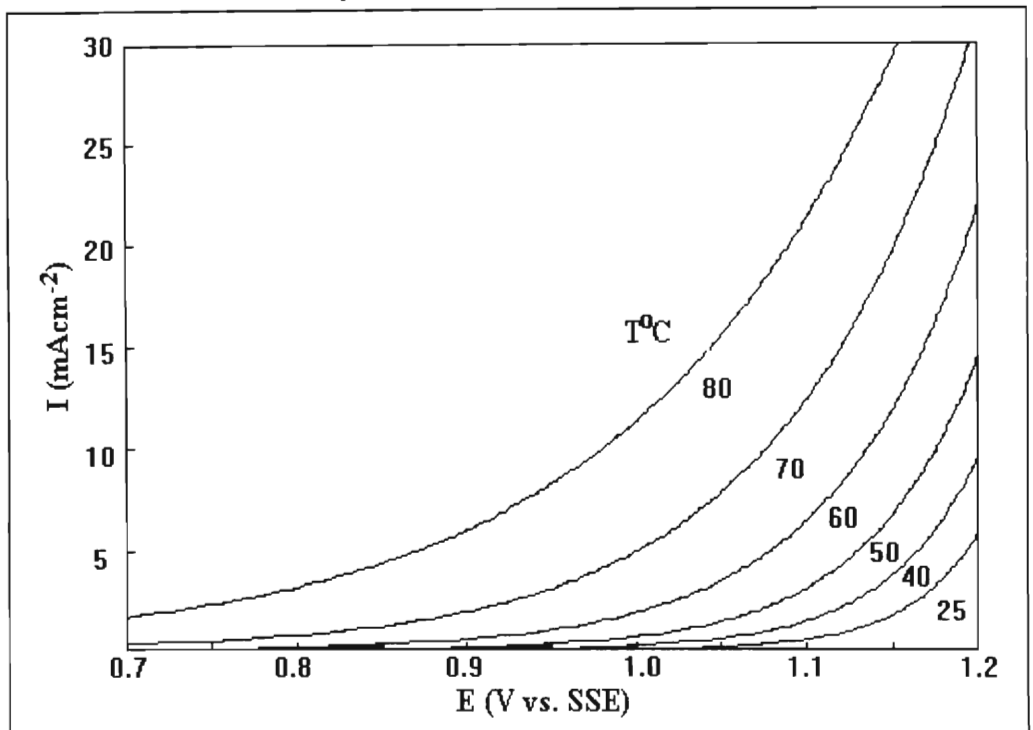

Fig. 5.4: Figure showing curves generated by the empirical equation for oxygen evolution.

Fig. 5.5 shows the result of correcting voltammograms obtained at 80°C (and 800 mV/s) with the empirical oxygen evolution curve. This voltammogram is shown because E_{pA} was found to increase with sweep rate and hence peak A is most significantly affected by oxygen evolution at the fastest sweep rate and highest temperature.

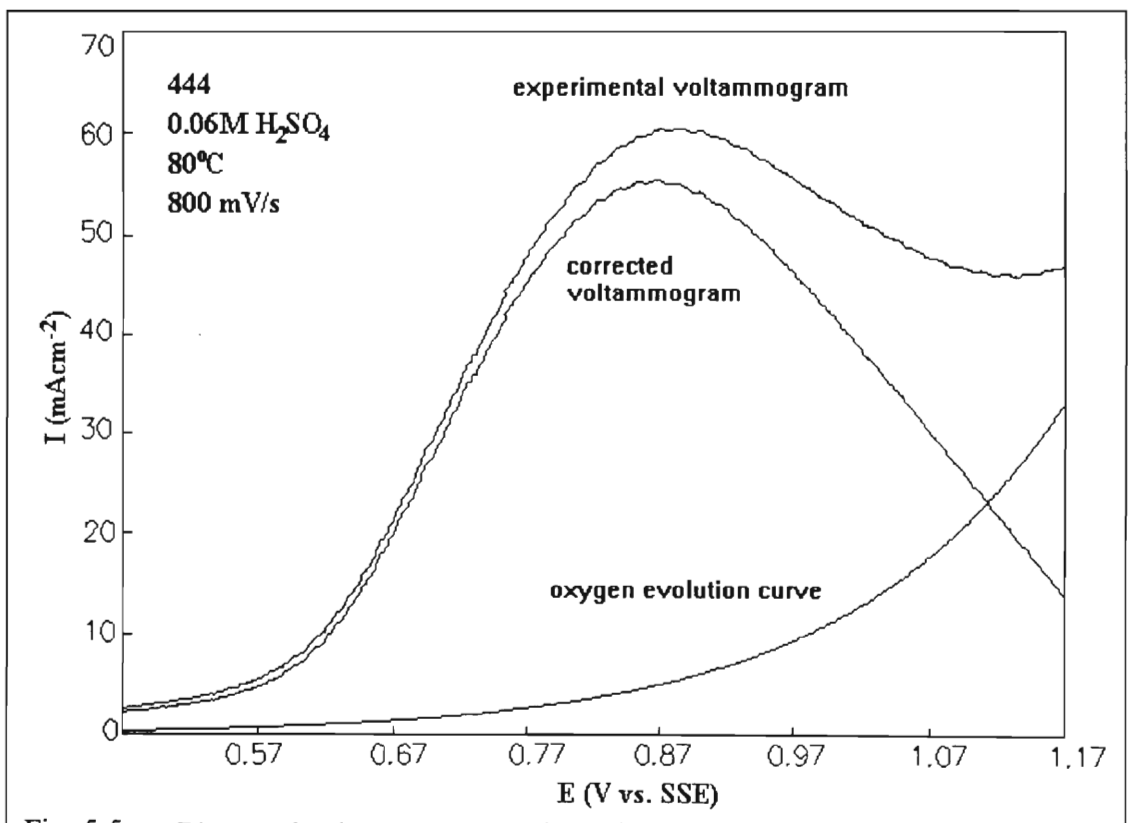

Fig. 5.5: Diagram showing a normal experimental voltammogram (444, 0.06M H_2SO_4, 80°C, 800 mV/s), the empirical oxygen evolution curve for 80°C and the corrected voltammogram which results from the subtraction of the oxygen evolution curve from the experimental voltammogram.

For the remainder of this chapter all voltammograms will be corrected for oxygen evolution unless otherwise stated. Fig. 5.6 shows a voltammogram with the cathodic sweep included, and it should be noted that the cathodic sweep nearly superimposes upon the anodic sweep and that peak A is closer to forming a plateau than a peak. Both of these results are diagnostic of a catalytic mechanism at slow sweep rates (*cf* section 2.3.2) and with the evidence of other results it will be suggested that H_3O^+ can act as a catalyst in its role in the dissolution of passivating oxides on stainless steels. However, the tendency of the cathodic sweep of the voltammogram to superimpose on the anodic sweep appears to be directly related to the concentration of the sulphate anion. In perchlorate and acetate solutions in similar conditions (in particular, at slow sweep rates) the cathodic sweep did not superimpose upon the anodic response as much as in the sulphate solution. It appears that the sulphate anion enhances the catalytic film dissolution process, possibly because of the high degree of porosity of temporarily passivating sulphate salts.

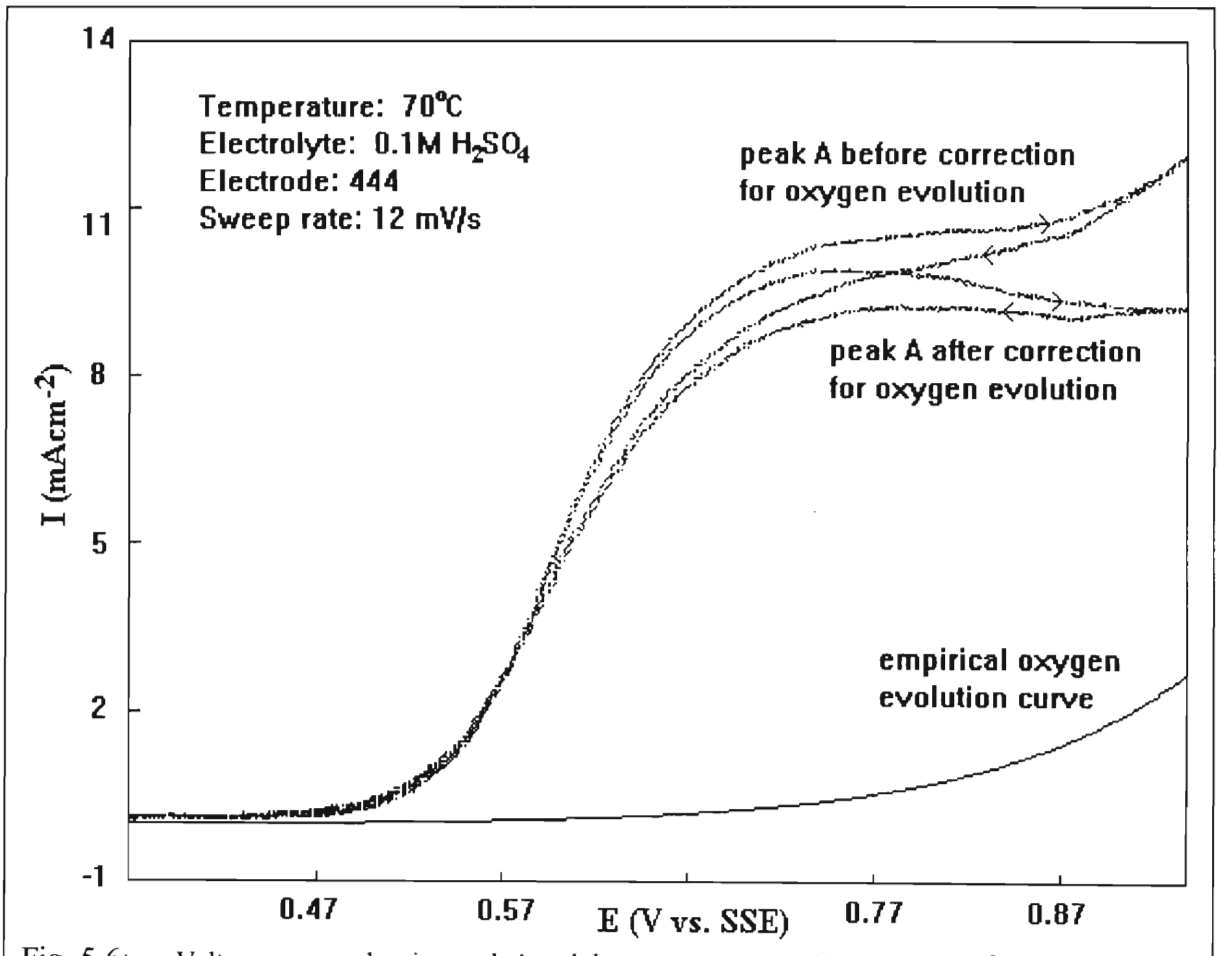

Fig. 5.6: Voltammogram showing peak A and the reverse sweep at 12 mV/s and 70°C. Comparison of the corrected voltammogram to voltammogram "c" of fig. 2.1 indicates the possibility of a catalytic mechanism contributing towards peak A.

It was found in perchloric and acetate solutions that if the sweep rate was not increased beyond approximately 300 mV/s, then the interference of oxygen evolution could be neglected. This was desirable as generating empirical equations was a highly time consuming process and some of the assumptions made in generating these equations are possibly not entirely valid (*cf* section 2.2.2). Accordingly, potential stop experiments and therefore oxygen evolution corrections were not performed in solutions containing acetate or perchlorate anions.

5.2. Voltammetric results

Figures 5.7 and 5.8 show the effect of sweep rate on peak A at 25°C and 80°C respectively.

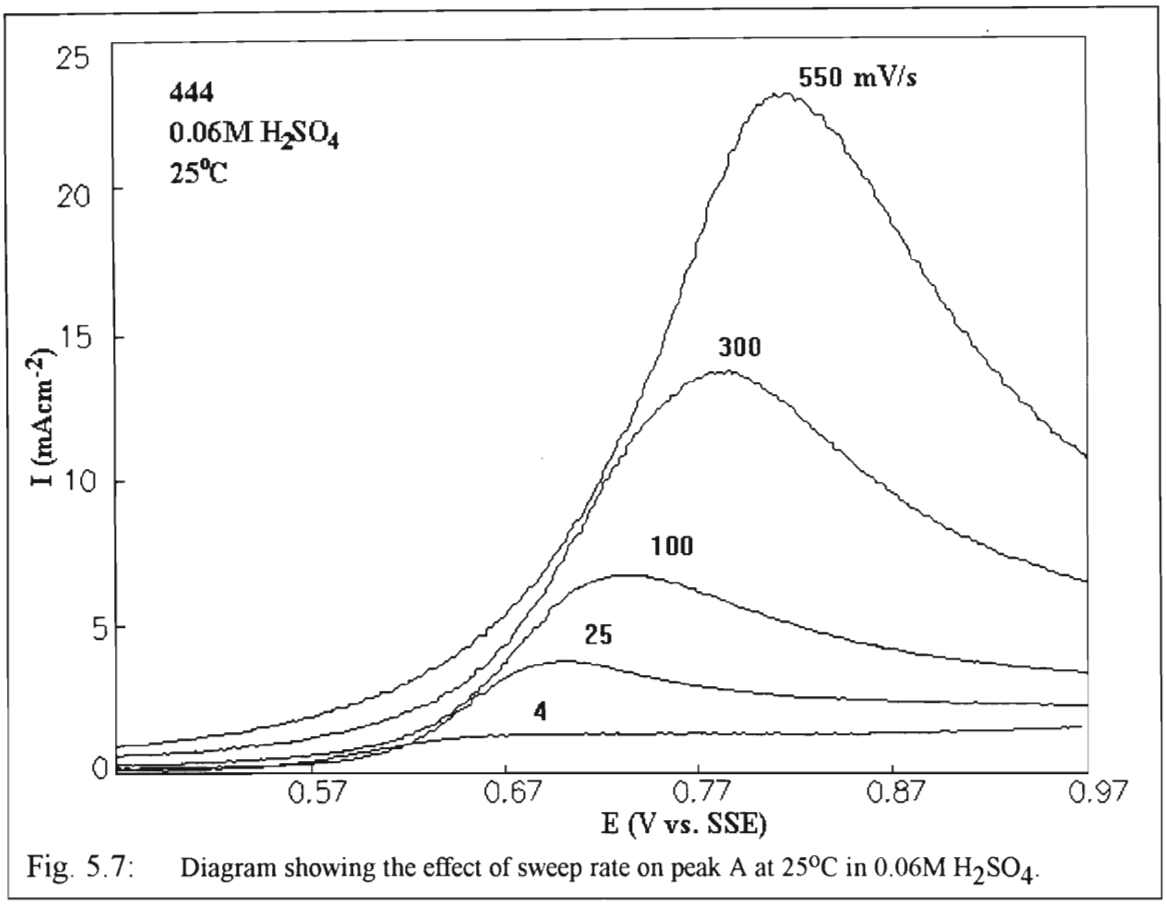

Fig. 5.7: Diagram showing the effect of sweep rate on peak A at 25°C in 0.06M H_2SO_4.

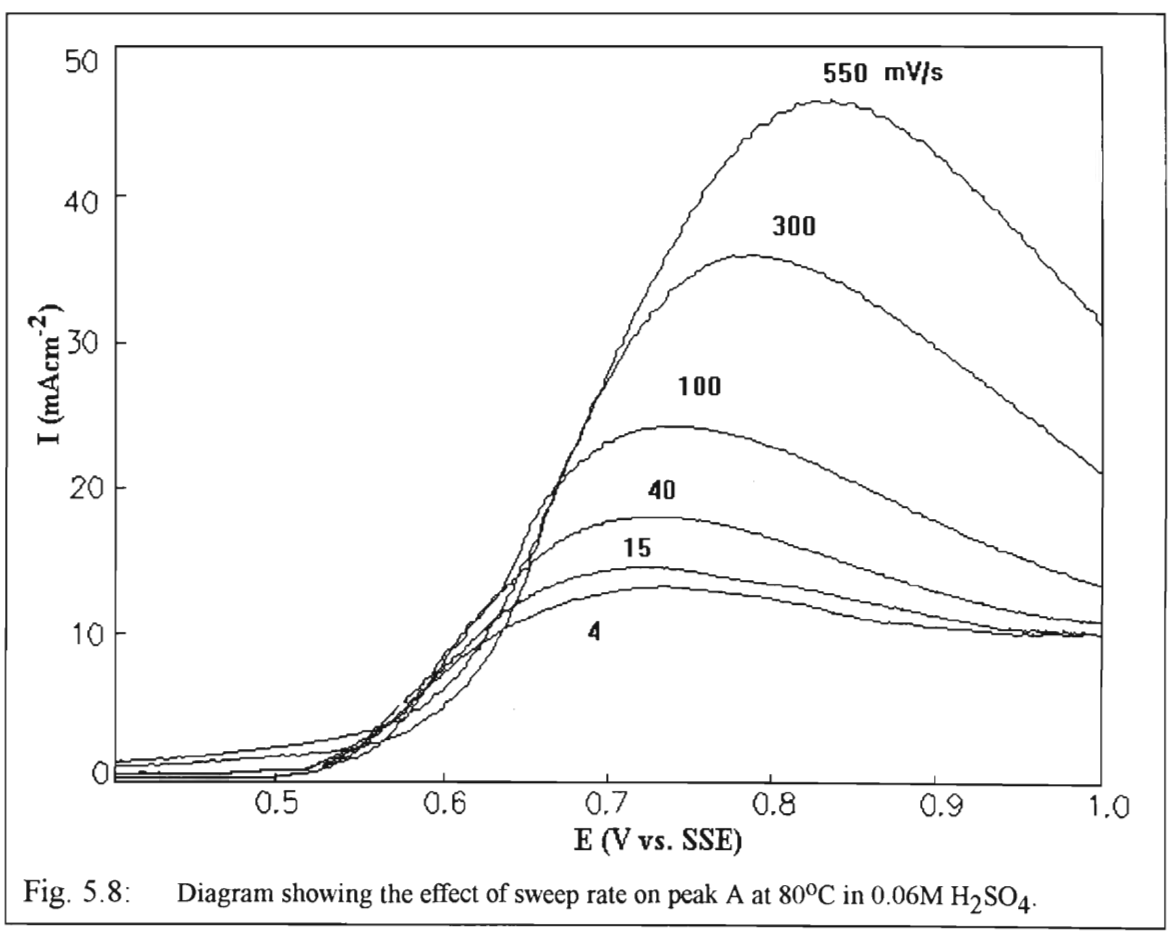

Fig. 5.8: Diagram showing the effect of sweep rate on peak A at 80°C in 0.06M H_2SO_4.

The 4 mV/s voltammogram at 25°C (fig. 5.7) forms a plateau, indicating a steady state, whereas the 4 mV/s voltammogram at 80°C (fig. 5.8) still exhibits a peak demonstrating that the processes are not in the steady state even at that slow sweep rate. E_{pA} increases with sweep rate (which is typical of irreversible reactions) which means that the peak A current responses from the slowest sweep rates will be least affected by oxygen evolution. Fig. 5.9 shows the effect of temperature on peak A at 200 mV/s. It appears that there is no general effect on E_{pA} with increase in temperature, but I_{pA} increases with increase in temperature.

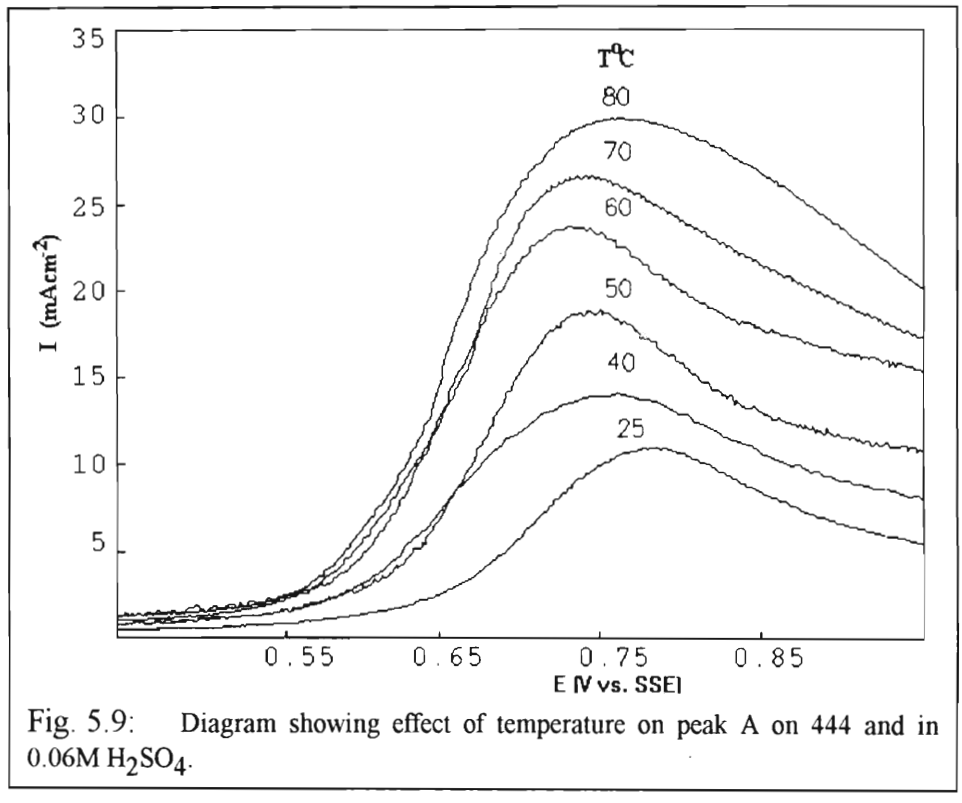

Fig. 5.9: Diagram showing effect of temperature on peak A on 444 and in 0.06M H_2SO_4.

Finally, fig. 5.10 shows the effect of pH on peak A. Clearly the hydronium ion concentration plays a significant role in the transpassive behaviour of Fe-Cr alloys. As the $[H^+]$ increases dissolution of the passivating oxides and probably also dissolution of the bare alloy increases in the transpassive region and E_{pA} increases positively.

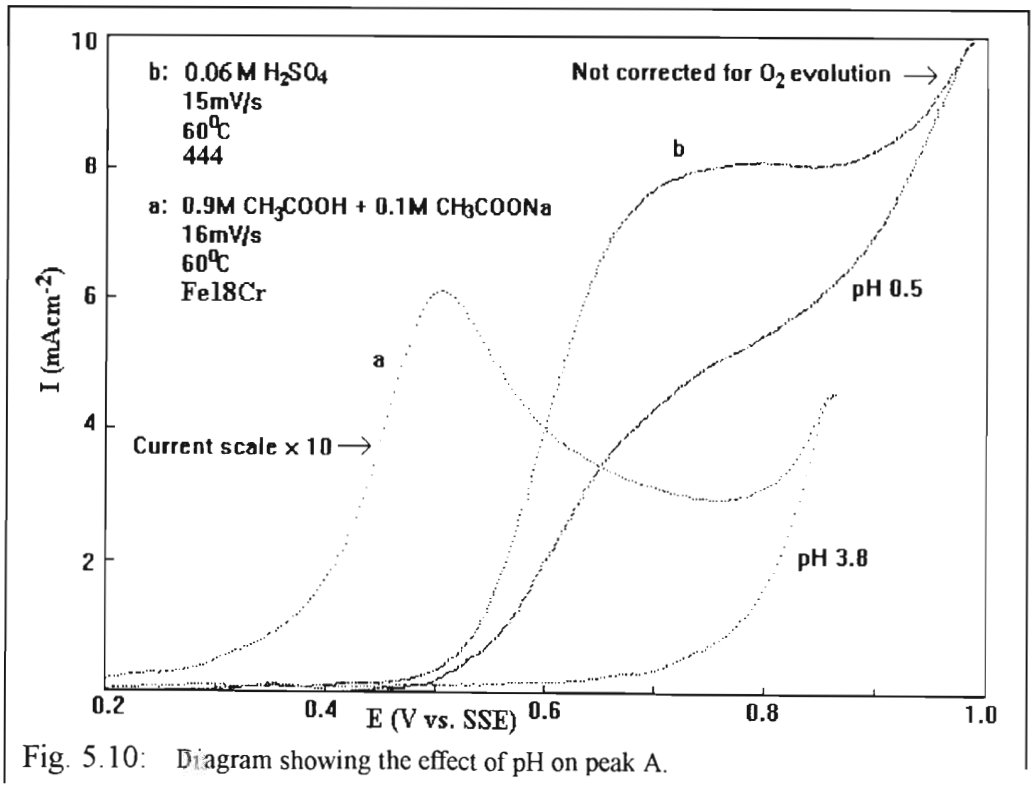

Fig. 5.10: Diagram showing the effect of pH on peak A.

5.3. Diffusion diagnostic results

The most significant results from the work on 444 in 0.06M H_2SO_4 were obtained from the diffusion diagnostic plots $\left(I_{pA}/\nu^{1/2} \; vs. \; \nu^{1/2}\right)$ that were obtained over the range of temperatures used. Fig. 5.11 shows these results.

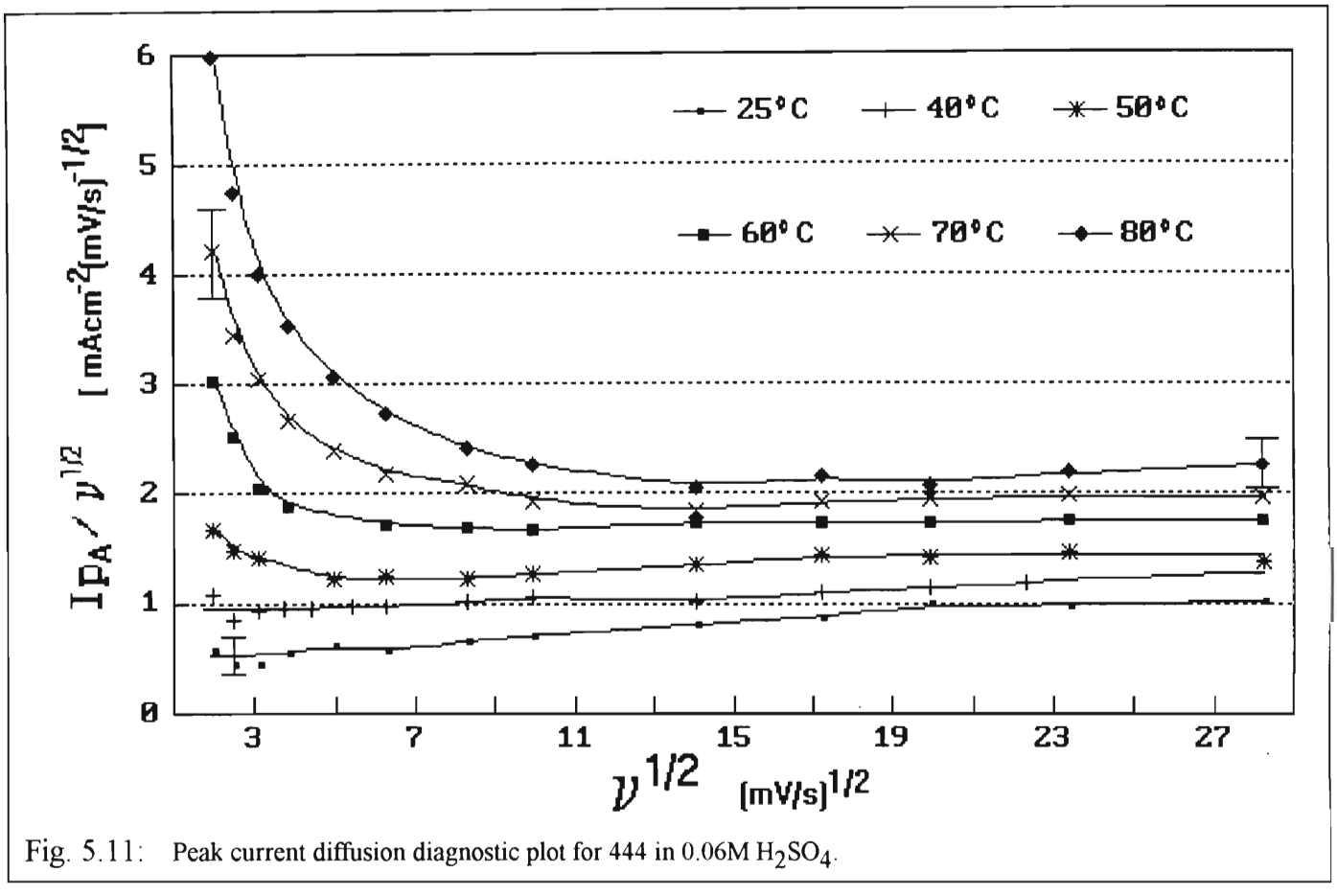

Fig. 5.11: Peak current diffusion diagnostic plot for 444 in 0.06M H_2SO_4.

At the lower temperatures (25, 40°C) and within experimental error, the plot approximates to a horizontal line and the processes contributing to peak A can be considered to be diffusion controlled. At the higher temperatures, however an increasingly large positive deviation from the horizontal occurs as the sweep rate is decreased. The following explanation is offered for this phenomenon:

Before entering the transpassive region, some passivating film exists on the electrode surface. The peak A current response must therefore involve oxidation of this film and possibly oxidation of the bare alloy as well. However, as long as the film remains intact over the electrode surface it is very likely that the rate of peak A processes will be controlled by the rate of transmission of ions through the film (be it by diffusion of ion vacancies or by diffusion through pores in the film) and this will result in $I_{pA} \propto \nu^{1/2}$. As the sweep rate is decreased more time is available for the oxidation, dissolution and breakdown of the film. The rate of oxidation will increase with temperature, as will dissolution, according to reactions such as

$$Fe_2O_3 + 6H^+ \rightleftharpoons 2Fe^{3+} + 3H_2O$$

Hence the experimental conditions where the greatest amount of the bare alloy will be exposed directly to the solution for the longest time will be at the highest temperatures and the slowest sweep rates. The

positive deviation in the diagnostic plot is then due to the additional oxidation reactions (such as Fe,Cr → Fe(III),Cr(III)) which occur to the greatest degree in the most aggressive conditions. These reactions will occur significantly when the alloy substrate is exposed directly to the solution. This does not occur when there is insufficient time (fast sweep rates) or energy (low temperatures) to appreciably break down the passive film. At the lower temperatures (and slower sweep rates), there is a slight negative deviation from the horizontal and this is explained in sections 5.5 and 6.1.1. It would appear that both a time factor and a required amount of available energy are needed to sufficiently break down the passivating film and expose at least some of the bare alloy surface to the solution.

Fig. 5.12 shows the effect of the oxygen evolution correction on the diffusion diagnostic plot. As is shown it gives the greatest effect at the slower sweep rates. However, the change is still not large and the qualitative result (the positive deviation from the horizontal at slow sweep rates) is unchanged.

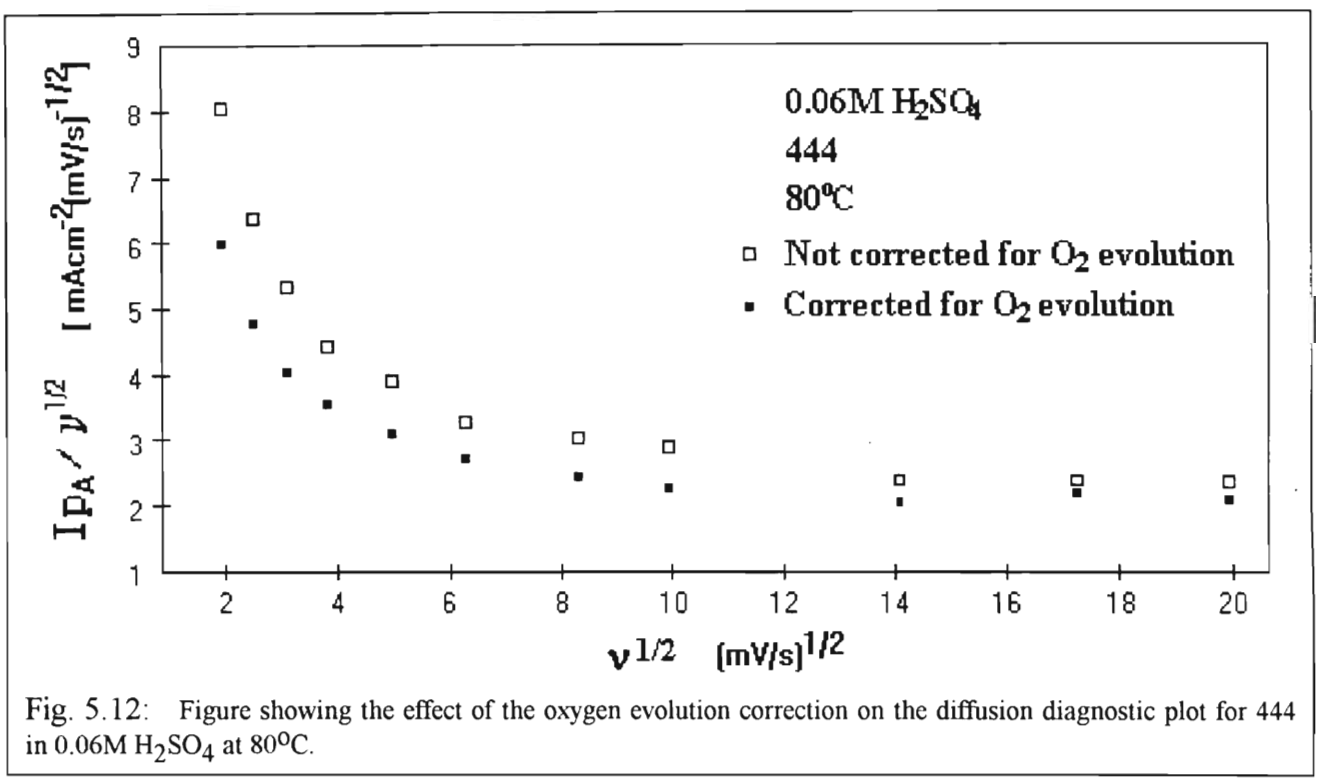

Fig. 5.12: Figure showing the effect of the oxygen evolution correction on the diffusion diagnostic plot for 444 in 0.06M H_2SO_4 at 80°C.

Another diagnostic for diffusion control in a porous passivating film is that $E_p \propto \nu^{1/2}$ (section 2.3.1). Accordingly fig. 5.13 shows a plot of $E_{pA}/\nu^{1/2}$ vs. $\nu^{1/2}$ for the range of temperatures used (corrected for oxygen evolution). Again a positive deviation occurs at slow sweep rates, but the points, within experimental error, superimpose for all temperatures. In other words E_{pA} for a particular sweep rate (on 444 in 0.06M H_2SO_4) is relatively independent of temperature. The positive deviation at slow sweep rates means that the point of maximum oxidation of the film / electrode occurs more positively than would be predicted by a model based on the diffusion of ions through pores in the film. Hence the pore model is either incorrect or insufficient for application to transpassive behaviour of Fe-Cr electrodes. It is possible that at the slower sweep rates, a more stable passive film is formed whilst the electrode is in the passive region (since it is there longer) and hence a more positive transpassive potential is required for its breakdown.

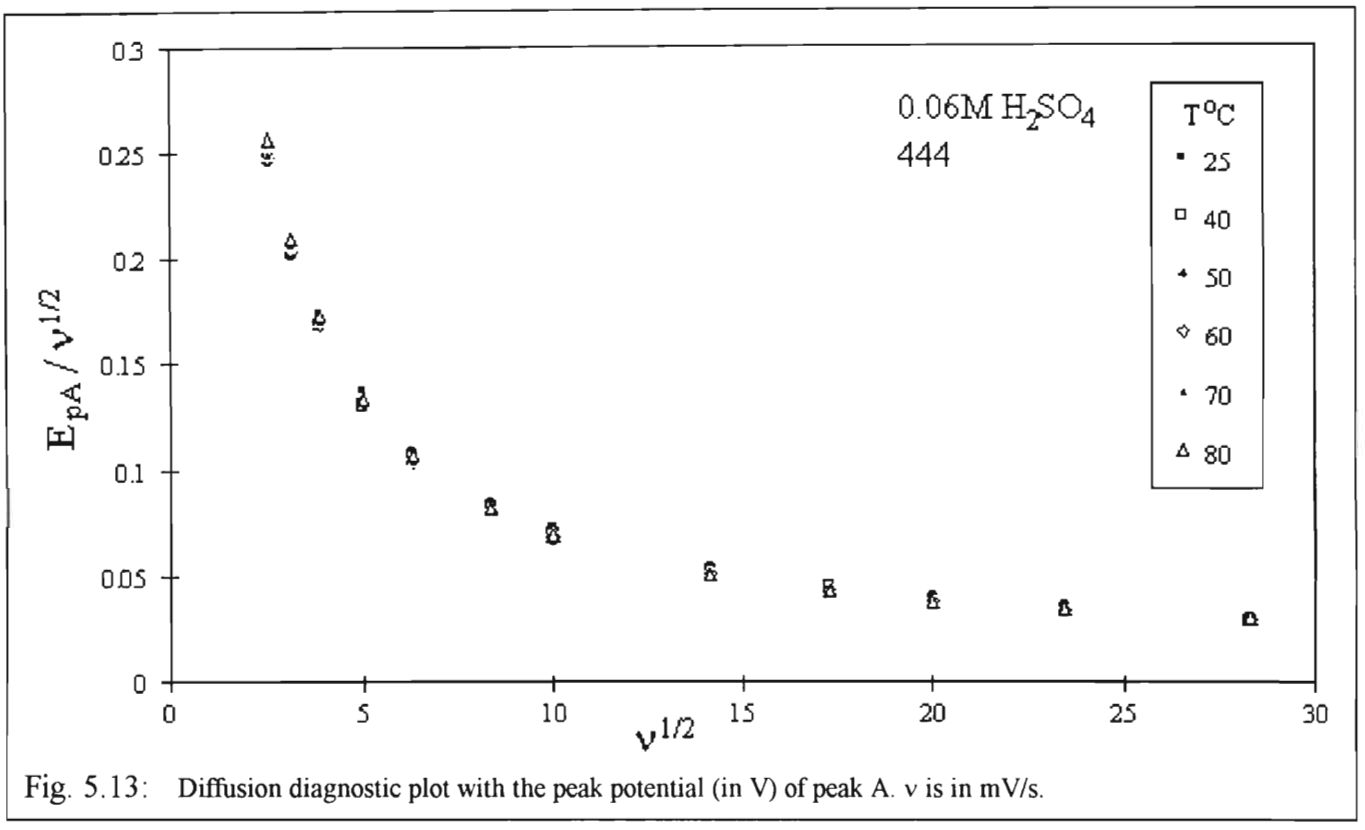

Fig. 5.13: Diffusion diagnostic plot with the peak potential (in V) of peak A. v is in mV/s.

Fig. 5.14 shows the effect of the oxygen evolution correction on the above diagnostic for 80°C. As before the effect is most pronounced at the slow sweep rates and the qualitative result is unchanged.

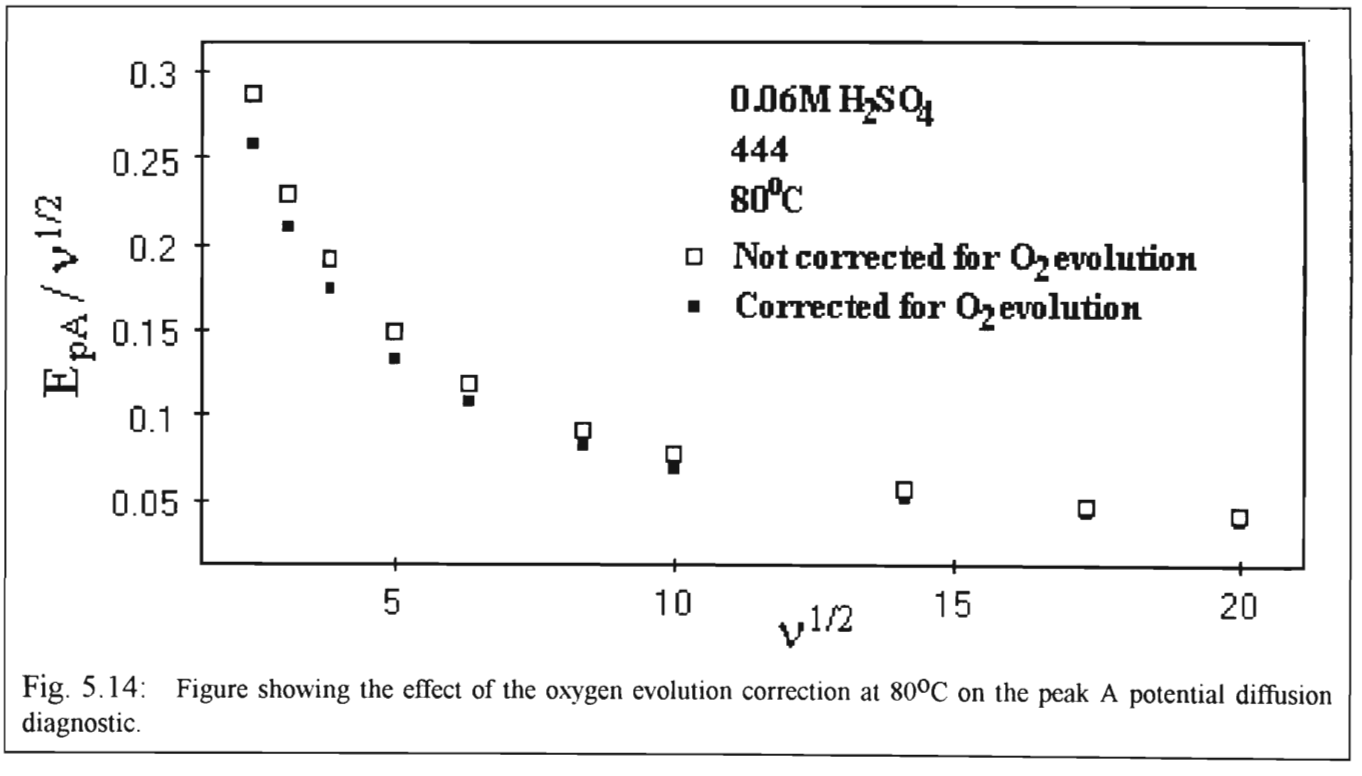

Fig. 5.14: Figure showing the effect of the oxygen evolution correction at 80°C on the peak A potential diffusion diagnostic.

5.4. Arrhenius plots

The Arrhenius equation is

$$\ln k = \ln A' - \frac{E_a}{RT} \tag{5.5}$$

where A' is a pre-exponential factor, k is the rate constant and E_a is the activation energy of a kinetically limited reaction. Applying this to peak A, the equation may be modified as follows

$$\ln I_{pA} = \ln A' - \frac{E_{a,pA}}{RT} \tag{5.6}$$

Here the peak height of peak A is considered to be the same as the rate constant for the overall reaction, and $E_{a,pA}$ is the apparent activation energy for the peak A processes. If a plot of the natural logarithm of the peak current density versus the inverse of temperature yields a straight line, then the value of the apparent activation energy may be obtained from the slope of the graph.

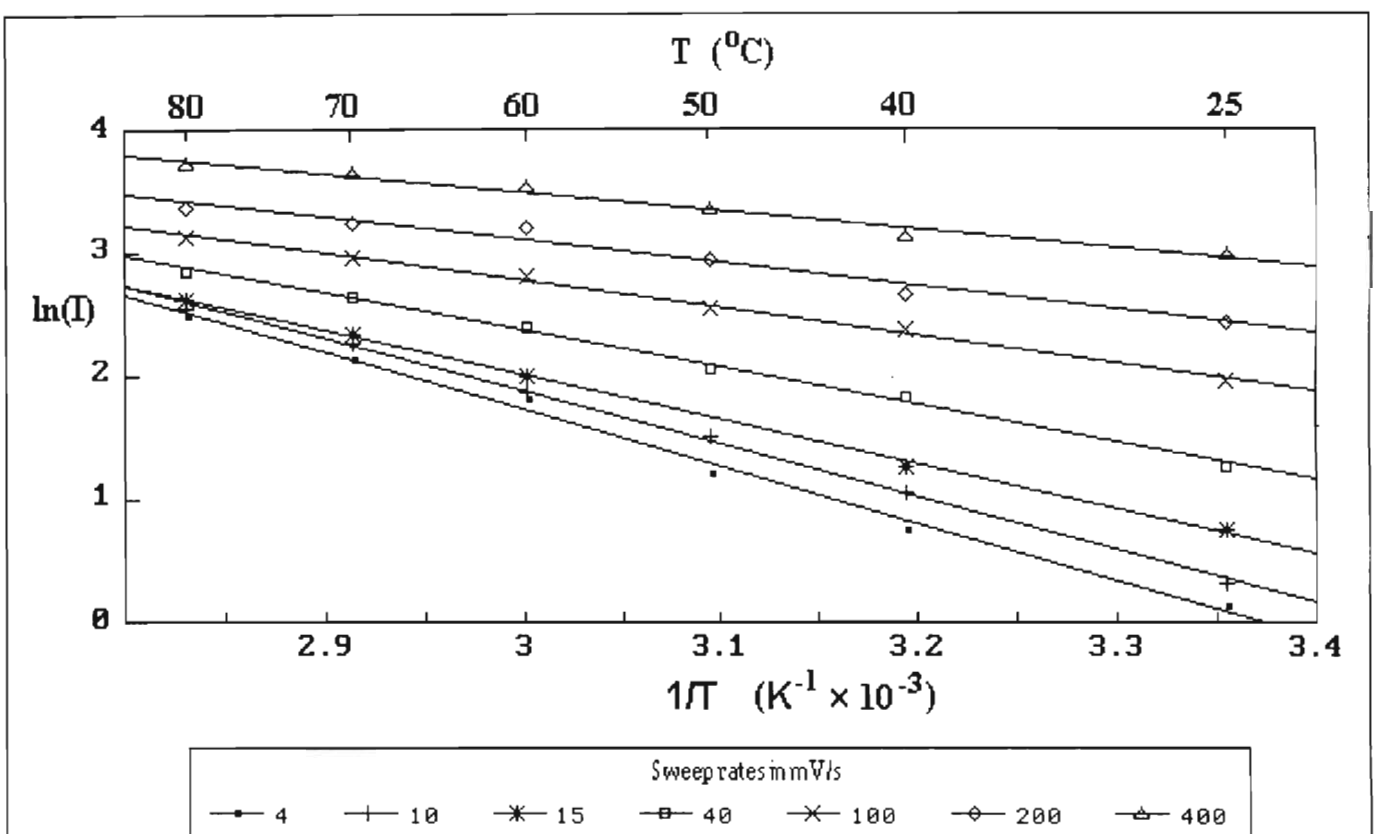

Fig. 5.15: Figure showing Arrhenius plots at a range of sweep rates for 444 in 0.06M H_2SO_4.

It should be noted that the diffusion diagnostic plots show that peak A processes are diffusion controlled at high sweep rates. Also, at slow sweep rates the additional reactions (due to breakdown of the passivating film) that occur are not necessarily kinetically limited. Hence it is necessary to use the terminology "apparent" activation energy. Fig. 5.15 shows Arrhenius plots for peak A data (444, 0.06M H_2SO_4) at a range of sweep rates

Table 5.2 shows the values of the apparent activation energies that were obtained compared to values obtained by Graham [52] in similar conditions.

ν (mV/s)	$E_{a,pA}$ (kJ/mole)	σ (kJ/mole)	$E_{a,pA}$ (kJ/mole) [52]
5	-	-	30.7
6.5	39.0	1.5	-
10	35.5	0.8	27.7
15	30.0	0.7	-
20	-	-	26.8
25	27.4	2.2	-
40	25.0	0.6	22.8
70	21.2	0.8	-
100	18.6	0.7	19.9
200	15.6	1.4	18.0
300	15.1	0.8	-
400	12.8	1.0	16.0
550	13.2	0.4	-

Table 5.2: Table showing apparent activation energies obtained on 444 in 0.06M H_2SO_4 and some values for comparison obtained by Graham [52] on Fe18Cr in 0.1M H_2SO_4.

As table 5.2 shows, and considering the difference in experimental conditions, reasonable correlation between the author's results and those of Graham were obtained. However, at slower sweep rates (less than 70 mV/s), the apparent activation energies were greater than those of Graham while at faster sweep rates the $E_{a,pA}$'s were less than those of Graham. At slower sweep rates this result may be due to the effect of the 2% Mo in 444. The beneficial effect of Mo in alloys containing chromium has already been alluded to (*cf* section 3.2). Hence if the 1.7% Mo in 444 results in a more compact, stable passive film than on Fe18Cr then the activation energy required for its breakdown would be greater. The process whereby Mo imparts greater stability to the passive film may have a slow rate constant which would explain the trend of the results at fast sweep rates. Fig. 5.16 shows the effect of sweep rate on the apparent activation energy.

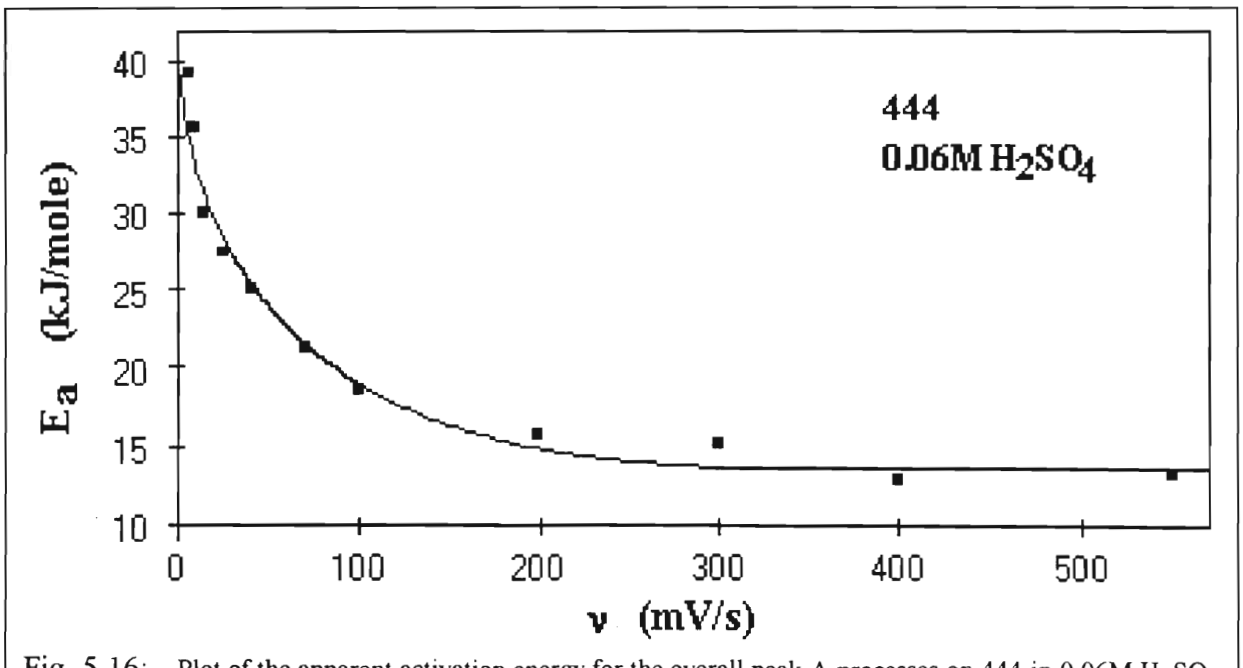

Fig. 5.16: Plot of the apparent activation energy for the overall peak A processes on 444 in 0.06M H_2SO_4 versus sweep rate.

According to fig. 5.16, the value of $E_{a,pA}$ becomes constant at fast sweep rates, whereas there is initially a sharp decrease of $E_{a,pA}$ with increase in ν. The following explanation is offered:

At slow sweep rates at least part of the overall peak A process is kinetically controlled. For example dissolution reactions such as $Fe_2O_3 + 6H^+ \rightleftharpoons 2Fe^{3+} + 3H_2O$ may be kinetically limited. Also at slow sweep rates plenty of time during the voltammetric sweep is spent in the passive region with the result that a stable, compact passive layer has time to form. As the sweep rate increases, the passive layer has less time to form, is easier to break down, and hence the apparent activation energy decreases. At faster sweep rates however, previous diffusion diagnostic plots show that the overall diffusion diagnostic process is diffusion controlled. Hence at these sweep rates the apparent activation energy does not reflect an activation energy barrier, which decreases with sweep rate. Rather, the apparent activation energy reflects a "diffusion barrier" which is not affected (or at least is not affected as much) by the stability of the passive film prior to voltammetric entry into the transpassive region.

5.5. Comparison to Fe18Cr data

The main difference between the alloys 444 and Fe18Cr is that 444 has 1.7% Mo. In order to see the effect of Mo on the transpassive region the peak A current responses were obtained for both alloys at a range of sweep rates in 0.06M H_2SO_4 at 25°C. Fig. 5.17 shows a peak A voltammogram obtained at 100 mV/s for both 444 and Fe18Cr.

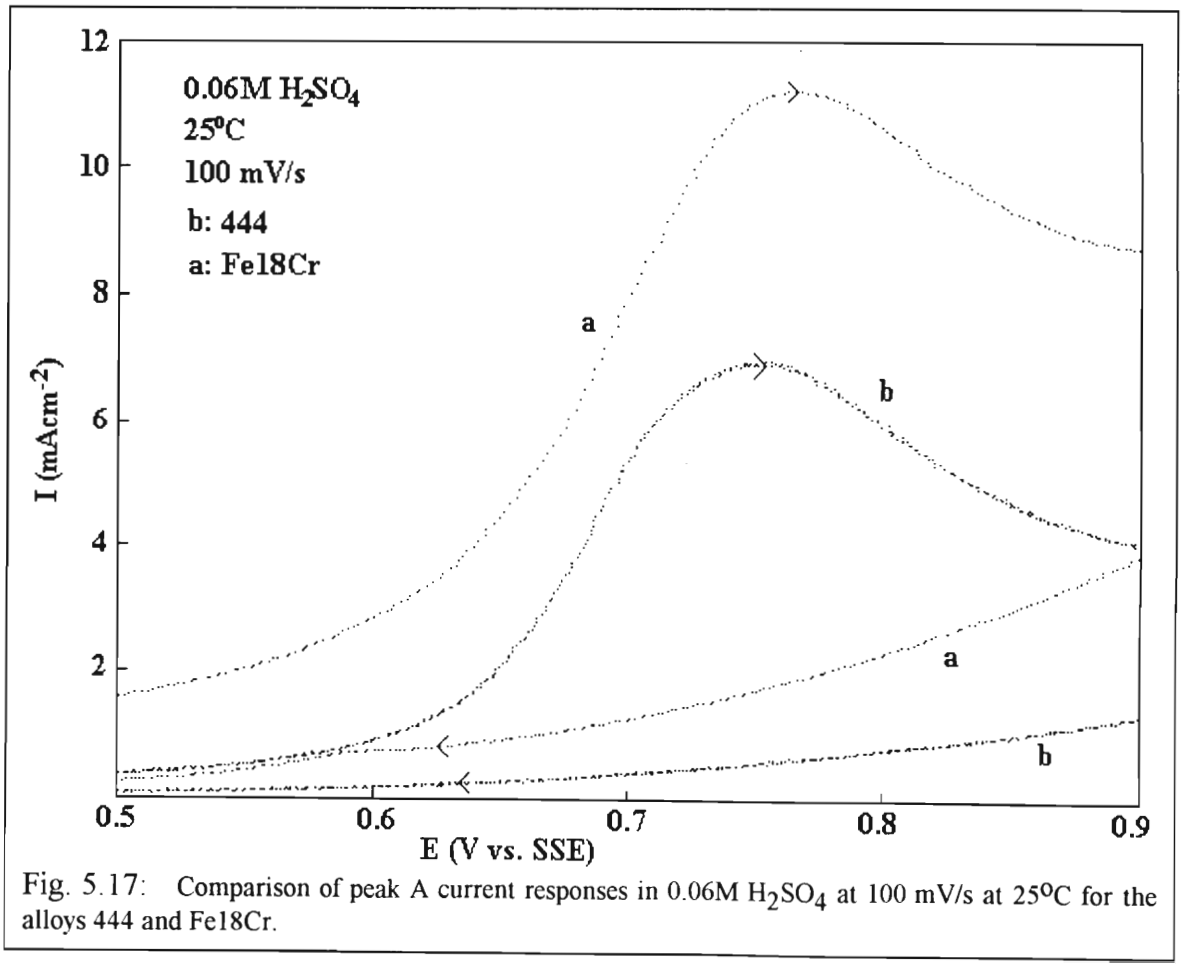

Fig. 5.17: Comparison of peak A current responses in 0.06M H_2SO_4 at 100 mV/s at 25°C for the alloys 444 and Fe18Cr.

The voltammograms are qualitatively similar (as has been found before [3]) but the peak height for Fe18Cr is significantly larger than for 444 and the peak potential of Fe18Cr is slightly positive (~20mV) of that of 444. This trend was found for all the sweep rates. Fig. 5.18 shows the diffusion diagnostic plot for both alloys at 25°C. The diagnostic plot for Fe18Cr gives, within experimental error, a horizontal line, indicating diffusion control of peak A processes at this temperature. The points for Fe18Cr are also all significantly larger in value than those for 444. However, the diagnostic plot for 444 increases slightly with increase in sweep rate. It is suggested that this result for 444 is due to the Mo component and can be partially explained if the passivating reaction involving Mo has a slow (rate determining) rate constant (compared to the passivating reactions involving Fe and Cr in Fe18Cr2Mo). If Mo reacts slowly, then at slow sweep rates its passivating influence is greater. Hence it is more difficult to break down the passive film in the transpassive region at slower sweep rates and therefore the current response would be less than if a uniform passive film over all sweep rates existed before entry into the transpassive region.

Therefore by assuming that the rate constant for the rate determining step of the passivating reaction(s) involving Mo is slow (compared to the rate constants for the rate determining steps of the passivating reactions involving Cr and Fe), the trends in the diffusion diagnostic data at 25°C and the trends in the variation of the apparent activation energy with sweep rate can be explained.

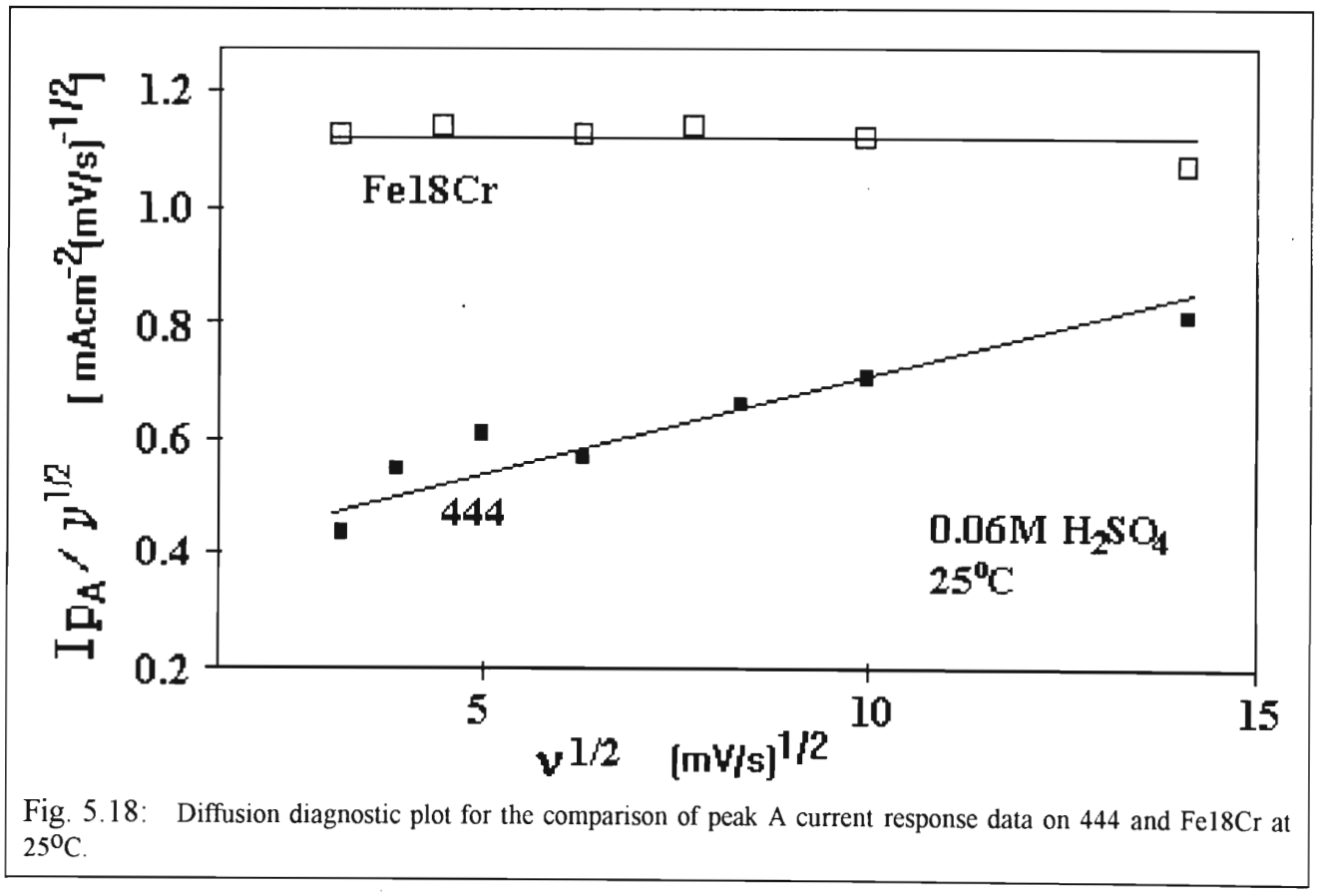

Fig. 5.18: Diffusion diagnostic plot for the comparison of peak A current response data on 444 and Fe18Cr at 25°C.

5.6. Final comments

In the beginning of the study only the 444 alloy was used. This was because, being the more corrosion resistant of the two, it was experimentally easier to use and far less time was spent on polishing 444 electrodes than was spent on polishing Fe18Cr electrodes. However, the previous results showed that the 1.7% Mo was a complicating, rather than a simplifying factor. Therefore the rest of the investigation was done with Fe18Cr.

The suggested explanation for the trends in the diffusion diagnostic plots needed further experimental validation. One way of investigating this would be to rotate the electrode. The peak A current response could be expected to be independant of rotation rate when transpassive reactions are predominantly solid state (i.e. when transport of ions within the film is rate determining). Since a high concentration of hydronium ions would favour dissolution of passivating metal oxides - which would then contribute towards breakdown of the passive film - a solid state mechanism (and therefore independance of the peak A current response) would be expected at a low hydronium ion concentration. Conversely, the peak A current response would be expected to be dependant on sweep rate at high acid concentrations. Therefore it was desirable to vary both the pH and the rotation rate in experiments as well as temperature and sweep rate. In order to have time to do this over a reasonable range of pH's, the temperatures and rotation rates used were limited to 25, 90°C (except in the pH 3.8 acetate buffer solution) and 0, 150 rad/s only, respectively. Apparent activation energies could therefore not be obtained for all but the pH 3.8 solution since only two points (from two temperatures) would be available for the Arrhenius plot.

An explanation of the secondary passivity exhibited in the voltammograms and investigations as to the possible reactions occuring in the transpassive region (in particular, is the peak A current response due mainly to oxidation of Cr species or Fe species ?) will be covered in chapter 6.

CHAPTER 6

6. VOLTAMMETRY AT A Fe18Cr ELECTRODE IN ACIDIC SOLUTIONS OF VARIABLE pH

This chapter is structured such that the voltammetric results for Fe18Cr in a selection of solutions (in order of increasing pH) are examined separately and then the overall results from the solutions of all the pH's used are examined. The two primary variables in these experiments were pH and sweep rate. The two secondary variables were temperature (25, 90°C) and rotation rate (0, 150 rad/s).

6.1. Voltammetric results in solutions of variable pH

Since it became apparent during the study that it was desirable to monitor the effect of the hydronium ion concentration without interference from anions, it became necessary to use acids with anions that are as "noble" (with respect to the alloy) as possible. Perchloric acid was therefore a better choice than sulphuric as the perchlorate ion is known to be relatively inert, whilst the sulphate anion tends to form temporarily passivating salt films. Unfortunately, at the higher pH's it was necessary to use a buffer in order to stabilise the pH. Acetate buffers were chosen because good results have been obtained with them previously [3]. However, Takahashi *et al* have proposed a mechanism for the active region on iron in acetate solutions where the acetate ion is involved in an adsorbed intermediate species, one of which is contained in a rds [72].

To check whether the acetate ion affects the transpassive region or not, an experiment was performed where two buffer solutions of the same pH (3.8) where made, but with different total analytical acetate ion concentrations. The first solution had $[OAc^-]$ = 1.0M and the second had $[OAc^-]$ = 0.1M. Cyclic voltammograms were obtained for each solution at 100 mV/s and 25°C. It was found that the value of I_{pA} for the second solution was just over half that of the first solution. Hence the acetate ion is involved in peak A processes. It was then decided that as the effect of the acid anion could not be removed, the next best thing would be to keep it consistent and hence all buffer solutions that were used had a total analytical acetate ion concentration of 1.0M. This high concentration was recommended by Takahashi *et al* [72] who found that low acetate ion concentrations gave artifacts due to insufficient buffering capacity.

6.1.1. pH 3.80: 0.9M CH_3COOH + 0.1M CH_3COONa

This solution gave good separation of peak A from oxygen evolution, particularly at the slower sweep rates and higher temperatures (*cf* fig. 3.9). The other important initial observation was that in this solution the current response at all potentials, sweep rates and temperatures was independent of rotation rate. All voltammograms in this section were obtained at 150 rad/s. In this case rotating the electrode merely had the practical use of freeing the electrode from bubbles e.g. in the oxygen evolution region. It is therefore very likely that at this pH transpassive processes are predominantly solid state. This also means that the passive film (and in particular the barrier layer) must remain appreciably intact during the voltammetric transition through peak A potentials. This is easily understood if dissolution reactions such as $Fe_2O_3 + 6H^+ \rightleftharpoons 2Fe^{3+} + 3H_2O$ are considered to be sensitive to the pH. It has been shown before that I_{pA} increases with increase in hydronium ion concentration [4,187]. This is because as the hydronium ion concentration increases, so does the degree of dissolution of passivating oxides in the transpassive region and more of the bare alloy surface is exposed directly to the solution. Hence at pH 3.8 (the least acidic solution used) it is possible that the barrier layer formed in the (primary) passive region remains mostly intact throughout the transpassive region prior to oxygen evolution. The peak A current response would then mostly be due to oxidation of cations within the film.

The voltammetric experiments in this solution were carried out at 60°C as well as the other two temperatures and hence it was possible to obtain values for apparent activation energies as in section 5.4. It was found that for sweep rates ≤ 100 mV/s the $E_{a,pA}$'s had an average value of 11.2 kJ/mole with a standard deviation of 0.5 kJ/mole. For 150 mV/s, $E_{a,pA}$ = 7.7 kJ/mole. It was difficult to obtain $E_{a,pA}$ values for faster sweep rates as at 25°C oxygen evolution interference became significant for $v > 150$ mV / s. Since dissolution reactions seem to play a minor role at this pH, it is not surprising that the apparent activation energy is initially independent of sweep rate.

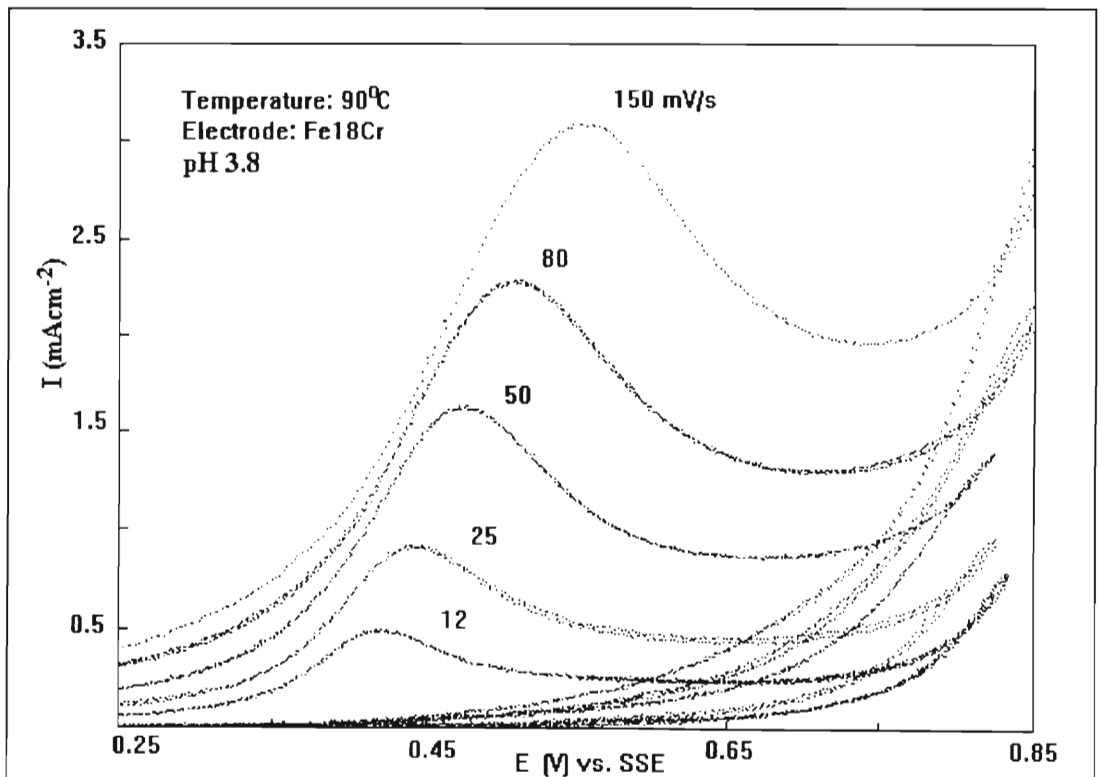

Fig. 6.1: Figure showing the effect of sweep rate on the peak A current response at 90°C in pH 3.8 acetate buffer solution.

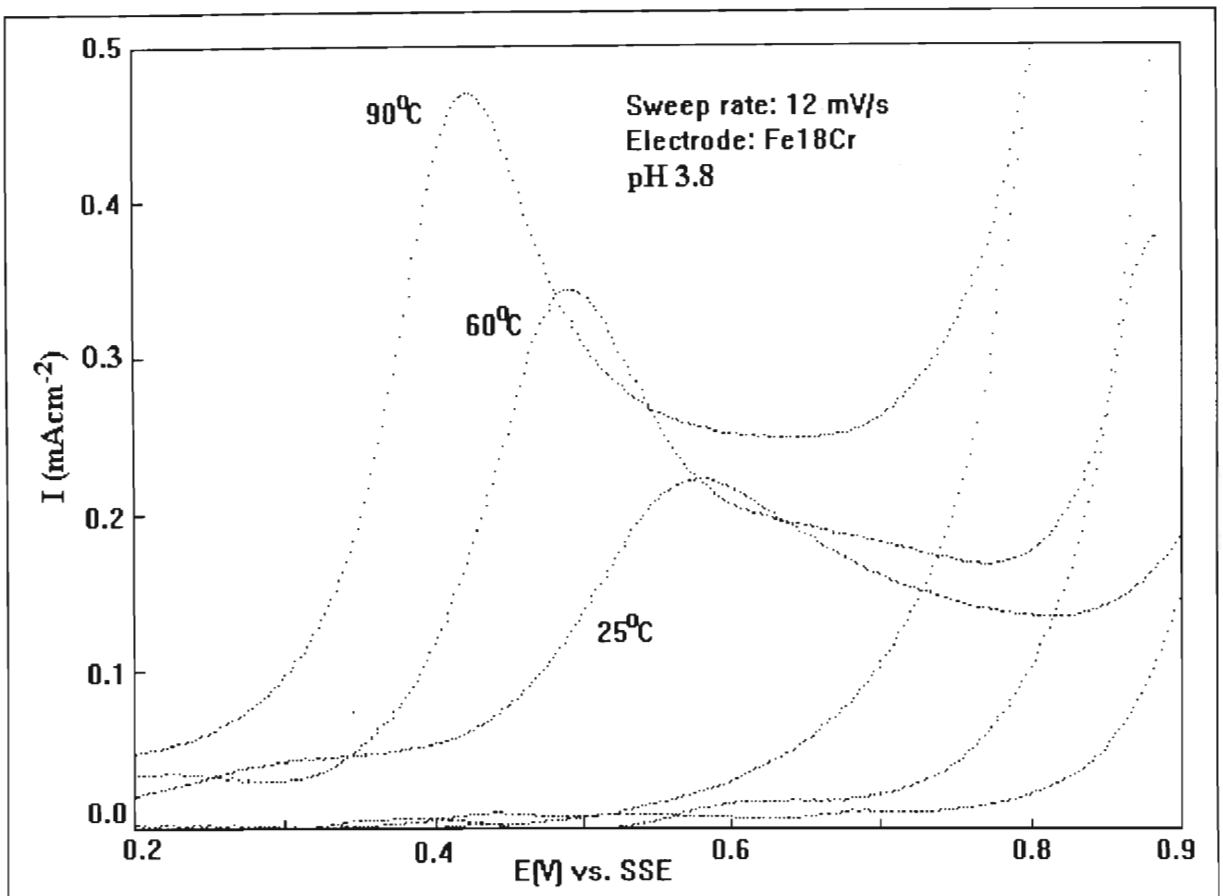

Fig. 6.2: Figure showing the effect of temperature on the peak A current response in pH 3.8 acetate buffer solution.

Figures 6.1 and 6.2 show the effect of sweep rate and temperature on the peak A current response, respectively. Fig. 6.3 shows the diffusion diagnostic plot generated from E_{pA} values and fig. 6.4 shows the diffusion diagnostic plot generated from I_{pA} values at 25 and 90°C.

Fig. 6.1 shows the gradual increase of I_{pA} and E_{pA} with sweep rate. The values of I_{pA} are shown quantitatively (as $I_{pA}/v^{1/2}$) in fig. 6.4. The results here are quite different to those for 444 in 0.06M H_2SO_4 (*cf* fig. 5.11). Instead of a positive deviation from the horizontal at slow sweep rates which increases with temperature, here a straight line with a positive slope (equivalent to a negative deviation from the horizontal at slow sweep rates) is obtained and this slope increases with temperature. The main difference in the experimental conditions used to obtain the results in figures 6.11 and 6.4 is that the former was obtained at a pH of 0.9 and the latter at a pH of 3.8. Again, if the forward rate of dissolution of passivating metal oxides (Fe_2O_3, Cr_2O_3 and others) is considered to be sensitive to pH (dissolution increasing as pH decreases), then the least dissolution will occur at the lowest pH. At slow sweep rates (in the pH 3.8 acetate solution) a compact passive film will have formed prior to voltammetric entry into the transpassive region. As the sweep rate is increased the passive film (prior to voltammetric entry into the transpassive region) becomes progressively less compact and protective (due to the electrode having spent progressively less time in the passive region). The resulting I_{pA} would be progressively larger than that predicted for the case where the limiting step is diffusion of ions (or ion vacancies) through a film which is consistently the same prior to voltammetric entry into the transpassive region for all sweep rates. This theoretical case would give a horizontal line in the diffusion diagnostic plot.

The positive slope of the (peak current) diagnostic plot is therefore probably due to the retarding effect that increasing the sweep rate has on the protective ability and degree of formation of the passive film prior to voltammetric entry into the transpassive region. As temperature increases, so do the rate constants of oxidation reactions (and the tensile stress on the passive film) and this retarding effect is therefore emphasised with the resultant increase in the slope of the diagnostic plot with temperature. McCrindle obtained cyclic voltammograms from 444 in various acidic media at very fast sweep rates (up to 50 V/s). He observed that peak A "disappeared into oxygen evolution" once the sweep rate was increased beyond a certain value, which was dependant on the electrolyte [188]. On further examination of these results it was noted that E_{tr} when peak A was present and E_{tr} when it had "disappeared" were almost exactly the same. It is therefore suggested that (instead of peak A disappearing into oxygen evolution) at the fastest sweep rates, the passive film is so incompletely developed that once the transpassive region is reached, rampant dissolution of the alloy substrate begins almost immediately and secondary passivity cannot be attained (no peak A). This then would be further evidence towards the suggestion that the transpassive behaviour of the anodic film is highly dependent on the "passivity" of the film before voltammetric entry into the transpassive region.

From figures 6.2 and 6.3 it can be seen that (unlike the results in 0.06M H_2SO_4 -*cf* fig. 5.13-) increasing the temperature decreases E_{pA} at a particular sweep rate. This may be because increasing the temperature at this pH raises the rate of dissolution of passivating metal oxides to a significant degree so that oxidation and or breakdown of the film is facilitated at a more negative potential than at the lower temperature (25°C). The peak potential diagnostic plot gave a positive deviation at slow sweep rates. Thus in strong and weak acids, Müller's pore resistance theory is not (totally) applicable to the transpassive behaviour of Fe-Cr alloys. The positive deviation in the peak potential diagnostic plot can again be explained by the hypothesis that a more protective passive film forms at slower sweep rates and hence greater mechanical stresses thereon and oxidation thereof are required (and hence greater potentials) than would be predicted by pore resistance theory.

Note that there are two competing effects:

1. Dissolution of passivating oxides by H^+ which is the predominant factor at pH 0.9 but does not occur appreciably at pH 3.8. At lower pH's dissolution of the anodic film in the transpassive region (and therefore I_{pA}) is enhanced (with respect to a diffusion controlled reaction) at the slower sweep rates.
2. The degree of formation of the passive film before voltammetric entry into the transpassive region. By "degree of formation of the passive film before voltammetric voltammetric entry into the transpassive region", the following is meant:
   In almost all of the voltammetric experiments performed for this thesis, the starting potential was negative of the passive region. Therefore, before transpassive potentials are reached, a passive film will exist on the electrode and the stability (or resistance to breakdown) of the passive film will depend on the time which it has had to form. i.e. the stability of the passive film will depend on the the sweep rate. For example, at a very fast sweep rate, the time spent in the passive region is small compared to the time spent at a slow sweep rate, and hence the passive film formed at the fast sweep

rate "before voltammetric entry into the transpassive region" (i.e. before E_{tr}) will be less stable than the passive film formed at the slow sweep rate and will be broken up more easily "after voltammetric entry into the transpassive region" (i.e. after E_{tr}) than the passive film formed at the slow sweep rate. The above factor is predominant in pH 3.8 solution where dissolution of passivating oxides is insignificant. When this effect is predominant, I_{pA} is enhanced (with respect to a diffusion controlled reaction) at faster sweep rates where the passive film is less well formed.

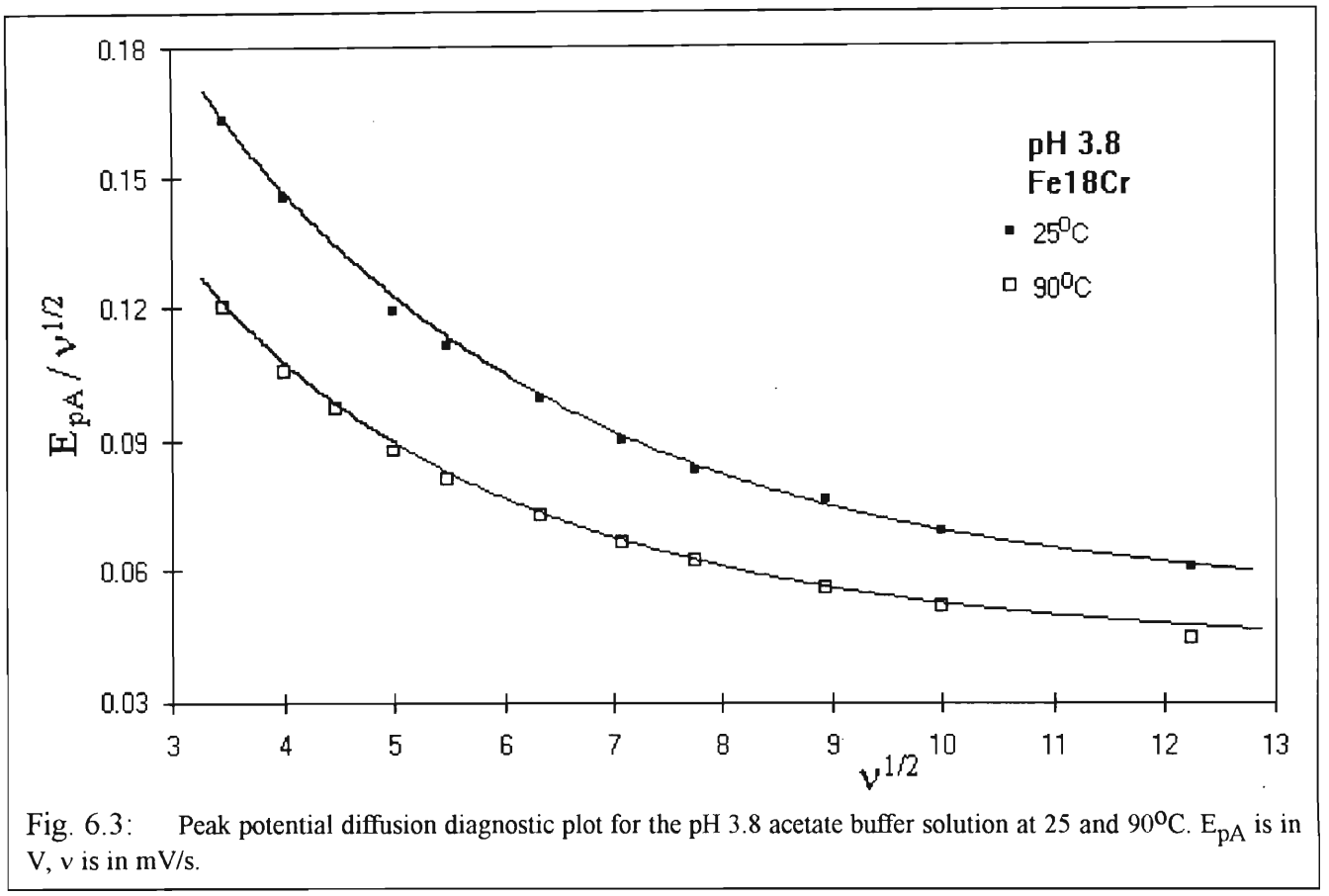

Fig. 6.3: Peak potential diffusion diagnostic plot for the pH 3.8 acetate buffer solution at 25 and 90°C. E_{pA} is in V, v is in mV/s.

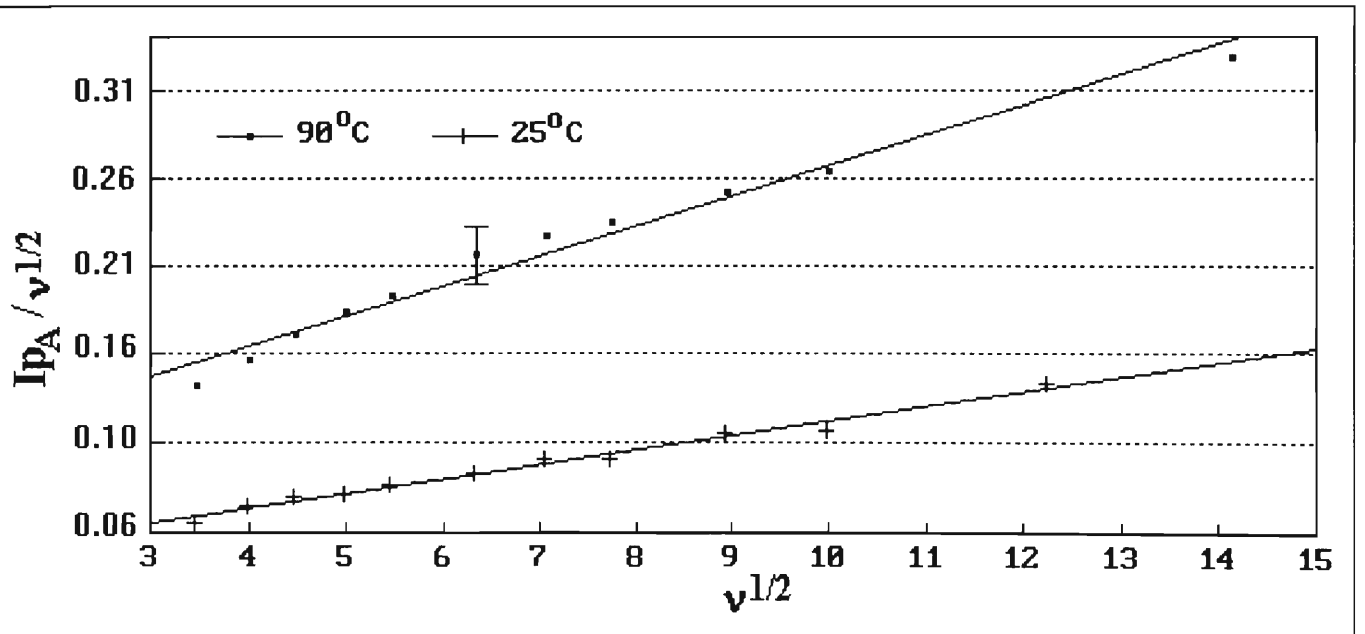

Fig. 6.4: Peak A current diffusion diagnostic plot for Fe18Cr in the pH 3.8 acetate buffer solution at 25 and 90°C

6.1.2. pH 2.40: 1.0M CH_3COOH

The results for this solution were qualitatively similar to those in the pH 3.8 acetate buffer solution and hence only the diagnostic plots of the results are shown. For this solution the voltammograms were also independent of rotation rate and, as with the pH 3.8 solution, 150 rad/s was used for all voltammograms. Fig. 6.5 shows the peak current diffusion diagnostic for this solution at 25 and 90°C. This plot is of particular interest because it represents an intermediate situation between the diagnostic plots for the weak and strong acid cases.

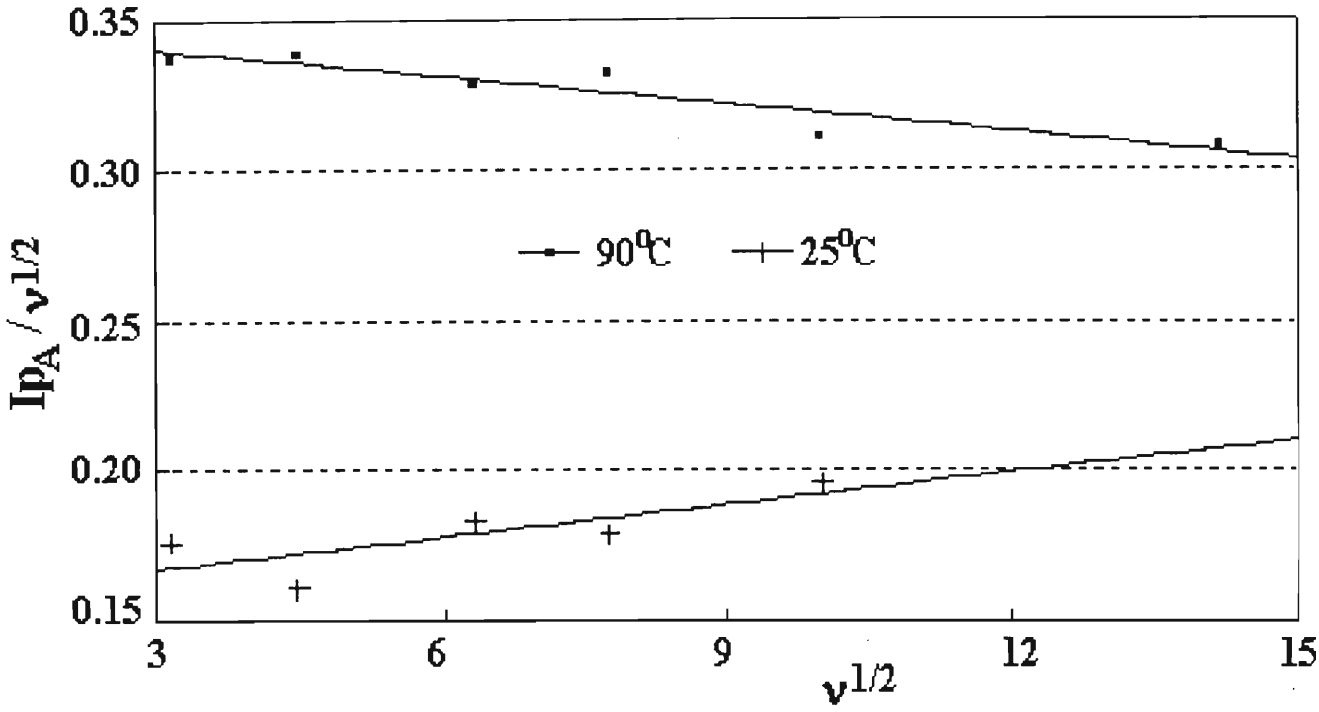

Fig. 6.5: Figure showing the peak current diffusion diagnostic plots for Fe18Cr in pH 2.4 solution.

At 25°C, the diagnostic best fit line has a positive slope (which is equivalent to an increasingly negative deviation from the horizontal as the sweep rate decreases). Thus at this temperature and pH, the degree of dissolution of the film at peak A potentials is not particularly significant. What is significant is the time spent in the passive region prior to voltammetric entry into the transpassive region. However, as in the pH 3.8 solution, the 90°C best fit line has a negative slope (which is equivalent to an increasingly positive deviation from the horizontal as the sweep rate decreases). This probably means that at this higher temperature, where the rate of the dissolution of passivating oxides is increased with respect to that at 25°C, the dissolution reaction(s) are significant. It will be shown in following sections that as the pH is decreased so the positive deviation from the horizontal of the peak current diffusion diagnostic plot at slow sweep rates and at constant temperature increases. The hydronium ion is therefore an active species. A general reaction for the dissolution of passivating oxides can now be defined

$$M_xO_y + 2yH^+ \rightleftharpoons xM^{2y/x+}_{(aq)} + yH_2O \qquad (6.1)$$

The reaction assumes oxides instead of oxyhydroxides, but the qualitative observation from either case is the same - by Le Chatelier's principle an increase in $[H^+]$ (or a decrease in pH) causes the reaction to shift

to the right. The more the reaction is shifted to the right the more likely it is that some of the bare alloy (or a greater surface area of the bare alloy) will be exposed directly to the solution.

Fig. 6.6 shows the peak potential diagnostic plot for the two temperatures and the results and interpretation are qualitatively the same as for the pH 3.8 solution.

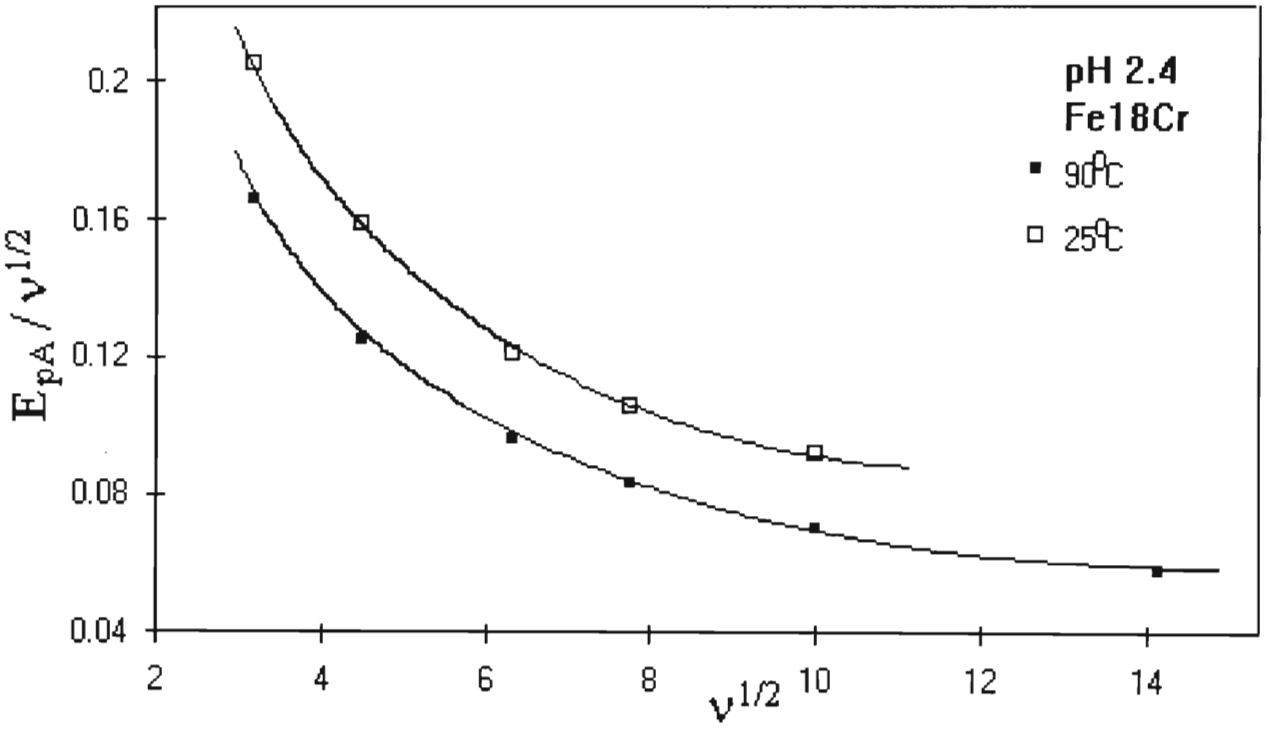

Fig. 6.6: Peak potential diffusion diagnostic plot for the pH 2.4 solution at 25 and 90°C.

6.1.3. pH 1.40: 0.02M H_2SO_4 + 0.94M CH_3COOH

This solution represented another intermediate situation as the peak current diagnostic plot at 90°C (fig. 6.7) gave a more significant deviation from the horizontal than in the pH 2.4 solution but a less significant deviation than in more acidic solutions, again showing the effect of decreasing the pH. The acetic acid was included because of the favourable affect that the acetate ion has in separating peak A from oxygen evolution. The solution was made up to an ionic strength of 1.00 as with the previous two solutions. The voltammograms were qualitatively similar to those of 444 in 0.1M H_2SO_4 and are not included here. Only data at 90°C was obtained for this solution.

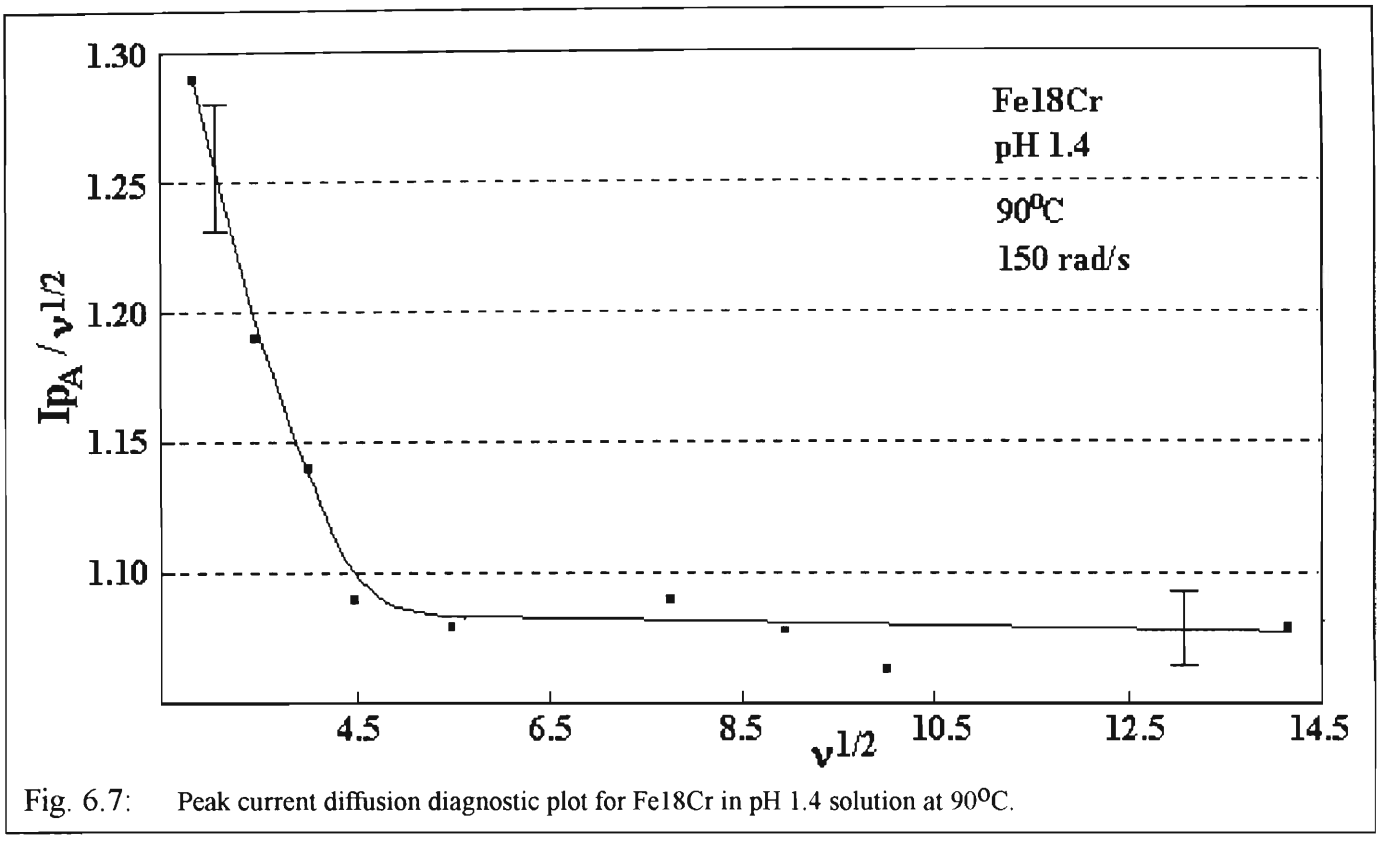

Fig. 6.7: Peak current diffusion diagnostic plot for Fe18Cr in pH 1.4 solution at 90°C.

The peak potential diagnostic plot is also not included here as it imparts no new information (a positive deviation at slow sweep rates is again obtained).

Note that a trend is forming. As pH decreases, an increasing positive deviation from the horizontal in the diffusion diagnostic plot at slow sweep rates is occuring. This continues to indicate the importance of H^+ in dissolution reactions at transpassive potentials.

6.1.4. pH 0.54: 0.290M $HClO_4$

This was the most acidic solution used and gave slightly better separation of peak A from oxygen evolution than in 0.06M H_2SO_4. Results in perchlorate solutions were important as the perchlorate anion is inert in these oxidative conditions. Therefore if the peak current diffusion diagnostic plots for peak A continued the previous trends in this solution (being the most acidic solution, it should give the greatest positive deviation from the horizontal at slow sweep rates) then these trends could definitely be attributed to the effect of the H^+ ion. Figures 6.8 and 6.9 show these diagnostic plots for 90 and 25°C respectively.

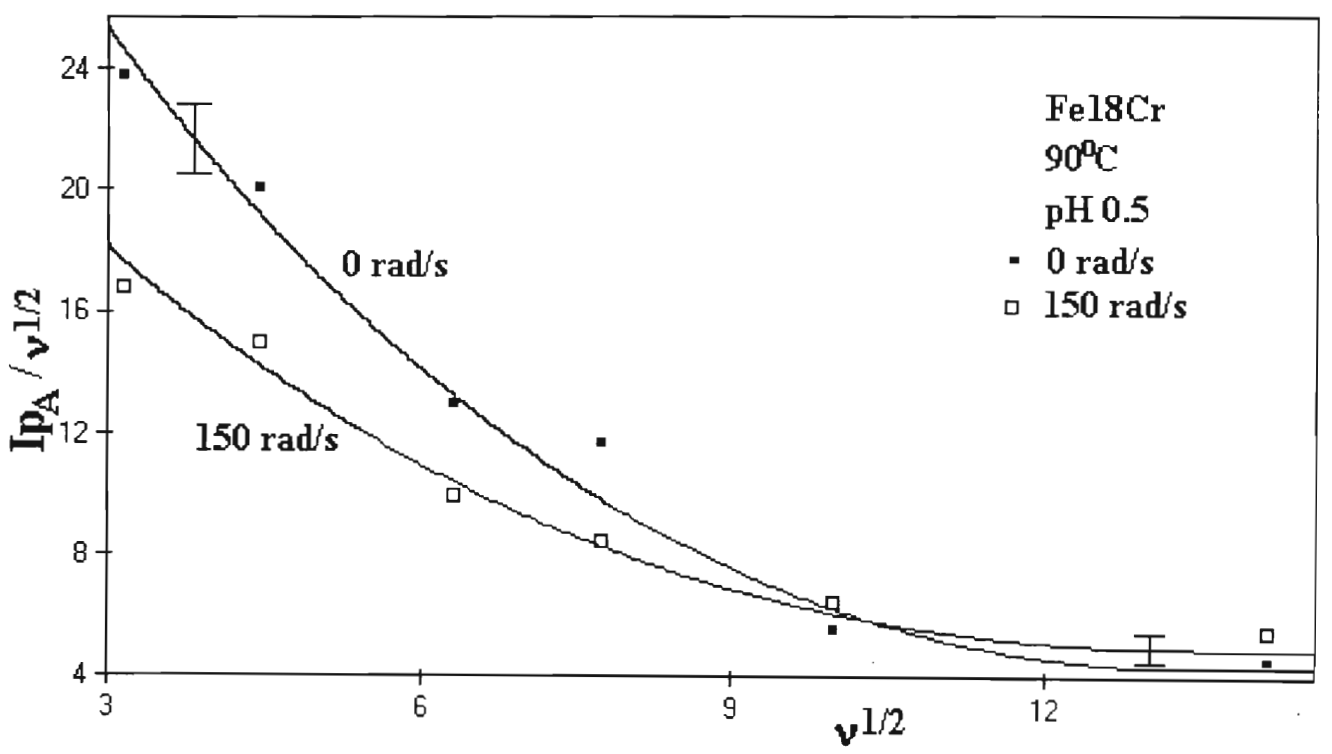

Fig. 6.8: Peak current diffusion diagnostic plot for peak A in the pH 0.5 solution at 90°C.

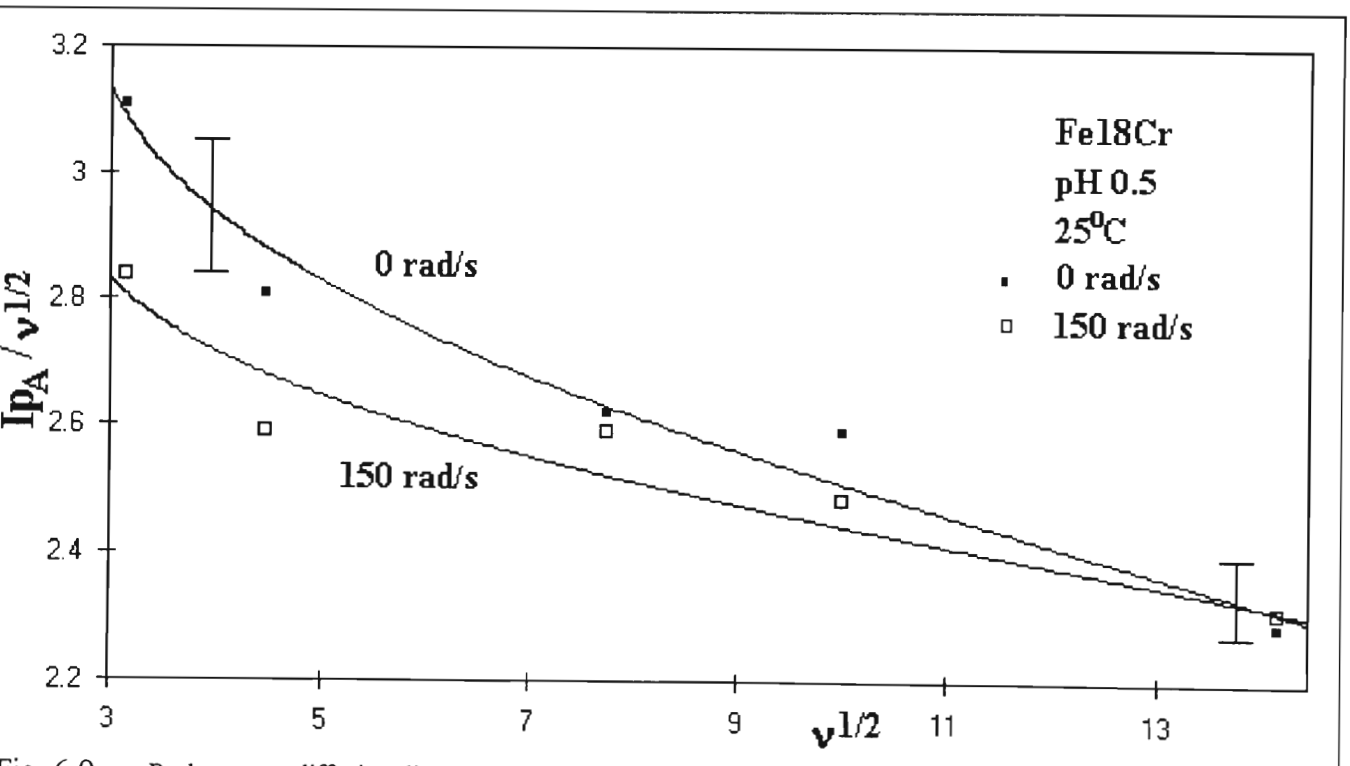

Fig. 6.9: Peak current diffusion diagnostic plot for peak A in the pH 0.5 solution at 25°C.

As the diagnostic plots show, there is significant deviation from the horizontal, beginning even at some of the faster sweep rates and also for the first time at 25°C . In order to further demonstrate the degree of this "deviation", fig. 6.10 shows some of the voltammograms that were obtained.

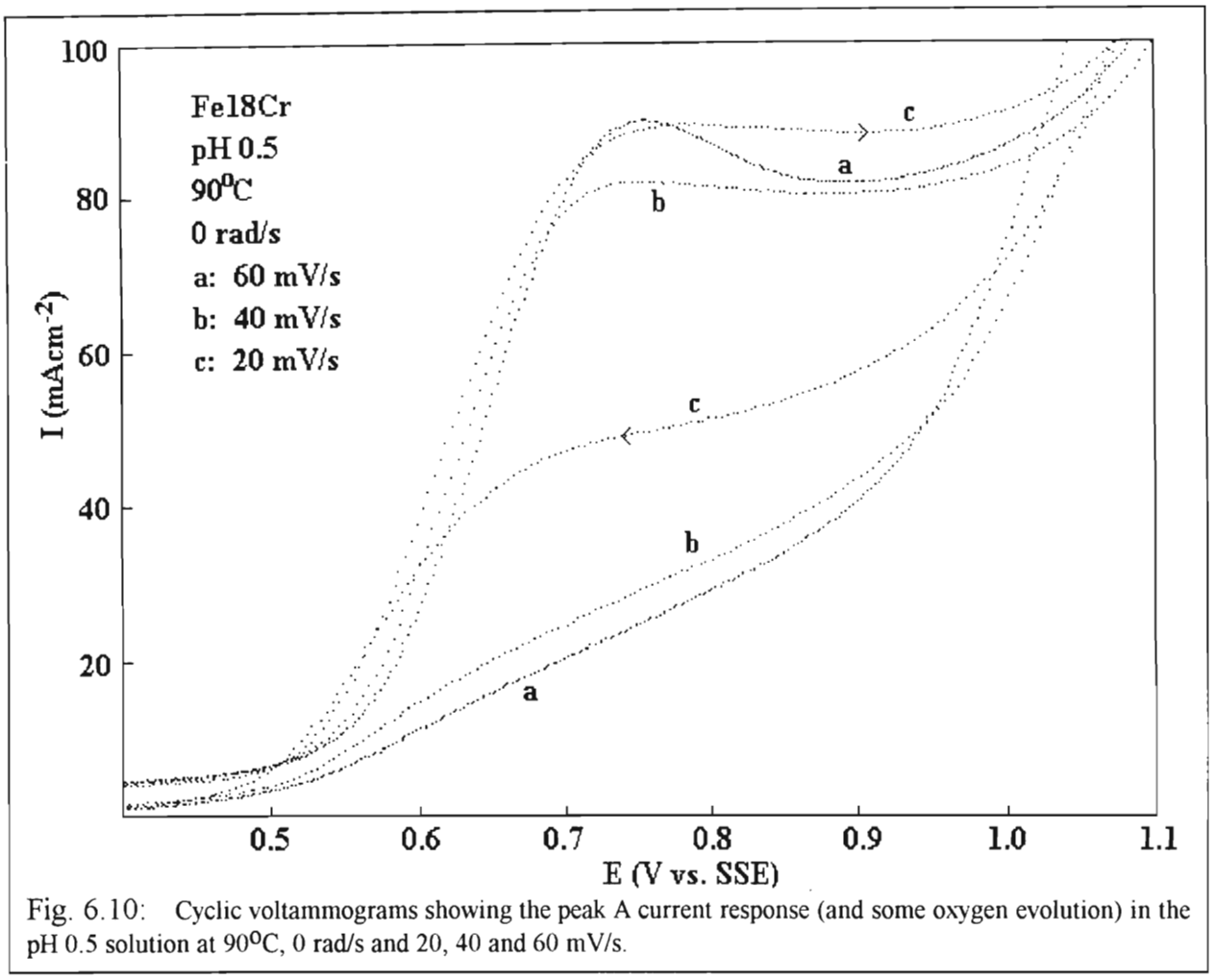

Fig. 6.10: Cyclic voltammograms showing the peak A current response (and some oxygen evolution) in the pH 0.5 solution at 90°C, 0 rad/s and 20, 40 and 60 mV/s.

Fig. 6.10 shows that in some cases as the sweep rate is decreased, the peak current increases. The explanation is that at this pH and temperature, the dissolution of passivating oxides[a] (*cf* reaction (6.1)) is a major component of peak A processes. As the sweep rate is decreased, more time is spent at peak A potentials and therefore more of the passivating oxides are removed, exposing more of the bare electrode directly to the solution. At this pH, the greater dissolution of the passive film (therefore providing a greater surface area of exposed alloy) as the sweep rate is decreased offsets the normal voltammetric effect of the increase of concentration gradient across the Nernst diffusion layer with increase in sweep rate. This does not happen at the highest pH (pH 3.8) because here the acid concentration is not sufficient for reaction (6.1) to be significant at transpassive potentials.

Fig. 6.10 also shows that as the sweep rate decreases, the reverse sweep of the voltammogram becomes closer to the forward sweep and the peak appears to form a plateau, although it is acknowledged that this latter observation may be due to oxygen evolution interference. Both of these effects were shown to be characteristic of a catalytic process (*cf* section 2.3.2). As the voltammograms in fig. 6.10 demonstrate, it was difficult to obtain E_{pA} values because of the plateau shapes of the peaks.

[a] In particular, the oxides of the barrier layer are dissolved.

Figures 6.8 and 6.9 also show that in this solution I_{pA} is dependant on rotation rate (this was in fact the case for all solutions more acidic than and including the pH 1.4 solution). The processes contributing to peak A are therefore at least partly governed by ions in solution (rather than ions in the anodic film). This is not surprising because in the most acidic solution the most dissolution of passivating oxides (and therefore also of the bare alloy itself) can be expected to occur. The protective barrier film is therefore also broken down to the greatest degree in the most acidic solution - this can be seen by comparing the size of the transpassive current densities in the various solutions at any one sweep rate as a function of pH.

Peak A processes are most dependent on rotation rate at the slowest sweep rate. At 10 mV/s and 90°C, I_{pA}(0 rad/s) was 42% larger than I_{pA}(150 rad/s). However, at the fastest sweep rates ($\nu \geq 100$ mV/s), and within experimental error, it appears that I_{pA} again becomes independent of rotation rate. Also, it was noticed that at fast sweep rates I_{pA}(150 rad/s) was consistently if only slightly larger than I_{pA}(0 rad/s). An explanation for the dependence of I_{pA} on rotation rate is suggested in section 6.4

6.2. Overall diffusion diagnostic results

In terms of the peak potentials, a general trend found was that as the pH decreased, E_{pA} moved positively. Between pH 3.8 and 0.5 at a constant sweep rate, E_{pA} could vary as much as 200 mV. Whether E_{pA} was affected by temperature was dependant on the solution. In sulphate solutions E_{pA} was mostly independent of temperature. In acetate solutions E_{pA} decreased with temperature. In the pH 0.5 perchlorate solution it was difficult to measure E_{pA} because of the broadness of peak A peaks and oxygen evolution interference. However, the positive deviation of the peak potential diagnostic plot at slow sweep rates was consistent for all pH's and temperatures.

Figures 6.11 and 6.12 show the peak current (for peak A) diffusion diagnostic plots for all pH's at 90 and 25°C respectively. $Log(I_{pA}/v^{1/2})$ was used on the y-axis instead of $I_{pA}/v^{1/2}$ in order that all the points might meaningfully be included on the scale (there was a range of over two orders of magnitude in the $I_{pA} / v^{1/2}$ values).

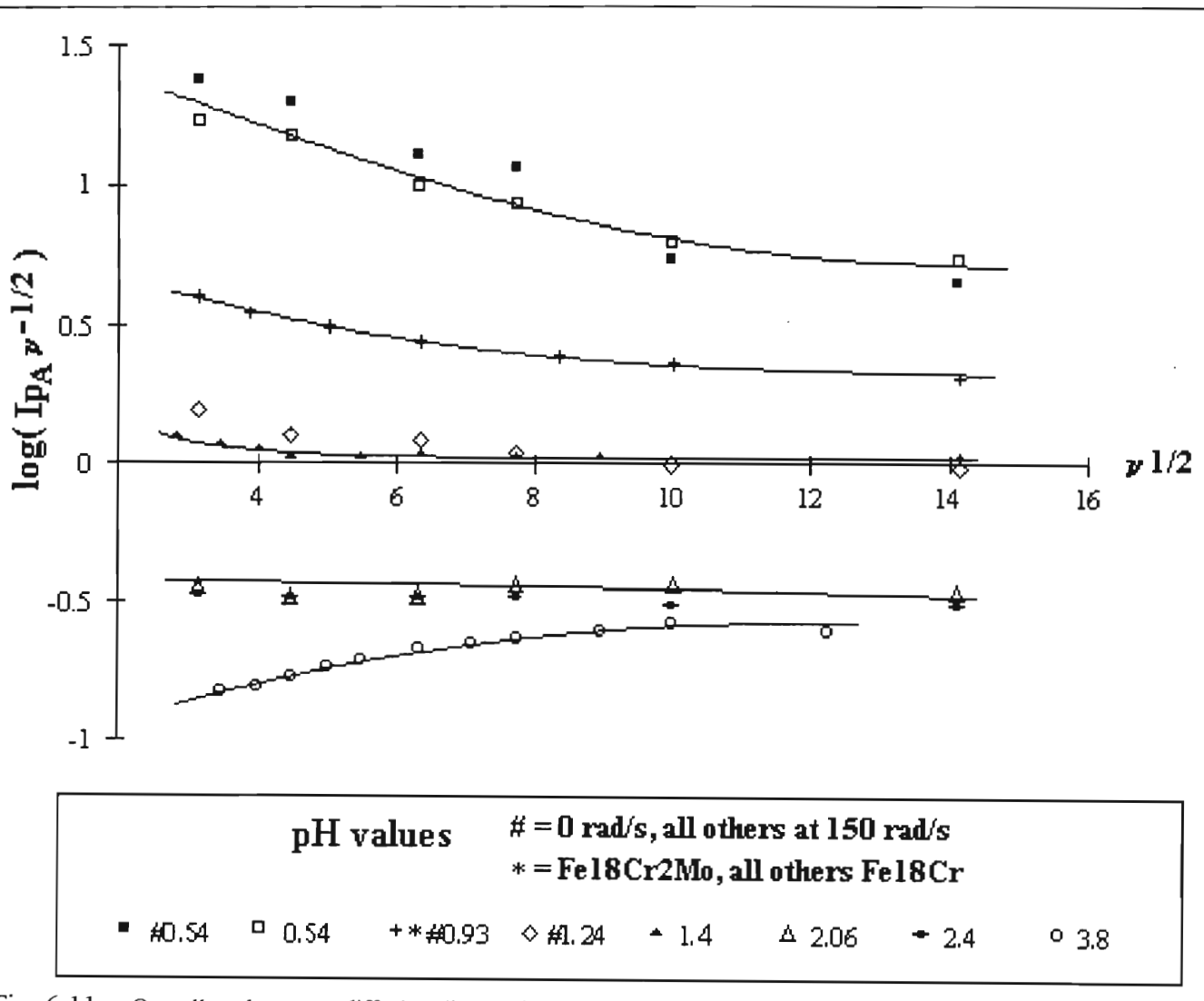

Fig. 6.11: Overall peak current diffusion diagnostic plot (for peak A) for all the solutions used, at 90°C.

Fig. 6.11 shows unequivocally the effect of pH on the peak A current response. As the solutions become more acidic the peak currents, in general, increase and the deviation from the horizontal at slow sweep rates changes from a negative to a positive one. Unfortunately, no quantitative correlation between

pH and I_{pA} could be made as the effect of anions such as acetate and sulphate cannot be quantified and definitely significantly affect peak A processes. The effect of pH, despite the interferences of the anions of the electrolytes is nevertheless clear.

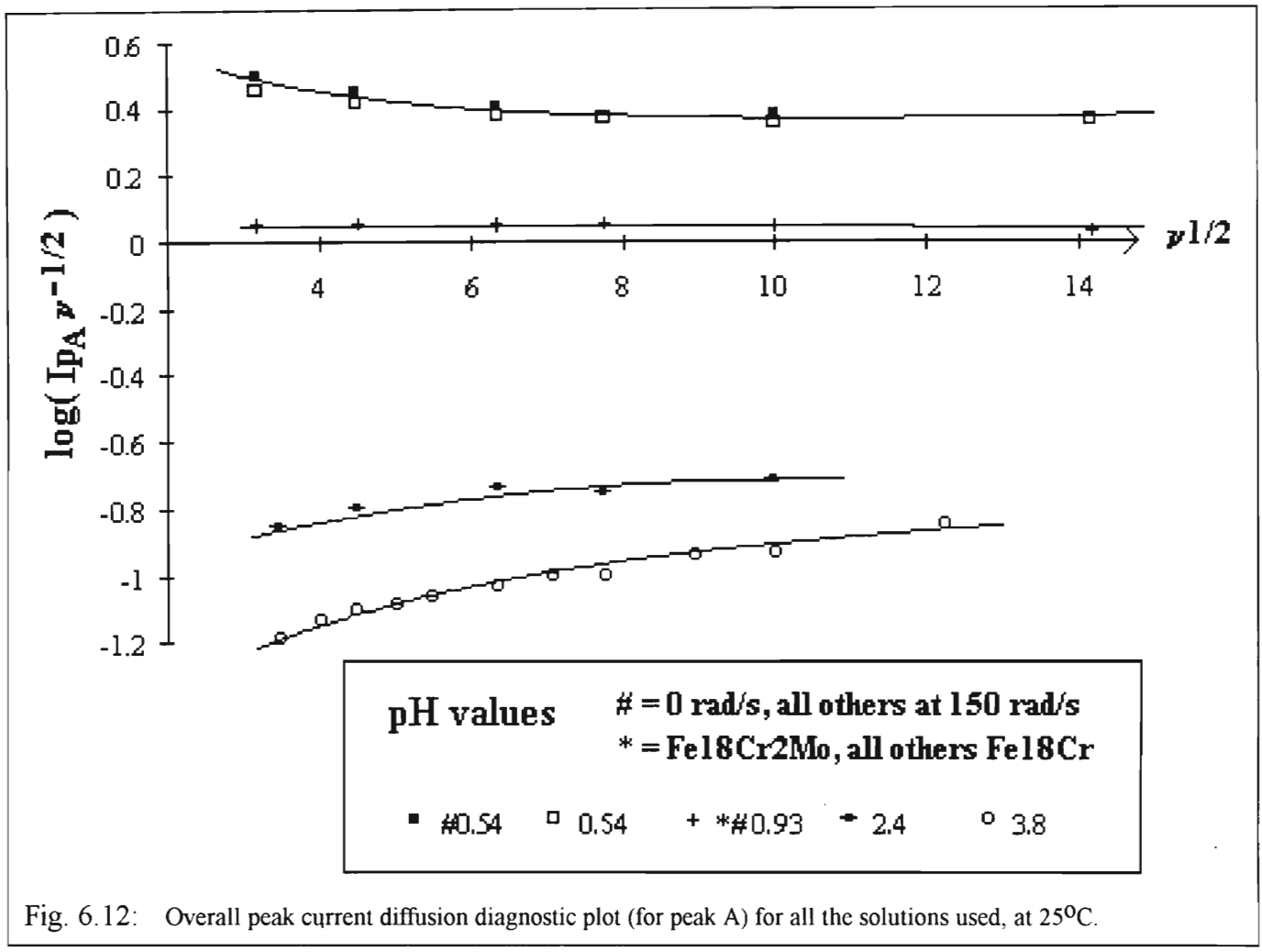

Fig. 6.12: Overall peak current diffusion diagnostic plot (for peak A) for all the solutions used, at 25°C.

The 25°C data gives the same qualitative results as the 90°C data except that, as is to be expected in the less aggressive -25°C- solutions, neither the peak currents nor the deviations from the horizontal in the diagnostic plots are as large as in the same solutions at 90°C.

6.2.1. Diffusion diagnostic results and the competition between activation and diffusion control of peak A processes

A final comment is that when a positive deviation from the horizontal (at slow sweep rates) is seen, this can be interpreted as a situation where **there is activation control rather than diffusion control**. However, the reason why there is activation control is because the conditions are such (low pH and high temperatures) that the protective passive film is being removed. Hence some of the substrate is being directly exposed to the solution so that there can be no diffusion limiting situations of substrate cations being transorted to the solution or solvent anions being transported to the substrate through an anodic film - the anodic film has been removed. Also, at slow sweep rates there is more time for the anodic film to be dissolved. As the sweep rate decreases, therefore, more of the electrode is exposed directly to the solution and there is a greater degree of activation control.

However, in conditions which do not favour the dissolution of the anodic film at transpassive potentials (higher pH), diffusion control will predominate because the anodic film, although it may become porous and less protective, remains largely intact and rates of reaction in the transpassive region are still limited by the transport of ions through the anodic film. In this case, decreasing the sweep rate has the opposite effect to that in the low pH, high temperature scenario. As the sweep rate is decreased, the time spent in the passive region is increased and the anodic film, before voltammetric entry into the transpassive region becomes more stable and more passivating (i.e. less amenable to the transport of ions within itself). Therefore, as the sweep rate decreases, diffusion through the anodic film becomes more difficult (at higher pH - e.g 3.8) and a negative deviation at slow sweep rates is obtained.

Therefore, for the experimental systems in this thesis, a positive deviation of the diffusion diagnostic plot at slow sweep rates reflects a system predominantly under activation control at the (slow) sweep rates which exhibit the positive deviation. A horizontal line, or a portion of a plot which contains a horizontal line reflects diffusion control. A negative deviation at slow sweep rates reflects diffusion control for the system over all the sweep rates contained in the plot.

6.3. Effect of addition of cations to the solution on peak A processes

So far the effect of pH has been considered in general terms and the dissolution of passivating oxides has been referred to. But the question remains - what passivating oxides ? Does Cr(X) dissolve or does Fe(III) and Fe(II) dissolve from the film and the electrode ? Or do both dissolve ? The major possibilities of peak A oxidation reactions that have been covered in the literature review are:

$$Cr(III) \rightarrow Cr(VI) \quad and \quad Fe(II) \rightarrow Fe(III)$$

The more detailed version of the former reaction has been suggested by Macdonald and others [11,13,177]

$$Cr_2O_3 + 5H_2O \rightarrow 2CrO_4^{2-} + 10H^+ + 6e^- \tag{6.2}$$

and the more detailed reaction for the oxidation of Fe(II) could be, for example

$$FeO + 2H^+ \rightarrow Fe^{3+}_{(aq)} + H_2O + e^- \tag{6.3}$$

It is important that reaction (6.2) produces protons whilst reaction (6.3) consumes them. The literature shows that all of Fe(II), Fe(III) and Cr(III) have been found in the passive film of Fe-Cr alloys in acidic solutions at potentials close to E_{tr} [11,146].

The following voltammetric experiments were therefore an attempt to see the effect of adding precisely each of the three above cations to some of the solutions which were used.

6.3.1. Addition of Fe(II) to pH 3.8 solution

Figures 6.13 and 6.14 show the effect of adding 0.01M Fe^{2+} to the pH 3.8 solution at 25°C and at 12 and 50 mV/s respectively.

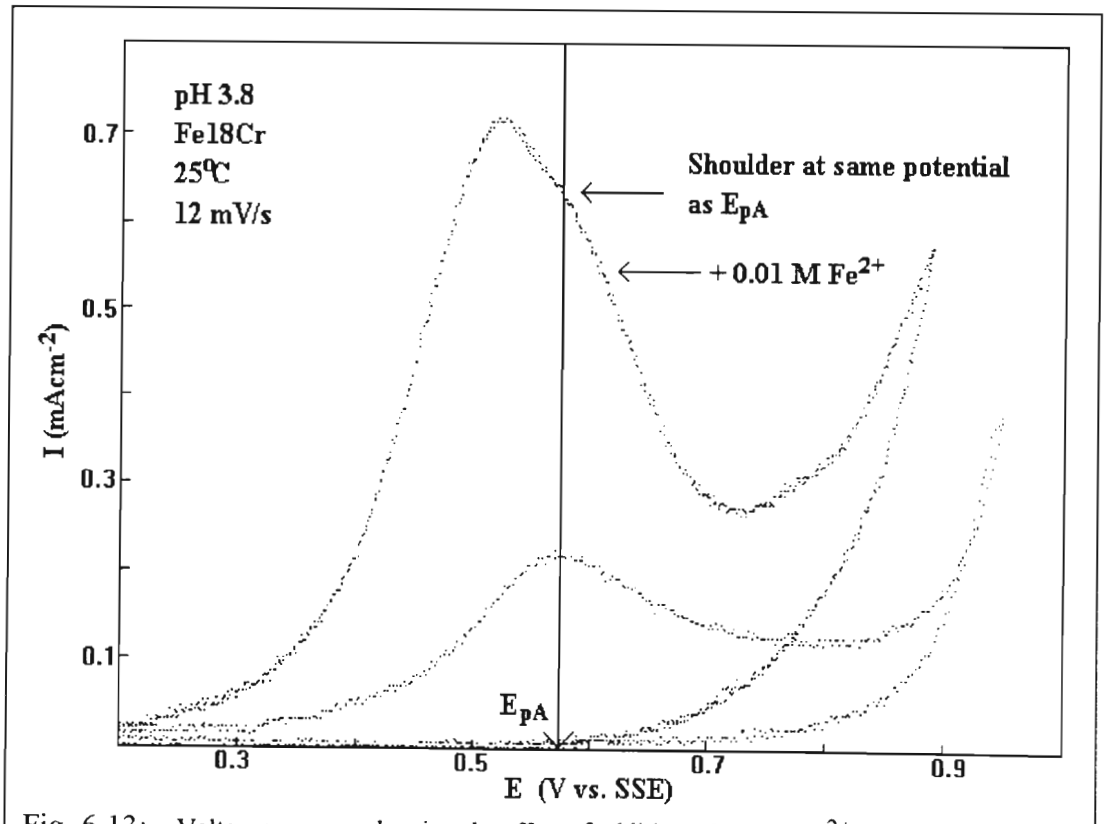

Fig. 6.13: Voltammograms showing the effect of addition of 0.01M Fe^{2+} to a pH 3.8 solution on the peak A current response at 25°C and 12 mV/s.

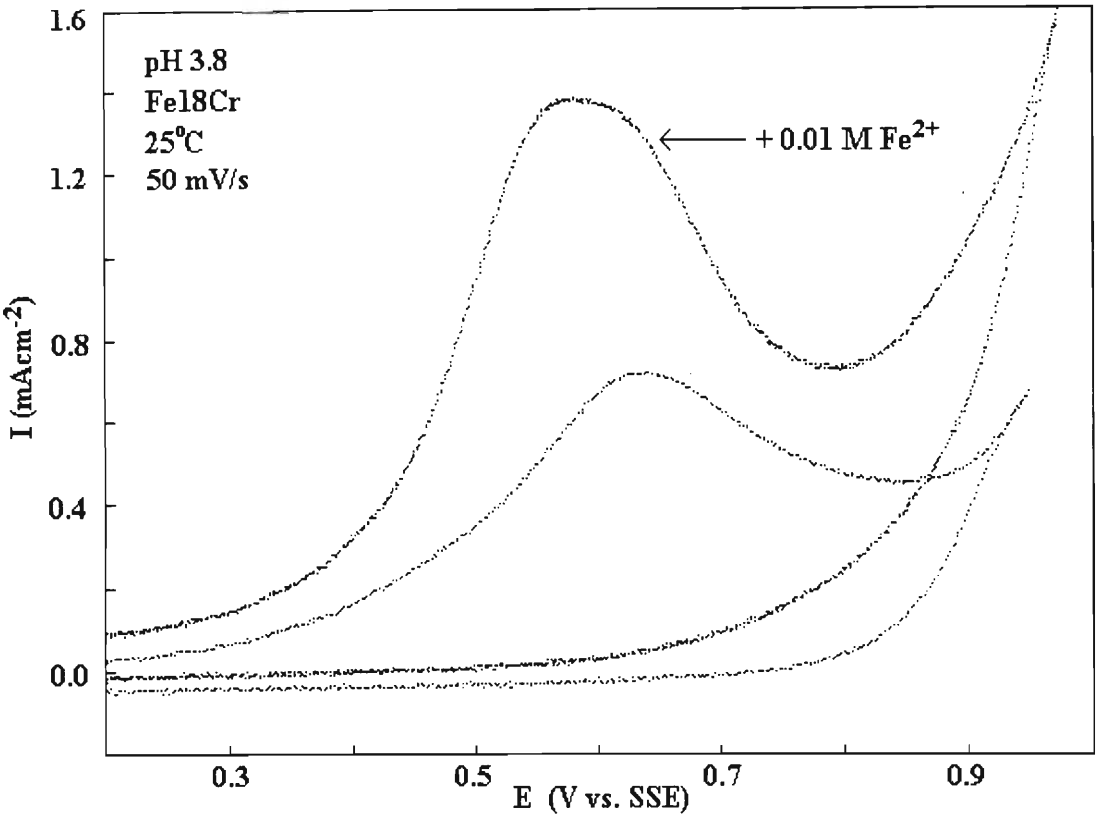

Fig. 6.14: Voltammograms showing the effect of addition of 0.01M Fe^{2+} to a pH 3.8 solution on the peak A current response at 25°C and 50 mV/s.

In fig. 6.13 the increase in peak A current response (at 12 mV/s) obtained by adding the 0.01M Fe^{2+} was 330%. Also, the peak potential of the Fe^{2+} CV is slightly negative of that of the normal pH 3.8 CV and a shoulder exists on the anodic side of the Fe^{2+} CV, the potential of which is exactly E_{pA}. It appears then that aqueous Fe^{2+} is oxidised at the electrode at potentials corresponding to the rising part of peak A. However, at this pH it was suggested that the passive film remains mostly intact during peak A potentials and that the peak A current response is mostly due to cations within the film being oxidised. It is perhaps not surprising that E_{pA} is slightly positive of the Fe^{2+} CV peak potential as in the normal pH 3.8 solution metal oxides, possibly within a stable lattice structure, are being oxidised whereas in the solution containing 0.01M Fe^{2+} aqueous ions are being oxidised.

In fig. 6.14 the shoulder at the faster sweep rate has disappeared into the Fe^{2+} CV peak itself, but the peak potential of the Fe^{2+} CV is still slightly negative of E_{pA} and the peak itself is broader than the normal pH 3.8 peak A peak. The main conclusion is that the oxidation of Fe(II) to Fe(III) can definitely occur at peak A potentials in pH 3.8 solution.

6.3.2. Addition of Fe(II), Fe(III) and Cr(III) to pH 0.5 solution

Each of the above ions (from AR $FeSO_4$, $Fe_2(SO_4)_3$, and $Cr(ClO_4)_3$ respectively) was made up into separate 0.3M $HClO_4$ solutions (pH 0.5) so that the concentration of the each cation was 0.04M in each 0.3M $HClO_4$ solution. CV's were then obtained for each of the above three solutions and for the usual 0.3M $HClO_4$ solution at 25°C and at 0 and 150 rad/s between 10 and 200 mV/s. The peak potentials and peak currents (of peak A) were then compared in various plots as a function of sweep rate.

It should be noted that the greatest change in the peak A current response was obtained with the solution containing the ferrous cation. Fig. 6.15 shows this effect at 40 mV/s. As in the pH 3.8 solution, the "ferrous peak A" is slightly negative (20 mV) of the normal peak A. As demonstrated by fig. 6.15, no shoulders on peak A were obtained in the experiments with the pH 0.5 solutions.

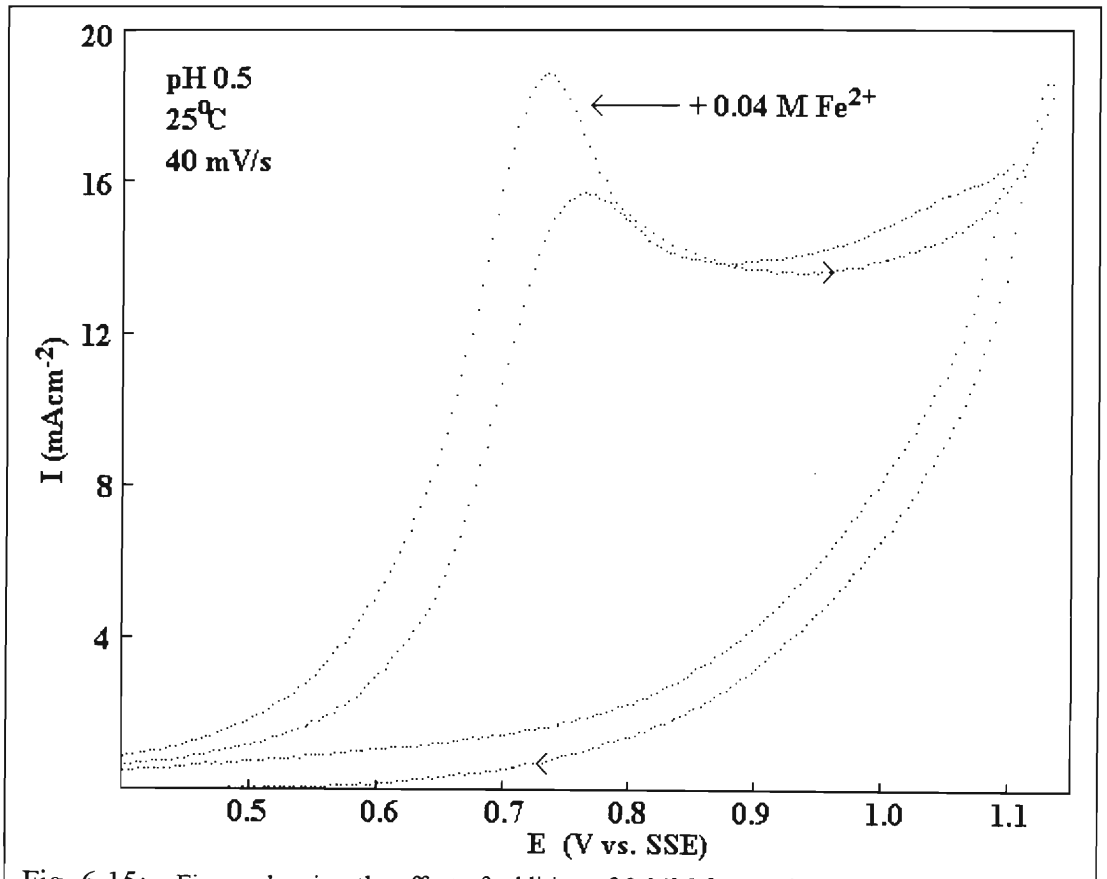

Fig. 6.15: Figure showing the effect of addition of 0.04M ferrous ion on the peak A current response in pH 0.5 solution at 25°C,40 mV/s and 0 rad/s.

The other plots are all shown consecutively as follows:

- Figures 6.16, 17, 18 show the effect of rotation on the peak current diffusion diagnostic plots of the solutions containing Fe^{2+}, Fe^{3+} and Cr^{3+} respectively.
- Figures 6.19 and 6.20 both show the superimposed peak current diffusion diagnostic plots for the usual pH 0.5 solution, and the same solution containing (separately) Fe^{2+}, Fe^{3+} and Cr^{3+} (i.e. four superimposed diagnostic plots per figure) at 150 and 0 rad/s respectively.
- Lastly, fig. 6.21 shows, for each of the four solutions, a plot of the peak A peak potential versus sweep rate. This plot shows the variations in E_{pA} more simply than the peak potential diagnostic plot.

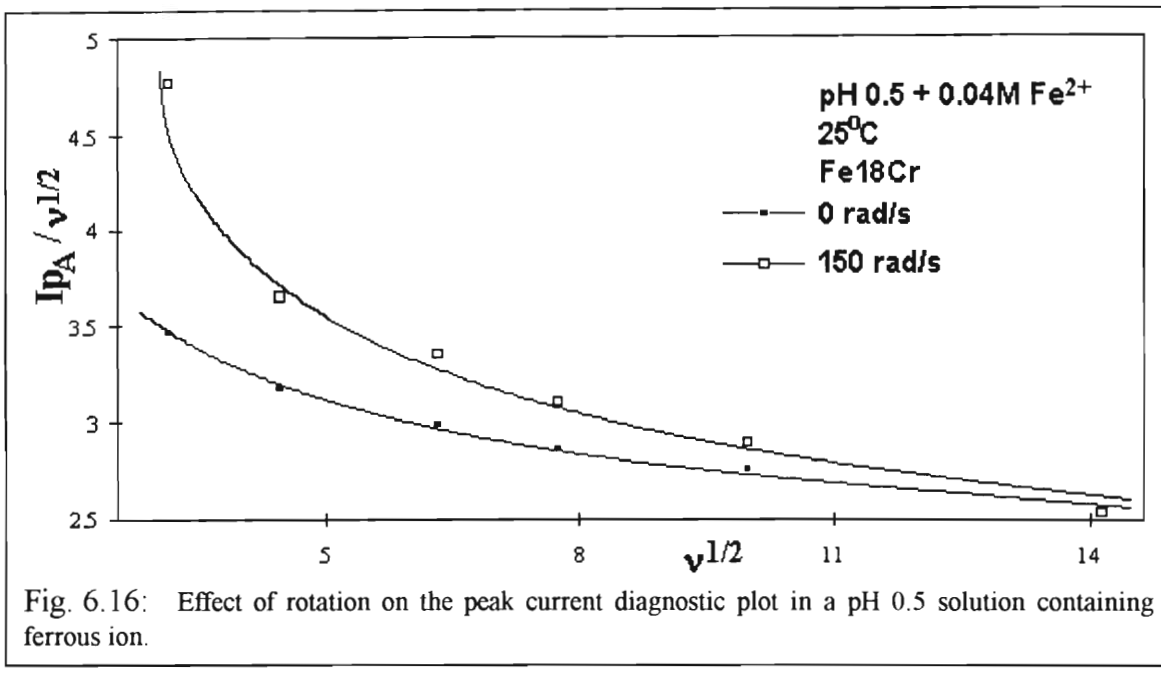

Fig. 6.16: Effect of rotation on the peak current diagnostic plot in a pH 0.5 solution containing ferrous ion.

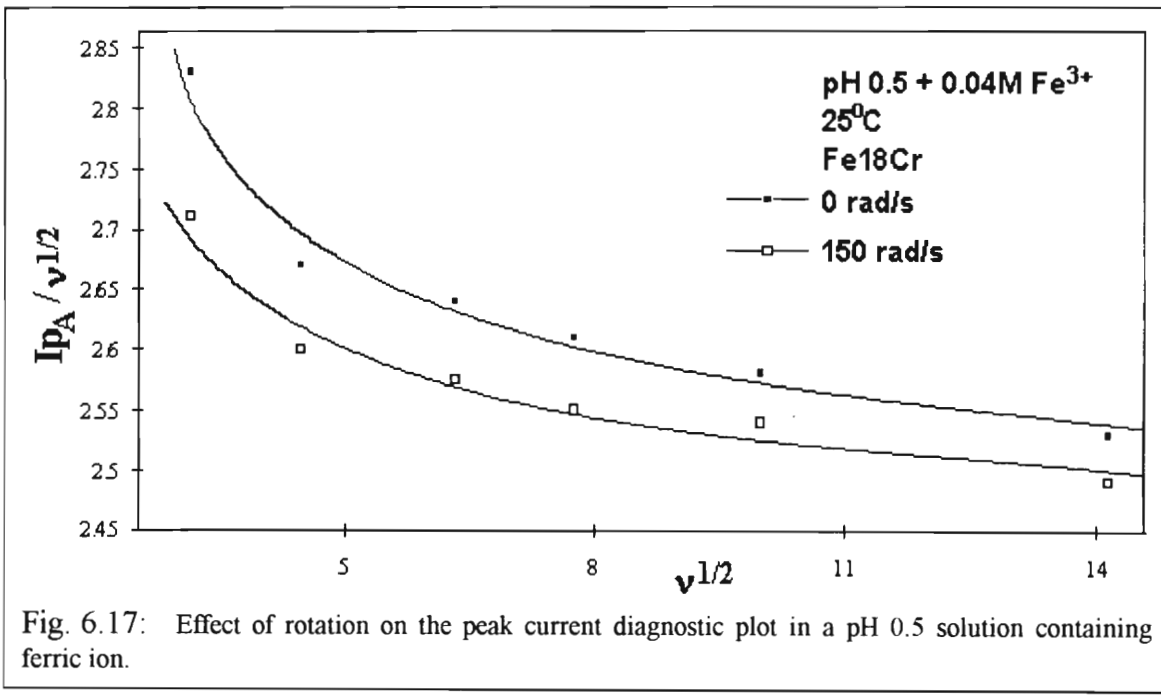

Fig. 6.17: Effect of rotation on the peak current diagnostic plot in a pH 0.5 solution containing ferric ion.

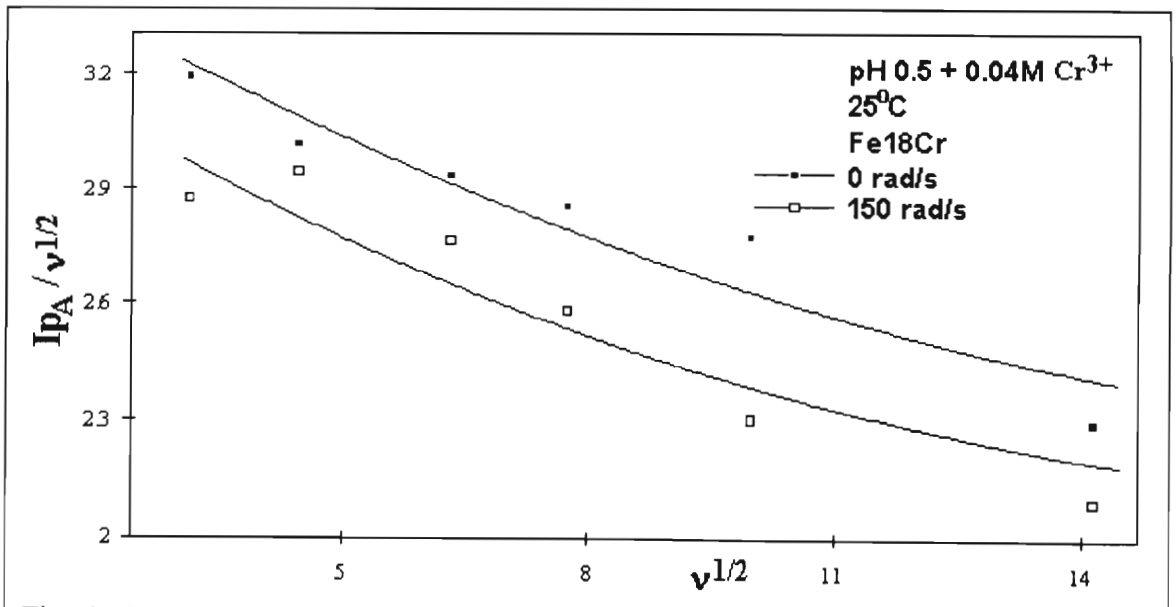

Fig. 6.18: Effect of rotation on the peak current diagnostic plot in a pH 0.5 solution containing chromic ion.

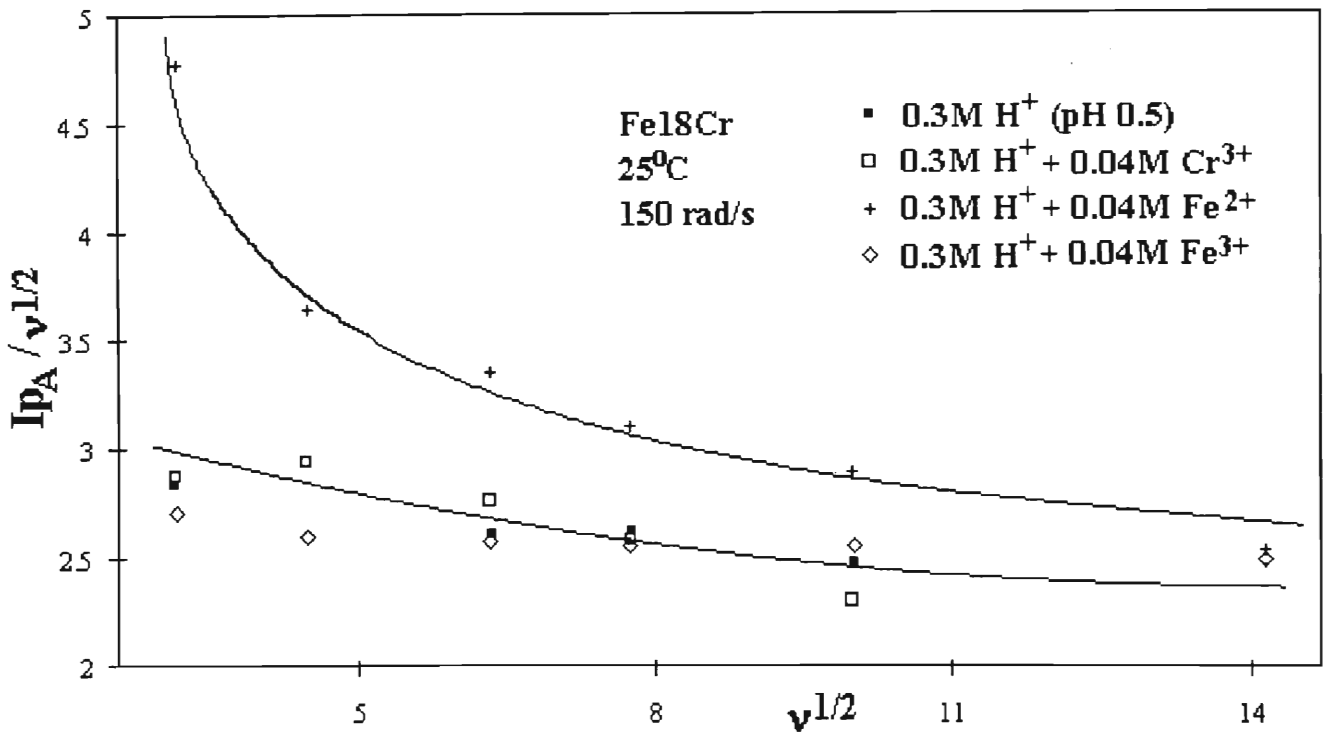

Fig. 6.19: Peak current diffusion diagnostic plots (of peak A) at 150 rad/s, pH 0.5 and 25°C showing the effect of addition of 0.04M Fe^{2+}, Fe^{3+} and Cr^{3+} to the pH 0.5 solution.

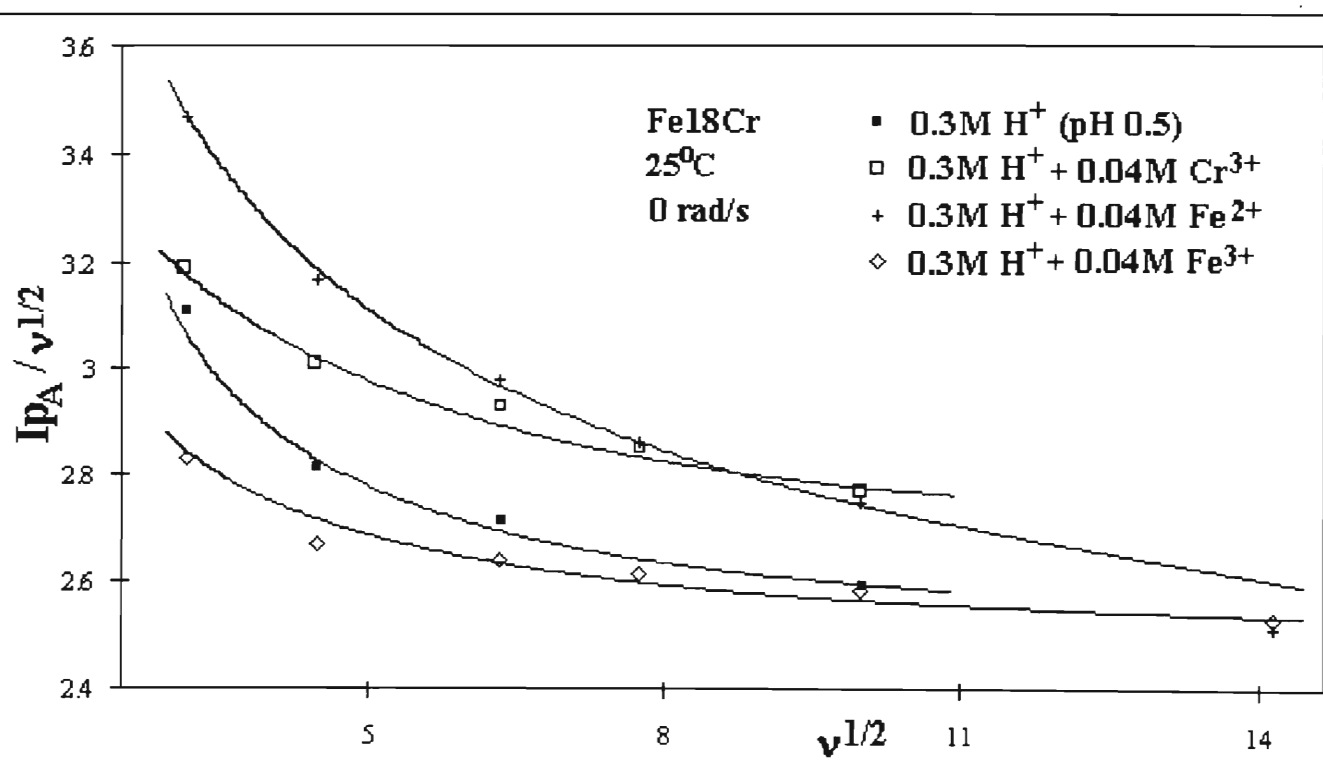

Fig. 6.20: Peak current diffusion diagnostic plots (of peak A) at 0 rad/s, pH 0.5 and 25°C showing the effect of addition of 0.04M Fe^{2+}, Fe^{3+} and Cr^{3+} to the pH 0.5 solution.

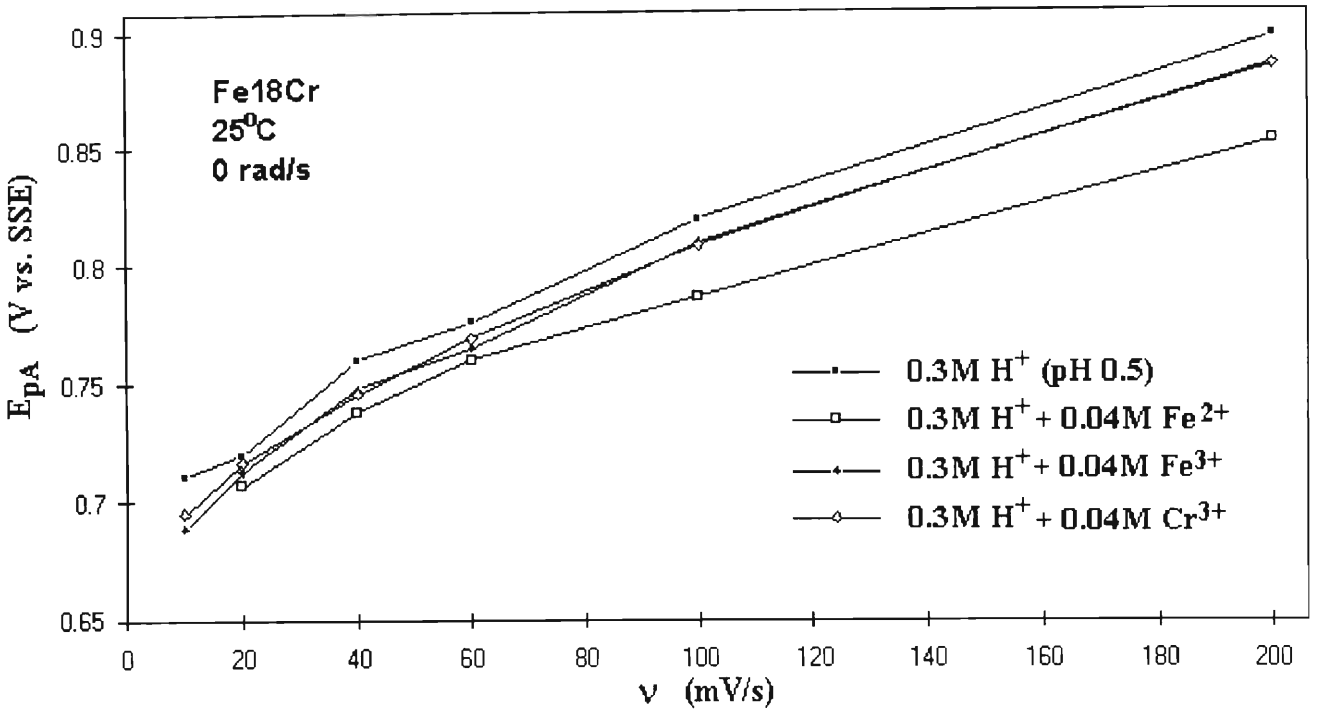

Fig. 6.21: Plots of the peak A peak potential versus sweep rate for each of the three pH 0.5 solutions containing (separately) 0.04M Fe^{2+}, Fe^{3+} and Cr^{3+} and for the usual pH 0.5 solution itself.

From fig. 6.21 it is evident that all the peak potentials (of peak A) of the solutions containing aqueous cations were slightly negative of the pH 0.5 solution. The following reason is suggested:

Peak A is mainly a current response due to a partial breakdown of a passive film followed by the formation of a temporary, less protective secondary "passive" film. The source of the cations within the secondary passive film must be from the dissolution products of the passive film breakdown and possibly from direct corrosion of the electrode itself, depending on the aggressiveness of experimental conditions. These will probably be cations such as Fe(III), Cr(III) and Cr(VI). If the concentration of these cations is increased artificially, then the conditions for secondary passivation (e.g. supersaturation) could be reached at an earlier stage then in the usual pH 0.5 solution. This would correspond to a peak potential in the solutions where ions necessary for secondary passivation are artificially introduced which is negative with respect to the peak potential in the usual pH 0.5 solution. The ferrous solution would provide a high concentration of ferric ions at the electrode/film - solution interface due to the oxidation of ferrous ions and resultant diffusion of Fe^{2+} towards the interface. This may be why the ferrous solution gives the most negative potentials.

6.3.2.1. The effect of rotating the electrode

One of the most significant result in this investigation was found as a result of rotating the electrode. Note that four solutions are being compared. The solutions were all at the same pH and only differed in the type (or the absence) of cations that were present. All cations were present at the same concentration - 0.04M. The solutions can be briefly listed as follows:

- 0.3M $HClO_4$ (pH 0.5) - the pH 0.5 solution
- 0.3M $HClO_4$ + 0.04M Fe^{2+} - the ferrous solution
- 0.3M $HClO_4$ + 0.04M Fe^{3+} - the ferric solution
- 0.3M $HClO_4$ + 0.04M Cr^{3+} - the chromic solution

Figures 6.9,16,17,18 show that for all of these solutions except the ferrous solution, I_{pA} decreased when the rotation rate was increased from 0 to 150 rad/s. This was reflected particularly at the slow sweep rates. However, for the ferrous solution, I_{pA} increased as rotation rate increased. Also, as shown in figures 6.19,20 the ferrous solution consistently gave the greatest increase in I_{pA} (with respect to the pH 0.5 solution).

It is suggested that the reason why I_{pA} might increase with rotation rate in a solution containing cations is:
The cation is oxidised in at the film / solution (or possibly electrode / solution) interface and hence its concentration in that region is depleted. The cation must be replenished by diffusion from the bulk solution. However, when the electrode is rotated, the Nernst diffusion layer thickness is decreased with the result that the distance from the bulk solution to the interface is reduced and cations may be replenished more efficiently. This would result in an increase in current.

However, it is suggested (and explained in section 6.4) that the effect of I_{pA} decreasing with increase in rotation rate is due to the hydronium ion rather than the addition of cations. There are two facts supporting this suggestion:

- I_{pA} decreased with increase in rotation rate for the usual pH 0.5 solution (no cations added).
- As previous results have shown I_{pA} became more dependant on rotation rate as the hydronium ion concentration increased.

There are therefore two competing effects in determining the dependence of I_{pA} on rotation rate.

- If the added cation in solution is oxidised at peak A potentials, then rotating the electrode will increase the current response.
- The high hydronium ion concentration (pH 0.5) results in a (as yet unexplained - *cf* section 6.4) decrease in the current response when the electrode is rotated.

In the case of ferrous ion the former of these above two effects is the predominant one, whereas in the case of the ferric and chromic ions, the latter case is the predominant one. The conclusion is that the oxidation of aqueous Fe(II) at peak A potentials is far more significant than the oxidation of aqueous Fe(III) or Cr(III). These results do not, of course, indicate to what extent oxidation of these ions occurs in the solid state. However, in this solution (most acidic used) dissolution of the passive film in the transpassive region would ensure that a maximum of aqueous (as opposed to solid state) oxidations would occur.

The peak potentials of all the above solutions were found to be independent of rotation rate.

6.3.2.2. The effect of aqueous ferrous ion

This has been largely covered in the previous section, but it should also be mentioned that the effect of ferrous ion addition was only significant in increasing I_{pA} at 150 rad/s as fig. 6.19 shows. At 0 rad/s however, I_{pA} was not significantly larger for the ferrous solution than for the other solutions.

It is reasonable to conclude that, of the three cations used, the ferrous cation is the most active **aqueous** cation at peak A potentials in pH 0.5 solution.

6.3.2.3. The effect of aqueous ferric ion

The effect of ferric ion can more clearly be seen at 0 rad/s (fig. 6.20), the reason being that at 150 rad/s fig. 6.19 shows that within experimental error, the diagnostic current values for the ferric, chromic and pH 0.5 solutions are the same. At 0 rad/s, however, I_{pA} for the ferric solution was generally less than for the pH 0.5 solution. Fe(III) is unlikely to oxidised to the only other higher Fe oxidation state - VI - in acidic solutions where Fe(VI) is unstable. Also, the aqueous Fe(III) would also be available for contributing towards secondary passivity by contributing towards supersaturation of cations near the interface, for example. It is therefore not surprising that adding Fe(III) to the solution reduces the peak A current response.

6.3.2.4. The effect of aqueous chromic ion

The effect of Cr(III) could best be seen at 0 rad/s. At this rotation rate, I_{pA} for the chromic solution was generally larger than for the pH 0.5 solution. Hence oxidation of aqueous Cr(III) does take place at peak A potentials in these experimental conditions, but not to the same extent as oxidation of aqueous Fe(II). The conclusion is that both the oxidation of Fe(II) and of Cr(III) contribute to the peak A current response and that if the oxidation of Cr species does comprise a significant portion of peak A processes then these oxidations must occur in the solid state - i.e. within the anodic film. This is in agreement with Haupt & Strehblow, who concluded that corrosion passivation currents on pure Cr are probably mostly (more than 90%) in the solid state [100].

6.4. Partial qualitative scheme for the transpassive behaviour of the anodic film on Fe-Cr alloys

Based on the results from chapters 5 and 6, the following qualitative scheme for transpassive processes on Fe-Cr alloys is suggested. It is acknowledged that the scheme entertains some speculation and that more supporting experimental evidence will be needed to validate it. These experiments will be suggested for future work.

The scheme covers the behaviour of the anodic film from the beginning of the passive film breakdown (E_{tr}) to the end of secondary passivity. This section is almost entirely occupied by what has been referred to as peak A. At E_{tr} the passive film begins to be oxidised and to partially break down. Whether this is due to tensile stresses, the action of cation vacancies, local acidification, a combination of these mechanisms or some other means is not known. Another point of debate (for which this scheme aims to provide an explanation) is whether the oxidation of Cr species is primarily responsible for the peak A current response (*cf* fig. 3.9) [10-13] or whether the oxidation of Fe species is responsible, as was indicated by the results of section 6.3 and by previous work in this laboratory [1,14]. It is this last question, in particular, that this scheme seeks to answer.

This study has shown that the hydronium ion plays an important role in transpassive behaviour. Increasing the $[H^+]$ not only increases the peak A current response but also gradually changes the peak A processes from apparently totally solid state (I_{pA} independent of ω at pH 3.8) to a situation where a significant proportion of peak A processes take place in the aqueous phase adjacent to the electrode (I_{pA} most dependent on ω at pH 0.5). The diagnostic plots at the lowest pH (and particularly at the highest temperature) are of the type which have been shown to indicate a catalytic reaction ($I_{pA}/\nu^{1/2}$ decreases with increasing sweep rate).

In view of these unique results concerning the hydronium ion and in order to resolve the debate over which species (Cr or Fe) are primarily responsible for the peak A current response, the following premise, referred to as the "acid premise", is proposed for Fe-Cr electrodes (but which may apply to most metal & alloy electrodes):

An acid solution will resist any reaction process that results in an overall increase in the acidity of the solution in the region of the electrode.

A qualification to the above premise would be:

The resistance of an acid solution to an increase in acidity is related to the original acidity of the solution. For example, a solution that is pH 0 will resist an increase in acidity far more than a solution which is pH 3.

The acid premise can be viewed as a a special case of Le Chatelier's principle. However, it is different from Le Chatelier's principle in one respect; namely that it is suggested that the acid principle not

only applies to equilibrium reactions, but also to irreversible reactions. The necessity for this difference from Le Chatelier in the acid premise will become apparent in its application in the partial explanation of transpassive voltammetric behaviour of Fe-Cr alloys in acid solutions:

One of the two popular manners in which Cr(III) is considered to react transpassively (eqn. (6.2)) is [11,12]

$$Cr_2O_3 + 5H_2O \rightarrow 2CrO_4^{2-} + 10H^+ + 6e^-$$

This equation contradicts the acid premise as hydronium ions are produced. The production of hydronium ions can be reduced if the above equation is written:

$$Cr_2O_3 + 5H_2O \rightarrow 2H_2CrO_4 + 6H^+ + 6e^- \qquad (6.4)$$

However, even eqn. (6.4) contradicts the acid premise.

So is it possible to oxidise chromic ion to chromate ion without a resultant increase in the acidity at the electrode ? The answer is yes and the following equations explore some of the ways in which the acid premise may be satisfied (these reactions do not describe a mechanism. Each reaction might occur separately and independently of the others):

$$4Cr_2O_3 + 6H^+ \rightarrow 3H_2CrO_4 + 5Cr^{3+} + 9e^- \qquad (6.5)$$

$$2Cr_2O_3 + 2H_2O \rightarrow 2H_2CrO_4 + 2Cr^{3+} + 6e^- \qquad (6.6)$$

$$Cr_2O_3 + Fe_2O_3 + 2H_2O \rightarrow 2H_2CrO_4 + 2Fe^{3+} + 6e^- \qquad (6.7)$$

$$Cr_2O_3 + 2Fe_2O_3 + 6H^+ \rightarrow 2H_2CrO_4 + 4Fe^{3+} + H_2O + 6e^- \qquad (6.8)$$

These reactions were derived after following these steps:

1. Reaction (6.4) requires 5 oxygen atoms to form two chromate ions from two chromic oxide molecules.
2. These oxygen molecules must either be supplied from water (in which case H^+ would be produced which is unacceptable in terms of the acid premise) or from other metal oxides in the film. The solution is deaerated so that no dissolved oxygen is available. Therefore the oxygen molecules must be supplied by other metal oxides.
3. In a Fe-Cr alloy only Cr-oxides and Fe-oxides are available in the anodic film. The most common oxides are ferric and chromic oxide.
4. If chromic oxide supplies its own oxygen atoms, then some chromic oxide molecules must dissolve as aqueous chromic ions (equations (6.5,6)).
5. Ferric oxide can also provide the necessary oxide ions if it dissolves as aqueous ferric ions (equations (6.7,8)).

In order to be consistent, H_2CrO_4 has been used instead of $HCrO_4^-$ or CrO_4^{2-}. However, Pourbaix diagrams show that as the acidity of the solution increases the chromate ion gradually associates more with

one and then two protons. Also, oxides of cations instead of oxyhydroxides or hydroxides have been used for consistency, but similar equations for hydroxides or oxyhydroxides could easily be generated.

A second manner in which the Cr(III) cation is considered to react at transpassive potentials is [115,116]

$$Cr_2O_3 + 3H_2O \rightarrow 2CrO_3 + 6H^+ + 6e^- \quad (6.9)$$

Comparing reactions (6.4) and (6.9), the former results in breakdown of the film (loss of passivating oxides) while the latter retains the chromic oxides within the film. It has been suggested that a layer of Cr_2O_3/CrO_3 oxides within an anodic film forms a glassy, protective structure [115,116]. So whether Cr(VI) is expelled into the solution or retained within the anodic film is vital in its effect on the onset of secondary passivity.

Reaction (6.9), however, also produces H^+ and is unacceptable in terms of the acid premise. The following reactions show how Cr_2O_3 can be oxidised to CrO_3 while satisfying the acid premise:

$$4Cr_2O_3 + 6H^+ \rightarrow 3CrO_3 + 5Cr^{3+} + 3H_2O + 9e^- \quad (6.10)$$

$$2Cr_2O_3 \rightarrow 2CrO_3 + 2Cr^{3+} + 6e^- \quad (6.11)$$

$$Cr_2O_3 + Fe_2O_3 \rightarrow 2CrO_3 + 2Fe^{3+} + 6e^- \quad (6.12)$$

If Fe(II) exists just prior to the transpassive region in the anodic film then a reaction such as (6.12) could be modified to

$$Cr_2O_3 + 3FeO \rightarrow 2CrO_3 + 3Fe^{2+} + 6e^- \quad (6.13)$$

and this would then be followed by

$$Fe^{2+}_{(aq)} \rightarrow Fe^{3+}_{(aq)} + e^- \quad (6.14)$$

The two sets of reactions describing the two possible oxidation products of Cr(III) at transpassive potentials differ in the way they affect their environment in two significant areas:

- As mentioned before reactions (6.5-8) result in the loss of passivating chromium species to the solution whereas reactions (6.10-12) keep the chromium species within the anodic film, albeit in a higher oxidation state. Therefore when reactions (6.10-12) occur, a greater current response would be expected than when reactions (6.5-8) occur.
- All the products of reactions (6.5-8) go into solution whereas only some of reactions (6.10-12) go into solution. Therefore when reactions (6.5-8) occur the current response is more likely to be dependent on rotation rate than when reactions (6.10-12) occur.

The next suggestion is that prior to voltammetric entry into the transpassive region (i.e. before E_{tr} is reached on the anodic sweep of a voltammetric experiment), the Cr-oxides exist predominantly in the inner

and middle parts of the passive film[a] as in the bipolar mechanism [11,115,116]. The Cr cations have a lower mobility than the Fe cations [115,116,], but migrate or diffuse towards the electrolyte - film interface during voltammetric progression through the transpassive region [11]. This would mean that Fe-oxides would dissolve preferentially to Cr-oxides which would explain the fact that ferric ions have previously been found in solution adjacent to the electrode (by atomic absorption and RRDE [1,3]) but chromium species have not yet been discovered in solution adjacent to the electrode. This also means that of reactions (6.5-8,10-12), reactions (6.7,8) and particularly, (6.12) and (6.13) would be favoured as Fe-oxides then dissolve preferentially.

However, in very acidic solutions - and at high temperatures -, it is likely that (between E_{tr} and E_{pA}) most of the passive film will be dissolved. Therefore in the most acidic solutions one would expect to find chromate ions in solution after passing through the transpassive region. However, in less acidic solutions, the passive film only partially breaks down - if it breaks down at all. Therefore in less acidic solutions one would expect to find only traces of chromate ion in solution after passing through the transpassive region, particularly at slow sweep rates. The obvious (future) experiment to validate this would be to obtain samples of the solution adjacent to the electrode from two experiments. Each experiment would involve holding a stationary Fe-Cr electrode at a transpassive potential for a time increment under identical conditions, but one would be in a strongly acidic and the other in a less acidic solution. AA analysis could then be performed on each solution to determine the concentration of Fe and Cr cations respectively.

The means of secondary passivation would again depend on pH. At low pH's, most of the original passive film will dissolve and Cr-oxides will be lost to solution as chromate ions. It is therefore suggested that ferric ions in solution precipitate to form a porous film according to

$$2Fe^{3+} + 3H_2O \rightleftharpoons Fe_2O_3 + 6H^+ \qquad (6.15)$$

Reaction (6.13) on its own disobeys the acid premise. However, secondary passivity is not very "passive" as shown by previous CV's - a significant current does flow and this could be explained by the following series of reactions which would be expected to occur just negative of E_{pA} and from there through the region of secondary passivity

$$Fe_{(s)} \rightarrow Fe^{2+} + 2e^- \qquad (6.16)$$

$$Fe^{2+} \rightarrow Fe^{3+} + e^- \qquad (6.17)$$

and the ferrous and ferric ions could be adsorbed or in solution. Reactions (6.16,17) would be followed by

$$2Fe^{3+} + 3H_2O \rightleftharpoons Fe_2O_3 + 6H^+ \qquad (6.15)$$

$$Fe_2O_3 + 2Fe + 6H^+ \rightarrow 4Fe^{2+} + 3H_2O + 2e^- \qquad (6.18)$$

and reaction (6.18) would be followed by reaction (6.17). Naturally Cr will also dissolve from the electrode when it is exposed directly to the solution during passivity breakdown, but this Cr will probably be quickly oxidised to chromate ions and lost to the solution. Reactions (6.15,18) are catalytic with respect to H^+, but for secondary passivity to be achieved the ferric oxide produced by reaction (6.15) would need to be in excess of the ferric oxide consumed by reaction (6.18) and by the dissolution of ferric oxide to

---

[a] In this case, the term "passive film" refers to the barrier layer.

aqueous ferric ions. This still results in a net production of H^+, however, and therefore secondary passivity will be resisted to a greater and greater degree as the pH decreases and the "stable" current that flows during the region of secondary passivity will increase as pH decreases.

If ferric (and ferrous) ions are considered to dissolve when Cr(III) is oxidised to Cr(VI), as required by the acid premise if Cr(III) has a low mobility within the anodic film, then the fact that ferric ions are predominantly found in solution [179] even though Cr species are being predominantly oxidised, is quite reconcileable in this scheme. For example, reactions (6.8,12) both show ferric ions dissolving preferentially even though chromic ions are being oxidised preferentially.

Reaction (6.15) can also be used to explain the rotation rate dependence of I_{pA} at low pH's. When reaction (6.15) occurs, an excess of H^+ is produced in the region of the electrode. This excess H^+ can be consumed, in order to satisfy the acid premise, in one of two ways:

- It can react, for example, with a metal oxide to produce aqueous metal cations and water.
- It can diffuse away from the electrode into the bulk solution. (The acid premise is only concerned with excess acid in the region of the electrode.)

By rotating the electrode (and thereby reducing the Nernst diffusion layer thickness) the excess H^+ may diffuse into the bulk solution more efficiently. Therefore when the electrode is rotated the reaction responsible for secondary passivity is resisted less and hence secondary passivity may be attained more easily, resulting in an I_{pA} which is smaller than when the electrode is stationary.

The means of secondary passivity in less acidic (higher pH) solutions would probably be through the oxidation of Cr_2O_3 to CrO_3. In the less acidic solutions the passive film is only partially - if at all - broken down. The Cr cations migrate (or diffuse) towards, but do not reach, the film - electrolyte interface. In this case secondary passivity would be brought about by the interaction of CrO_3 and Cr_2O_3 oxides to form a glassy, non-conducting layer which nevertheless is not as protective as the initial passive barrier layer perhaps due to an increased porosity of the anodic film (since, by the acid premise, oxidation of Cr(III) to Cr(VI) must include dissolution of some other oxides to aqueous cations simultaneously).

This scheme does neglect the action of electrolyte anions. Therefore any future work should be done in acids where the anions are as noble as possible towards the electrode (e.g. $HClO_4$ and HBF_4).

Finally, the deviations of the peak current diffusion diagnostic plot can be explained in more detail using the acid premise. In the pH 0.5 solution, the greatest deviation from the horizontal was obtained at slow sweep rates. This is because at the slower sweep rates, more time is spent at each point in the transpassive region, and the acidity of the solution resists formation of protective metal oxides. Also, the more protective chromic oxides are lost to the solution as chromate ions. As the sweep rate increases, less time is available for complete dissolution of the original passive film and more chromic oxides may be left in the film (since they must be transported from the inner region of the film to the film / electrolyte

interface before dissolving), perhaps being oxidised to CrO_3 instead of being lost to the solution as chromate ions.

In the pH 3.8 solution, a negative deviation from the horizontal was obtained at slow sweep rates and this can be attributed to the low mobility of Cr cations within the anodic film. This low mobility is accentuated at slow sweep rates where the degree of formation (and compactness) of the passive film is greater than at fast sweep rates. At slow sweep rates, sufficient CrO_3 is obtained to render the anodic film "glassy" fairly early on in the transpassive region (probably slightly negative to E_{pA}) whereas at fast sweep rates this occurs ay more positive potentials than with slow sweep rates.

In conclusion, this partial scheme has as its pivotal point the acid premise. This acid premise was deduced from the initially perplexing nature of the variation of voltammetric results with pH and can be used to explain, or at the least not contradict, all the results obtained.

6.5. A cathodic peak A in 72% $HClO_4$

A voltammetric experiment was performed with AR 72% $HClO_4$ as the solution and at 25°C. A sweep rate of 100 mV/s was used. The initial potential was -1.0V as usual, but in this case as soon as the electrode had been lowered into the acid, the voltammetric sweep was begun immediately. This was done in order to avoid immediate rampant general corrosion. In this case the first cycle was taken for the result. This is shown in fig. 6.22.

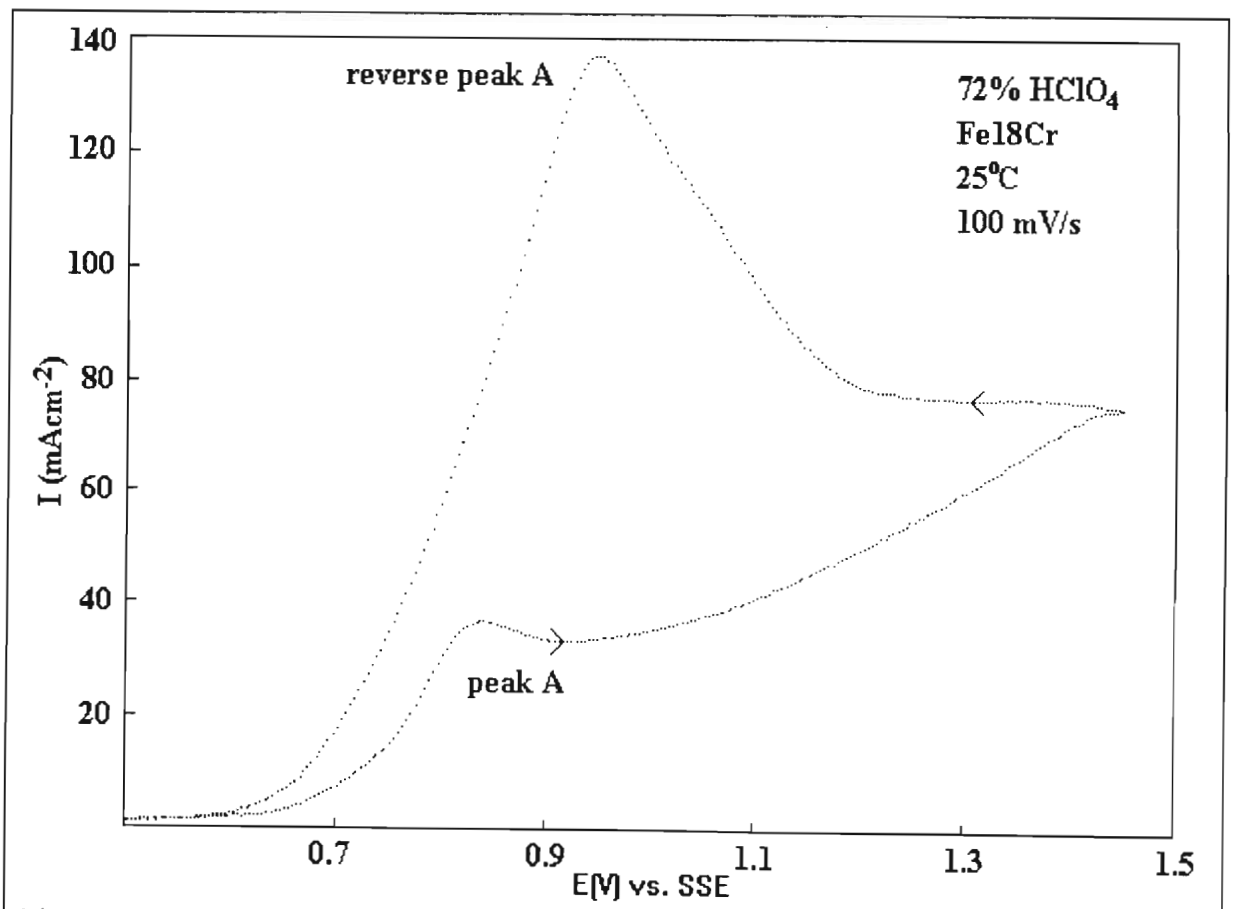

Fig. 6.22: Cyclic voltammogram in 72% $HClO_4$ at 100 mV/s, 0 rad/s and 25°C showing the reverse "peak A" on the cathodic sweep.

Fig. 6.22 shows a typical peak A response on the forward sweep, but displays an anodic peak on the cathodic sweep which has a peak height of over 350% larger than I_{pA}. Fletcher *et al.* have used this phenomenon as diagnostic of nucleation / growth kinetics in the case where intercrystal collisions are statistically improbable [189]. Fig. 6.23 shows a result where they have obtained the reverse peak for a reaction governed by nucleation / growth kinetics. Fletcher obtained the results for a reduction process (negative potential and current). The theory should also apply qualitatively to an oxidation process (positive potential and current) as in this study. The importance of this result is reflected in chapter 7, where chronoamperometic results, in the form of rising transients are strong evidence for a nucleation mechanism when the electrode is stepped to a transpassive potential. The above data could therefore be viewed as voltammetric confirmation of a chronoamperometrically established phenomenon.

The question as to why the reverse peak only shows itself in this (the most aggressive) solution. This can be understood if corrosion pits can be considered to nucleate and grow in the same way as nuclei that grow by electrocrystallisation - i.e. on an inactive surface (*cf* Ch. 8). In this very aggressive solution, it would not be surprising to have near-rampant pitting corrosion on the reverse sweep (i.e. growth of pitting "nuclei") while still in the transpassive region. In a similar study by Magaino *et al*, (for Fe13Cr in 65% H_3PO_4 + 20% H_2SO_4 [190]) SEM analyses of the electrode after dissolution in the transpassive region showed little overlap of the corrosion pits. This is in fact an important condition of Fletcher's for the occurence of the reverse peak. In less aggressive solutions, metal oxide nuclei are probably able to form and overlap, thus protecting the substrate before a peak can occur on the reverse sweep.

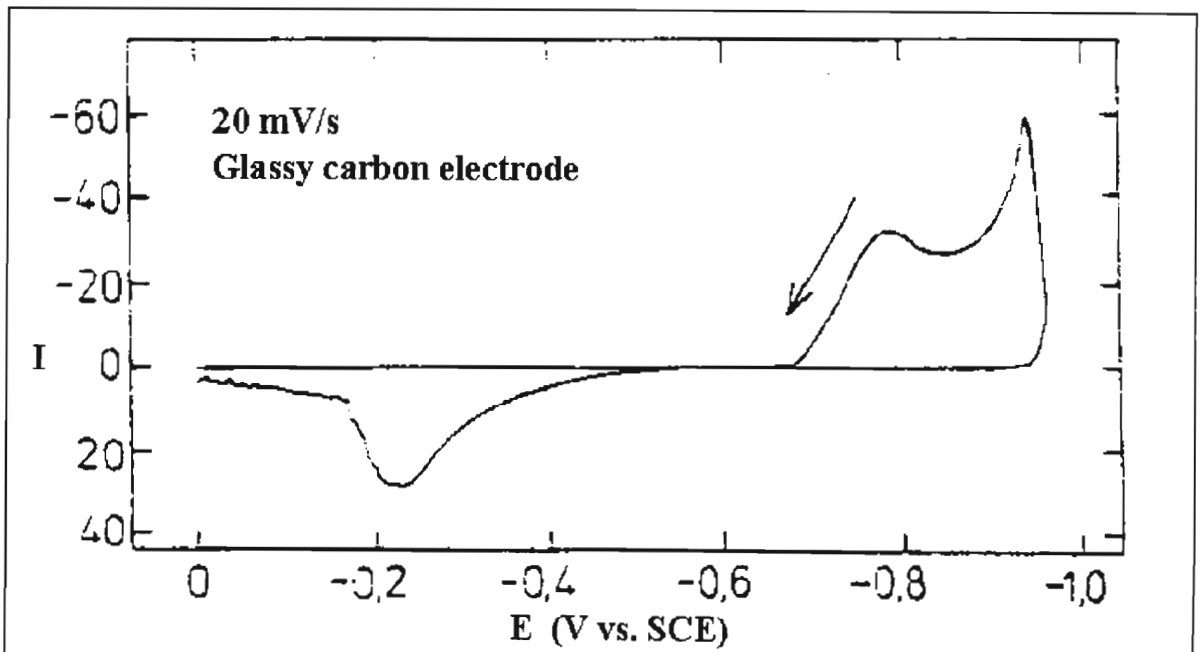

Fig. 6.23: Cyclic voltammogram at 20 mV/s and 25°C for the deposition of cobalt on glassy carbon. The electrolyte was 0.4M $Co(NH_4)_2(SO_4)_2$ dissolved in aqueous solution [189]. Current is in $mAcm^{-2}$.

Two further points can be stressed as a result of this section

- Firstly, pitting corrosion may occur in the absence of chloride provided the potential is sufficiently positive [190].
- Secondly, it is suggested that these corrosion pits may be treated in the same way and by the same theory as nuclei in electrocrytallisation studies [191]. This concept is developed in chapter 8.

CHAPTER 7

7. CHRONOAMPEROMETRY ON Fe-Cr ELECTRODES

The purpose of this part of the investigation was to study the phenomenon of the rising transient (*cf* section 3.4.2) under a variation of experimental conditions, in particular pH, starting and finishing potentials, and the number of potential steps. Apparent activation energies for the proposed nucleation processes have been obtained by plotting I_{max} versus 1/T (Arrhenius plots) [51] but according to the model in chapter 8, a large proportion of the nucleation (and growth) processes are diffusion controlled and therefore do not have an activation energy associated with them. Instead the behaviour of the processes leading to the rising transient have been investigated at ambient temperature (25°C) under a variety of experimental conditions. This can be considered as a first step in the general investigation of nucleation and other processes leading to rising transients. Unless otherwise stated, all transients were obtained at 0 rad/s. The Fe18Cr electrode was used for all chronoamperometric experiments.

A system is used to convey the potential step information and will be briefly described here in order to avoid confusion.

Fig. 7.1 shows a general diagram which can be used to describe the potential steps and time intervals in a potential step experiment. E_1' is the initial potential, or the potential from which the first potential step is made. Unless otherwise stated, the last step of the electrode pretreatment was to hold the electrode at E_1' for 30 seconds before the first potential step. If the experiment involves a single potential step, then E_2' is the final potential, but if the experiment involves a double potential step then E_3' is the final potential and E_2' is the intermediate potential. The beginning of the experiment (t = 0) is taken as the instantaneous time of the first potential step. In a double step experiment, t_1 is the duration of time spent at potential E_2' and $(t_2 - t_1)$ is the duration of time spent at E_3', both of which were usually 1 or 2 seconds. In some double step experiments $E_1' = E_3'$, but E_3' was always either equal to or negative of E_1'. A diagram such as fig. 7.1 is included in most chronoamperograms.

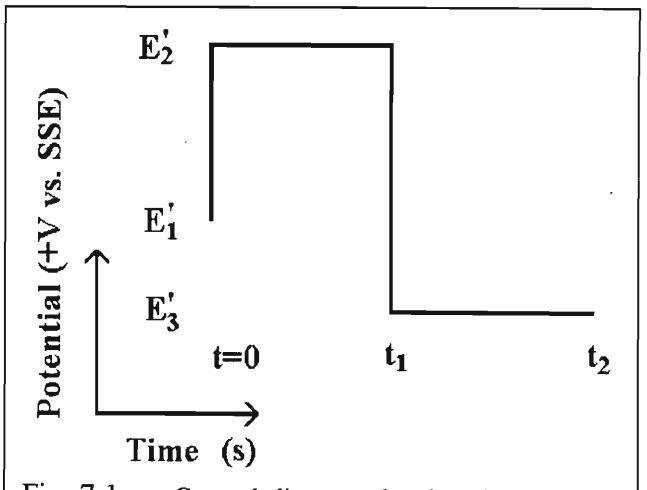

Fig. 7.1: General diagram showing the graphical means of describing a potential step experiment.

7.1. Acetate solution: pH 3.8

Most of the experiments in this solution were double potential step experiments. It was as a result of the second potential step that a reverse rising transient was discovered for this system. It is standard procedure to provide a polarisation curve as a reference for the potential steps imposed on the electrode and so fig. 7.2 shows a polarisation curve in pH 3.8 solution at 25°C.

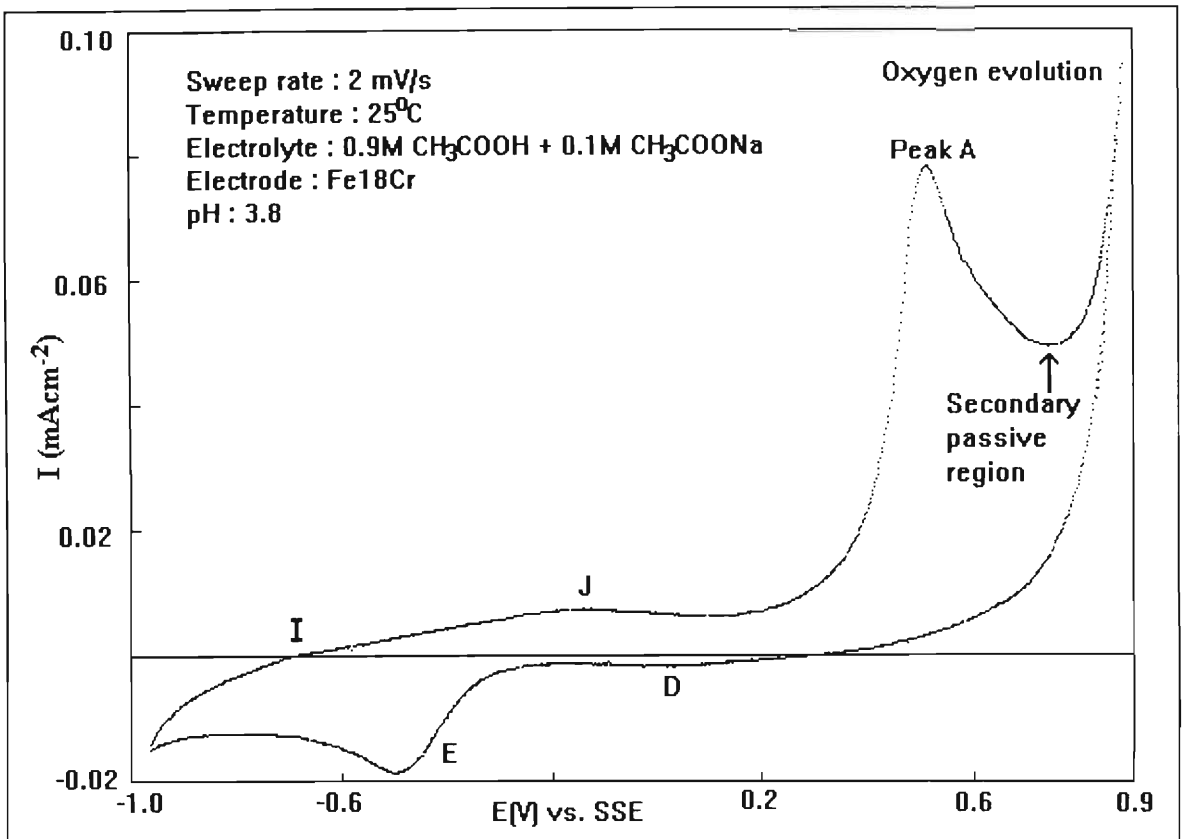

Fig. 7.2: Polarisation curve for Fe18Cr in pH 3.8 solution at 25°C and 2 mV/s.

As can be seen from the above polarisation curve, -0.7V (vs. SSE) is the potential (in an anodic sweep) at which the overall current response is zero. In first set of experiments -0.7V was therefore used as the starting potential (E_1'). A second potential step was imposed exactly 1.0 second after the first one, but with $E_3' = E_1'$. Fig. 7.3 shows the results for the first set of experiments.

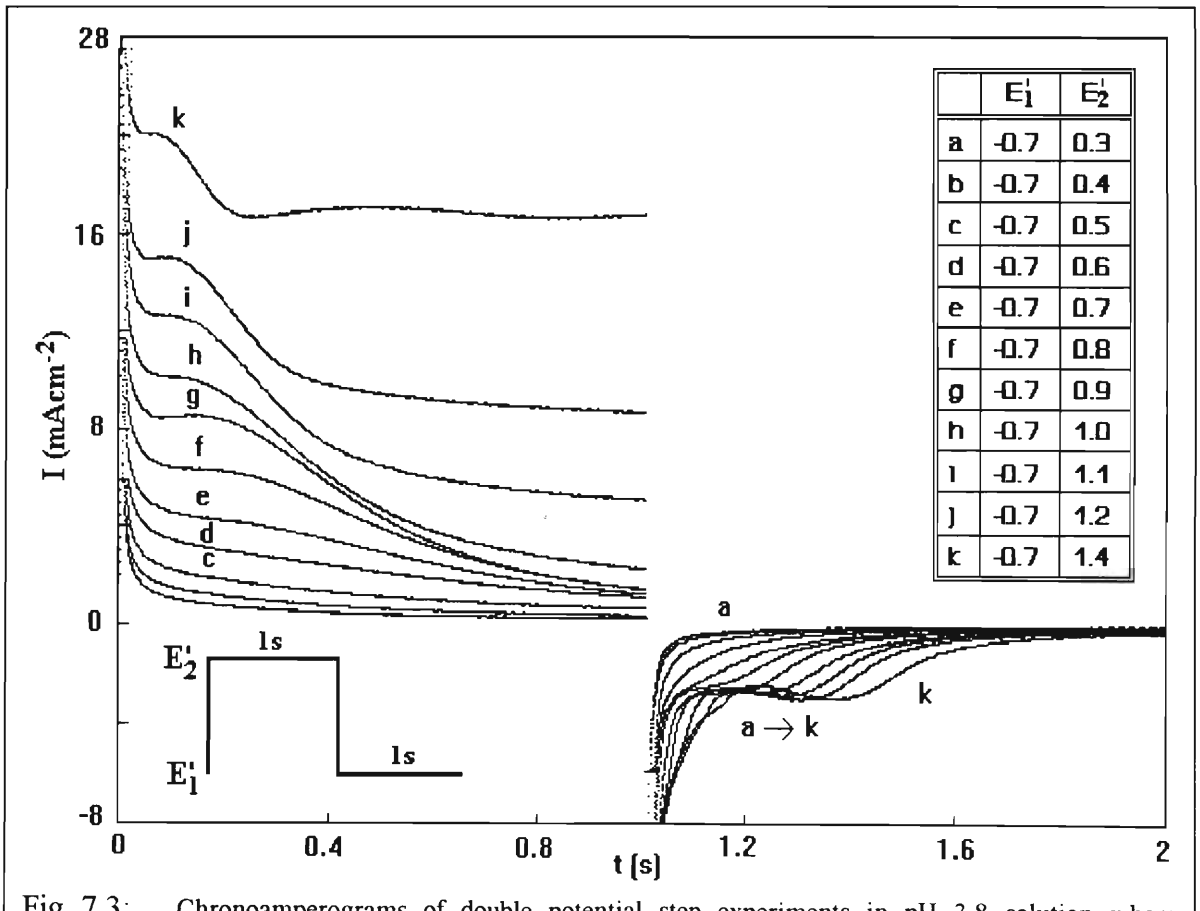

	E_1'	E_2'
a	-0.7	0.3
b	-0.7	0.4
c	-0.7	0.5
d	-0.7	0.6
e	-0.7	0.7
f	-0.7	0.8
g	-0.7	0.9
h	-0.7	1.0
i	-0.7	1.1
j	-0.7	1.2
k	-0.7	1.4

Fig. 7.3: Chronoamperograms of double potential step experiments in pH 3.8 solution where $E_1' = E_3' = -0.7V$ and E_2' is varied. The electrode is Fe18Cr in pH 3.8 solution at 25°C and 0 rad/s.

Fig. 7.3 confirms previous data and adds some new discoveries. Considering the first second of the chronoamperograms (i.e. the current response to the first potential step), the result that stepping into the passive region gives a falling transient and stepping into the transpassive region gives a rising transient was confirmed. Also, it should be noted that by examining the levelling off parts of the chronoamperograms (i.e. I_{lev}), that oxygen evolution interference only becomes significant when $E_2' > 1.0V$. Only when E_2' is increased to 1.1V does I_{lev} increase significantly from the corresponding values of I_{lev} for $E_2' \leq 1.0V$, thus indicating significant oxygen interference for the $-0.7 \rightarrow 1.1V$ potential step. This is an example of why the polarisation curve (which predicted significant oxygen evolution interference for $E_2' \geq 0.9V$) can only be taken as a rough guide for making decisions about the potential steps to be used in a chronoamperometric experiment. This is because a polarisation experiment involves a gradual change in the anodic film whereas a chronoamperometric experiment involves an (almost) instantaneous change in the anodic film (or a change from no film or a pre-existent film to an anodic film). The processes in each type of experiment would therefore be different and care must be exercised in relating the results of voltammetric and polarisation experiments to the results of chronoamperometric experiments. The observation that as E_2' increases, I_{max} increases and t_{max} decreases was also confirmed in fig. 7.3 and this was explained in section 3.4.2.

Considering the last second of the chronoamperograms (i.e. the current response to the second potential step), it can be seen that a "reverse" or cathodic rising transient has been obtained. This is the first time that this phenomenon has been seen on Fe-Cr alloys, although reverse rising transients have also been obtained on carbon steel in 1M NaOH [192]. The manner in which the reverse rising transient is affected by the value of E_2' is clearly shown - as E_2' increases the rising portion of the transient becomes more distinct and **both** $|I_{max}|$ and t_{max} (for the reverse rising transient) increase.

It was suspected that the reverse rising transient was due to a reduction of the anodic film that was formed while the electrode was at the transpassive potential. This reduction probably occurred by pitting of the transpassively formed film, hence increasing the surface area and causing the rise in the reverse transient. As E_2' increased, a greater volume of film was generated (as indicated by the normal rising transients). As a result a greater reduction current (larger "reverse" I_{max}) would be generated in reducing and a longer time (larger "reverse" t_{max}) would be needed to reduce it all. In order to provide evidence for this idea the following experiments were designed:
E_1' (= E_3') was set at -0.7V and E_2' was set at 0.9V. The variable in this set of experiments was t_1 - the time spent at potential E_2'. The idea was that if the time spent at E_2' was sufficiently short such that a transpassive film could not form, then a reverse rising transient would not be obtained. This would happen provided that the above proposed explanation for the reverse rising transient was correct. Fig. 7.4 shows the results obtained for this set of experiments. The results clearly show that as t_1 is reduced so the reverse transient gradually changes from a rising transient to a falling transient.

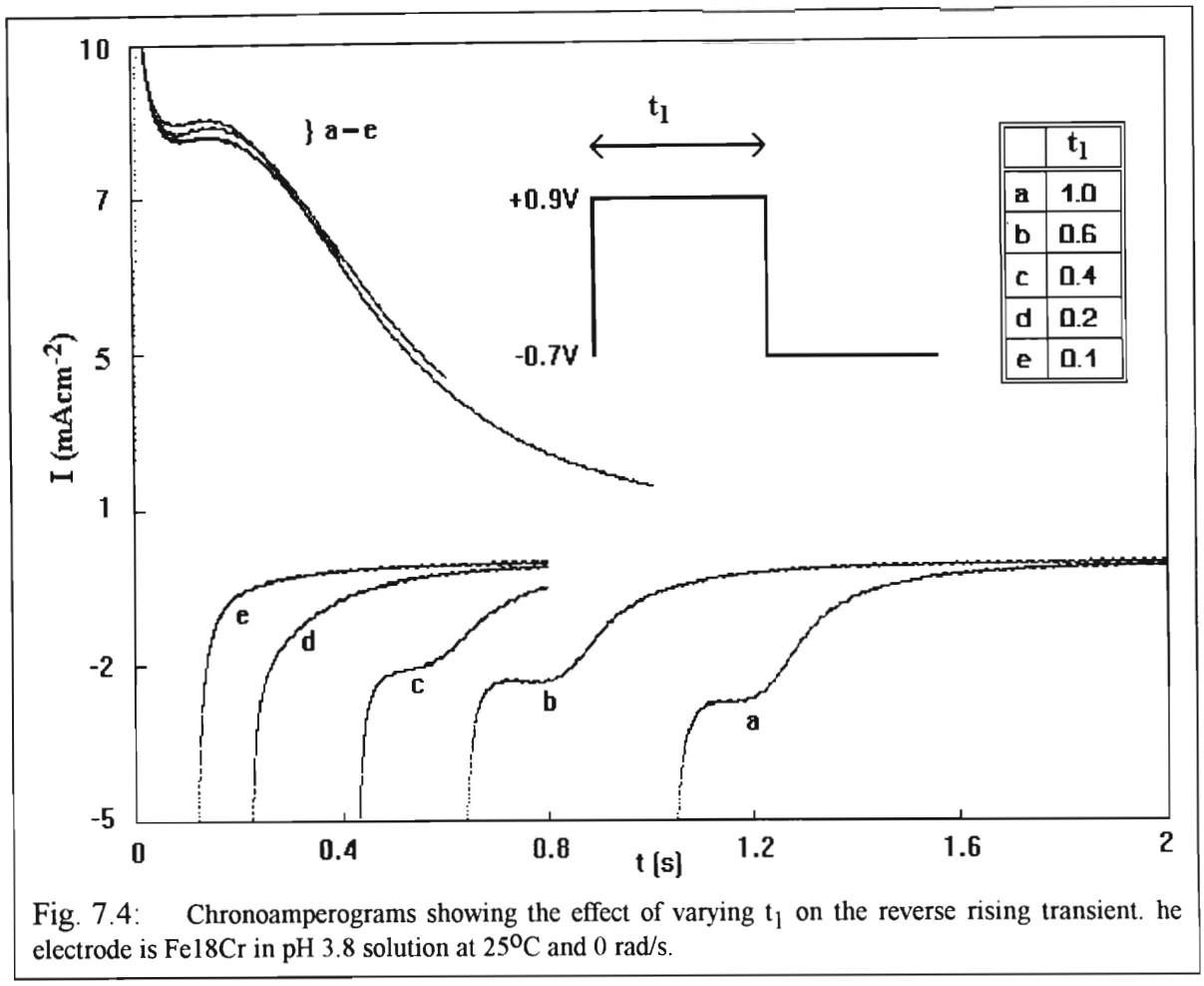

Fig. 7.4: Chronoamperograms showing the effect of varying t_1 on the reverse rising transient. he electrode is Fe18Cr in pH 3.8 solution at 25°C and 0 rad/s.

One other set of experiments was conducted to investigate the reverse rising transient. In these experiments the final potential (E_3') was varied but the initial (E_1') and final potentials were again kept equal. Fig. 7.5 shows the results.

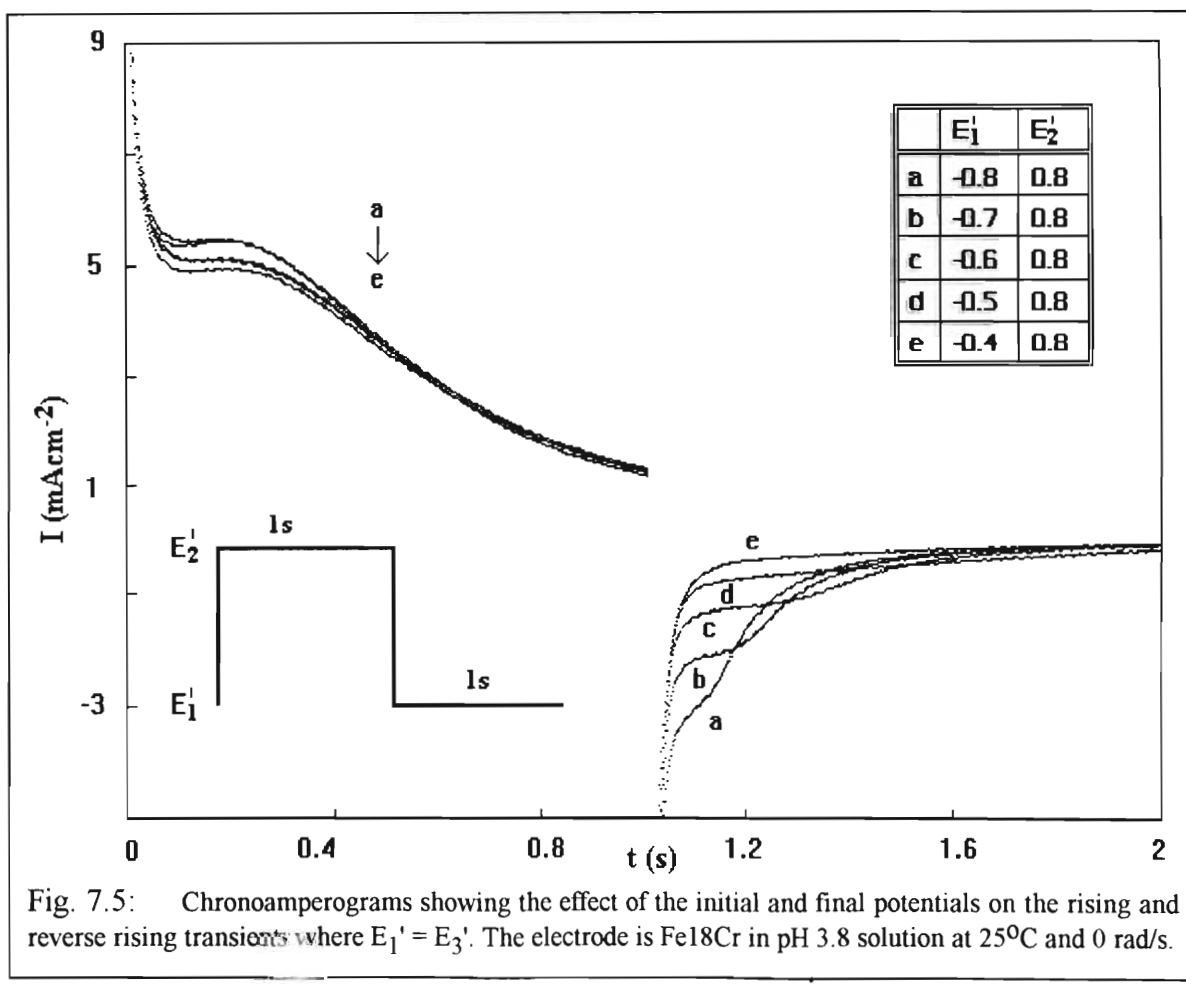

Fig. 7.5: Chronoamperograms showing the effect of the initial and final potentials on the rising and reverse rising transients where $E_1' = E_3'$. The electrode is Fe18Cr in pH 3.8 solution at 25°C and 0 rad/s.

One observation from fig. 7.5 is that the (normal) rising transient is independent of the initial potential within that range (-0.8 to -0.4V vs. SSE) of initial potentials. The other observation is that as the size of the potential step from E_2' to E_3' is increased by making E_3' more negative then the "reverse" t_{max} decreases and the "reverse" $|I_{max}|$ increases. This is analogous behaviour to the normal rising transient when E_2' is increased.

One other important aspect of the reverse rising transient is the fact that it establishes the presence of an anodic film. As fig. 7.3 showed, the reverse rising transient occurred for potentials (of E_2') up to 1.4V. This is a good indication that secondary passivity does not stop at the onset of oxygen evolution, but extends well into oxygen evolution. This would also mean that for the transpassive potential regions of interest (e.g. 0.6 - 1.0V vs. SSE in voltammetric peak A studies), the transpassive anodic film behaviour is not affected by oxygen evolution. This was an assumption used in the theory developed for the oxygen evolution correction (section 2.2.2).

The -0.7 → 1.4 → -0.7 chronoamperogram shown in fig. 7.3 is of interest because two rising portions are evident in the (first) transient. This has been shown to be due to the formation of consecutive layers by polynuclear nucleation [67].

Two other sets of experiments were performed, the object of both being to investigate the effect of varying E_1' within the passive region. In the first set of experiments (fig. 7.6) E_1' was consistently equal to E_3' . In the second set (fig. 7.7) E_3' was consistently set at -0.7V.

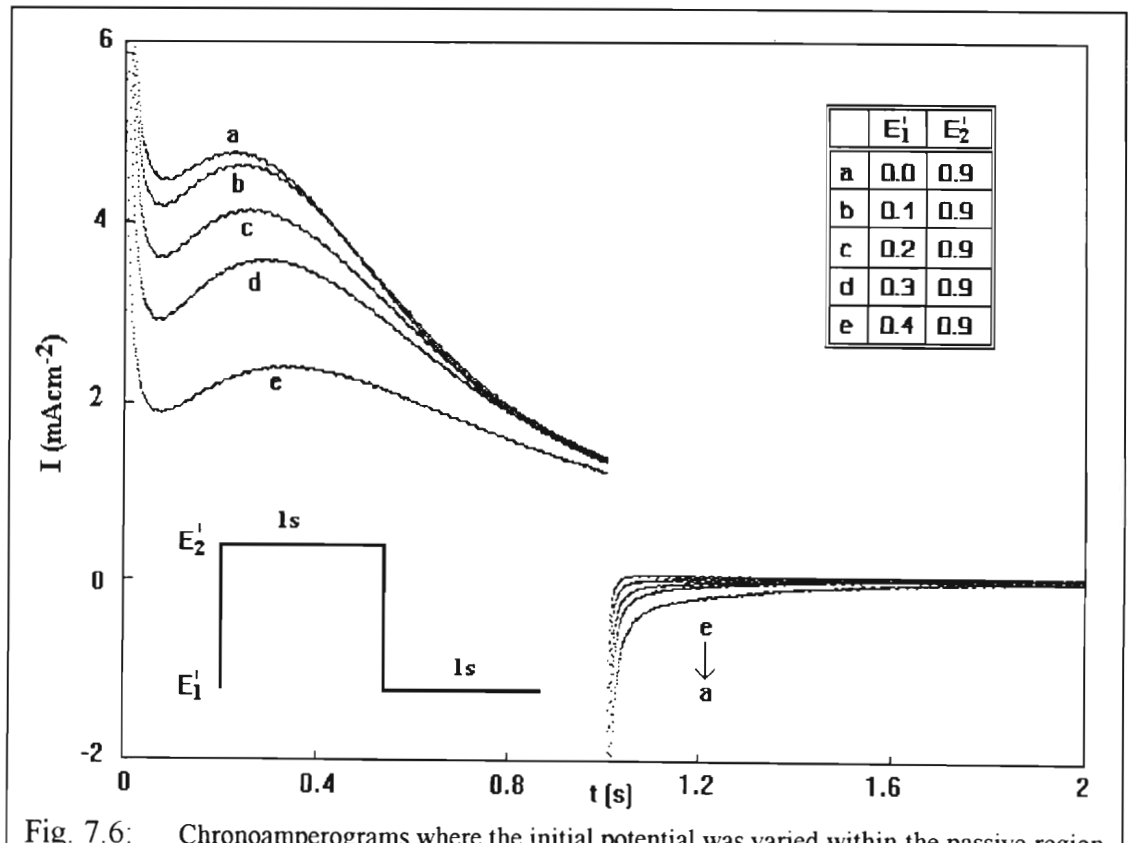

Fig. 7.6: Chronoamperograms where the initial potential was varied within the passive region and $E_1' = E_3'$. The electrode is Fe18Cr in pH 3.8 solution at 25°C and 0 rad/s.

Fig. 7.6 shows that rising transients can still be obtained when using passive region potentials as the starting potential. However, t_{max} increases and I_{max} decreases as E_1' is increased. Also, I_{max} in general is

about 50% (or more) smaller than when the starting potential was -0.7V. However, the rising transients are far better defined - the rising part of the "peak" is far clearer - when passive region potentials are used as the initial potential. It should also be noted that with E_3' in the passive region, no reverse rising transients are obtained.

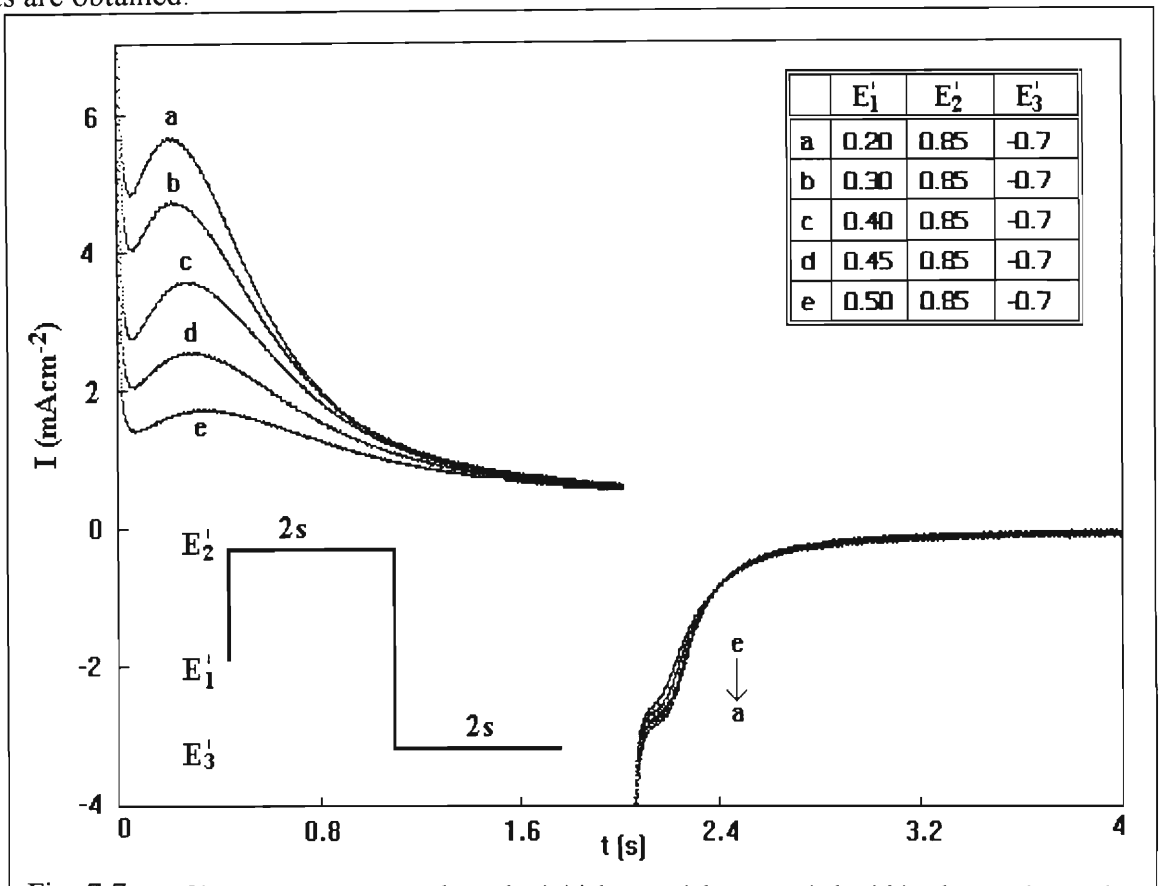

	E_1'	E_2'	E_3'
a	0.20	0.85	-0.7
b	0.30	0.85	-0.7
c	0.40	0.85	-0.7
d	0.45	0.85	-0.7
e	0.50	0.85	-0.7

Fig. 7.7: Chronoamperograms where the initial potential was varied within the passive region and E_3' = -0.7V. The electrode is Fe18Cr in pH 3.8 solution at 25°C and 0 rad/s.

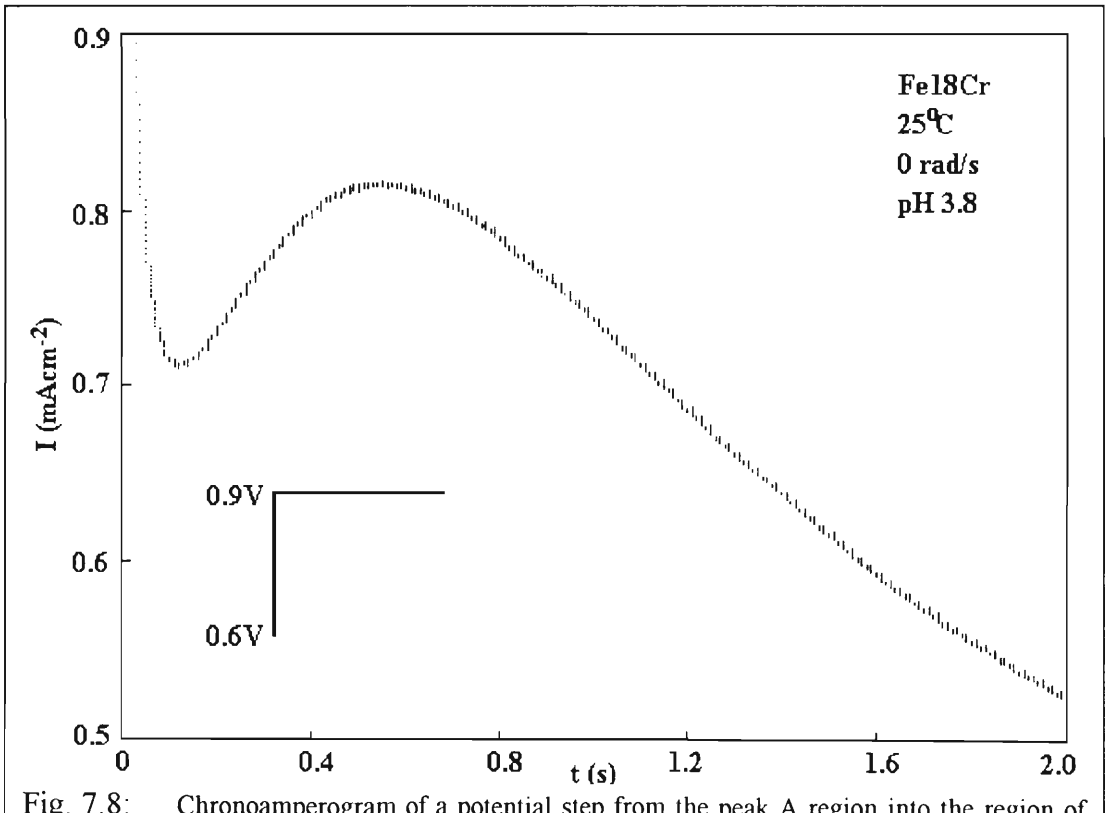

Fig. 7.8: Chronoamperogram of a potential step from the peak A region into the region of secondary passivity. The electrode is Fe18Cr in pH 3.8 solution at 25°C and 0 rad/s. The electrode was held at 0.6V for 30s before the potential step.

Fig. 7.7 shows that the reverse rising transient is independent of starting potential (E_1') when E_1' is in the passive region. Fig. 7.8 shows an unusual result. The potential step is from 0.6V (vs. SSE) to 0.9V (peak A region to region of secondary passivity) and a rising transient is still obtained.

Figures 7.5-8 all show the importance of stepping to the transpassive region in order to obtain the rising transient and more notably, the fact that stepping to the region of secondary passivity, rather than the peak A region will be more likely to induce a rising transient. This is perhaps not surprising because the peak A region is a region of general dissolution of the electrode whereas a stable anodic film exists in the secondary passive region. Therefore a film would be more encouraged to form when stepping to the secondary passive region than to the peak A region and according to the model in chapter 8, the nucleation and growth of the film is one of the two contributors to the rising part of the transient (the other being temporary pitting corrosion of the electrode).

7.1.1. The effect of addition of cations to the pH 3.8 solution

Fe^{2+}, Fe^{3+} and Cr^{3+} (each in concentrations of 0.04M) were added separately to three pH 3.8 solutions. Before a chronoamperometric experiment was attempted, cyclic voltammograms were obtained in each of the above solutions and a normal pH 3.8 solution at a slow sweep rate (10 mV/s). The electrode was always polished between the cyvlic voltammetric and chronoamperometric experiments. Fig. 7.9 shows the cyclic voltammograms that were obtained.

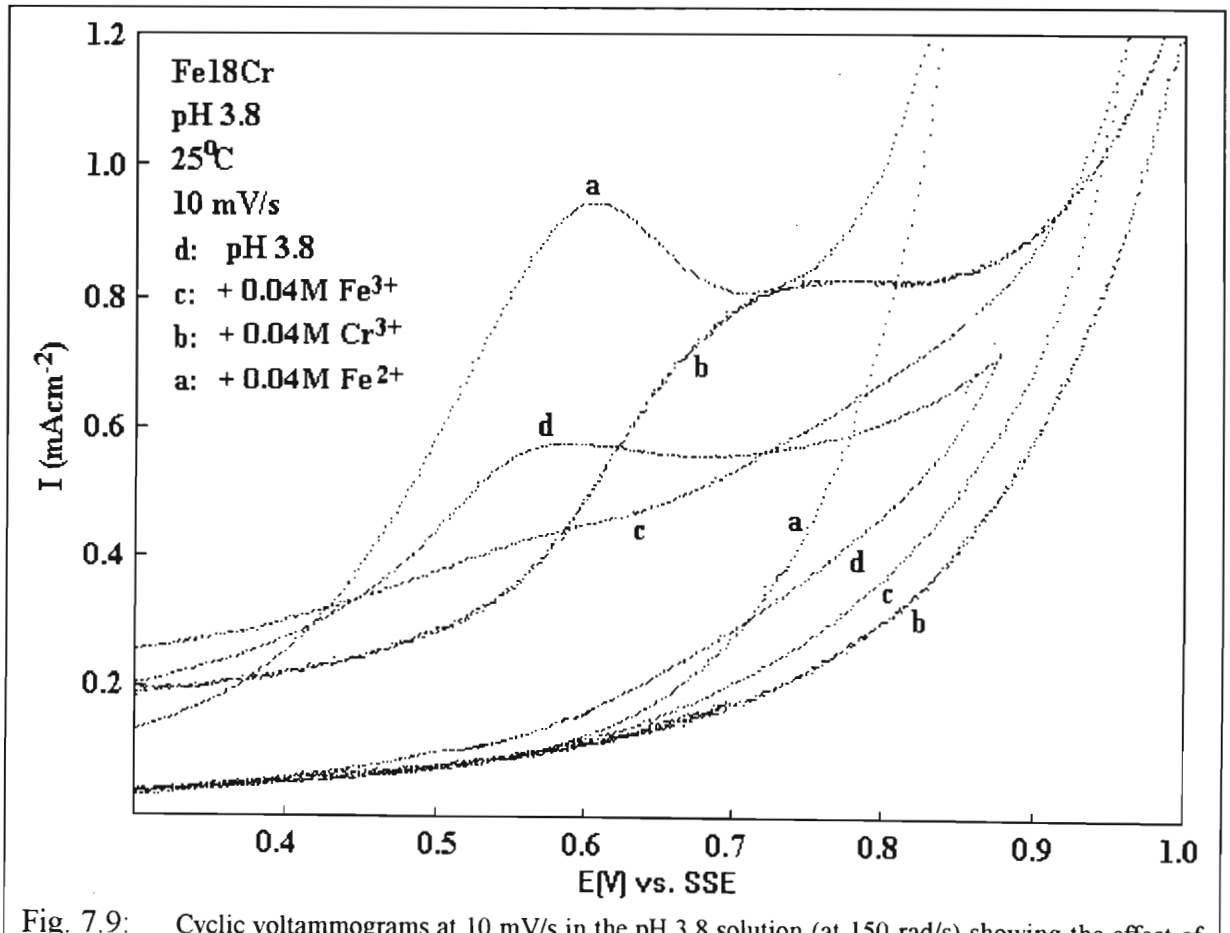

Fig. 7.9: Cyclic voltammograms at 10 mV/s in the pH 3.8 solution (at 150 rad/s) showing the effect of addition of cations Fe^{2+}, Fe^{3+} and Cr^{3+} (separately) at a concentration of 0.04M.

The effect of adding Fe^{2+} is the same as has been obtained in results shown in chapter 7. The addition of Fe^{3+}, however, has almost totally suppressed the peak A current response. This can be explained if Fe(III) is considered to be a major agent in secondary passivity. The addition of aqueous Fe(III) would then hasten secondary passivity. The addition of Cr^{3+} increases E_{pA} and I_{pA}. I_{pA} is probably increased because of the additional Cr(III) → Cr(VI) reactions. E_{pA} is probably increased because aqueous Cr(III) may strengthen the passive film (before voltammetric entry into the passive film) by reacting to form Cr_2O_3 (in the passive region) and thus a more positive potential is needed to break down the passive film than in the normal pH 3.8 solution.

A set of chronoamperometric experiments was then carried out. In one single step experiment for each solution, the potential was stepped from 0.3V (passive region) to 0.82V (secondary passivity).

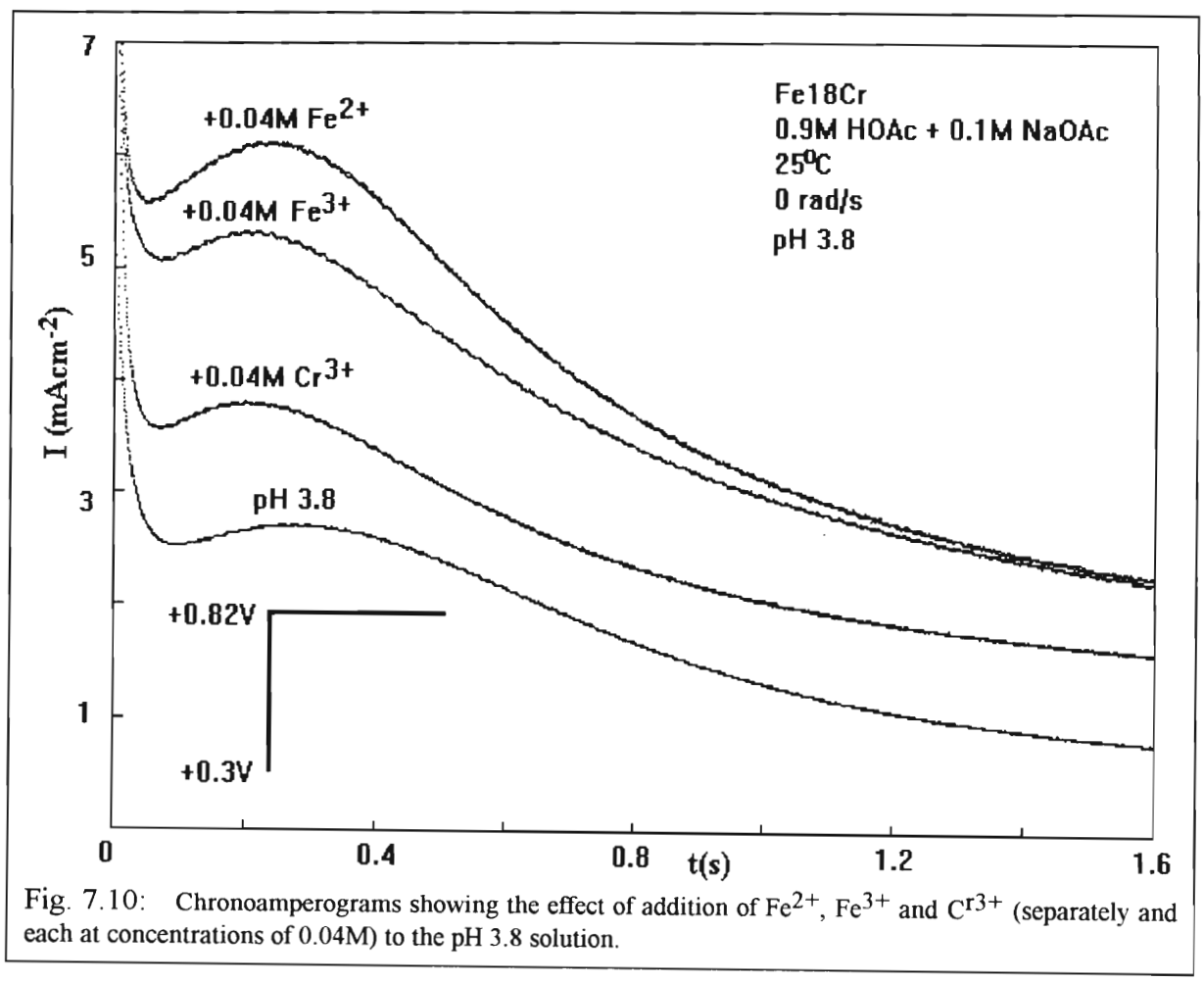

Fig. 7.10: Chronoamperograms showing the effect of addition of Fe^{2+}, Fe^{3+} and Cr^{3+} (separately and each at concentrations of 0.04M) to the pH 3.8 solution.

According to fig. 7.10, the addition of Cr^{3+} has the least effect on the rising transient. The Fe^{3+} solution increases I_{max} more than the Cr^{3+} solution does. This unexpected result may be because experimental conditions (e.g. a favourable pH) are such that the Fe(III)→Fe(VI) oxidation reaction is favoured and Fe(VI) may exist in a metastable state for very short times. As is expected, the Fe^{2+} solution increases I_{max} to the greatest extent (Of all the three above aqueous ions, Fe^{2+} was shown - in chapter 7 - to contribute most to the current response at transpassive potentials).

7.2. Perchlorate solution: pH 0.5

As is usual, the polarisation curve for this solution (at 2 mV/s) is shown first (Fig. 7.11).

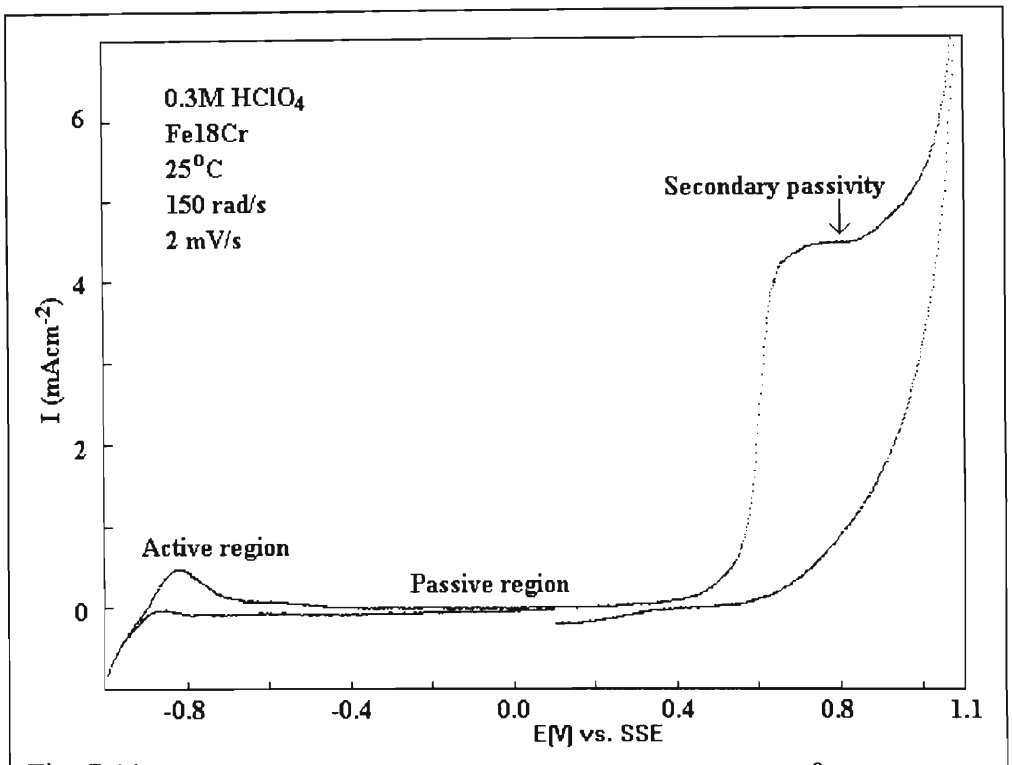

Fig. 7.11: Polarisation curve of Fe18Cr in the pH 0.5 solution at 25°C, 2 mV/s and 150 rad/s. Here the starting potential was +0.1V and the potential was initially swept cathodically to the negative limit.

Fig. 7.12 shows the transient data obtained in this solution at 25°C and 0 rad/s from single step experiments.

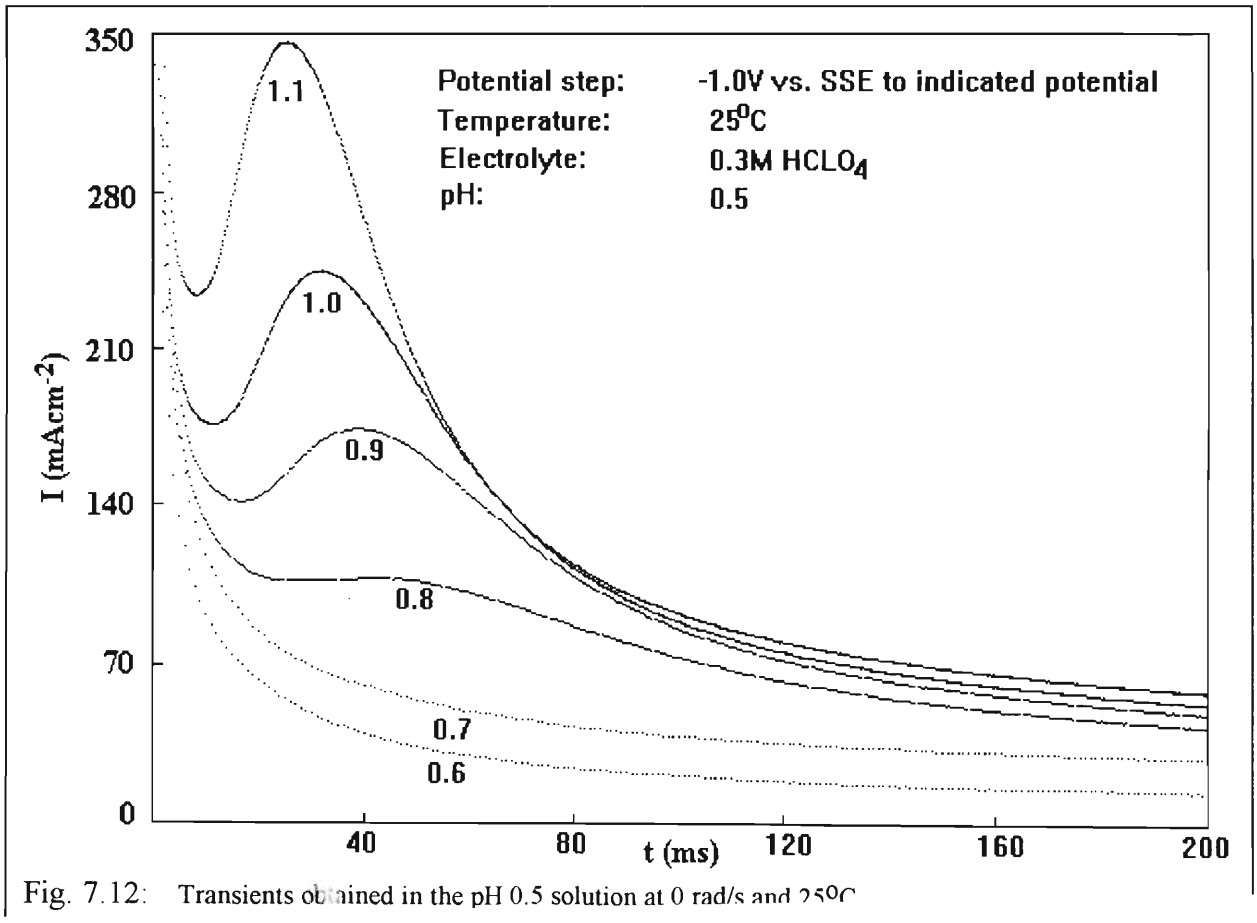

Fig. 7.12: Transients obtained in the pH 0.5 solution at 0 rad/s and 25°C

A reverse rising transient was not found at this pH (0.5). The reason for this is probably due to the fact that t_{max}'s in general are reduced by approximately one order of magnitude from the pH 3.8 to the pH 0.5 solution. The processes causing the reverse rising transient may still occur, but if so they occur at such short times after the second potential step that they are obscured by the double layer charging current.

In comparing the rising transients of fig. 7.12 to those obtained in the pH 3.8 solution, two observations can immediately be made. Firstly, the range of t_{max} in the pH 3.8 solution was approximately 0.2 to 0.4 seconds whereas in the pH 0.5 solution the range of t_{max} is approximately 0.02 to 0.05 seconds. Secondly, whereas the range of I_{max} in the pH 3.8 solution was 2 - 20 $mAcm^{-2}$, in the pH 0.5 solution the range is 100 - 500 $mAcm^{-2}$. Clearly the increase in acid concentration from pH 3.8 to 0.5 greatly increases the rate of dissolution of material from the electrode. Therefore not only is the hydronium ion involved in dissolution of passivating metal oxides, but it is definitely also involved in the direct dissolution of the base alloy, possibly in a catalytic or semi-catalytic manner.

Fig. 7.12 shows that the values of I_{lev} for the potential steps -1.0V $\rightarrow$ 0.8,0.9,1.0, and 1.1V are very close. If there was significant oxygen evolution interference at the 1.1V potential (as the polarisation curve would indicate) then the value of I_{lev} for the step to 1.1V should be a great deal larger than that for the step to 0.8V. This is further evidence for the facts that oxygen evolution interference in a chronoamperometric experiment cannot be accurately predicted by a polarisation curve and for the suggestion that secondary passivity exists well into the oxygen evolution region.

The effect of rotating the electrode is shown in fig. 7.13 for a potential step of -1.0 $\rightarrow$ +1.0V.

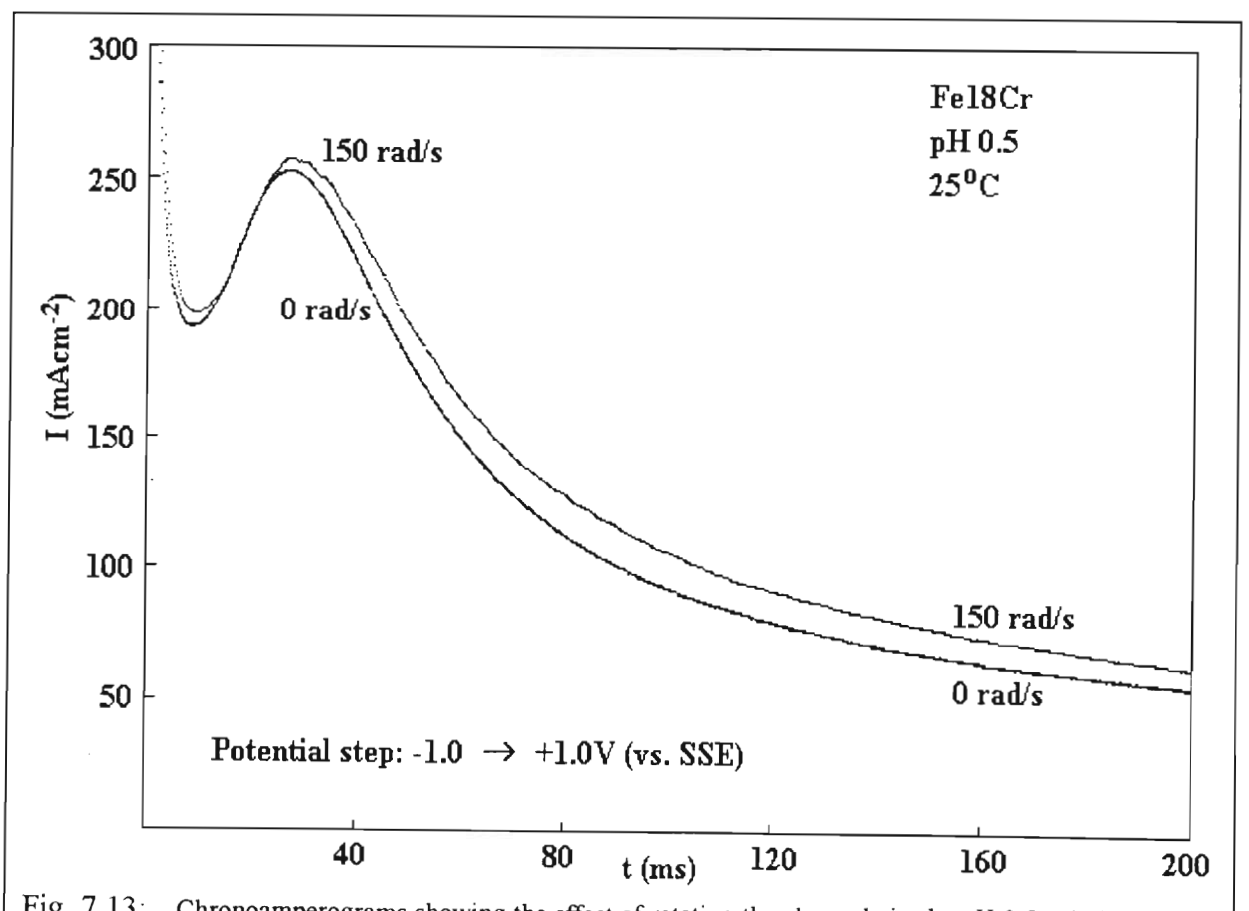

Fig. 7.13: Chronoamperograms showing the effect of rotating the electrode in the pH 0.5 solution for the

From fig. 7.13, the main effect of rotating the electrode is to increase the current response, particularly after t_{max}. This is probably due to the increased efficiency of removal of oxidation products when the electrode is rotated. t_{max} is also slightly larger when the electrode is rotated, which is to be expected if supersaturation of material must occur adjacent to the electrode prior to nucleation and growth of the passivating film.

One consistent observation in the investigation of rising transients was that the potential to which the electrode was stepped had to be in the transpassive region in order for a rising, rather than a falling transient to be obtained. The reason for this was thought to be that the nucleation and growth of the passivating anodic film occurs very quickly (particularly when stepping to the passive region) and if the experimental conditions are not such that the formation of a passivating anodic film can be delayed, then the rising transient would be obscured by the double layer charging current. Stepping to the transpassive region probably delays the formation of a passivating film, simply due to the temporarily rampant pitting corrosion of the electrode induced by the highly positive potential to which the electrode is stepped.

It was thought that the aggressive conditions previously only obtained by stepping to the transpassive region could also be obtained by raising the temperature of the solution. Fig. 7.14 shows the results of stepping to the passive region at 90°C in pH 0.5 solution. Reproducibility could only be obtained when the electrode was rotated during the experiment and so the transients were obtained at 150 rad/s. A reproducible transient could not be obtained when stepping to the transpassive region, probably because of the unchecked, general corrosion that occurred when stepping to those potentials.

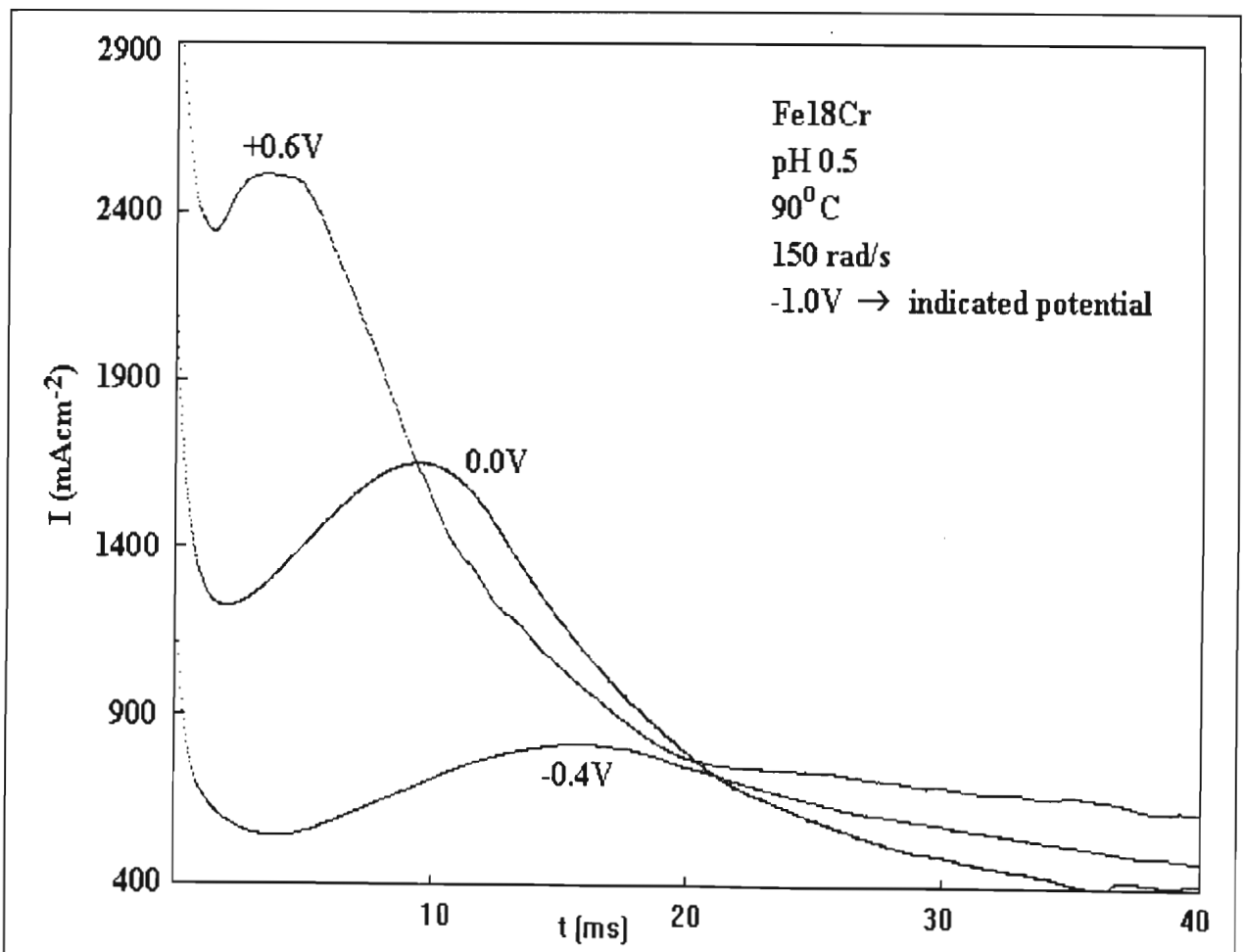

Fig. 7.14: Chronoamperograms showing rising transients obtained when stepping to the passive region at 90°C in the pH 0.5 solution.

One transient that was obtained at 90°C is shown separately (fig. 8,15). This involved a potential step of -1.0V → -0.6V, into what is suspected (at 90°C) to be the active region.

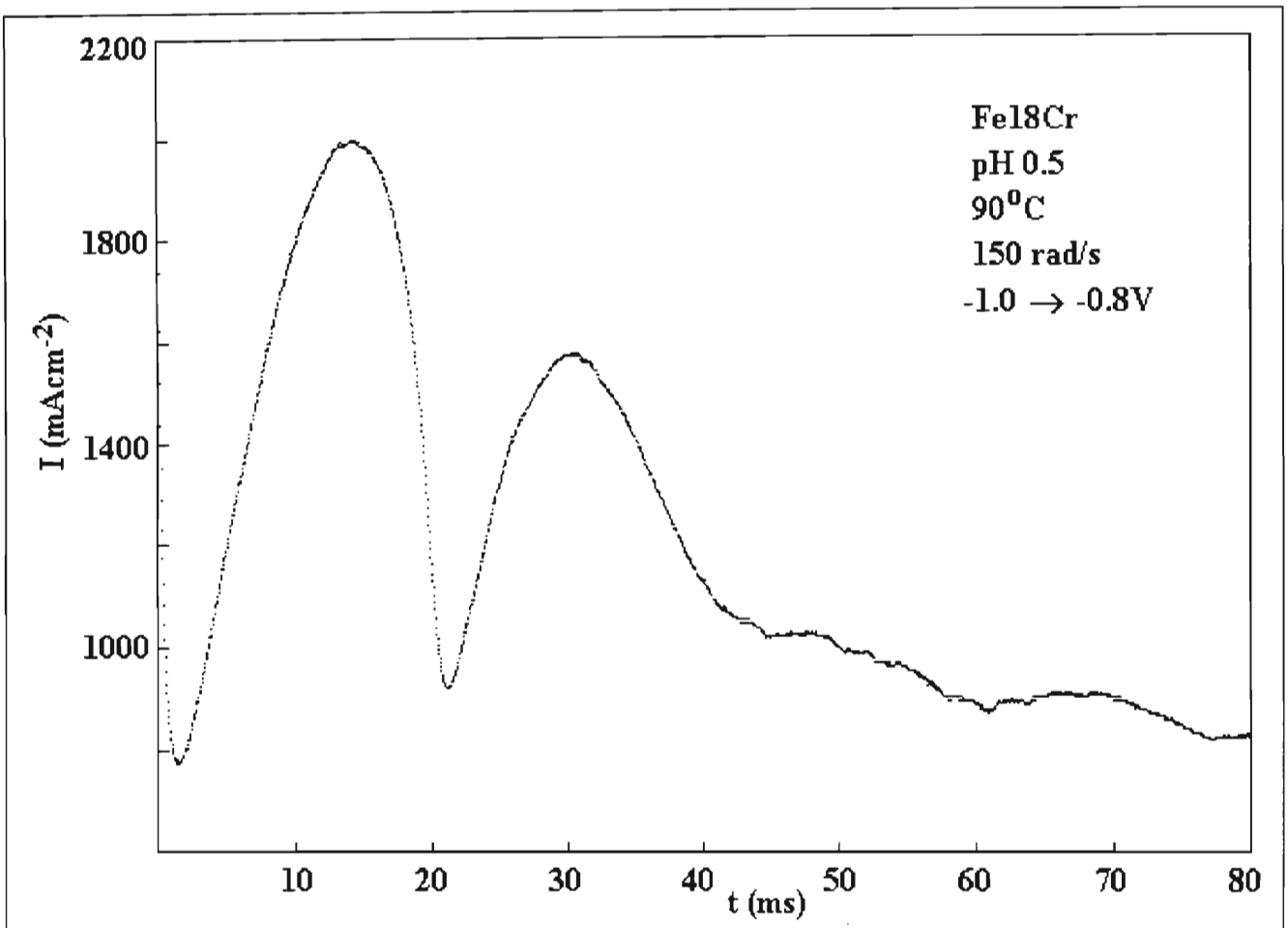

Fig. 7.15: Chronoamperogram showing a double rising transient obtained from stepping into the active region in the pH 0.5 solution at 90°C.

Fig. 7.15 shows a double rising transient. One cause of a number of rises in a transient has been shown to be the formation of consecutive layers in an anodic film [67]. Since the active region is a region of general dissolution, it is possible that the initial film formed is highly porous, hence allowing further dissolution, nucleation and growth of another layer of film.

The reproducible regime used for the chronoamperometric experiments at 90°C and in pH 0.5 solution was, out of necessity, different. The regime simply consisted of switching on the electrode before immersion (to the starting potential of -1.0V), immersing the electrode in the solution, holding that potential (-1.0V) for 5 seconds only, and then stepping to the desired potential.

7.2.1. The effect of addition of cations to the pH 0.5 solution

Fe^{2+}, Fe^{3+} and Cr^{3+} (each in concentrations of 0.04M, as with the pH 3.8 solution) were added separately to three pH 0.5 solutions. Each of the three solutions was then used in a set of four single potential step experiments at 25°C and 0 rad/s - namely stepping from -1.0V to 0.8, 0.9, 1.0 and 1.1V vs. SSE. 0.8V was the first potential at which the transient displayed a "rise". The results for each solution were qualitatively similar for the normal pH 0.5 solution, although the values of I_{max} and t_{max} differed. Fig. 7.16 compares the transients obtained at 25°C for each of the solutions for the potential step $-1.0 \rightarrow +1.0$V.

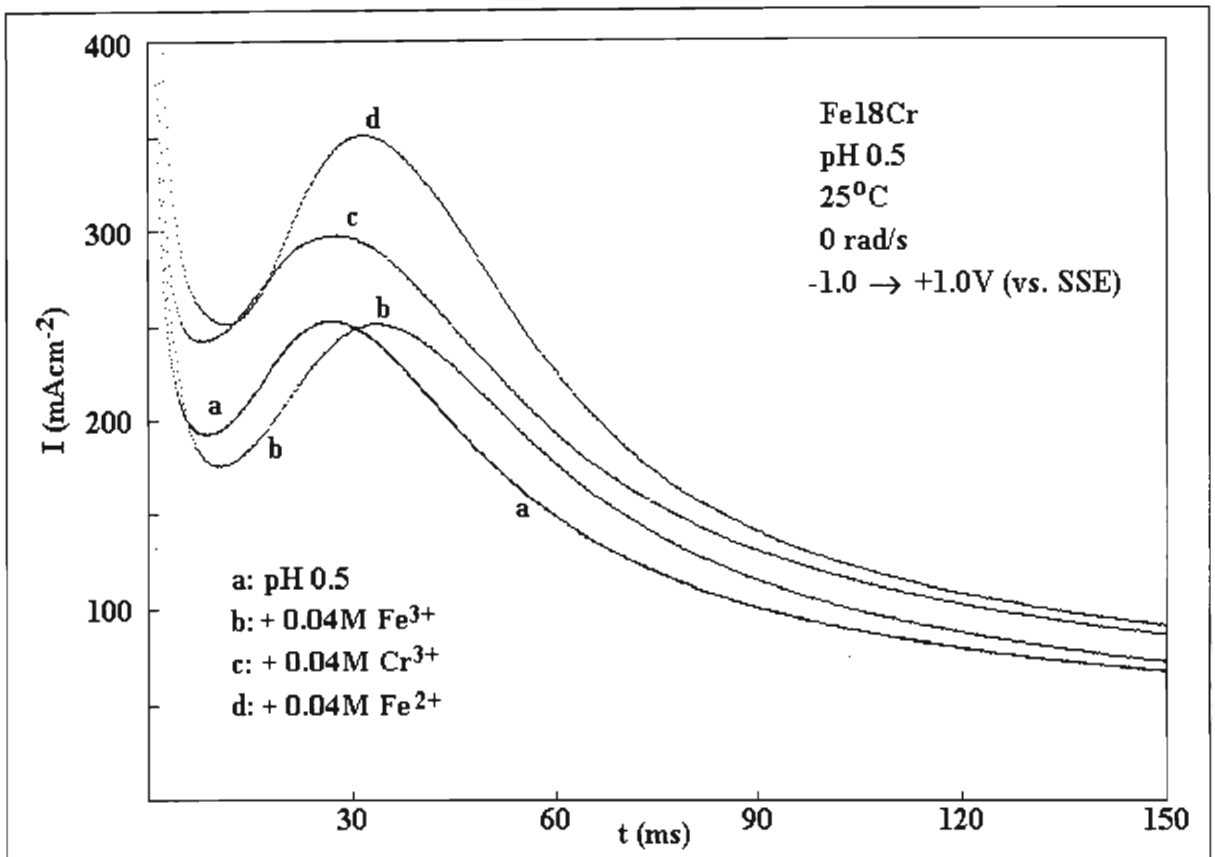

Fig. 7.16: Chronoamperograms showing the effect of addition of cations Fe^{2+}, Fe^{3+} and Cr^{3+} (separately) at a concentration of 0.04M to the pH 0.5 solution at 25°C and 150 rad/s for the potentials step -1.0V → +1.0V.

Fig. 7.16 shows that the addition of Fe^{3+} to the solution does not increase I_{max}, but t_{max} is increased. Since I_{max} is not increased (unlike in the pH 3.8 solution) it can be concluded that this pH is not conducive towards the Fe(III) → Fe(VI) oxidation reaction, which is consistent with current thought [91]. The fact that t_{max} is increased means that the addition of Fe^{3+} impairs the nucleation and growth of the anodic film, thus lengthening the time for it to form. This can be explained if an equilibrium reaction such as

$$Fe^{2+}_{(aq)} \rightleftharpoons Fe^{3+}_{(aq)} + e^{-}$$

is considered to occur. The addition of aqueous Fe^{3+} would then, by Le-Chatelier's principle, shift the equilibrium to the left and delay the formation (by nucleation and growth) of ferric oxides.

The addition of chromic ions raises I_{max}, but as before, the addition of ferrous ions raises I_{max} the most. These results support Graham's suggestion that iron dissolves preferentially (*cf* section 3.4.2) in these potential step experiments.

Figures 7.17,18 show the variation of I_{max} and t_{max} (respectively) with potential step for each of the four pH 0.5 solutions at 25°C.

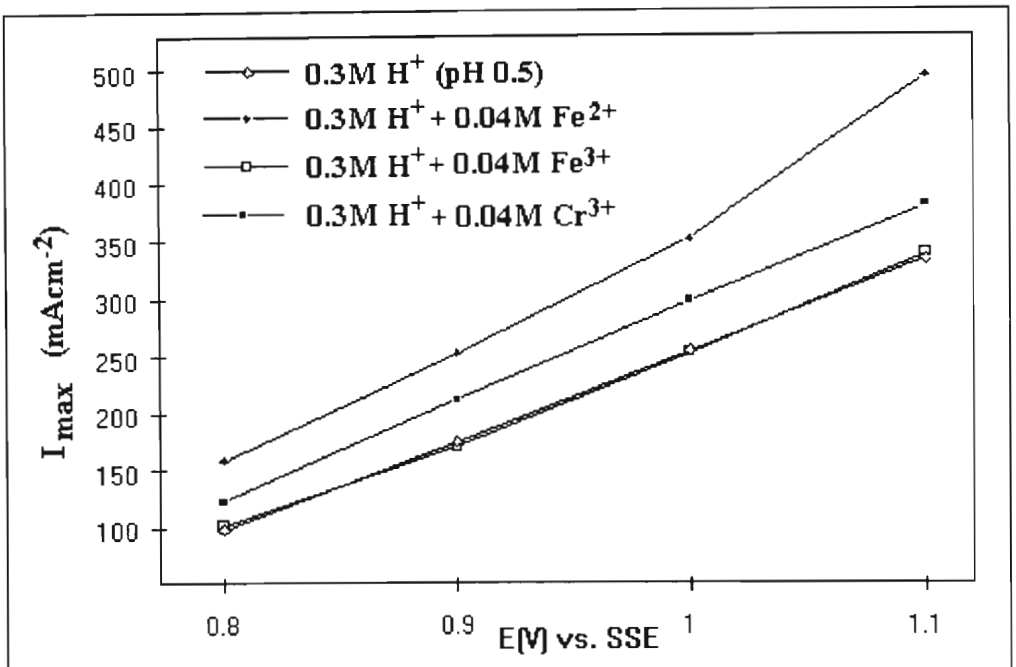

Fig. 7.17: Plot of I_{max} versus E_2' for each of the four pH 0.5 solutions used, at 25°C and 0 rad/s.

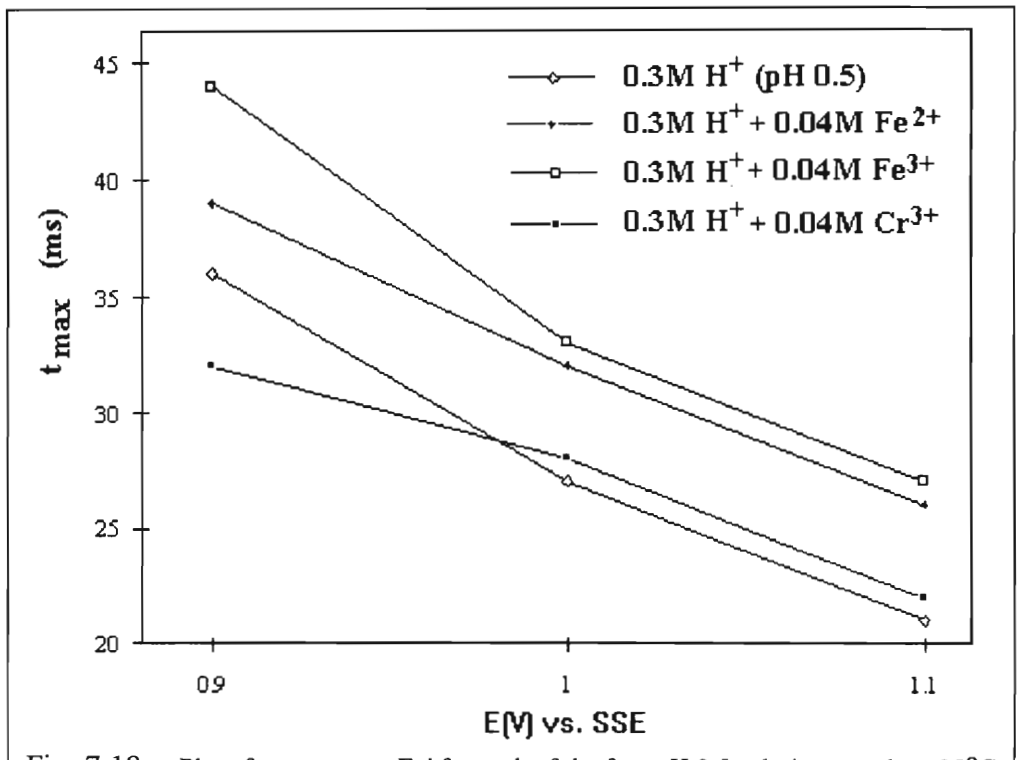

Fig. 7.18: Plot of t_{max} versus E_2' for each of the four pH 0.5 solutions used, at 25°C and 0 rad/s

The values of t_{max} for $E_2' = 0.8V$ in fig. 7.18 were left out because the chronoamperometric peaks for the potential step to 0.8V were very wide and shallow (they formed plateaus), so that t_{max} could not accurately be found. The corresponding I_{max} values could, however, be easily found as the current density value of the plateau. Fig. 7.17 shows the same trends for all the potential steps as shown in fig. 7.16 for the potential step to 1.0V. Generally, the ferrous ions increased I_{max} by 70 - 100 $mAcm^{-2}$ and the chromic ions increased I_{max} by 20 - 40 $mAcm^{-2}$. Fig. 7.18 shows that the ferric ions increased t_{max} the most, followed by ferrous ions, whilst the chromic ions had the least overall effect on t_{max}.

CHAPTER 8

8. QUANTITATIVE MODEL FOR RISING TRANSIENTS

8.1. Introductory theory

For the sake of simplicity, all equations will be given in terms of the time after the potential step, t, and P_i's, where P_i is any coefficient of t or of an exponential term or it is a time term itself. For example, equation (2.1) - the equation for the current due to instantaneous charge transfer controlled conical nuclei undergoing sudden death - can be written in the simplified form

$$I = P_A\left\{\exp\left(-P_B(t-P_C)^2\right)-\exp\left(-P_B t^2\right)\right\} \tag{8.1}$$

where $P_{A,B,C}$ are defined in equation (2.55). Note that the P_i's used in this chapter will be used independently of those in chapter 2.

The concept of (sudden) "death" of nuclei was introduced in section 2.4.1.3. This simply involves the cessation of growth of a nucleus at a certain rigid, predefined height from the electrode surface. The concept of "slow death" will now be introduced. Qualitatively, slow death can be thought of as a gradual process whereby nuclei stop growing. No one nucleus may "die" at the same time or exact dimensional size as another. For example, consider the growth of pits into an (Fe18Cr) electrode after a potential step into the transpassive region. At some point, an oxide or salt film will nucleate or precipitate over the electrode surface. As a pit is filled with this passivating oxide or salt, it effectively "dies". However, not all the pits will be filled with the passivating substance simultaneously. If the film forms by nucleation, then it might take a finite time for a pit to be reached by a growing (passivating) nucleus, and this finite time would be independent of a particular pit dimension. Hence the pits die gradually - the number of corroding pits is slowly reduced. Quantitatively, if the death of cones in equation (8.1) were to be "slow", then this could be indicated by the insertion of one additional parameter as shown

$$I = P_A\left\{\exp\left(-\frac{P_B}{P_D}(t-P_C)^2\right)-\exp\left(-P_B t^2\right)\right\} \tag{8.2}$$

where P_D is a dimensionless parameter with the condition $P_D \geq 1$. If $P_D \to \infty$, then the limiting situation of the following equation arises

$$I = P_A\left\{1-\exp\left(-P_B t^2\right)\right\} \tag{8.3}$$

and this is simply the equation for charge transfer controlled instantaneous conical nucleation, where the current levels out at I_{max} ($I_{max} = I_{lev}$). If $P_D = 1$ then the limiting situation of equation (8.1) is attained, where, after t_{max}, the current rapidly diminishes to zero.

Current theory on formation and growth of nuclei can be summarised in the following three questions:

1. Are the nuclei right angle cones or hemispheres ?
2. Is the growth of the nuclei charge transfer or diffusion controlled ?
3. Do the nuclei form instantaneously or progressively ?

It is acknowledged that these questions do not cover all possible situations. For example, growth of nuclei as spherical caps has been considered. Also, another type of kinetic control (e.g. the rate of a chemical reaction) may be important. These questions only consider limiting situations (e.g. instantaneous versus progressive nucleation). However, at this early stage of development of the model, and for the sake of simplicity, only the situations considered by these previous three questions (and the possibility of slow or sudden death of nuclei) will be considered.

8.2. Description of the model

It is proposed that there are three primary contributions towards the rising transient current responses of a Fe-Cr electrode:

A. A diffusion controlled dissolution current, which decays with the root of time. This has also been proposed for the deposition of Ag_2O on a silver electrode [61]. This can be described by the following term

$$\frac{P_9}{t^{1/2}}$$

B. A current due to the "pitting nucleation" of conical, charge transfer controlled nuclei which form instantaneously after the potential step. The term "pitting nucleation" needs some explanation: Generally, pitting refers to a loss of material from the anodic film or from the substrate at specific, localised sites. Nucleation refers to growth (or gain) of material on the substrate (or on top of an already established inner anodic film) at localised or active sites. Pitting nucleation (or pitting nuclei) is a term which simply implies that **the growth of pits can be described in the same way and by the same equations as the growth of nuclei**. This is a unique form of pitting since it occurs in the absence of chloride. It has been shown before that pitting will occur without halide ions provided the potential is sufficiently positive [52,190]. This approach in the treatment of pit growth is not new and has been successfully and quantitatively applied to the growth of hemispherical pits [191]. There is only one significant difference in the growth kinetics of pits and of "true" nuclei. It is simply that the growth of a nucleus may be (diffusion) limited by the rate at which material is supplied to it whereas material is always available at the edges of the pit. Thus pitting nucleation is more likely to be charge-transfer controlled than "true" nucleation.

These pitting nuclei undergo a slow death upon the formation of a passivating oxide / salt (see **C.**). A finite time is required before passivating substances can nucleate on the electrode surface and this time is defined as P_7 (in seconds). The death of the pitting nuclei is "slow" (it does not occur only when pits reach certain rigidly defined dimensions) simply because the passivating nuclei do not necessarily form directly on top of the pits. Since the death of pits depends on their being covered by passivating nuclei, and a particular passivating nucleus can occur at a totally random distance from a pit, it can be seen that some pits will be large, and some small when they "die" (stop growing).

When $t < P_7$, then the current due to the pitting of the electrode is

$$P_1\left\{1-\exp\left(-P_2\,t^2\right)\right\}$$

and when $t \geq P_7$, then the current contribution from the pitting of the electrode (when the pits themselves are undergoing a slow death) is

$$P_1\left\{\exp\left(-\frac{P_2}{P_5}(t-P_7)^2\right)-\exp\left(-P_2 t^2\right)\right\}$$

Fig. 8.1 shows a simplified representation of the initiation, growth, and death of a pit, according to the nucleation model.

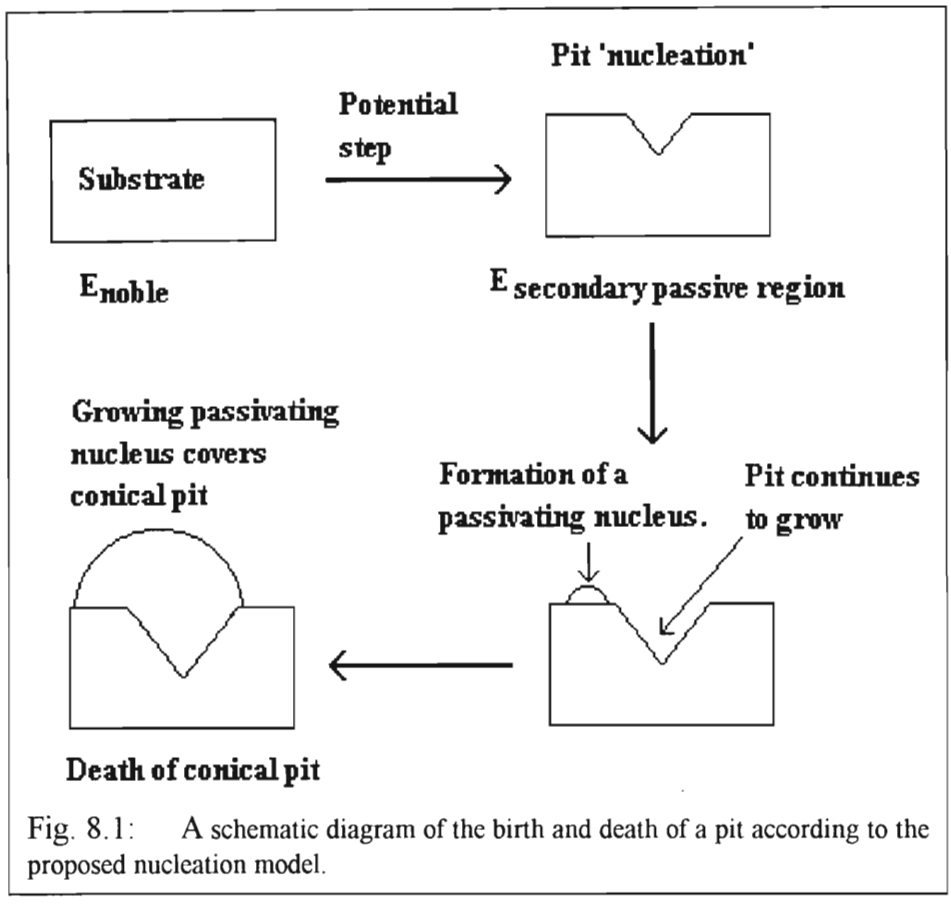

Fig. 8.1: A schematic diagram of the birth and death of a pit according to the proposed nucleation model.

C. Finally, it is suggested that the passivating substance[a] will nucleate progressively and grow in a diffusion controlled manner as hemispheres. The level of supersaturation required for further precipitation in the region of a precipitated nucleus is lost immediately after the initial precipitation, and the nucleus grows by the diffusion of cations from the electrode surface in two ways:

(i) Cations formed by oxidation of the electrode underneath the nucleus can diffuse through pores in the growing nucleus to the edges of the nucleus. In this case "death" occurs when and if the growing nucleus becomes more compact and the pores close up.

(ii) Adsorbed cations formed by oxidation of a portion of the electrode that is not yet covered by the passivating substance may diffuse along the surface of the electrode to the edge of a nucleus. In this case "death" occurs progressively as the surface of the electrode is covered.

---

[a] This passivating substance will form a passive film. In the early stages of development of this model, no differentiation is made between the barrier layer and the outer, porous layers of a passive film. However, the passivating nuclei can definitely be said to form the inner part (if not all) of the resulting anodic film. Note that the potentials to which Fe-Cr electrodes were stepped to obtain a rising transient usually corresponded to the region of secondary passivity, where the secondary "passive" film does not contain the more protective barrier layer, but rather a porous and only slightly protective film.

In both cases it can be envisaged that death of the hemispherical nuclei is slow and that the greater the porosity of the passivating substance, the slower the death of its constituent nuclei. The time at which these nuclei begin to grow will be the same as the time of the beginning of the slow death of the conical pits (P_7). The time when the slow death of these nuclei starts is defined as $P_7 + P_8$. Hence at $P_7 \leq t < P_7 + P_8$, ("death" of passivating nuclei has not yet begun) the contribution to the current by the hemispherical nuclei is given by

$$\frac{P_3}{(t - P_7)^{1/2}}\left\{1 - \exp\left[-P_4(t - P_7)^2\right]\right\}$$

and the contribution to the current by the hemispherical nuclei at $t \geq P_7 + P_8$ is given by

$$\frac{P_3}{(t - P_7)^{1/2}}\left\{\exp\left[-\frac{P_4}{P_6}(t - P_7 - P_8)^2\right] - \exp\left[-P_4(t - P_7)^2\right]\right\}$$

Putting it all together, the model is as follows:

At $t < P_7$,

$$I = \frac{P_9}{t^{1/2}} + P_1\left\{1 - \exp\left(-P_2 t^2\right)\right\}$$

at $P_7 \leq t < P_7 + P_8$,

$$I = \frac{P_9}{t^{1/2}} + P_1\left\{\exp\left(-\frac{P_2}{P_5}(t - P_7)^2\right) - \exp\left(-P_2 t^2\right)\right\} + \frac{P_3}{(t - P_7)^{1/2}}\left\{1 - \exp\left[-P_4(t - P_7)^2\right]\right\}$$

and at $t \geq P_7 + P_8$,

$$I = \frac{P_9}{t^{1/2}} + P_1\left\{\exp\left(-\frac{P_2}{P_5}(t - P_7)^2\right) - \exp\left(-P_2 t^2\right)\right\} + \frac{P_3}{(t - P_7)^{1/2}}\left\{\exp\left[-\frac{P_4}{P_6}(t - P_7 - P_8)^2\right] - \exp\left[-P_4(t - P_7)^2\right]\right\}$$

The theoretical meanings of the P_i's which have not already been defined, are given in table 8.1 and are obtained from parallel models in the literature (*cf* section 2.4.1). It must be noted that the exact meanings of the parameters in this model will differ from those in the literature, due to the fundamental difference that in the literature, the solution is almost always considered to be the source of nucleating material (electrocrystallisation) i.e. the nucleating material is a predissolved solute in the solution, whereas in this model the Fe-Cr electrode is the source of nucleating material. In the table a subscript "c" means that the term is specific to the **c**onical pitting nuclei, a subscript "h" means that the term is specific to the **h**emispherical nuclei, and a subscript "d" means that the term is specific to the **d**issolution process(es).

Parameter	Theoretical meaning	Reference
P_1	$n_c F k''$	64
P_2	$\pi M_c^2 k'^2 N_{o,c} / \rho_c^2$	64
P_3	$n_h F D_h^{1/2} C_h^* / \pi^{1/2}$	59
P_4	$4\sqrt{2}\,\pi^{3/2} M_h^{1/2} C_h^{*1/2} D_h A_{k,h} / 3\rho_h^{1/2}$	59
P_9	$n_d F D_d^{1/2} C_d^* / \pi^{1/2}$	61

Table 8.1: Definitions of the P_i parameters used in the nucleation model, **according to electrocrystallisation theory**.

Two inconsistencies in the definitions of the parameters based on electrocrystallisation models were noted:

- Any use of a bulk concentration term, C^*, is invalid as the concentration of the active material in the bulk solution is always zero (the active material is not pre dissolved in the solvent).
- Since the conical nuclei are in fact pits, it is meaningless to use the density term, ρ_c.

Clearly, most of the P_i's used in the nucleation model will have to be defined independently of the traditional literature definitions which are based on electrocrystallisation theory. However, the above definitions are a good rough guide of the meanings of the P_i's. At this early stage of development of the model, the rough guide of the above definitions is taken to be sufficient.

8.3. Results

A program (NUCMODEL.BAS, *cf* appendix B) was written by the author to fit this model to experimental rising transients by means of a simple iterative process. In order to explain the parameter which describes the degree to which the theoretical transient fits the experimental transient, it should be noted that δ'' is defined as

$$\delta'' = \sum_{i=1}^{m} \left| I_{e,i} - I_{t,i} \right|^2$$

where δ'' is the sum of the squares of the absolute values of the differences between the experimental current values (I_e) and the theoretical current (I_t) values, when there are m experimental points. The factor which describes the degree of fit of the theoretical to the experimental transient is then defined as

$$\delta_f = \frac{\delta'' \times 10^5}{m \times I_{\max}^2}$$

It was observed during the procedure of curve fitting that a good fit was obtained for $\delta_f \leq 4$. It should also be mentioned that the fitting procedure was only used for points at times $\geq t_{min}$. The reason was that the initial falling portion of the transient has a double layer charging current contribution and including this region in the fitting procedure would result in a positive unknown error in the value of P_9. When diagrams of the theoretical curves were generated, any overlap between the theoretical and experimental curves before I_{min} would then indicate that the initial falling current probably has a large diffusion controlled dissolution component.

The model has been applied to two rising transients, each of which represents an extreme of experimental conditions. The first involved a potential step of -1.0 to +1.0V vs. SSE (i.e. from the pre-active to the secondary passive region) in 0.3M $HClO_4$ (pH 0.5) at 25°C and the final value of the fitting parameter, δ_f, was 2.5. Fig. 8.2 shows the theoretical and experimental transients for these conditions and fig. 8.3 shows the individual contribution of each of the three proposed processes to the overall theoretical current.

The second experimental transient involved a potential step of +0.4 to +0.85V (i.e. from the passive to the secondary passive region) in acetate buffer solution (pH 3.8) at 25°C and the final value of δ_f was 3.5. Fig. 8.4 shows the theoretical and experimental transients for these conditions and fig. 8.5 shows the individual contribution of each of the three proposed processes to the overall theoretical current. It should be noted that the program that fits theoretical transients to experimental transients, being essentially an iterative process, could ideally be allowed to continue *ad infinitum* (thereby continuously reducing the value of the fitting parameter - albeit by progressively smaller and smaller amounts), but had to be stopped as soon as a reasonable fit was obtained.

The values of the P_i's obtained for each of the above rising transients are tabulated in table 8.2

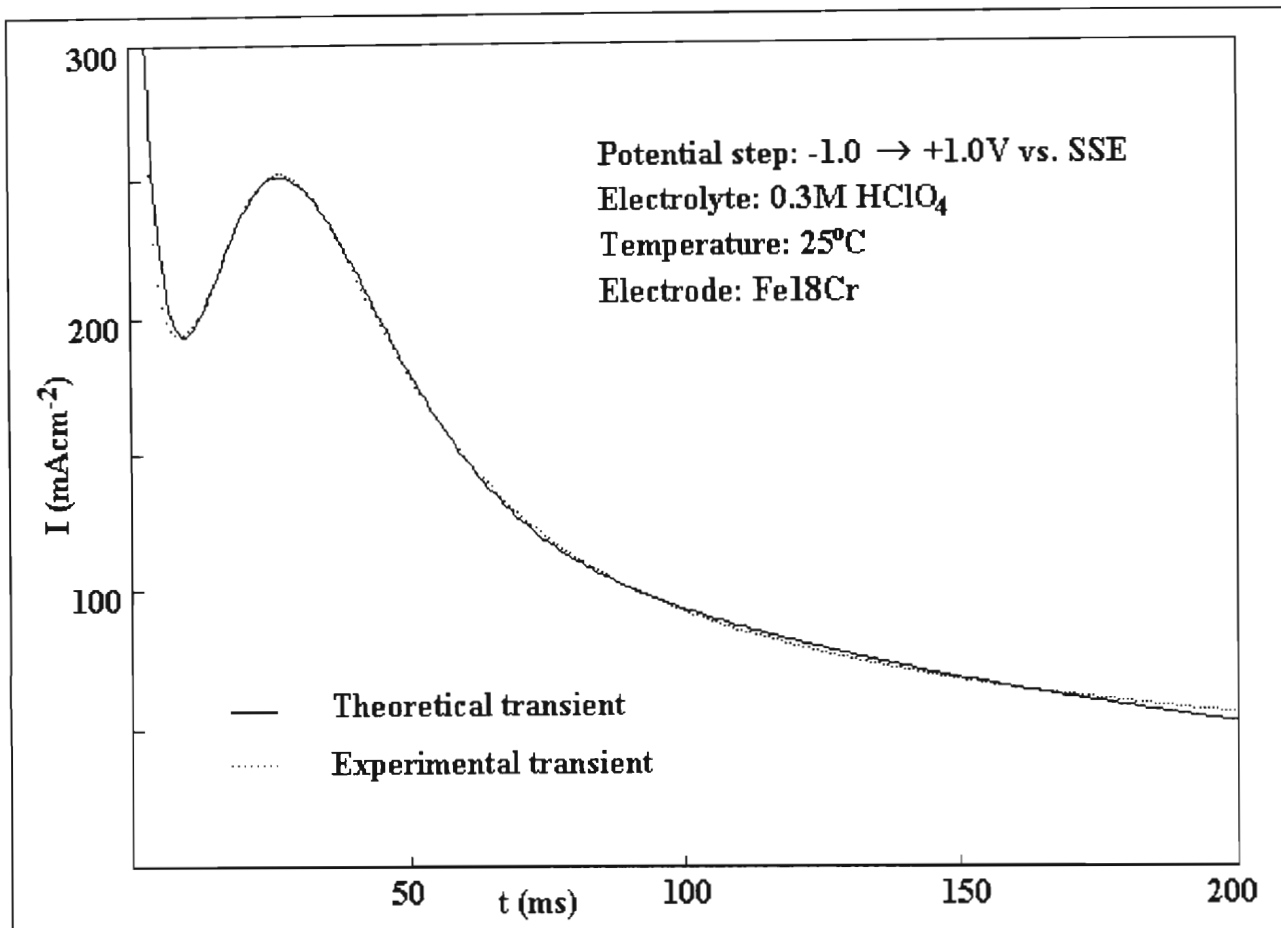

Fig 8.2: Diagram showing experimental transient (at pH 0.5) and the theoretical transient generated from the proposed nucleation model.

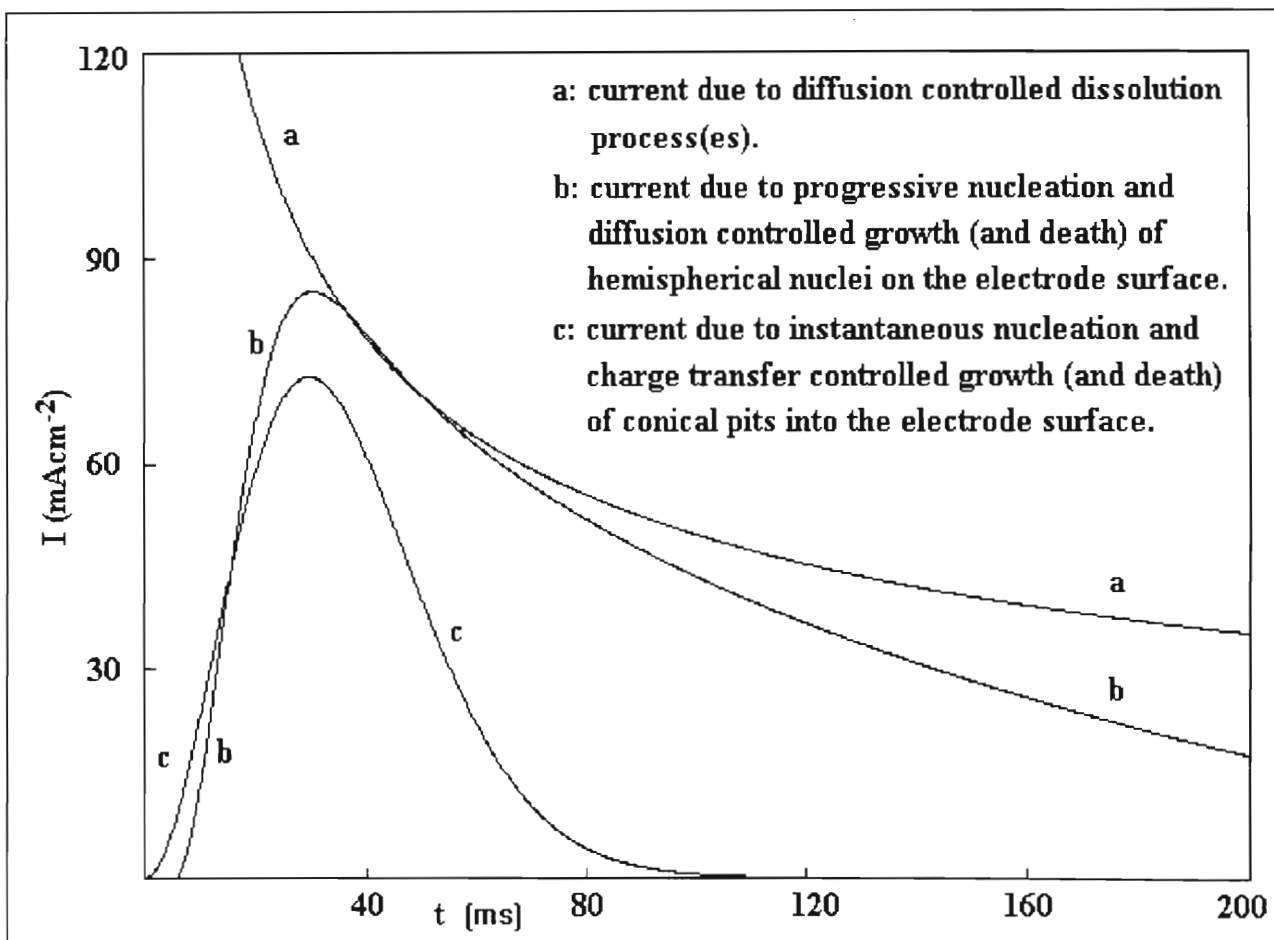

Fig 8.3: Diagram showing the individual contributions of each process in the proposed nucleation model to the overall theoretical transient in fig 8.2.

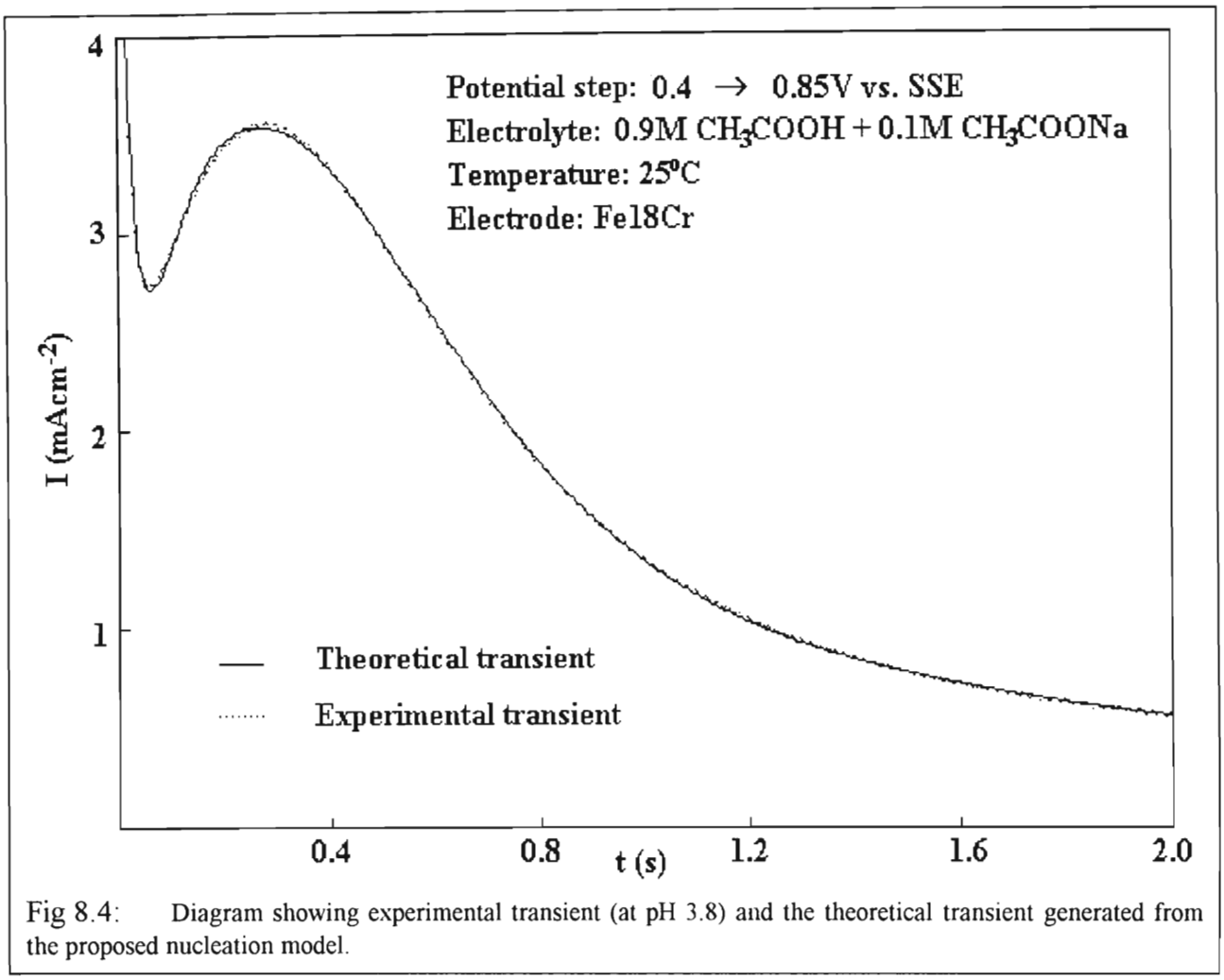

Fig 8.4: Diagram showing experimental transient (at pH 3.8) and the theoretical transient generated from the proposed nucleation model.

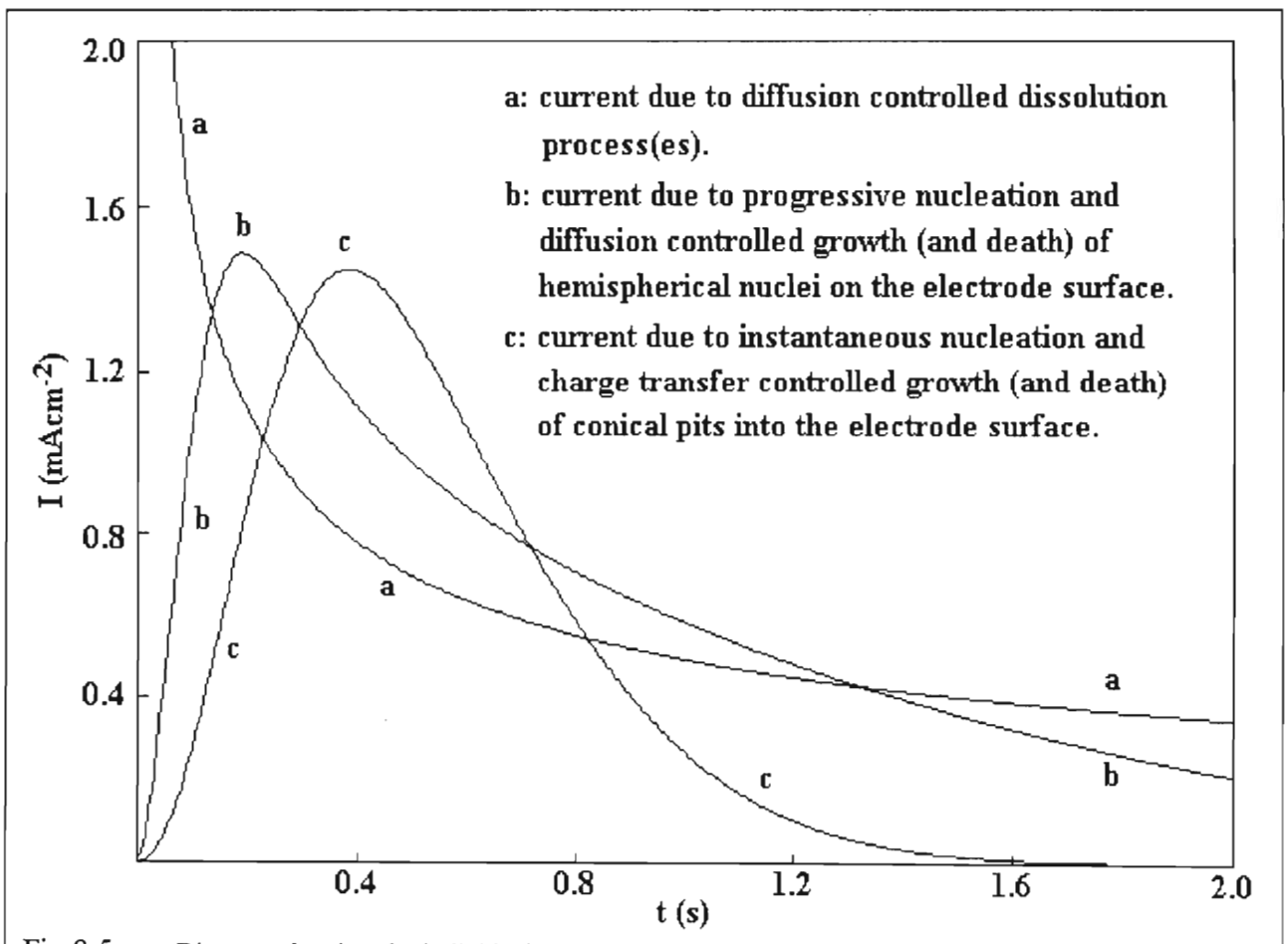

Fig 8.5: Diagram showing the individual contributions of each process in the proposed nucleation model to the overall theoretical transient in fig 8.4.

8.4. Discussion

Transient	P_1	P_2	P_3	P_4	P_5	P_6	P_7 (s)	P_8 (s)	P_9
pH 0.5, -1.0 → 1.0 V, fig 8.2	144	1933	16.3	4141	3.06	217	0.0054	1.0×10^{-6}	15.67
pH 3.8, 0.4 → 0.85 V, fig 8.4	2.58	14.4	1.25	44.7	6.37	127	1.0×10^{-5}	0.0100	0.722

Table 8.2: List of the values of the parameters that were obtained from fitting the proposed nucleation model to the indicated experimental transients.

It is evident from figs 8.3 and 8.5 that the current due to dissolution processes appears to be the largest contributor to the overall charge that is generated. It is therefore suggested that at least two, and probably all three of the following dissolution processes contribute to the overall diffusion controlled dissolution current (which is represented by curve "a" in figs 8.3 and 8.5):

1. The dissolution of a pre-existent layer. For the experimental transient corresponding to the 0.4 to 0.85V potential step (fig. 8.4), this pre-existent layer is, of course, the passive layer. The passive layer contains Fe(II) and Cr(III) which can be oxidised to Fe(III) and Cr(VI) immediately after the potential step. Note that this process will also contribute to the supersaturation required for deposition of passivating nuclei. However the other transient (-1.0 to 1.0 V) has as its initial potential, a pre-active "noble" potential. However some evidence has been gathered for the existence of a pre-existent layer, even at these potentials (*cf* Ch 9). Of course, if the pre-existent layer is totally removed after the potential step then this current contribution will rapidly diminish to zero.
2. A certain percentage of cations will be lost to the solution (and therefore do not contribute to a passivating film) at a diffusion controlled rate. The charge associated with the original oxidation of the electrode to this lost percentage of cations will be incorporated in curve "a" of figures 8.3 and 8.5.
3. After a passivating film has been established and passivating nuclei have started to "die", a non-destructive dissolution of cations through the passive film may occur through pores in the passive film or through cation diffusivity (point defect model) or by migration. This dissolution will also be diffusion controlled. These cations will not contribute to further growth of passivating nuclei and are lost to the solution. This last effect might contribute considerably to the steady-state current, I_{lev}, of rising transients.

It is acknowledged that it would be better to separate these three contributions instead of assuming that they all contribute to one overall diffusion controlled dissolution current. However, doing this would result in an unmanageable number of parameters in the model. This assumption has been found to be workable, if not ideal in the theoretical sense. More advanced versions of this model may be able to separate these contributions to the diffusion controlled dissolution current, but in the early stages of its development the assumption that curve "a" is the sum of three dissolution processes is considered to be reasonable.

Examining the table of the values obtained for the P_i's and figures 8.2-5 leads to the following observations of the effect of each parameter on the current to the theoretical rising transient:

P_1 The important theoretical constant that this parameter contains is the rate constant for the growth of conical pits vertically into the electrode (k''). The effect of increasing P_1 on the theoretical transient is simply to increase I_{max} (P_1 is a pre-exponential term). Hence the interpretation is that as the rate at which pits grow vertically into the electrode increases, so the current maximum of the rising transient increases.

P_2 This contains the rate constant for the horizontal growth of conical pits (k') and the term for the number of active sites ($N_{o,c}$). As P_2 is increased, t_{max} (time of the current peak) of the theoretical transient decreases. The interpretation is that the faster the pitting nuclei coalesce (thereby reducing surface area) the faster the current response will once again decrease.

P_3 The main constant in this parameter is the diffusion coefficient. The larger the value thereof, the more quickly diffusing species can be incorporated into nuclei - the effect is to raise the value of I_{max}, as with P_1. P_9 is analogous to P_3, in that the important term is again the diffusion coefficient, but the effect of increasing P_9 is to increase the dissolution current as a whole which increases I_{max}, t_{max}, I_{min} and I_{lev}.

P_4 The main term here is the nucleation rate constant ($A_{k,h}$). This will in turn be dependant on the rate at which the required level of supersaturation is achieved. As P_4 is increased, t_{max} decreases (as with P_2).

P_5 P_5 and P_6 are the parameters describing the "slowness of death" of the conical pitting and hemispherical passivating nuclei respectively and their effect has already been described (*cf* page 125). The value of P_6 for both fitted transients was far larger than the value of P_5 which correctly indicates that the death of pitting nuclei is far more sudden than the death of passivating nuclei.

P_7 The times (in seconds) represented by P_7 and (P_7 + P_8) are the times that mark the beginning of the slow death of conical pitting and hemispherical passivating nuclei respectively. The effect of increasing either (or both) P_7 or P_8 would be to increase t_{min}, I_{max} and t_{max} (if P_7 and or P_8 are decreased, the nuclei "die" earlier and the current maximum is retarded, but is reached more quickly) and to decrease I_{min} (the time and current of the local minimum before the rising part of the transient).

The reason for choosing cones for the theoretical 3-D shape of the pits was that it has been shown (by computer simulation) that the vertical growth of corrosion pits (i.e. into the electrode) at very positive potentials usually exceeds horizontal growth [140]. A hemisphere grows equally in the horizontal and vertical directions, whereas a right circular cone has a separate rate constant governing each of these modes of growth. The reason for choosing hemispheres for the theoretical 3-D shape of the passivating nuclei was that SEM analysis has shown that 3-D nuclei on Fe-Cr alloys are of a roughly hemispherical shape [52].

This nucleation model was initially developed for the nucleation and growth of an anodic film at transpassive potentials, where it has been shown that pitting does occur in the absence of chloride

anions [89]. However, can the model be applied to rising transients obtained when stepping to passive potentials (cf fig. 7.14) where pitting in the absence of chloride ions is not known [88-90] ? Indeed, at passive potentials and before the formation of the passive film, general corrosion occurs whereas pitting corrosion does not. General corrosion is simply a highly delocalised corrosion happening simultaneously and to the same extent over all of the exposed surface of the substrate. Now, if the horizontal growth rate of conical pits is considered to be far in excess of the vertical growth rate, **and if the conical pits overlap significantly**, then the case of general corrosion is closely approximated. This is illustrated, for a single conical pit in fig. 8.6.

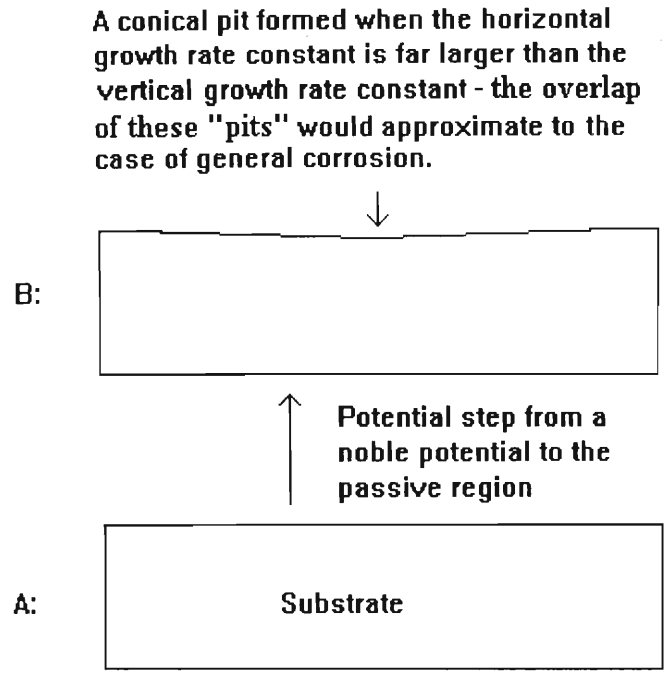

Fig. 8.6: Diagram demonstrating the case when conical pits may approximate general corrosion. "A" refers to the substrate at a noble potential. "B" refers to the substrate just after a potential step to the passive region has been performed and just before the formation of a passive film.

One disadvantage of this model is the large number of parameters it requires (nine). A resulting criticism is that in the iterative process of curve fitting, many local minima, each giving different values for the nine parameters, could be obtained. In order to find the correct local minimum (which should also give the best overall fit), a great deal of thought must go into the initial guesses for the nine parameters. If an incorrect local minimum does occur, it can usually be spotted by the theoretically unlikely values of the parameters that it produces. Also, a certain range of possible values for the parameters may be specified, so that the programme cannot consider theoretically impossible or unlikely values of the parameters (e.g. negative time values for P_7 and P_8 are not allowed). By taking these precautions, it is suggested that incorrect local minima can be avoided.

An advantage of this model is its flexibility towards adaptation and improvement. In an earlier stage of development, the case where only the dissolution process(es) and pitting nuclei were assumed to contribute to the current was considered. When this was found to be insufficient, it was simple to "add" the contribution to the current from growing, passivating hemispherical nuclei.

However, the single most important advantage of the model - as demonstrated by its application to rising transients in two extremes of experimental situations - is that it works !

CHAPTER 9

9. THE SCRATCH EXPERIMENT FOR DETERMINATION OF A PRE-EXISTENT FILM

One question which is pertinent in the interpretation of data (particularly chronoamperometric) concerning the anodic film on Fe-Cr and other alloys is:
Does a film exist at the cathodic starting potential (usually ~ -1.0V vs. SSE) of an experiment or does the physical and electrochemical pretreatment of the electrode ensure that the bare surface of the alloy is exposed at the onset of an electrochemical experiment ?

This question arose out of discussions with Dr D.D. Macdonald in his August 1992 visit to the University of Natal. The significance of this question can be seen, for example, in the modelling of chronoamperometric rising transient data. On the application of an anodic potential step from a so called "noble" potential (overall current at that potential = 0) the first reaction step might not be dissolution of the bare alloy, but rather dissolution of the pre-existent film. This would present an important difference in any quantitative model. The model in chapter 8 allows for the existence of a pre-existent film and assumes that it dissolves in a diffusion controlled manner on the application of an anodic potential step.

The question of the possibility of a pre-existent film has been addressed before by Frankenthal in his work on Fe24Cr in 1M H_2SO_4 and he concluded that after his electrochemical etching there was not a pre-existent film [130]. Other authors (such as Shoesmith) have found pre-existent films on other substrates, such as lead and copper, and these results point to the necessity of determining whether a pre-existent film can be found on Fe-Cr alloys or not.

The purpose of the scratch experiment was merely to determine whether a pre-existent film can be found on Fe18Cr in 0.06M H_2SO_4. This can then serve as an indication whether the pursuit of further work in this area is viable. The experimental method is described in section 4.7.1.3. The "noble" potential that was chosen was -0.95V. The idea was that if there was no pre-existent film, then scratching the electrode at the "noble" potential should not alter the current response significantly, and if there was a current response, then it would be independent of rotation rate. If there was a pre-existent film, however (and if the electrode provided material for the formation of the pre-existent film) then scratching the electrode would definitely give an anodic current response as some of the electrode would dissolve so as to replenish the film. If the electrode is rotated, then more dissolution would occur as some cations would also be lost to the bulk solution. Therefore, increasing the rotation rate would increase the current response until some critical rotation rate above either the loss of cations (or other film material) to the bulk solution reaches a constant, diffusion limited level or the rate at which the substrate is oxidised becomes activation limited.

The range of rotation rates used was from 10 to 350 rad/s. In general, after the culet of the diamond made contact with the electrode, there was an initial sharp rise in current, followed by a levelling out to a

plateau current. The plateau current was maintained presumedly due to the fact that the culet of the diamond was in contact with the electrode throughout the experiment. Fig. 9.1 shows the values of the plateau currents versus the rotation rate used.

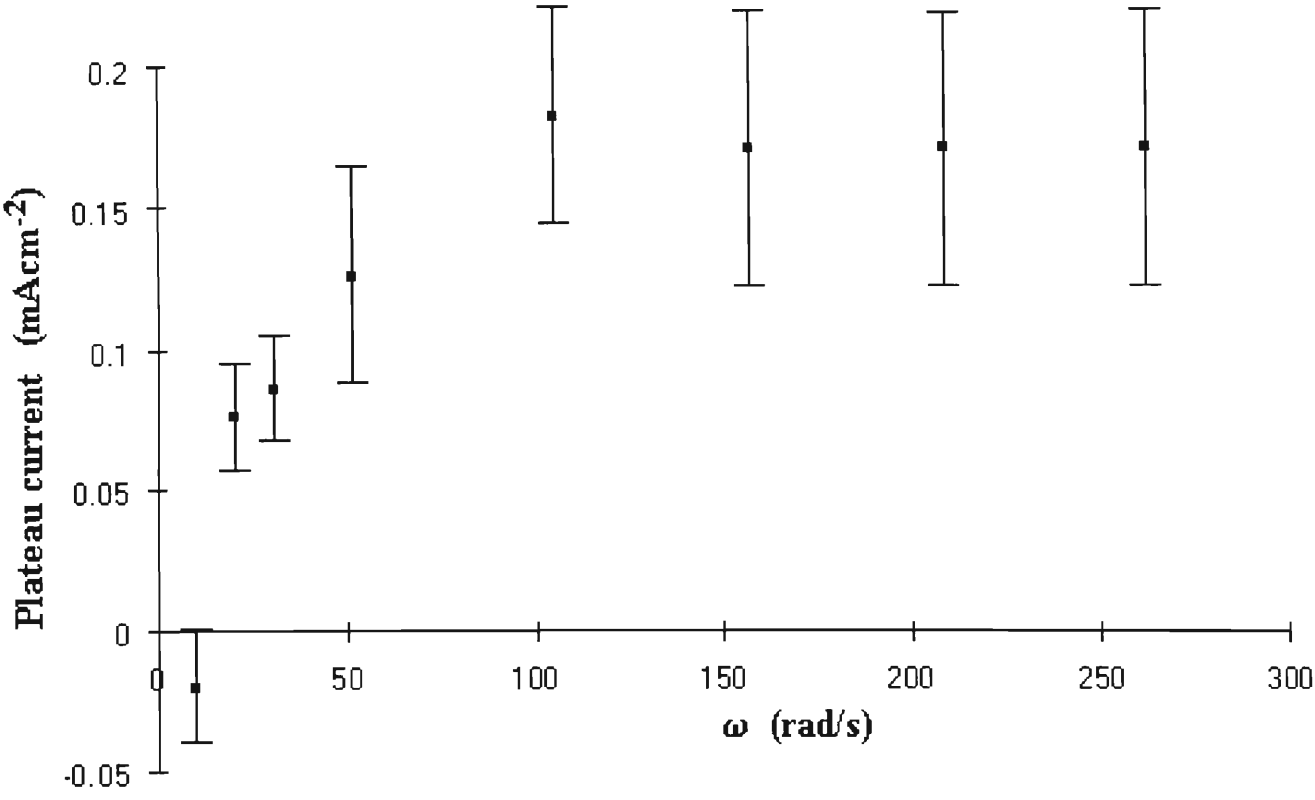

Fig. 9.1: Plot of the plateau current obtained in the scratch experiment versus the rotation rate used. The electrolyte was 0.06M H_2SO_4. The "noble" potential was -0.95V (vs. SSE) at 25°C.

As fig. 9.1 shows, the plateau current was indeed dependent on rotation rate. However, two experimental problems should be noted:

- Because the electrode was rotated, the scratch in the electrode was always circular. Because of this, it was difficult to keep the scratched area of the electrode constant.
- As the rotation rate increased so did the noise in the current response. Computer smoothing procedures had to be used and even after the smoothing, a large uncertainty error still existed. All plateau currents for rotation rates ≥ 150 rad/s largely overlapped and so an average value (as shown) was taken.

Both of the above problems resulted in the error bars shown in fig. 9.1. Any future experiments of this nature would need to be designed so as minimise the noise problem. However, even with the error bars, it can still be seen that the plateau current was dependent on rotation rate for $0 \leq \omega \leq 100$ rad/s. Therefore some evidence exists for a pre-existent film on Fe18Cr in 0.06M H_2SO_4 at 25°C.

Fig. 9.2 shows two of the scratch current responses that were obtained. Of course, the curves have both been smoothed for presentation, but the error bars give the spread of the noise that was obtained.

Once the fact of a pre-existent film arises, other questions immediately present themselves, such as:

What is the protective or passivating ability of the pre-existent film ?

The suppression of the active region current response on Fe-Cr alloys could be explained by a protective pre-existent film, for example. This would definitely be a subject of future work, but is beyond this preliminary investigation. It would not be surprising, however, to find that the existence, protectiveness, thickness and composition of the pre-existent film would all be pH dependent.

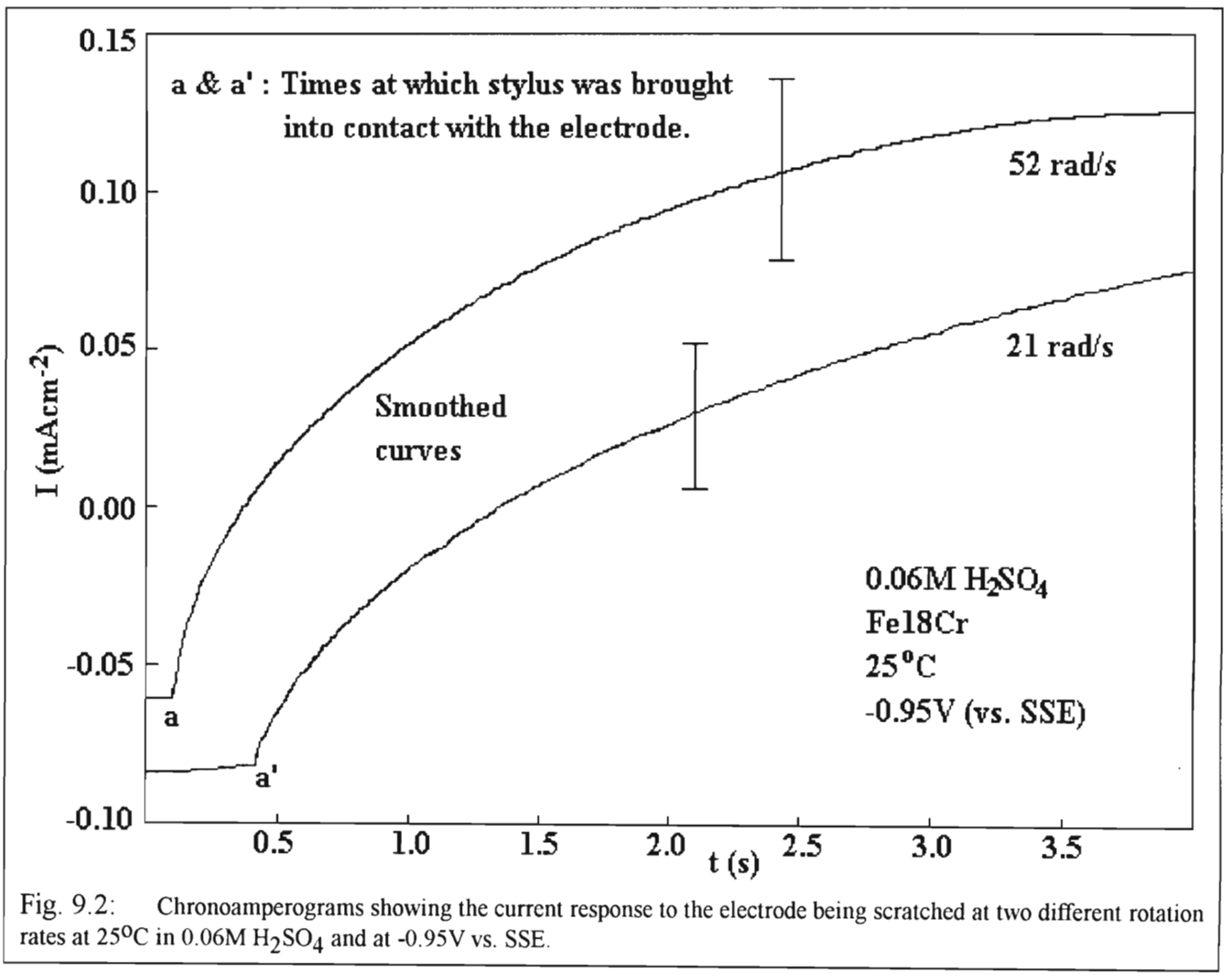

Fig. 9.2: Chronoamperograms showing the current response to the electrode being scratched at two different rotation rates at 25°C in 0.06M H_2SO_4 and at -0.95V vs. SSE.

CONCLUSIONS

1. A method has been developed for the correction of the current due to oxygen evolution on the peak A current response (which occurs in the potential range 0.6 - 0.9V vs. SSE). The validity of the method depends on the assumption that oxygen evolution does not chemically interfere with anodic film processes. The method has been applied to 444 in 0.06M H_2SO_4 and the results were qualitatively acceptable. The "kink" that always occurs in the "potential stop" method is evidence of the fact that more than one oxidative process contributes towards peak A.

2. The application of a peak current diffusion diagnostic ($Ip/v^{1/2}$ vs $v^{1/2}$) to peak A has been shown to be valid. The diagnostic was applied in solutions of pH varying from 0.5 to 3.8. At the smallest pH, the greatest positive deviation from a horizontal line (the horizontal line would indicate diffusion control) at slow sweep rates was found whereas the largest pH solution gave the greatest negative deviation from the horizontal at slow sweep rates. Intermediate pH's showed a gradual transition between these two extremes. These trends have been explained in terms of the degree of formation of the passive film before voltammetric entry into the passive region, the degree of dissolution of the anodic film (which increased with increase in acidity), the time spent at transpassive dissolution potentials (i.e. the sweep rate) and the proposed manner in which Fe-oxides and Cr-oxides behave within the film at transpassive potentials.

3. The diffusion diagnostic results were used to explain the competition between diffusion control and activation control (of peak A processes) as follows:
   When conditions are such that a maximum area of the electrode is exposed directly to the solution at transpassive potentials (low pH -e.g. pH 0.5- and slow sweep rates -less than 60 mV/s) then the peak A processes will be activation controlled. When conditions are such that the anodic film (which was formed in the passive region before voltammetric entry into the transpassive region) remains intact throughout the peak A potential range (higher pH's -e.g pH 3.8), then peak A processes are diffusion limited. In particular, the peak A processes are limited by the transport of ions between the alloy / film interface and the film / solution interface when the anodic film remains intact throughout the peak A potential range.

4. RDE experiments showed that at pH 3.8 transpassive processes were predominantly solid state whereas at pH 0.5 the transport of ions in solution was shown to play a significant part in peak A processes. Intermediate pH's showed a gradual transition between these two extremes. It was found at pH 0.5 that rotating the electrode decreased the peak A current response and this was attributed to the more efficient removal of excess H^+ generated in the formation of passivating oxides. According to the acid premise, passivating oxide formation would be resisted (with the degree of resistance directly related to the acidity of the bulk solution) unless the excess H^+ could be removed or consumed.

5. The addition of ferric, ferrous and chromic ions to solutions for CV experiments showed that of the three aqueous ions, the ferrous ion is most active at peak A potentials, followed by the chromic ion. The addition of ferric ion decreased the peak A current response, probably due to the ability of the added ferric ions to contribute towards the supersaturation needed prior to nucleation and growth of passivating ferric oxides on the electrode surface. On rotating the electrode, only the transpassive current response of the ferrous solution increased - those of the ferric and chromic solutions decreased - showing that the removal of excess H^+ (which results in a decrease of I_{pA} as ω increases) was more important than the removal of oxidation products in the ferric and chromic solutions from the electrode (which would result in an increase of I_{pA} as ω increases).

6. In the explanation of voltammetric results, the premise that an acid solution will resist any process that increases the acidity (relative to the acidity in the bulk solution) in the region of the electrode has been found to be important. Using this acid premise, (and the assumption that Cr(III) has a low mobility within the anodic fim) it was shown that the oxidation of Cr(III) to Cr(VI) at peak A potentials can only occur with a synergistic dissolution of ferrous and ferric oxides. Therefore, although the oxidation step Cr(III) $\rightarrow$ Cr(VI) is suspected to be responsible for the peak current response, this reaction will occur concurrently with the release of ferric cations from the anodic film to the solution. An exception to this is that in very aggressive conditions (pH 0.5, 90°C), the anodic film (at peak A potentials) is almost completely dissolved, and the peak A current response can be considered to be due to oxidation of both Cr(0), Fe(0) directly from the substrate to their highest stable oxidation states.

7. Chronoamperomertic studies have confirmed the existence of the rising transient, usually obtained when stepping to the transpassive region. These studies have also shown that increasing the hydromium ion concentration not only increases dissolution of the anodic film, but when the alloy substrate is exposed directly to the solution, it also increases dissolution of the alloy substrate. In addition a "reverse" rising transient, obtained when stepping cathodically from the transpassive region, has been discovered. This is the first time that this "reverse" rising transient has been seen on Fe-Cr alloys. It was shown that the occurence of the reverse rising transient is dependent on the presence of a transpassive anodic film before the cathodic potential step is imposed. In addition, reverse rising transient data shows that a stable anodic film - and hence probably secondary passivity - exists well into the oxygen evolution region. This conclusion is supported elsewhere in the literature [90].

8. A quantitative model has been developed to describe the chronoamperomtric rising transient obtained on Fe18Cr when the electrode is stepped to the transpassive region. This model considers the growth of pits into the electrode as equivalent to the growth of charge transfer controlled nuclei. These "pitting nuclei" undergo a "sudden death" when they are covered by a passivating oxide. The passivating oxide itself is formed by a 3-D nucleation and growth mechanism. The model allows for the diffusion controlled dissolution of a pre-existent film. A component of the transient is a diffusion controlled dissolution contribution, which may be the sum of a number of dissolution reactions. The

model has been sucessfully applied to two rising transients, one from pH 3.8, and the other from pH 0.5 solution.

9. In very aggressive conditions (pH 0.5, 90°C) a rising transient was obtained on Fe18Cr when stepping to the passive region. This was explained by the suggestion that the anodic film nucleates and grows normally very quickly (in less than 1ms) when stepping to the passive region. The rising transient is therefore superimposed on the double layer charging current. Stepping to the transpassive region or imposing very aggressive conditions when stepping to the passive region (such as 90°C, pH 0.5) both have the effect of slowing down the growth of the anodic film, simply due to the initial rampant corrosion of the electrode. The rising transient is then obtained in a time span sufficiently long so as not to be overshadowed by the double layer charging current. In a separate experiment, a rising transient was obtained on Fe when stepping to the passive region in mild conditions (pH 3.8, 25°C). This shows that it is the Cr in Fe18Cr which is responsible for the increased rate of formation of the anodic film.

10. The results of scratching an Fe18Cr electrode at a cathodic "noble" potential (-0.95V vs. SSE) with rotation rate as a variable indicate that a pre-existent film may be present at that potential. These results do not indicate the nature or content of the suspected pre-existent film and merely serve as a springboard for more exploratory work.

FUTURE WORK

1. It has become apparent that a large portion of transpassive processes on Fe-Cr alloys (pH depending) are solid-state. CV is a technique better suited to investigating electrochemistry in solution, rather than in the solid state. Electochemical impedance spectroscopy, however, is useful for investigating processes within the anodic film as demonstrated by D.D. Macdonald in the development of his point defect model. An EIS study of the transpassive behaviour of anodic films on Fe-Cr alloys could be worthwhile.

2. One way of gaining evidence for the partial scheme for transpassive processes outlined in section 6.4 would be to undertake an atomic absorption study. This would involve holding an electrode at a transpassive potential (no rotation) and after a suitable time increment, taking a sample of the solution adjacent to the electrode and analysing for total Fe and Cr (ionic) concentrations. The main variable would be pH and the object would be firstly to see how the individual Fe and Cr ionic concentrations vary with pH (the scheme would predict a decrease in individual concentrations with increase in pH) and secondly to observe the change in the ratio of Fe cations to Cr cations with pH (the scheme would predict an increase in this ratio with increase in pH).

3. In order to better understand the effect of the hydronium ion, any future work should involve electrolytes with an anion which is as noble towards the electrode as possible (e.g. $HClO_4$ and HBF_4).

4. Room for a great deal more chronoamperometric work exists. Temperature was not used as a primary variable in this study and could be used in future studies. The behaviour of the reverse rising transient, for example, would be worth investigating at 90°C. The model for the rising transient can be further developed and attempts can be made to "fit" it to as much of the existing rising transient data as possible. This would give a better understanding of the meaning and implications of the parameters of the model.

5. Cyclic voltammetry could also be attempted over a greater range of pH's. In particular, it may be useful to investigate pure iron in bicarbonate solutions - which gives a peak A response [15] probably due to analogous processes to those responsible for the peak A current response on the Fe18Cr electrode. The advantage is that using Fe only simplifies the resulting analysis - only Fe and its ionic forms can be responsible for anodic film behaviour.

6. A chronoamperometric study on pure Fe would also be informative and would provide more information as to the role of Cr by the comparison of Fe and Fe-Cr transients.

7. One study which would be particularly imformative is a voltammetric study of Fe-Cr alloys where the Cr% is the main variable, varying from 1 - 30%. In the literature, only APC's with varying Cr% have been reported. This would give additional invaluable information on the role of Cr. The difficulty in the acquisition of the alloys themselves is probably why this sort of study has not been undertaken before.

8. A project that would be further evidence towards the cathodic pitting hypothesis (generated to explain the reverse rising transient) would be to use SEM to take a picture of the film on the electrode after a reverse rising transient has been obtained. The pictures should then show the pits in the anodic film.

9. A test which can be used in future experiments where it is desirable to detect the presence of aqueous ferric ions would be to inject potassium thiocyanate solution at the electrode (at 0 rad/s, of course). The resulting $Fe(SCN)_3$ complex gives a deep red colouration. The injection of the KSCN solution could be performed by filling a second luggin capillary with the KSCN solution, positioning the tip close to the electrode and then opening the tap of the second luggin capillary when desired.

10. Clearly, more work on the scratch experiment for the determination of a pre-existent film is necessary. The initial work would need to focus on ways of reducing the noise of the current response when the electrode is being scratched.

REFERENCES

[1] F. Graham, *An Electrochemical Study of the Passivation of Stainless Steels*, MSc. Thesis, University of Natal - Durban, (1986), section 5.3

[2] F. Salibas, *Electrochemical Studies on Steels*, MSc. Thesis, University of Natal - Durban, (1983), Ch 5

[3] R. McCrindle, *An Electrochemical Investigation of the Passive Film on Stainless Steel*, MSc. Thesis, University of Natal - Durban, (1988), Ch 6-10

[4] F. M. Delnick, N. Hackerman, *Passivity of Metals*, R.P. Frankenthal, K. Kruger (editors), Electrochem. Soc. Inc., Princeton, New York, (1978), 116

[5] W. Schmickler, *ibid*, 102

[6] J. Ord, D. Desmet, *J. Electrochem. Soc.*, **113**, (1966), 1285

[7] R. Moshtev, *Electrochim. Acta.*, **16**, (1971), 2039

[8] M. Abyaneh, M. Fleischmann, *J. Electroanal. Chem.*, **119**, (1981), 187, 197

[9] F. Graham, *An Electrochemical Study of the Passivation of Stainless Steels*, MSc. Thesis, University of Natal - Durban, (1986), sections 4.4, 4.10, 5.5

[10] M. Prazak, V. Prazak, V. Cihal, *Z. Electrochem.*, **62(6/7)**, (1958), 739

[11] R. Kirchheim *et al*, *Corros. Sci.*, **29(7)**, (1989), 899

[12] D. D. Macdonald, *J. Electrochem. Soc.*, **139**, (1992), published in December

[13] S. Haupt, H. Strehblow *et al*, *Surf. Interface. Anal.*, **9**, (1986), 357

[14] R. McCrindle, *An Electrochemical Investigation of the Passive Film on Stainless Steel*, MSc. Thesis, University of Natal - Durban, (1988), 60

[15] C. Rangel, R. Leitao, I. Fonseca, *Electrochim. Acta.*, **34(2)**, (1989), 255

[16] M. Slabbert, F. Robinson, *Stainless Steel*, **22(5)**, (1986), 31

[17] E. R. Brown, R. F. Large, *Physical methods of chemistry*, Vol.2A, A. Weissburger, B.W. Rossiter (editors), Wiley-Interscience, New York, (1971), Ch 4

[18] V. C. Levich, *Acta. Physiochem.* URSS, **17**, (1942), 257

[19] R. Armstrong, *Corros. Sci.*, **11**, (1971), 693

[20] R. D. Armstrong, M. Henderson, H. Thirsk, *J. Electroanal. Chem.*, **35**, (1972), 119

[21] R. D. Armstrong, M. Henderson, H. Thirsk, *J. Electroanal. Chem.*, **39**, (1972), 222

[22] Southampton Electrochemistry Group, *Instrumental methods in Electrochemistry*, T.J. Kemp (editor), Ellis Horwood, Chichester, (1985), section 1.3

[23] *ibid.* section 4.2

[24] M. Datta, H. Mathieu, D. Landolt, *J. Electrochem. Soc.*, **131(11)**, (1984), 2484

[25] C. Courty, H. Mathieu, D. Landolt, *Electrochim. Acta.*, **36**, (1991), 1623

[26] J. E. B. Randles, *Trans. Faraday. Soc.*, **44**, (1948), 327

[27] A. Sevcik, *Coll. Czech. Chem. Comm.*, **13**, (1958), 349

[28] Southampton Electrochemistry Group, *Instrumental methods in Electrochemistry*, T.J. Kemp (editor), Ellis Horwood, Chichester, (1985), Ch 6

[29] W. J. Müller, *Trans. Faraday. Soc.*, **27**, (1931), 731

[30] D. D. Macdonald, *Transient Techniques in Electrochemistry*, Plenum Press, New York, (1977), section 8.4.2

[31] N. de Tacconi, A. Calandra, A. Arvia, *Electrochim. Acta.*, **18**. (1973), 571

[32] A. Calandra, N. de Tacconi, R. Pereiro, A. Arvia, *Electrochim. Acta.*, **19,** (1974), 901

[33] R. Nicholson, I. Shain, *Anal. Chem.*, **36(4)**, (1964), 706

[34] D. Evans, *Phys. Chem.*, **76(8)**, (1972), 1160

[35] R. Nicholson, I. Shain, *Anal. Chem.*, **37(2)**, (1965), 178

[36] M. Hulbert, I. Shain, *Anal. Chem.*, **42(2)**, (1970), 162

[37] D. Sawyer, J. Roberts, *Experimental Electrochemistry for Chemists*, Wiley, (1974), 336-339

[38] M. Xiang, *J. Electroanal. Chem.*, **242**, (1988), 63

[39] P. Andricacos, H. Cheh, *J. Electrochem. Soc.*, **127(10)**, (1980), 2153

[40] T. Berzins, P. Delahay, *J. Amer. Chem. Soc.*, **75**, (1953), 555

[41] P. Andricacos, P. Ross, *J. Electrochem. Soc.*, **130(6)**, (1983), 1340, 1353

[42] D. Devilliers, F. Lantelme, M. Chelma, *Electrochim. Acta.*, **31(10)**, (1986), 1235

[43] N. D. Tomashov, B.P. Chernova, *Passivation and Protection of Metals against Corrosion*, Plenum Press, New York, (1967)

[44] S.W. Dean, Jr., W.D. France, Jr., S.J. Ketcham, *Handbook on Corrosion Testing and Evaluation*, W.H. Ailor (editor), J. Wiley and sons, New York, (1971)

[45] A.J. Bard, L.R. Faulkner, *Electrochemical Methods - Fundamentals and Applications*, J. Wiley and sons, Inc., New York, (1980), 232

[46] A. Ramamurthy, S. Rangarajan, *Electrochim. Acta.*, **26**, (1981), 111

[47] A. J. Bard, L.R. Faulkner, *Electrochemical Methods - Fundamentals and Applications*, J. Wiley and sons, Inc., New York, (1980), Ch 5

[48] Southampton Electrochemistry Group, *Instrumental methods in Electrochemistry*, T.J. Kemp (editor), Ellis Horwood, Chichester, (1985), Ch 2

[49] P. Allen, A. Hickling, *Trans. Faraday. Soc.*, **53**, (1957), 1626

[50] F. Graham, H. Brookes, *Electrochim. Acta.*, **33**, (1988), 1475

[51] F. Graham, *An Electrochemical Study of the Passivation of Stainless Steels*, MSc. Thesis, University of Natal - Durban, (1986), section 5.5

[52] F. Graham, PhD. Thesis, University of Natal - Durban, (1993), Ch 5-6, to be published

[53] D. D. Macdonald, *Transient Techniques in Electrochemistry*, Plenum Press, New York, (1977), 278

[54] Southampton Electrochemistry Group, *Instrumental methods in Electrochemistry*, T.J. Kemp (editor), Ellis Horwood, Chichester, (1985), Ch 9

[55] M. Fleishmann, H. Thirsk, *J. Electrochem. Soc.*, **110**, (1963), 688

[56] A. Bewick, M. Fleishmann, H. Thirsk, *Trans. Faraday. Soc.*, **58**, (1962), 2200

[57] G. Hills, D. Schiffrin, J. Thompson, *Electrochim. Acta.*, **19**, (1974), 657

[58] G. Gunawardena, G. Hills, I. Montenegro, B. Scharifker, *J. Electroanal. Chem.*, **138**, (1982), 225

[59] B. Scharifker, G. Hills, *Electrochim. Acta.*, **28**, (1983), 879

[60] B. Scharifker, J. Mostany, *J. Electroanal. Chem.*, **177**, (1984), 13

[61] C. Alonso, R. Salvarezza, J. Vara, A. Arvia, *Electrochim. Acta.*, **35**, (1990), 489

[62] M. Abyaneh, *J. Electroanal. Chem.*, **209**, (1986), 1

[63] M. Abyaneh, *Electrochim. Acta.*, **36**, (1991), 727

[64] R. Armstrong, M. Fleischmann. H. Thirsk, *J. Electroanal. Chem.*, **11**, (1966), 208

[65] M. Sluyters-Rehbach, J.Wijenberg, E. Bosco, J. Sluyters, *J. Electroanal. Chem.*, **236**, (1987), 1

[66] M. Abyaneh, *Electrochim. Acta.*, **27(9)** , (1982), 1329

[67] W. Obretenov, *Electrochim. Acta.*, **33(4)**, (1988), 487

[68] E. Bosco, S. Rangarajan, *J. Electroanal. Chem.*, **134**, (1982), 213

[69] M. Abyaneh, G. Halvorsen, *J. Electroanal. Chem.*, **149**, (1983), 263

[70] F. Graham, *An Electrochemical Study of the Passivation of Stainless Steels*, MSc. Thesis, University of Natal - Durban, (1986), sections 2.4, 5.2

[71] F. Salibas, *Electrochemical Studies on Steels*, MSc. Thesis, University of Natal - Durban, (1983), 117

[72] K. Takahashi, A. Bardwell, B. Macdougall, M. Graham, *Electrochim. Acta.*, **37**, (1992), 477

[73] P. Lorbeer, W. Lorenz, *Passivity of Metals*, R.P. Frankenthal, J. Kruger (editors), Electrochem. Soc. Inc., Princeton, New York, (1978), 607

[74] J. Bessone, L. Karakaya, P. Lorbeer, W. Lorenz, *Electrochim. Acta.*, **22**, (1977), 1147

[75] M. Keddam, O. Mattos, H. Takenouti, *J. Electrochem. Soc.*, **128**, (1981), 257

[76] J. O'M. Bockris, D. Drazic, A. Despic, *Electrochim. Acta.*, **4**, (1961), 325

[77] I. Epelboin, C. Gabrielli, M. Keddam, H. Takenouti, *J. Electrochem. Soc.*, **20**, (1975), 913

[78] M. Janik-Czachor, *J. Electrochem. Soc.*, **128**, (1981), 513C

[79] H. Schwieckert, W. Lorenz, H. Friedburg, *J. Electrochem. Soc.*, **127**, (1980), 1693

[80] H. Schwieckert, W. Lorenz, H. Friedburg, *J. Electrochem. Soc.*, **128**, (1981), 1295

[81] D. Gilroy, B. Conway, *J. Phys. Chem.*, **69**, (1965), 1257

[82] G. Larramona, C. Gutierrez, *J. Electrochem. Soc.*, **136**, (1989), 2171

[83] P. Russell, J. Newman, *J. Electrochem. Soc.*, **133**, (1986), 59

[84] P. Pintauro, S. Roy, *J. Electrochem. Soc.*, **139**, (1992), 177

[85] O. Riggs, Jr., *Corrosion*, **20**, (1964), 275t

[86] F. Graham, *An Electrochemical Study of the Passivation of Stainless Steels*, MSc. Thesis, University of Natal - Durban, (1986), 80

[87] C. M. Rangel, I. Fonseca, R. Leitao, *Electrochim. Acta.*, **31**, (1986), 1659

[88] Z. Szklarska-Smialowski, W. Kozlowski, *J. Electrochem. Soc.*, **131**, (1984), 234

[89] Z. Szklarska-Smialowski, W. Kozlowski, *J. Electrochem. Soc.*, **131**, (1984), 723

[90] Z. Szklarska-Smialowski, W. Kozlowski, *Corrosion*, **40**, (1984), 595

[91] F. Beck, R. Kauss and Oberst, *Electrochim. Acta.*, **30**, (1985), 173

[92] F. Salibas, *Electrochemical Studies on Steels*, MSc. Thesis, University of Natal - Durban, (1983), 122

[93] K. E. Heusler, *Passivity of Metals*, R.P. Frankenthal, J. Kruger (editors), Electrochem. Soc. Inc., Princeton, New York, (1978), 771

[94] Ya. Kolotyrkin, *Electrochim. Acta.*, **25**, (1980), 89

[95] M. El-Basiouny, S. Haruyama, *Corros. Sci.*, **17**, (1977), 405

[96] M. Shlepakov, A. Sukhotin, Yu. Pa. Kostikov, V. Strykanov, *Elektrokhimiya*, **18**, (1982), 1430

[97] M. Shlepakov, A. Sukhotin, Yu. Pa. Kostikov, *Elektrokhimiya*, **18**, (1982), 1433

[98] A. Sukhotin *et al.*, *Elektrokhimiya*, **16**, (1980), 1403

[99] M. Shlepakov, A. Sukhotin, *Zasch. Met.*, **20**, (1984), 25. *Chem. Abs.*, **102**, (1985), 139718h

[100] S. Haupt, H. Strehblow, *J. Electroanal. Chem.*, **216**, (1987), 229

[101] Th. Heumann, H. Panesar, *J. Electrochem. Soc.*, **110**, (1963), 629

[102] L. Wikstrom, K. Nobe, *J. Electrochem. Soc.*, **116**, (1969), 525

[103] M. Hull, *J. Electroanal. Chem.*, **38**, (1973), 143

[104] H. Uhlig, P. Bond, H. Feller, *J. Electrochem. Soc.*, **110**, (1963), 650

[105] J. Johnson, C. Chi, C. Chen, W. James, Corrosion, 26, (1970), 238

[106] K. Sugimoto, Y. Sawada, *Corros. Sci.*, **17**, (1977), 425

[107] R. Arnstrong, J. Harrison, *J. Electroanal. Chem.*, **36**, (1972), 79

[108] R. Arnstrong, J. Harrison, H. Thirsk, *Corros. Sci.*, **10**, (1970), 679

[109] M. Janik-Czachor, G. Wood, G. Thompson, *Br. Corros. J.*, **15**, (1980), 154

[110] J. Galvele, *J. Electrochem. Soc.*, **123**, (1976), 464

[111] T. Hoar, *Corros. Sci.*, **7**, (1967), 355

[112] N. Sato, K. Kudo, T. Noda, *Electrochim. Acta.*, **16**, (1971), 1909

[113] N. Sato, *J. Electrochem. Soc.*, **129**, (1982), 255

[114] J. R. Galvele, *Passivity of Metals*, R.P. Frankenthal, J. Kruger (editors), Electrochem. Soc. Inc., Princeton, New York, (1978), 285

[115] A. Brooks, C. Clayton, K. Doss, Y. Lu, *J. Electrochem. Soc.*, **133**, (1986), 2459

[116] C. Clayton, Y. Lu, *J. Electrochem. Soc.*, **133**, (1986), 2465

[117] D. Macdonald, M. Urquidi-Macdonald, *J. Electrochem. Soc.*, **137**, (1990), 2395

[118] D. Macdonald, S. Biaggio, H. Song, *J. Electrochem. Soc.*, **139**, (1991), 170

[119] M. Urquidi-Macdonald, D. Macdonald, *J. Electrochem. Soc.*, **136**, (1989), 961

[120] D. Macdonald, S. Smedley, *Electrochim. Acta.*, **35**, (1990), 1949

[121] D. T. Larson, Corros. Sci., **19**, (1979), 657

[122] R. E. White, J. O'M. Bockris, B.E. Conway, E. Yeager (editors), *Comprehensive Treatise of Electrochemistry*, Vol 8, Plenum Press, New York, (1984), Ch 5 - 10

[123] Southampton Electrochemistry Group, *Instrumental methods in Electrochemistry*, T.J. Kemp (editor), Ellis Horwood, Chichester, (1985), Ch 10

[124] K. Asami, K. Hashimoto, S. Shimodaira, *Corros. Sci.*, **16**, (1976), 529

[125] I. Olefjord, B.O. Elfstrom, *Corrosion*, **38**, (1982), 46

[126] M. Frolicher, A.Hugot-Le Goff, V. Jovancicevic, *Passivity of metals and semiconductors,* M. Froment (editor), Elsevier, Amsterdam, (1983), 85

[127] T. Ohtsuka, K. Azumi, N. Sato, *ibid*, 199

[128] R. P. Frankenthal, *J. Electrochem. Soc.*, **114**, (1967), 542

[129] R. P. Frankenthal, *J. Electrochem. Soc.*, **116**, (1969), 580

[130] R. P. Frankenthal, *J. Electrochem. Soc.*, **116**, (1969), 1646

[131] H. Saito, T. Shibata, G. Okamoto, *Corros. Sci.*, **19** (1979), 693

[132] G. Okamoto, *Corros. Sci.*, **13**, (1973), 471

[133] G. Okamoto,T. Shibata, *Corros. Sci.*, **10**, (1970), 371

[134] N. Nielsen, T. Rhodin, *Z. Electrochem*, **62**, (1958), 707

[135] G. Long, J. Kruger, D. Black, M. Kuriyama, *J. Electroanal. Chem.*,**150**, (1983), 603

[136] I. Olefjord, B. Brox, *Passivity of metals and semiconductors,* M. Froment (editor), Elsevier, Amsterdam, (1983), 561

[137] C. L. McBee, J.Kruger, *Electrochim Acta*, **17**, (1972), 1337

[138] Y. C. Lu, R.C. Clayton, *J. Electrochem. Soc.*, **132**, (1985), 2517

[139] M. Kerkar, J. Robinson, A. Forty, *Faraday. Discuss. Chem. Soc.*, **89**, (1990), 31

[140] D. Williams, R. Newman, Q. Song, R. Kelly, *Nature*, **350**, (1991), 216

[141] J. Castle, J. Qiu, *J. Electrochem. Soc.*, **137**, (1990), 2031

[142] G. Burstein, P. Marshall, *Corros. Sci.*, **24**, (1984), 449

[143] P. Marshall, G. Burstein, *Corros. Sci.*, **24**, (1984), 463

[144] V. Mitrovic-Scepanovic, B. MacDougall, M. Graham, *Corros. Sci.*, **24**, (1984), 479

[145] N. Ramasubramanian, N. Preocanin, R. Davidson, *J. Electrochem. Soc.*, **132**, (1985), 793

[146] C. Calinski, H. Strehblow, *J. Electrochem. Soc.*, **136**, (1989), 1328

[147] J. Kruger, *Corros. Sci.*, **29**, (1989), 149

[148] J. Holliday, R. Frankenthal, *J. Electrochem. Soc.*, **119**, (1972), 1190

[149] S. Tjong, R. Hoffman, E. Yeager, *J. Electrochem. Soc.*, **129**, (1982), 1662

[150] A. P. Bond , *J. Electroochem. Soc*, **120**, (1973), 603

[151] E. A. Lizlovs, A.P. Bond, *J. Electrochem. Soc*, **122**, (1975), 719

[152] M. A. Streicher, *Corrosion*, **30**, (1974), 77

[153] J. Galvele, J. Lumsden, R. Staehle, *J. Electrochem. Soc.*, **125**, (1978), 1204

[154] I. Olefjord, *Materials Science and Engineering*, **142**, (1980), 161

[155] A. Yaniv, J. Lumsden, R.Staehle, *J. Electrochem. Soc.*, **124**, (1977), 490

[156] K. Asami, M. Naka, K. Hashimoto, T. Masumoto, *J. Electrochem. Soc.*, **127**, (1980), 2130

[157] K. Hashimoto, K. Asami, K. Teramoto, *Corros. Sci.*, **19**, (1979), 3

[158] K. Hashimoto, K. Asami, *Corros. Sci.*, **19**, (1979), 1007

[159] K. Hashimoto, K. Asami, M. Naka, *Corros. Sci.*, **19**, (1979), 857

[160] G. Hultquist *et al.*, *Corros. Sci.*, **27**, (1987), 937

[161] I. Olefjord, B.Brox, U. Jelvestam., *J. Electrochem. Soc.*, **132**, (1985), 2852

[162] I. Olefjord, B.O. Elfstrom,*Corros. Sci.*, **15**, (1975), 697

[163] C. Leygraf *et al, Corros. Sci.*, **19**, (1979), 343

[164] G. Hultquist, C. Leygraf, D. Brune, *J. Electrochem. Soc.*, **131**, (1984), 1773

[165] I. Olefjord, B.Brox, U. Jelvestam., *Proc. Electrochem. Soc.*, (1984) , 388

[166] H. Ogawa, H. Omata, I. Otoh, H. Okada, *Corrosion*, **34**, (1978), 52

[167] M. da Cunha Belo *et al*, *J. Electrochem. Soc.*, **124**, (1977), 1317

[168] K. Hashimoto, K. Asami, *Corros. Sci.*, **19**, (1979), 251

[169] R. Berneron, J. Charbonnier, R. Namder-Irani, J. Manenc, *Corros. Sci.*, **20**, (1980), 899

[170] J. Mathieu, H. Mathieu, D. Landolt, *J. Electrochem. Soc.*, **125**, (1978), 1039

[171] R. Chaudhary, W. Schultz, *J. App. Electrochem.*, **14**, (1984), 349

[172] M. Datta, H. Mathieu, D. Landolt, *Electrochim. Acta.*, **24**, (1979), 843

[173] A. Paola, *Electrochim. Acta.*, **34**, (1989), 203

[174] B. Cahan, C-T. Chen, *J. Electrochem. Soc.*, **129**, (1982), 921

[175] J. Gluszek, G. Freeman, J. Baron, J. Kubicki, *Corrosion*, **41**, (1985), 527

[176] G. Bianchi, A. Cerquetti, F. Mazza, S. Torchio, *Corros. Sci.*, **12**, (1972), 495

[177] S. Clough, T. Pinchback, *J. Materials for Energy Systems*, **1**, (1979), 55

[178] Th. Heumann, R. Schürmann, *Z. Electrochem.*, **65**, (1961), 560

[179] J. Wilford, H. Brookes, J. Bayles, unpublished results.

[180] J. Ambrose, R. Barradas, K. Belinko, D. Shoesmith, *J. Colloid. Interfac. Sci.*, **47**, (1974), 441

[181] L. Franke, W. Forker, *Electrochim. Acta.*, **20**, (1975), 775

[182] D. Landolt, *Passivity of Metals*, R.P. Frankenthal, J. Kruger (editors), Electrochem. Soc. Inc., Princeton, New York, (1978), 484

[183] F. Graham, *An Electrochemical Study of the Passivation of Stainless Steels*, MSc. Thesis, University of Natal - Durban, (1986), Ch 4

[184] B. MacDougall, M. Graham, *Electrochim. Acta.*, **26**, (1981), 705

[185] Southampton Electrochemistry Group, *Instrumental methods in Electrochemistry*, T.J. Kemp (editor), Ellis Horwood, Chichester, (1985), Ch 11

[186] Conway et al., Modern Aspects of Electrochemistry, No. 16, Plenum Press, (1985), 182

[187] R. McCrindle, *An Electrochemical Investigation of the Passive Film on Stainless Steel*, MSc. Thesis, University of Natal - Durban, (1988), 202-204

[188] *ibid*, Ch 11

[189] S. Fletcher et al., *J. Electroanal. Chem.*, **159**, (1983), 267

[190] S. Magaino, M. Matlosz, D. Landolt, *J. Electrochem. Soc.*, **140**, (1993), 1365

[191] T. Okada, *J. Electrochem. Soc.*, **131**, (1984), 241

[192] D.D. Macdonald, B. Roberts, *Electrochim. Acta.*, **23**, (1978), 557

APPENDIX A

The following tables list most of the values of I_{pA} and a selection of the values of E_{pA} that were obtained during the cyclic voltammetric work on Fe18Cr2Mo and Fe18Cr.

Tables of values of I_{pA} and E_{pA}

	Temperature (°C)											
	25	50	60	70	80	80	25	50	60	70	80	80
	I_{pA} (mAcm^{-2})						E_{pA} (V vs. SSE)					
ν (mV/s)	Corrected for O_2 evolution					*	Corrected for O_2 evolution					*
4	1.14	3.36	6.05	8.45	12.0	16.1	-	-	-	-	-	-
6.5	1.13	3.78	6.41	8.82	12.1	16.2	0.625	0.646	0.631	0.637	0.654	0.732
10	1.38	4.48	6.50	9.65	12.7	16.8	0.632	0.649	0.642	0.656	0.662	0.722
15	2.13	-	7.29	10.3	13.7	17.1	0.675	-	0.652	0.660	0.668	0.739
25	3.03	6.07	10.6	12.0	15.4	19.4	0.687	0.660	0.657	0.662	0.670	0.740
40	3.57	7.83	10.8	13.9	17.2	20.7	0.687	0.667	0.660	0.669	0.678	0.743
70	5.49	10.2	14.1	17.6	20.2	25.2	0.717	0.682	0.676	0.669	0.683	0.757
100	7.04	12.7	16.6	19.2	22.6	28.7	0.730	0.697	0.685	0.676	0.685	0.757
200	11.4	19.0	24.6	25.9	28.9	33.6	0.773	0.730	0.715	0.710	0.710	0.790
300	15.1	24.8	29.9	33.4	37.5	41.0	0.804	0.753	0.742	0.730	0.740	0.799
400	19.7	28.5	34.5	38.7	41.4	47.2	0.809	0.769	0.757	0.764	0.753	0.807
550	22.9	34.1	41.1	46.5	51.5	-	0.850	0.797	0.792	0.777	0.804	-
800	28.8	39.1	49.9	55.6	64.4	-	0.878	0.831	0.820	0.82	0.846	-

Table A1: Table of I_{pA} and E_{pA} values obtained from 444 in the 0.06M H_2SO_4 solution (pH 0.93). In these experiments, $E_1 = E_2 \sim -1.0$V. E_3 was +1.0 - +1.2V. "-" means that the data point for a particular set of conditions was not or could not reliably be measured. "*" means that the data points in the column of the asterisk were not corrected for oxygen evolution. $\omega = 0$ rad/s.

	Temperature (°C)					
	25	60	90	25	60	90
ν (mV/s)	**I_{pA} ($mAcm^{-2}$)**			**E_{pA} (V vs. SSE)**		
12	0.226	0.355	0.515	0.565	0.486	0.417
16	0.298	0.444	0.625	0.582	0.500	0.422
20	0.355	0.544	0.762	-	0.509	0.434
25	0.407	0.685	0.917	0.596	0.516	0.438
30	0.476	0.779	1.06	0.610	0.526	0.444
40	0.587	0.971	1.38	0.629	0.549	0.460
50	0.711	1.19	1.61	0.637	0.560	0.469
60	0.779	1.36	1.83	0.644	0.572	0.482
80	1.03	1.73	2.26	0.682	0.595	0.501
100	1.17	1.99	2.65	0.690	0.613	0.518
150	1.75	2.39	3.07	0.739	0.635	0.544
200	-	3.26	4.65	-	0.674	0.597
300	-	3.74	-	-	0.699	-

Table A2: Lists of I_{pA} and E_{pA} values from Fe18Cr in pH 3.8 acetate buffer solution. Here, $E_1 = E_2 \sim$ 0.9V and $E_3 \sim$ +0.9V vs. SSE. ω = 150 rad/s.

	Temperature = 90°C						
	pH						
	2.40	2.06	1.40	1.24	1.24	0.54	0.54
ν (mV/s)	150 rad/s	150 rad/s	150 rad/s	0 rad/s	150 rad/s	0 rad/s	150 rad/s
8	-	-	3.64	-	-	-	-
10	1.07	1.14	-	5.00	3.73	75.1	53.0
16	-	-	4.58	-	-	-	-
20	1.52	1.43	4.86	5.73	4.82	89.5	66.8
40	2.08	2.07	7.02	7.64	6.72	81.7	62.4
60	2.58	2.82	8.46	8.55	8.27	90.0	65.2
100	3.11	3.67	10.56	10.18	11.36	55.2	62.4
200	4.36	4.77	15.27	13.54	-	64.1	76.8
E_1	-0.95	-1.01	-1.1	-0.9	-0.9	0.05	0.05
E_2	-0.95	-1.01	-1.1	-0.9	-0.9	-1.02	-1.02
E_3	0.95	+0.9 - +1.1	+1.0 - +1.2	+1.0 - +1.2	+1.0 - +1.2	+1.0 - +1.2	+1.0 - +1.2

Table A3: Table listing I_{pA} values for Fe18Cr in solutions used other than pH 3.80 and 0.93 at 90°C.

	Temperature = 25°C		
	pH		
	2.4	0.54	0.54
ν (mV/s)	150 rad/s	0 rad/s	150 rad/s
10	0.555	9.83	9.01
20	0.718	12.60	11.56
40	1.16	15.52	15.03
60	1.39	20.25	20.25
100	1.96	25.95	24.81
200	-	32.34	32.68
E_1	-0.90	0.10	0.10
E_2	-0.90	-1.00	-1.00
E_3	1.10	1.17	1.17

Table A4: Table listing I_{pA} values for Fe18Cr in solutions used other than pH 3.80 and 0.93 at 25°C.

	pH 0.5					
	+0.04M Fe^{2+}	+0.04M Fe^{2+}	+0.04M Fe^{3+}	+0.04M Fe^{3+}	+0.04M Cr^{3+}	+0.04M Cr^{3+}
ν (mV/s)	0 rad/s	150 rad/s	0 rad/s	150 rad/s	0 rad/s	150 rad/s
10	10.97	15.09	8.96	8.58	10.10	9.07
20	14.17	16.34	11.94	11.67	13.46	13.19
40	18.84	21.17	16.12	15.74	16.02	13.84
60	22.15	24.05	20.02	19.76	22.10	19.98
100	27.58	28.89	25.90	25.41	27.69	23.07
200	35.50	35.78	35.88	35.34	32.41	29.64

Table A5: Table of I_{pA} values obtained with Fe18Cr in the pH 0.5 solution at 25°C showing the effect of addition of cations.

APPENDIX B

Programs for collection and processing of digital data

The writing of programs for the collection and processing of data (from the Nicolet 3091 digital oscilloscope) represents a significant portion of the work undertaken in the thesis. Several programs were written, but only the three most original and unique programs have been included in this chapter. Briefly, they are:

- COLLVER7.BAS - This is a two part programme and the most complex of the three. One part deals with the collection of digital data sent from the Nicolet oscilloscope, and the other part deals with the processing of this data into ASCII data files.
- GRAPH.BAS - This programme was written because of a defficiency in all the commercial graphics software that the author has seen. Although most graphics programmes will draw graphs with multiple sets of Y data, they only allow for one set of X data which is common to all the Y data. This program draws graphs where multiple sets of both X and Y data are allowed.
- NUCMODEL.BAS - This program fits the nucleation model to experimental rising transient data by an iterative process.

All the above programs were written in the language QBASIC 1.0. This is the new version of BASIC that comes with DOS 5.0 and replaces GW-BASIC. It has the following advantages over its predecessor :-

- It dispenses with the need for numbering lines and has a text editor (for cutting & pasting) together with mouse support.
- Procedures may be used, thus enhancing structured programming.
- Dynamic arrays are available and a string variable may contain up to 32767 characters, which is useful for storing waveform data (one waveform may contain up to 20095 characters) in one string.
- It contains all the usual basic commands and a number of new ones such as the CASE and DO...UNTIL control structure statements. Thus the simplicity of BASIC is kept and is combined with many of the powerful features of a modularised language such as PASCAL.
- A pull-down menu system is provided, and this includes a debugging menu with a step by step command debugging feature (and a tracer) and an option for setting breakpoints in the program.
- A comprehensive help system is provided.

QBASIC 1.0 is, however, a translator-based language. It was used because BASIC seems to one of the main programming languages used in electrochemistry and programs such as COLLVER7 are based on older programs which were written in APPLESOFT BASIC. Also, the programs written are not yet sufficiently long and complex for the inefficiency of the translator to be a major problem. QBASIC 1.0 was found to be the most powerful and simplest version of BASIC available.

COLLVER7.BAS

In the listing of these programs, a courier font has been used in order to retain the indentation and structure of the programs as seen in QBASIC's text editor. Note that an apostrophe - ' - is an abbreviation for the REM statement. All comments are preceded by an apostrophe. Some comments not included in the program code are given and these will be given in the usual times roman font.

The program fullfils two major roles. The collection part of the program collects waveforms from the oscilloscope. A single waveform is usually transferred as a 20000 character string, which the program collects and dumps in a "rawdata" file. All waveforms can only be obtained in the Y - t (current or potential versus time) form. Therefore to get I - E (current versus potential) data, two waveforms (I-t and E-t) would have to be recorded and stored. The program can then process the data strings to ASCII data files. This program was written expressly for the NICOLET 3091 oscilloscope.

```
'************************* COLLVER7.BAS ********************************
'
'Written by C.Tonkinson for the Electrochemistry research laboratory,
'Chemistry Department, University of Natal, Durban, July 1991.
'
'The program has two main parts, viz. a part that collects data from a
'NICOLET 3091 oscilloscope and a part that processes the data into a
'formatted ASCII file. Both parts function separately and independently
'of each other.
'
'COLLECTION :
'If one waveform is being transferred, then it will be transferred as 20000
'characters with 5 characters to a number, where the first character is
'either a blank or a minus sign indicating the sign of the 4 digit number.
'The data will be transferred in the following manner after the RS-232
'button on the oscilloscope has been pressed:-
' 5 character identifier, then a delimiter (an e.g. of a delimiter is a
' carriage return followed by a line feed)
' 100 mS delay
' 20000 characters of waveform data, then a delimiter
' 100 mS delay
' 40 characters of normalization data, then a delimiter
'
'Normalization data, by means of a formula given in the Nicolet users
'manual (cf page 155), is used to obtain actual voltage and time values from the
'4 digit numbers. The normalization data is divided as follows :-
'
'Characters 1-5 and 6-10 (RESET VZERO & RESET HZERO). These are used only
'when the user defines the location of zero volts and time with the
'NUMERICS RESET button on the NICOLET. They represent the vertical location
'of zero volts (ranging from -2048 to 2047) and the horizontal location of
'zero time (ranging from 0000 to 3999) respectively. If NUMERICS RESET is
'not used, then the position of zero volts is taken as the vertical centre
'of the screen, even when the DC OFFSET adjust dial is used. The position
```

```
'of zero time is determined by the position of the screen cursor. These two
'numbers are not used in the program, but can be incorporated.
'
'Characters 11-15 are not used (always zero)
'
'Characters 16-20 (HZERO). These represent the horizontal location of zero
'time and are defined by the position of the cursor on the NICOLET screen.
'If unused, as with this program then the position of zero time is assumed
'to be at the left of the screen.
'
'Characters 21-25 and 26-30 (VNORM DIGIT & VNORM POWER). These are scale
'numbers which, when used in the following formula, gives the vertical
'scale factor. Multipling a data value by this factor gives its vertical
'component in mV :
'vnorm! = (VNORM DIGIT - 5) * 10 ^ (VNORM POWER - 12)
'y-component (mV) = 4 digit number * vnorm!
'
'Characters 31-35 and 36-40 (HNORM DIGIT & HNORM POWER). Similarly, a time
'scale factor is obtained from these two numbers using the analogous
'formula. Multiplying a data value by this factor gives its horizontal
'component in seconds.
'
'The NICOLET can send two waveforms at a time. This corresponds to
'having the SAVE switch in the "save" position. Each waveform
'will be transferred as 10000 characters in the following manner:-
' 5 character identifier, then a delimiter.
' 100 mS delay
' 10000 characters of waveform data, then a delimiter
' 100 mS delay
' 40 characters of normalization data, then a delimiter
' 100 mS delay
' 10000 caharacters of waveform data, then a delimiter
' 100 mS delay
' 40 characters of normalization data, then a delimiter
'
'The only character in the identifier of use is the fifth one. Its value
'corresponds to the following meanings :
' 0 - Channel A data. SAVE switch in the 'on' position. i.e. 1 waveform
' 1 - Channel B data. SAVE switch in the 'on' position
' 2 - Channel A data. SAVE switch in the 'save' position. i.e. 2 waveforms
' 3 - Channel B data. SAVE switch in the 'save' position
'This character could be used in a future errorchecking routine.
'
'Before the program can accept a waveform, 4 parameters must be entered :-
'(1) area! - This is the area of the electrode. Here, a null value can be
'entered and the area value may be appended to the raw data file just
'before processing.
'(2) IV! - This is the voltage to current conversion factor.
'(3) ONEorTWO% - an integer number indicating whether the SAVE switch will
'be in the "on" ( ONEorTWO% = 1 ) or the "save" ( ONEorTWO% = 2 ) position
'at the time of data collection.
'(4) XYorIT$ - a string variable indicating whether the data will come from
'one channel ( In this case the x-axis will be time and the y-axis will be
```

```
'current. This is referred to as I-t data and XYorIT$ = "I" ) or from both
'of the channels. In the case where both channels are used, the y-axis from
'channel B and the y-axis from channel A are later processed to form the y
'and x-axes of of the new data set. Time may be optionally set as a third
'axis. This is referred to as XY data (XYorIT$ = "X"), and channel B is
'always assumed to contain the current-time curve and channel A the
'potential-time curve. Also, when XYorIT$ is set as "X", the program
'expects the current curve to be sent first.
'
'The program therefore allows for 4 types of data -
'(1) XY data, 2 curves (processed to form 1 set of data or 1 curve)
'(2) XY data, 4 curves (processed to form 2 sets of data or 2 curves)
'(3) It data, 1 curve
'(4) It data, 2 curves
'
'After these parameters have been entered, the program then waits for data.
'When the RS-232 button on the NICOLET is pressed, the program collects all
'the characters sent (20051 when the SAVE button is in the "on" position
'and 20095 when it's in the "save" position) and dumps them into a single
'string variable. It then saves the string variable, together with the 4
'parameters to a file. It then waits for more data. If the next set of data
'is the second curve of a set of XY data, the program saves it to the same
'file. In this manner the program becomes automatic and must only be
'attended to when one or more of the parameters needs to be changed. This
'is a necessary feature as it allows the user to limit his attention to his
'experiments, and not having to worry about the computer. In order to be
'automatic, the program must generate its own filenames. The first 3
'letters of each filename are "raw". The extension is "chr" if
'XYorIT$ = "I" (since this corresponds to chronoamperometric work) and
'"cyv" if XYorIT$ = "X" (since this corresponds to cyclic voltammetry). The
'4th to 8th letters are 5 digits. The 5 digit number for the first file
'that was saved with this program was 00001. The program increments this
'number represented by the 5 digits by 1 and the 5 digits are saved in a
'separate file called "number.cnt" each time a set of data is saved. Thus
'the filename of the 123rd file to be saved which is XY data is
'"raw00123.cyv".
'
'PROCESSING:
'
'The processing of raw data takes place in various stages. The no. of times
'each stage occurs depends on the type of data.
'Stage 1: All the information corresponding to a waveform is loaded into a
'string variable.
'Stage 2: The long string variable is subdivided into the separate data
'points and the normalization numbers. At this point all the numbers are
'contained in an array of string variables, all of length 5 characters.
'It must be noted that QBASIC allocates a maximum of 64K to arrays. One
'waveform will have a maximum of 4000 data points, which is worth 32K with
'single precision variables.
'Stage 3: The array of string variables are converteted to a numeric array.
'Stage 4: The numeric variables within the array corresponding to data
'points are normalised.
'The normalised data is saved in columns in an ASCII file.
```

```
'
'The program can automatically process all raw data files it has listed in
'a file called "rawfiles.dir" (The collection part of the program appends
'filenames of raw data files to this file as it saves them) or it can
'selectively process files specified by the user.
'
'
'There are 7 additional files which the program uses. These files must be
'kept in the same directory as the program file :-
'
'DIRECTRY.DAT - This contains the two pathnames for the location of raw
'data files and processed data files.
'WRONGFILS.DAT - This file is used during the processing part of the
'program. If the program cannot find a raw data file, instead of stopping,
'it writes the name of the file it cannot find to WRONGFILS.DAT, skips to
'the next raw data file in the list, and at the end of processing, displays
'the names, if any, of the files it could not find.
'RAWFILES.DIR - This file contains a list of all the raw data files that
'have not yet been processed.
'NOFILES.DIR - This file only contains a number - the number of raw data
'files which have not yet been processed.
'NUMBER.CNT - This file keeps the 5 digit number which is used in data
'filenames.
'EXPINFO.DAT - This contains the most recent values of the 4 abovementioned
'parameters.
'SAVETIME.DAT - This contains one of the letters "y" or "n", indicating
'whether the process part of the program should calculate and save time
'values as well as current and potential or not.
'
'It should also be noted that the NICOLET has 8 switches, the last 7 of
'which affect the data transmission via the RS232 card. The settings as
'used for this program are :-
'switches 1,4,5,6,7,8 closed. switches 2,3 open.
'Switches 2,3 and 4 set the baud rate. The setting here is 9600 baud (for
'further information consult the NICOLET users manual). Switch 6 sets the
'parity, 7 sets parity checking and 8 sets the no. of stop bits. Changes in
'the position of these switches can be accomodated by changing the relevant
'parameters in the two OPEN COM statements in the main module. Switch 5
'sets the characters that are contained in a delimeter. If this switch is
'set in the open position then, near the beginning of the main module,
'change the initialisation value of saveSAVE% to 20090 and that of saveON%
'to 20048.
'
'-------------------------------------------------------------------------
```

```
'THE MAIN MODULE
'Within any QBASIC 1.0 main module procedures and global variables are
'declared. The main module contains the main menu, the data collection code
'and two errorchecking routines as the ON ERROR GOTO statement (as well as
'any other event trapping statement and the GOSUB statement) will only
'refer to a label within the main module.
'
'Declare all the procedures
DECLARE SUB saveareas ()                                          '(page 174)
DECLARE SUB inputfiles (filename$(), m%)                          '(page 165)
DECLARE SUB stringtoval (whichno1%, no2%)                         '(page 177)
DECLARE SUB process1 (whichno1%, whichno4%, no2%, no3%, current%, time%,
                      whicharea%)                                 '(page 173)
DECLARE SUB savedata (directory$, check1file$, anumber%)          '(page 176)
DECLARE SUB increment ()                                          '(page 165)
DECLARE SUB datain ()                                             '(page 163)
DECLARE SUB changeDATAdirs (rawdir$, processdir$)                 '(page 162)
DECLARE SUB process (rdir$, pdir$)                                '(page 166)
DECLARE SUB getexpinfo ()                                         '(page 163)
'COMMON SHARED declares global variables
'The meaning of suffixes on variables are as follows :-
'! - single precision numeric : % - integer : $ - string
'dat$() - array used to store the string data for waveforms in process ()
'dat!() - array used to store converted string to numeric values
'dt!() - array used to store normalized numeric data point values
'other variables explained as encountered
COMMON SHARED dats$(), dat!(), dt!(), no4%(), no1%(), area!()
COMMON SHARED IV!, area!, XYorIT$, ONEorTWO%, data$, wrong$, saveSAVE%
COMMON SHARED number$, lngth%, choose$, check1$, check1name$, saveON%
COMMON SHARED rawdir$, processir$
'If "directry.dat" isn't found go to the nofile label
ON ERROR GOTO nofile
OPEN "directry.dat" FOR INPUT AS #1
'Get the raw and processed data file path names
 INPUT #1, rawdir$, processdir$
CLOSE #1
'Turn off error checking
ON ERROR GOTO 0
'initialise the 4 experimental parameters
IV! = 0: area! = 0: XYorIT$ = "": ONEorTWO% = 0
'comno% - default COM port no. is 1
'wrong$ - given value of "y" when process () can't find a raw data file
comno% = 1: wrong$ = "n"
'saveSAVE% and saveON% - The no. of characters that the NICOLET sends
'after the RS232 button has been pressed is 20095 when the SAVE switch is
'in the "save" position and 20051 when it is in the "on" position.
comon$ = "n": checkfile$ = "y": check1file$ = "n"
saveSAVE% = 20095: saveON% = 20051
CLS : LOCATE 8
beginofmenu:
'If event trapping for activity at a COM port is on - i.e. if
'comon$ = "y" - then turn it off
IF comon$ = "y" THEN COM(comno%) OFF: comon$ = "n"
```

```
CLS : LOCATE 3
PRINT "1.)  Collect waveforms and save to disk."
PRINT "2.)  Process waveforms and save to disk."
PRINT "3.)  Set COM port number - default is 2."
PRINT "4.)  Set active data subdirectories."
PRINT "5.)  Quit.": PRINT
INPUT "Enter number of option : ", number%
SELECT CASE number%
 CASE 1
  GOSUB collect
 CASE 2
  CALL process(rawdir$, processdir$)
 CASE 3
  INPUT "Enter no. of COM port (1 or 2 only - default is 2.)", comno%
  IF comno% <> 1 AND comno% <> 2 THEN comno% = 2
 CASE 4
  CALL changeDATAdirs(rawdir$, processdir$)
 CASE 5
  END
 CASE ELSE
  GOTO beginofmenu
END SELECT
GOTO beginofmenu

'Option 1 of the main menu has been selected.
collect:
'checkfile$ is initialised as "y" when the program starts and when
'process() has finished processing a set of data. It is used as a check to
'whether the option of emptying rawfiles.dir of all its old names should be
'given.
IF checkfile$ = "y" THEN
 checkfile$ = "n": check1file$ = "y"
 PRINT "Empty 'rawfiles.dir' of all previous filenames ? (y/n). "
 INPUT " - <Enter> for a quick no - : ", choose$
 CLS
END IF
'Call the procedure which gets the 4 experimental values.
CALL getexpinfo
CLS
'Check to see that a value for XYorIT$ has been entered
IF XYorIT$ = "" THEN
exitTHEroutine:
 CLS : LOCATE 5
 PRINT "You have not entered the processing constants correctly."
 PRINT "Please do so on returning to the main menu."
 PRINT "Press any key to continue."
 WHILE INKEY$ = "": WEND
 GOTO beginofmenu
END IF

'count% is used in the collection of XY data. 2 seperate waveforms must be
'sent (one from each channel -the RS232 button must be pressed twice- ).
'These 2 waveforms are saved in the same file. If count% = 2, then waveform
```

```
'data is appended to the most recent file, rather than a new file being
'created.
count% = 0
IF comno% = 1 THEN
 'Open and initialize COM1 for I/O with these specifications:-
 'baud rate of 9600, no parity, 8 data bits per byte, 1 stop bit.
 'turn off data carrier detect, clear to send, data set ready and
 'don't'wait for open communications lines. Suppress detection of request
 'to send and set the receive buffer at 20480 bytes (max. of 20095 bytes
 'involved here). Open the commonications port as a sequential file
 OPEN "com1:9600,n,8,1,cd0,cs0,ds0,op0,rs,rb20480" FOR INPUT AS #1
ELSEIF comno% = 2 THEN
 OPEN "com2:9600,n,8,1,cd0,cs0,ds0,op0,rs,rb20480" FOR INPUT AS #1
ELSE GOTO exitTHEroutine
END IF
'when activity is detected at COM1 go to the label `getdata'
ON COM(comno%) GOSUB getdata

beginofcollect:
'switch communications port event trapping on i.e. make the ON COM
'statement active
COM(comno%) ON: comon$ = "y"
IF XYorIT$ = "X" THEN
 count% = count% + 1: IF count% = 3 THEN count% = 1
END IF
nearbeginofcollect:
IF XYorIT$ = "X" THEN
 LOCATE 7
 PRINT "In CV work, always transmit the current (Y of XY) waveform(s)
        first."
 PRINT "Otherwise the processing part of the program gives garbage."
 PRINT "This will be channel B on the nicolet."
END IF
LOCATE 12
'The next set of code causes the computer to wait until :
'- either the escape or tab key is pressed. The only other way to exit the
'loop is for the communications port event trapping to be activated.
PRINT "Waiting for data - Press <Escape> to go to main menu,"
PRINT "or <Tab> to reset experimental constants."
WHILE INKEY$ <> CHR$(27)
 IF INKEY$ = CHR$(9) THEN
  CALL getexpinfo
  CLS
  GOTO nearbeginofcollect
 END IF
WEND
CLOSE #1
GOTO beginofmenu

getdata:
CLS : LOCATE 12
PRINT "Getting data - please wait."
'Call the data collection procedure
```

```
CALL datain
'Turn off COM event trapping
COM(comno%) OFF: comon$ = "n"
'If the waveform is It data ot the first (current) waveform in XY data then
'call the procedure which increments the 5 digit number by 1.
IF XYorIT$ = "I" OR (XYorIT$ = "X" AND count% = 1) THEN
 CALL increment
END IF
'Call the procedure which saves waveform data. Parameters in brackets mean
'that those parameters will not be changed in the procedure.
CALL savedata((rawdir$), check1file$, (count%))
'initialize the waveform data string variable to free menory. It contains
'either 20051 or 20095 characters.
data$ = ""
'Go back and wait for more data
RETURN beginofcollect

nofile:
CLOSE #1: CLS : LOCATE 5: skip1$ = "y"
PRINT "The file 'directry.dat' does not exist or does not have both"
PRINT "pathname entries. Enter them now."
PRINT "Press any key to continue."
WHILE INKEY$ = "": WEND
CALL changeDATAdirs(rawdir$, processdir$)
GOTO beginofmenu

wrongname:
'this is the routine to which the procedure process() branches if it cannot
'find the name of a raw data file it is meant to process. check1$ is a
'variable which is given the value of "n" each time process() is called,
but
'whilst process() is running. If a `wrong file' is found, it is given the
'value of "y". Filenames are only appended to wrongfil.dat when check1$
'= "y", otherwise the previous contents of wrongfil.dat are deleted.
IF check1$ = "n" THEN
 check1$ = "y"
 OPEN "wrongfil.dat" FOR OUTPUT AS #1
  PRINT #1, check1name$  'check1name$ is the "wrong file" name.
 CLOSE #1
ELSEIF check1$ = "y" THEN
 OPEN "wrongfil.dat" FOR APPEND AS #1
  PRINT #1, check1name$
 CLOSE #1
END IF
'This is a marker to let process() know that it must skip to the next raw
'data filename in its list or else end the procedure.
wrong$ = "y"
'Go to the line after the one which caused the error
RESUME NEXT

'-------------------------------------------------------------------------
```

```
'This procedure changes the pathnames for the raw and processed data files.

SUB changeDATAdirs (rawdir$, processdir$)

PRINT "Current data subdirectories are :-"
PRINT "1.) Raw data - "; rawdir$
PRINT "2.) Processed data - "; processdir$
PRINT "Change 1, 2 or 3 for both ?"
PRINT "Enter 1, 2, 3 or else any other integer to keep current values."
INPUT skip2%

IF skip2% > 0 AND skip2% < 4 THEN
   PRINT "Give drive and full pathname. "
  END IF
  SELECT CASE skip2%
   CASE 1
    INPUT rawdir$
   CASE 2
    INPUT processdir$
   CASE 3
    PRINT "Enter raw data subdirectory first."
    INPUT rawdir$, processdir$
   CASE ELSE
    EXIT SUB
  END SELECT
  IF RIGHT$(rawdir$, 1) <> "\" THEN
   rawdir$ = rawdir$ + "\"
  END IF
  IF RIGHT$(processdir$, 1) <> "\" THEN
   processdir$ = processdir$ + "\"
  END IF
  OPEN "directry.dat" FOR OUTPUT AS #1
   WRITE #1, rawdir$, processdir$
  CLOSE #1

END SUB
```

```
'This collects the character data sent after the RS232 button is pressed.
'It dumps all the character data into one string variable.

SUB datain
data$ = ""
IF ONEorTWO% = 1 THEN
 len1% = saveON%
ELSEIF ONEorTWO% = 2 THEN
 len1% = saveSAVE%
ELSE
 EXIT SUB
END IF

'While the receive buffer has not yet received len1% characters (20051 if
'ONEorTWO% = 1 and 20095 if ONEorTWO% = 2) do nothing.
WHILE LOC(1) < len1%
WEND
'Put everything that is in the receive buffer into data$
data$ = INPUT$(len1%, #1)

END SUB


'--------------------------------------------------------------------------

'This procedure gets the 4 experimental constants (ONEorTWO%, XYorIT$, IV!
'and area!) and saves them to the file expinfo.dat.

SUB getexpinfo
REDIM menuchoice$(1 TO 7), info$(1 TO 4)
'These variables are shared with all procedures
SHARED IV!, area!, XYorIT$, ONEorTWO%
'Declare local variables
STATIC number%, i%, yn$
'Get the last set of values that were entered for the 4 experimental
constants
OPEN "expinfo.dat" FOR INPUT AS #2
 FOR i% = 1 TO 4
  INPUT #2, info$(i%)
 NEXT i%
CLOSE #2
CLS
menuchoice$(1) = "1.) I/V (mA/mV) "
menuchoice$(2) = "2.) Area (cm2) - 0 or [Enter] means the value is to be
                      appended later "
menuchoice$(3) = "3.) X/Y data or I/t data. [X/I] "
menuchoice$(4) = "4.) One or Two sets of curves -<save> off/on- [1/2] "
menuchoice$(5) = "5.) All of the above."
menuchoice$(6) = "6.) No changes."
begin:
PRINT "Which of the following experimental constants"
PRINT "do you wish to set/change (default values shown) ?"
FOR i% = 1 TO 4
```

```
 PRINT menuchoice$(i%); ": "; info$(i%)
NEXT i%
FOR i% = 5 TO 6
 PRINT menuchoice$(i%)
NEXT i%
PRINT : INPUT "Enter a number : ", number%
IF number% > 0 AND number% < 5 THEN PRINT "Enter experimental constant."
SELECT CASE number%
 CASE 1
  INPUT info$(1)
 CASE 2
  INPUT info$(2)
 CASE 3
  INPUT info$(3)
 CASE 4
  INPUT info$(4)
 CASE 5
  PRINT "Enter the 4 processing constants, each seperated by a comma only."
  INPUT info$(1), info$(2), info$(3), info$(4)
 CASE 6
  IV! = VAL(info$(1)): area! = VAL(info$(2))
  XYorIT$ = info$(3): ONEorTWO% = VAL(info$(4))
  EXIT SUB
 CASE ELSE
  GOTO begin
END SELECT
IF info$(3) = "x" THEN info$(3) = "X"
IF info$(3) = "i" THEN info$(3) = "I"
IV! = VAL(info$(1)): area! = VAL(info$(2))
XYorIT$ = info$(3): ONEorTWO% = VAL(info$(4))
CLS
LOCATE 3
FOR i% = 1 TO 4
 PRINT menuchoice$(i%); ": "; info$(i%)
NEXT i%
checkinfo:
LOCATE 9
INPUT "Everything correct (n /- <Enter> accepts - ) ?", yn$
SELECT CASE yn$
 CASE "n"
  GOTO begin
 CASE ""
  OPEN "expinfo.dat" FOR OUTPUT AS #2
   FOR i% = 1 TO 4
    PRINT #2, info$(i%)
   NEXT i%
  CLOSE #2
  GOTO endhere
 CASE ELSE
  GOTO checkinfo
END SELECT

endhere:
```

```
END SUB

'This gets the 5 digit number used in data filenames from number.cnt,
'increments it by one, and saves it to number.cnt.
SUB increment
number$ = "": number% = 0
OPEN "number.cnt" FOR INPUT AS #2
INPUT #2, number$
CLOSE #2
number% = VAL(number$) + 1
number$ = STR$(number%)
'Get rid of leading or trailing spaces
number$ = LTRIM$(number$): number$ = RTRIM$(number$)
'If the numeric varaible (number%) was not 5 digits long, then add the
'character "0" the necessary amount of times in order to make the string
'variable (number$) 5 digits long.
FOR i% = 1 TO (5 - LEN(number$))
number$ = "0" + number$
NEXT i%
OPEN "number.cnt" FOR OUTPUT AS #2
WRITE #2, number$
CLOSE #2
END SUB

'--------------------------------------------------------------------------

'This procedure gets the number (m%) of files there are to be processed
'from nofiles.dir and then gets m% (i.e. all) the filenames contained in
'rawfiles.dir

SUB inputfiles (filename$(), m%)

OPEN "nofiles.dir" FOR INPUT AS #1
 INPUT #1, m%
CLOSE #1
REDIM filename$(m%)
OPEN "rawfiles.dir" FOR INPUT AS #1
FOR i% = 1 TO m%
 INPUT #1, filename$(i%)
NEXT i%
CLOSE #1

END SUB

'--------------------------------------------------------------------------
```

```
'This procedure controls the processing part of the program. It deals with
'data according to the way in which it was stored, as briefly described in
'the program introduction in the main module. The parameters contain the
'names of the raw data and processed data paths.
'
SUB process (rdir$, pdir$)

'STATIC declares local variables
STATIC k%, i%, j%, m%, menuno%, fileno$, count%
'The no1% and no4% arrays contain numbers that define limits of loops.
'For example 4008 * 5 = 20080, the number of waveform and normalization
'characters sent when the SAVE button is in the `save' position.
REDIM no1%(1 TO 3), no4%(1 TO 2), area!(1 TO 2)
no1%(1) = 2008: no1%(2) = 4016: no1%(3) = 4008
no4%(1) = 1: no4%(2) = 2009
IV% = 0: m% = 1: current% = 0: time% = 0: whicharea% = 1: somewrong$ = "n"
count% = 0: check1$ = "n"
'filename$() will contain the names of all the files to be processed. The
'outermost loop will loop exactly m% times.
REDIM filename$(m%)

menu:
CLS : LOCATE 4
PRINT "1) Set save time option. "
'If area value(s) were not originally entered, they can now be appended to
'the raw data file(s) before processing. This option will be used in the
case
'where two waveforms contribute to one raw data file, but the waveforms
'were obtained with electrodes of differing areas.
PRINT "2) Append area values onto collected waveform files. "
PRINT "3) Examine files in rawfiles.dir "
PRINT "4) Specify files to be processed."
PRINT "5) Process files from rawfiles.dir. "
PRINT "6) Go back to the main menu. ": PRINT
INPUT "Enter a number : ", menuno%
SELECT CASE menuno%
 CASE 1
  INPUT "Save time values to disk as well as X & Y data ? (y/n) ",
savetime$
  OPEN "savetime.dat" FOR OUTPUT AS #1
   WRITE #1, savetime$
  CLOSE #1
 CASE 2
  CALL saveareas
 CASE 3
  CLS
  OPEN "rawfiles.dir" FOR INPUT AS #1
   DO
    count% = count% + 1
    INPUT #1, line$
    PRINT line$
    'at the end of a page, wait for a keystoke
    IF count% / 25 = INT(count% / 25) THEN WHILE INKEY$ = "": WEND
```

```
   LOOP UNTIL EOF(1)
  CLOSE #1
  WHILE INKEY$ = "": WEND
 CASE 4
  INPUT "No of files to be processed ?", m%
  REDIM filename$(m%)
  FOR i% = 1 TO m%
   PRINT "Enter the number and extension of file no. "; i%; "."
   INPUT filenum$, ext$
   digit$ = STRING$((5 - LEN(filenum$)), "0") + filenum$
   filename$(i%) = rdir$ + "raw" + digit$ + "." + ext$
  NEXT i%
  GOTO start
 CASE 5
  'call the procedure which reads rawfiles.dir and nofiles.dir
  CALL inputfiles(filename$(), m%)
  GOTO start
 CASE 6
  EXIT SUB
END SELECT
GOTO menu
CLS

start:
FOR k% = 1 TO m%
 PRINT "Now processing '"; filename$(k%); "'."
 subtract% = m% - k%
 PRINT "There are "; subtract%; " raw data files to be processed
       afterwards."
 'The string waveform data is saved in the array dat$ - one waveform per
 'variable. REDIM clears the contents of prevoius values of the array and
 'initialises it.
 REDIM dats$(2)
 intermediate$ = RIGHT$(filename$(k%), 9)
 endofname$ = RIGHT$(filename$(k%), 3)
 ON ERROR GOTO wrongname
 check1name$ = filename$(k%)
 OPEN filename$(k%) FOR INPUT AS #1
 'wrong$ = "y" only if process() could not find filename$(k%)
 IF wrong$ = "y" THEN
  'There is at least one unfound file.
  somewrong$ = "y"
  wrong$ = "n"
  GOTO continue   'skip to the end of the outermost loop
 END IF
 ON ERROR GOTO 0
 SELECT CASE endofname$
 'the case where the last 3 letters of the raw data filename are "chr"
 'i.e. It is chronoamperometric data.
 CASE "chr"

  'get the variables describing whether one or two area values will be
  'used, the length of the waveform data, and the I/V conversion factor.
```

```
 INPUT #1, areacheck$, lngth%, IV!
 'put the data for one waveform in dats$(1)
 dats$(1) = INPUT$(lngth%, #1)
 'get the value(s) of the area(s)
 IF areacheck$ = "y" OR areacheck$ = "1" THEN
  WHILE area!(1) = 0 AND NOT EOF(1)
   INPUT #1, area!(1)
  WEND
  area!(2) = area!(1)
 ELSEIF areacheck$ = "2" THEN
  WHILE area!(1) = 0 AND NOT EOF(1)
   INPUT #1, area!(1), area!(2)
  WEND
 END IF
 IF area!(1) = 0 THEN
  PRINT "Area values have not been appended."
  PRINT "Press a key to go to the menu and append them."
  WHILE INKEY$ = "": WEND
  CLOSE
  GOTO menu
 END IF
CLOSE #1
no2% = 1: current% = 1: time% = 1
IF lngth% = (saveON% + 2) THEN    'i.e. if there is one waveform only

 'In the array dt!, the first identifier refers to the data point, the
 'second to the first (or second) waveform and the third refers to whether
 'the variable is a time value (2) or a current or potential value (1).
 REDIM dat!(1 TO 4008, 1 TO 1), dt!(1 TO 4000, 1 TO 1, 1 TO 2)
 'the general variable whichnox% is used as the index for the arrays of
 'type nox% when these arrays are used as parameters in procedures.
 'no2% is always equal to 1 or 2 and no4% can range from 1 to 4. They are
 'used as indeces in arrays such as dt!. no2% refers to the nth waveform
 'or pair of waveforms that were sent in one transfer (one press of the
 'RS232  button) in the dat! array and no3% refers to the nth single (i.e
 'it refers seperately to each of a pair of waveforms that were delivered
 'simultaneously) waveform in the dt! array.
 whichno1% = 3: whichno4% = 1: no3% = 1: whicharea% = 1
 'Call the procedure which converts the no2%'th waveform to
 'no1% (whichno1%=4008 in this case) numeric values.
 CALL stringtoval(whichno1%, no2%)
 ERASE dats$  'free memory
 'Call the procedure which normalises the numeric values obtained in
 'stringtoval(). If curent% = 1 then current is calculated, else potential
 'is calculated. If time% = 1 then time is calculated, else it is not.
 CALL process1(whichno1%, whichno4%, no2%, no3%, current%, time%,
whicharea%)
 ERASE dat!   'free memory
 'A processed file name begins with the letters "pro" or "pra" or "pra",
 'the later two being used in the case when two waveforms were transferred
 'at once. Otherwise the processed data file name is the same as the raw
 'data file name.
 newfilename$ = pdir$ + "pro" + intermediate$
```

```
 PRINT "Now writing to '"; newfilename$; "'."
 OPEN newfilename$ FOR OUTPUT AS #1
 PRINT #1, "current    time"
  FOR i% = 1 TO 4000
   PRINT #1, USING "+#.###^^^^ "; dt!(i%, no3%, 1); dt!(i%, no3%, 2)
  NEXT i%
 CLOSE #1
 ERASE dt!     'free memory

ELSEIF lngth% = (saveSAVE% + 2) THEN

 REDIM dat!(1 TO 4016, 1 TO 1), dt!(1 TO 2000, 1 TO 2, 1 TO 2)
 whichno1% = 2
 CALL stringtoval(whichno1%, no2%)
 ERASE dats$
 FOR i% = 1 TO 2
  whichno1% = i%: whichno4% = i%: no3% = i%: whicharea% = i%
  CALL process1(whichno1%, whichno4%, no2%, no3%, current%, time%,
                whicharea%)
 NEXT i%
 ERASE dat!
 REDIM newfilename$(2)
 newfilename$(1) = pdir$ + "prA" + intermediate$
 newfilename$(2) = pdir$ + "prB" + intermediate$
 FOR i% = 1 TO 2
 PRINT "Now writing to '"; newfilename$(i%); "'."
  OPEN newfilename$(i%) FOR OUTPUT AS #1
  PRINT #1, "current    time"
  FOR j% = 1 TO 2000
   PRINT #1, USING "+#.###^^^^ "; dt!(j%, i%, 1); dt!(j%, i%, 2)
  NEXT j%
  CLOSE #1
 NEXT i%
 ERASE dt!

END IF
CASE "cyv"    'i.e XY data

 OPEN "savetime.dat" FOR INPUT AS #2
  'if savetime$ = "y" then time values will be saved as well as current
  'and potential in XY data.
  INPUT #2, savetime$
 CLOSE #2
 REDIM dat!(1 TO 4016, 1 TO 2)
 INPUT #1, areacheck$, lngth%, IV!
 FOR i% = 1 TO 2
  dats$(i%) = INPUT$(lngth%, #1)
  no2% = i%
  IF lngth% = (saveON% + 2) THEN
   whichno1% = 3: repeat$ = "n"
  ELSEIF lngth% = (saveSAVE% + 2) THEN
   whichno1% = 2: repeat$ = "y"
  END IF
```

```
 CALL stringtoval(whichno1%, no2%)
 dats$(i%) = ""
NEXT i%
ERASE dats$
IF areacheck$ = "y" OR areacheck$ = "1" THEN
 WHILE area!(1) = 0 AND NOT EOF(1)
  INPUT #1, area!(1)
 WEND
 area!(2) = area!(1)
ELSEIF areacheck$ = "2" THEN
 WHILE area!(1) = 0 AND NOT EOF(1)
  INPUT #1, area!(1), area!(2)
 WEND
END IF
IF area!(1) = 0 THEN
 PRINT "Area values have not been appended."
 PRINT "Press a key to go to the menu and append them."
 WHILE INKEY$ = "": WEND
 CLOSE
 GOTO menu
END IF
CLOSE #1

IF repeat$ = "n" THEN
 IF savetime$ = "y" THEN
  REDIM dt!(1 TO 4000, 1 TO 2, 1 TO 2)
 ELSE
  REDIM dt!(1 TO 4000, 1 TO 2, 1 TO 1)
 END IF
 FOR i% = 1 TO 2
  'MUST keep no2% as i%
  no2% = i%: no3% = i%:
  IF savetime$ = "y" THEN
   time% = i%
  ELSE
   time% = 2
  END IF
  current% = i%: whichno1% = 3: whichno4% = 1: whicharea% = i%
  CALL process1(whichno1%, whichno4%, no2%, no3%, current%, time%,
                whicharea%)
 NEXT i%
 ERASE dat!
 newfilename$ = pdir$ + "pro" + intermediate$
 PRINT "Now writing to '"; newfilename$; "'."
 OPEN newfilename$ FOR OUTPUT AS #1
 IF savetime$ = "y" THEN
  PRINT #1, "current    potential   time"
  FOR j% = 1 TO 4000
   PRINT #1, USING "+#.###^^^^ "; dt!(j%, 1, 1); dt!(j%, 2, 1);
                                  dt!(j%, 1, 2)
  NEXT j%
 ELSE
  PRINT #1, "current    potential"
```

```
  FOR j% = 1 TO 4000
   PRINT #1, USING "+#.###^^^^ "; dt!(j%, 1, 1); dt!(j%, 2, 1)
  NEXT j%
 END IF
 ERASE dt!
 CLOSE #1

ELSEIF repeat$ = "y" THEN
 IF savetime$ = "y" THEN
  REDIM dt!(1 TO 2000, 1 TO 4, 1 TO 2)
 ELSE
  REDIM dt!(1 TO 2000, 1 TO 4, 1 TO 1)
 END IF

 FOR i% = 1 TO 2
  'In this case we have a total of 4 waveforms in one raw data file. The
  'first and the third and then the second and the fourth must be
  'combined to form seperate processed data files, remembering that the
  'first two will be current-time data and the second two will be
  'potential-time data. These four waveforms are processed using two
  'loops, where j% is the inner loop counter. In both the cases where
  'j% = 1, current is calculated, and for these times, no3% is given the
  'value of 1 and then 2. In both occasions where j% = 2, potential is
  'calculated and no3% is given the value 3 and then 4.
  no2% = i%: current% = i%
  IF savetime$ = "y" THEN
   time% = i%
  ELSE
   time% = 2
  END IF
  FOR j% = 1 TO 2
   'The values which no3% has, in order, are 1,2,3,4. The current values
   'calculated when no3% = 1 are combined with the potential values
   'calculated when no3% = 3. and they are saved together as a "pra"
   'file. The other two are saved as a "prb" file.
   no3% = i% * i% - i% + j%
   whichno1% = j%: whichno4% = j%: whicharea% = j%
   CALL process1(whichno1%, whichno4%, no2%, no3%, current%, time%,
                 whicharea%)
  NEXT j%
 NEXT i%
 ERASE dat!
 REDIM newfilename$(2)
 newfilename$(1) = pdir$ + "prA" + intermediate$
 newfilename$(2) = pdir$ + "prB" + intermediate$
 FOR i% = 1 TO 2
  PRINT "Now writing to '"; newfilename$(i%); "'."
  OPEN newfilename$(i%) FOR OUTPUT AS #1
  IF savetime$ = "y" THEN
   PRINT #1, "current    potential   time"
   FOR j% = 1 TO 2000
    PRINT #1, USING "+#.###^^^^ "; dt!(j%, i%, 1); dt!(j%, (i% + 2), 1);
                                   dt(j%, i%, 2)
```

```
     NEXT j%
    ELSE
     PRINT #1, "current    potential"
     FOR j% = 1 TO 2000
      PRINT #1, USING "+#.###^^^^ "; dt!(j%  , i%, 1); dt!(j%, (i% + 2), 1)
     NEXT j%
    END IF
    CLOSE #1
   NEXT i%
   ERASE dt!
  END IF

 END SELECT

continue:
NEXT k%

'If any raw data files could not be found in this run of process(), then
'print out their names .
IF somewrong$ = "y" THEN
 PRINT : PRINT "The following files were not found : ": PRINT
 OPEN "wrongfil.dat" FOR INPUT AS #1
  DO
   INPUT #1, wrongfile$
   PRINT wrongfile$
  LOOP UNTIL EOF(1)
 CLOSE #1
END IF
somewrong$ = "n"

PRINT "Finished! - press any key to continue."
WHILE INKEY$ = "": WEND
GOTO menu


END SUB


'------------------------------------------------------------------------
```

```
'This procedure takes numeric values contained in the array dat! and
'normalises them to give current (mAcm-2), potential (mV), or time (s)
'values.

SUB process1 (whichno1%, whichno4%, no2%, no3%, current%, time%,
whicharea%)
STATIC i%
t% = 0
PRINT "Now normalising numeric data. Cycle no. "; no3%
'The normalisation data was at the end of the string data$ and now will be
'at the end ot the array dat!. no1%(whichno1%) refers to the last variable
'in the array dat!.
vnorm! = (dat!((no1%(whichno1%) - 3), no2%) - 5) *
         10 ^ (dat!((no1%(whichno1%) - 2), no2%) - 12)
hnorm! = (dat!((no1%(whichno1%) - 1), no2%) - 5) *
         10 ^ (dat!(no1%(whichno1%), no2%) - 12)
REM hzero! = dat!((no1%(whichno1%) - 4), no2%)
FOR i% = no4%(whichno4%) TO (no1%(whichno1%) - 8)
t% = t% + 1
 IF current% = 1 THEN
  'find the current in Acm-2.
  dt!(t%, no3%, 1) = (dat!(i%, no2%) * vnorm! * IV!) / area!(whicharea%)
 ELSE
  'find the potential in mV.
  dt!(t%, no3%, 1) = dat!(i%, no2%) * vnorm!
 END IF
 IF time% = 1 THEN
  dt!(t%, no3%, 2) = t% * hnorm!
 END IF
NEXT i%
END SUB


'-------------------------------------------------------------------------
```

```
'If raw data has to be collected when the area of the elecrode is not known
'a null value for the area may be enterd and the area (or areas)
'corresponding to a waveform (or 2 or 4 waveforms in one raw data file) can
'be appended to the raw data file before processing.

SUB saveareas

CLS : STATIC m%, i%
m% = 1
REDIM filename$(m%)
INPUT "Specify files to be appended or use Rawfiles.dir (S/R) "; which$
IF which$ = "s" OR which$ = "S" THEN
 INPUT "Enter first and last filenumbers :"; first%, last%
ask:
 CLS
 INPUT "XY or It data (x/i) :", xi$
 IF xi$ = "i" OR xi$ = "I" THEN
  endbit$ = ".chr"
  ELSEIF xi$ = "x" OR xi$ = "X" THEN
   endbit$ = ".cyv"
  ELSE
   GOTO ask
 END IF

 m% = last% - first% + 1
 REDIM filename$(m% + 1)

 j% = 0
 FOR i% = first% TO last%
  j% = j% + 1
  ln% = 5 - LEN(LTRIM$(STR$(i%)))
  num$ = STRING$(ln%, "0") + LTRIM$(STR$(i%))
  filename$(j%) = rawdir$ + "raw" + num$ + endbit$
 NEXT i%

 ELSE
 IF which$ = "r" OR which$ = "R" THEN
  'Get all the raw data filenames and the no. (m%) of raw data files.
  CALL inputfiles(filename$(), m%)
 END IF
END IF

REDIM areacheck$(m%)
FOR i% = 1 TO m%
 OPEN filename$(i%) FOR INPUT AS #1
 'Get the areacheck$ variable. If it is equal to 1 or 2, then 1 or 2 area
 'values respectively must be appended to the raw data file concerned.
 INPUT #1, areacheck$(i%)
 CLOSE #1
NEXT i%
defineareas:
CLS : LOCATE 3
INPUT "How many different area values will you be entering ? ", noareas%
REDIM areas!(noareas%)
FOR i% = 1 TO noareas%
```

```
 PRINT "Enter value of area no. "; i%; " (cm2) : "
 INPUT areas!(i%)
NEXT i%

CLS : LOCATE 3
FOR i% = 1 TO noareas%
 PRINT i%; ".) "; areas!(i%)
NEXT i%

LOCATE (5 + noareas%)
INPUT "Correct ([Enter] = yes ) ? ", gonext$
IF gonext$ <> "" THEN GOTO defineareas

'Go through all the raw data files, checking each to see if area values
'need to be entered, and if so prompt for the no. corresponding to any of
'the area values already entered.
FOR i% = 1 TO m%
 CLS
 FOR j% = 1 TO noareas%
  PRINT j%; ".) "; areas!(j%)
 NEXT j%
 LOCATE (5 + noareas%)
 SELECT CASE areacheck$(i%)
 CASE "1"
  IF noareas% > 1 THEN
   PRINT "Enter the number corresponding to the area of the electrode used"
   PRINT "for the waveform in file "; filename$(i%); "."
   INPUT one%
   OPEN filename$(i%) FOR APPEND AS #1
    WRITE #1, areas!(one%)
   CLOSE #1
  ELSE
   OPEN filename$(i%) FOR APPEND AS #1
    WRITE #1, areas!(1)
   CLOSE #1
  END IF
 CASE "2"
  IF noareas% > 1 THEN
   PRINT "Enter the two numbers corresponding to the areas of the
          electrodes"
   PRINT "used for the first and second waveforms in file "; filename$(i%)
   INPUT ", respectively. : ", one%, two%
   OPEN filename$(i%) FOR APPEND AS #1
    WRITE #1, areas!(one%), areas!(two%)
   CLOSE #1
  ELSE
   OPEN filename$(i%) FOR APPEND AS #1
    WRITE #1, areas!(1), areas!(1)
   CLOSE #1
  END IF
 END SELECT
 NEXT i%


END SUB
```

```
'This procedure saves raw data and experimental parameters to a raw data
'file.

SUB savedata (directory$, check1file$, anumber%)

m% = 0

'If the area value originally entered was the null value, then the no. of
'area values which are still to be appended are saved in areacheck$, else
'areacheck$ is given the value which indicates that area values do not have
'to be appended.
IF area! = 0 THEN
 areacheck$ = LTRIM$(STR$(ONEorTWO%))
ELSEIF area! > 0 THEN
 areacheck$ = "y"
END IF

IF XYorIT$ = "X" THEN
 filename$ = directory$ + "raw" + number$ + ".cyv"
END IF
IF XYorIT$ = "I" THEN
 filename$ = directory$ + "raw" + number$ + ".chr"
 LOCATE 1: PRINT "Saving data as "; filename$; "."
 OPEN filename$ FOR OUTPUT AS #2
  'Write the variable containing area value information, what the length of
  'the raw data string after saving it will be, and the I/V conversion
  'factor.
  WRITE #2, areacheck$, (LEN(data$) + 2), IV!
  PRINT #2, data$
  IF area! > 0 THEN PRINT #2, area!
 CLOSE #2
ELSEIF XYorIT$ = "X" AND anumber% = 1 THEN
 LOCATE 1: PRINT "Saving data as "; filename$; "."
 OPEN filename$ FOR OUTPUT AS #2
  WRITE #2, areacheck$, (LEN(data$) + 2), IV!
  PRINT #2, data$
 CLOSE #2
 'If the raw data currently being saved is the second set of curve(s) of XY
 'data from the NICOLET, then append it to the same file in which the first
 'set of XY data was saved.
ELSEIF XYorIT$ = "X" AND anumber% = 2 THEN
 LOCATE 1: PRINT "Appending data as "; filename$; "."
 OPEN filename$ FOR APPEND AS #2
  PRINT #2, data$
  IF area! > 0 THEN PRINT #2, area!
 CLOSE #2
END IF

'Now append (or clear and then write to if choose$ = "y") the raw data
'filename to rawfiles.dir and increment the no. in nofiles.dir by 1.
IF XYorIT$ = "X" AND anumber% = 2 THEN GOTO endit
IF (choose$ = "y" OR choose$ = "Y") AND check1file$ = "y" THEN
 OPEN "rawfiles.dir" FOR OUTPUT AS #2
```

```
END IF
IF (choose$ = "n" OR choose$ = "") OR ((choose$ = "y" OR choose$ = "Y") AND
check1file$ = "n") THEN
 OPEN "nofiles.dir" FOR INPUT AS #2
  INPUT #2, m%
 CLOSE #2
 OPEN "rawfiles.dir" FOR APPEND AS #2
END IF
WRITE #2, filename$
CLOSE #2
m% = m% + 1
OPEN "nofiles.dir" FOR OUTPUT AS #2
 WRITE #2, m%
CLOSE #2
check1file$ = "n"

endit:

END SUB

'------------------------------------------------------------------------

'This procedure converts all the raw data in the string variable data$ to
'the numeric values. 5 characters per numeric value. The numeric values are
'stored in the dat! array.

SUB stringtoval (whichno1%, no2%)
PRINT "Now converting string data to numeric data. Cycle no. "; no2%
STATIC i%
f% = 0
FOR i% = 1 TO 6
 f% = f% + 1
tryagain:
 SELECT CASE MID$(dats$(no2%), f%, 1)
  CASE " "
   GOTO proceed
  CASE "+"
   GOTO proceed
  CASE "-"
   GOTO proceed
  CASE "0"
   GOTO proceed
  CASE "1"
   GOTO proceed
  CASE "2"
   GOTO proceed
  CASE "3"
   GOTO proceed
  CASE "4"
   GOTO proceed
  CASE "5"
   GOTO proceed
  CASE "6"
```

```
    GOTO proceed
   CASE "7"
    GOTO proceed
   CASE "8"
    GOTO proceed
   CASE "9"
    GOTO proceed
   CASE ELSE
    f% = f% + 1
    GOTO tryagain
  END SELECT
proceed:
NEXT i%

FOR i% = 1 TO no1%(whichno1%)
  'while the f% character is a carriage return or line feed, increment f%
  'by 1. i.e. skip carriage returns or line feeds.

  WHILE MID$(dats$(no2%), f%, 1) = CHR$(10) OR MID$(dats$(no2%), f%, 1) =
                                               CHR$(13)
   f% = f% + 1
  WEND

  dat!(i%, no2%) = VAL(MID$(dats$(no2%), f%, 5))
  f% = f% + 5
NEXT i%

END SUB


'-------------------------------------------------------------------------

'******************** END OF COLLVER7.BAS ********************************
```

GRAPH.BAS

This is a relatively simple program with one major useful feature. It can draw multiple graphs with multiple sets of Y data **and** multiple sets of X-data. It does not label or number axes. The idea is that once the graph is drawn, it can be cut and pasted into Windows Paintbrush and the labelling and numbering is done in that application (Windows and a 386 PC are needed). This program is designed to take data files in the format produced by COLLVER7.BAS. The user must enter the scale to be used and a VGA screen is required, although the program could be adjusted for a monochrome screen. In future work, it may be worthwhile incorporating this program as a subroutine into COLLVER7.BAS in order to obtain graphs automatically on the PC screen within seconds after the NICOLET oscilloscope has finished transmitting waveform data.

```
'************************GRAPH.BAS*****************************************

'Written by C.Tonkinson for the Electrochemistry research laboratory,
'Chemistry Department, University of Natal, Durban, July 1991.

'datasub$ contains the path where data files (generated from COLLVER7.BAS)
beginhere:
datasub$ = "f:\data\pr"
CLS
ask:
CLS
INPUT "XY or It data (x/i) :", xi$
IF xi$ = "i" OR xi$ = "I" THEN
 endbit$ = ".chr"
 ELSEIF xi$ = "x" OR xi$ = "X" THEN
  endbit$ = ".cyv"
 ELSE
  GOTO ask
END IF
vars% = 2: plot% = 2: varpos%(1) = 2: varpos%(2) = 1
INPUT "How many files to be plotted ? ", nofiles%
REDIM filename$(nofiles%), num$(nofiles%), abc$(nofiles%), lorp$(nofiles%)
FOR i% = 1 TO nofiles%
'The letter asked for in the line below refers to the third letter in the
'processed file filename. e.g. the letter for pra00157.cyv would be "a".
'When these filenames are generated by COLLVER7.BAS, only the third letter
'and the 5 digit number are variable.
 PRINT "Enter the letter & number of file no. "; i%; ","
 PRINT "and print lines or points (l/p) - default is l "
 INPUT abc$(i%), num$(i%), lorp$(i%)
 'Here the filename(s) are generated from previous input information.
 IF lorp$(i%) = "" THEN lorp$(i%) = "l"
 ln% = 5 - LEN(LTRIM$(num$(i%)))
 num$(i%) = STRING$(ln%, "0") + num$(i%)
 filename$(i%) = datasub$ + abc$(i%) + num$(i%) + endbit$
NEXT i%
setscale:
```

```
'The user sets the scale and the increment for the positioning of
'tickmarks on the axes.
PRINT "Enter consecutively the following values to be used in the"
PRINT "plotting of the graph :-"
PRINT "Ymax, Ymin, Yincrement, Xmax, Xmin, Xincrement."
INPUT ymax!, ymin!, yinc!, xmax!, xmin!, xinc!
INPUT "plot every 'n'th point - give n - ", stepno%
'Go to VGA graphics mode for the output screen
SCREEN 12
'Draw a rectangle in the screen.
LINE (0, 0)-(639, 470), 15, BF
LINE (60, 50)-(580, 430), 0, B
'Set the size of the portion of the screen in which graphics will be
'written
VIEW (60, 50)-(580, 430)
'Scale the graphics rectangle of the screen such that the maximum and
'minimum values given by the user correspond to the corners of the
'rectangle.
WINDOW (xmin!, ymax!)-(xmax!, ymin!)
'Calculate the number of, and draw tickmarks on the X and Y axes
noincx% = INT((xmax! - xmin!) / xinc!)
noincy% = INT((ymax! - ymin!) / yinc!)
FOR i% = 0 TO noincy%
 ybit! = ymin! + yinc! * i%
 LINE (xmin!, ybit!)-(xmin! + .01 * (xmax! - xmin!), ybit!), 0
NEXT i%
FOR i% = 0 TO noincx%
 xbit! = xmin! + xinc! * i%
 LINE (xbit!, ymin!)-(xbit!, ymin + .01 * (ymax! - ymin!)), 0
NEXT i%

FOR i% = 1 TO nofiles%
 OPEN filename$(i%) FOR INPUT AS #1
 'In the ASCII format used by collver7.bas, each variable takes up 12
 'characters. The length of the file in bytes is divided by dividor% to get
 'the no. of rows in the file.
 divisor% = 12 * vars%
 IF LOF(1) / divisor% = INT(LOF(1) / divisor%) THEN
  filength% = LOF(1) / divisor% - 1
 ELSE
  filength% = INT(LOF(1) / divisor%)
 END IF
 REDIM var!(1 TO vars%, 1 TO filength%)
  FOR j% = 1 TO filength%
   FOR k% = 1 TO vars%
    INPUT #1, var!(k%, j%)
   NEXT k%
  NEXT j%
 CLOSE #1
 'This section takes each point in the data file and writes them to the
 'screen by writing lines between them.
 IF lorp$(i%) = "l" THEN
  FOR j% = (stepno% + 1) TO filength% STEP stepno%
```

```
   FOR k% = 2 TO plot%
    LINE (var!(varpos%(1), j% - stepno%), var!(varpos%(k%), j% - stepno%))-
         (var!(varpos%(1), j%), var!(varpos%(k%), j%)), 0
   NEXT k%
  NEXT j%
 ELSE
 'This section takes each point in the data file and writes them to the
 'screen by drawing that point literally as a point on the screen.
  IF lorp$(i%) = "p" THEN
   FOR j% = stepno% TO filength% STEP stepno%
    FOR k% = 2 TO plot%
     PSET (var!(varpos%(1), j%), var!(varpos%(k%), j%)), 0
    NEXT k%
   NEXT j%
  END IF
 END IF
NEXT i%
ERASE var!

'The graph(s) have finished being drawn and are currently displayed.
'The next line says do nothing until a key is pressed.
WHILE INKEY$ = "": WEND
'Go back to text mode for the output screen
SCREEN 0, 0, 0
INPUT "Change scale and replot (c), plot new graph (p),
       or quit <Enter> ? ", cpq$
SELECT CASE cpq$
 CASE "c"
  GOTO setscale
 CASE "p"
  GOTO beginhere
END SELECT


***************************** END OF GRAPH.BAS ******************************
```

NUCMODEL.BAS

This is the initial program which was designed to fit the nucleation model described in chapter 5 to experimental data which is in the ASCII format provided by COLLVER.BAS. The process is basically an iterative one and can be simply summarised as follows:

There are 9 parameters in the model. Nine initial guesses for these parameters (and lower and upper boundaries which the parameters are not allowed to exceed) are supplied by the user. The program then generates a curve from those nine parameters. Then the program calculates the fitting parameter, δ_f (called `fit!` in the program), which is defined in section 7.3 and is a measure of the fit between the experimental and theoretical (generated from the nine parameters) curves. (Usually a good fit has been obtained when `fit!` < 4.)

The program then takes the first parameter (P_1 - called `p!(1)` in the main module of the programme -) and adds a user stipulated fraction of P_1 - called `in!(1)` in the main module - to itself to give a new parameter, called `n!(1)` in the main module. A new theoretical curve is generated with `n!(1)` instead of `p!(1)` and δ_f is then calculated. One of three courses of action is then taken:

1. If δ_f is reduced from its original value (i.e. a slightly better fit) then the value of P_1 is set equal to the value of `n!(1)`. A procedure (`iterate`) is called and repeats the above process until the value of `n!(1)` is increased to a point which causes δ_f to increase. The current value of P_1 is then retained.
2. If δ_f is increased or equal to its original value, then `in!(1)` is subtracted from P_1 to give a new value of `n!(1)`. Again a theoretical curve is calculated by using the new `n!(1)` value and if δ_f is reduced then the `iterate` procedure is called as in the first option.
3. If neither increasing or decreasing P_1 by the user-stipulated fraction of itself causes δ_f to be decreased, then P_1 retains its original value.

The process in the above paragraph is then repeated for each of the nine parameters. After that, new values of `in!(1-9)` are generated. The new values of `in!(1-9)` are based on the new, slightly improved values of the P_i parameters and are also slightly decreased in value from the previous cycle. The nine parameters are once again optimised using the `iterate` procedure, followed by another adjustment and decrease in the `in!(1-9)` values. This cycle is basically continued *ad infinitum*, although there are conditions which when met will cause the program to stop. However, it is better for the user to keep an eye on the results which are printed out on the screen after every optimisation of each parameter together with the value of δ_f generated from those parameters. The user can then decide when a sufficiently good fit has been obtained and and stop the programme with the Ctrl-Break keystroke combination.

This is defintely not an advanced model fitting programme (for example it creates a bias towards the initial parameters that it optimises) but is sufficient for the early stages of development of the nucleation model.

```
**********************************NUCMODEL.BAS*********************************

'Written by C.Tonkinson for the Electrochemistry research laboratory,
'Chemistry Department, University of Natal, Durban, December 1992.

DECLARE SUB iterate (sign$, b!(), k%, inc!, dd!) 'cddsre2.bas
DECLARE FUNCTION diff! (m!())
COMMON SHARED filength%, cur!(), time!(), p!(), pl!(), ph!(), skip$,
              count%, newinc!
CLS
'The name and path of the data to which the nucleation model is to be
'fitted is generated.
INPUT "Letter and Number of data file to analyse "; abc$, num$
ln% = 5 - LEN(LTRIM$(num$))
num$ = STRING$(ln%, "0") + num$
file$ = "f:\data\pr" + abc$ + num$ + ".chr"

'The arrays which will contain, respectively, the initial parameter guesses
'and the lower and upper allowed values of the parameters are declared.
REDIM p!(1 TO 9), pl!(1 TO 9), ph!(1 TO 9)
'The values to be stored in the above arrays are read.
OPEN "d:\temp\pall3no4.dat" FOR INPUT AS #1
FOR i% = 1 TO 9
 INPUT #1, p!(i%), pl!(i%), ph!(i%)
NEXT i%
CLOSE #1

maxcur! = -100
'The experimental data file is opened and the current and time values
'therein are read into the cur!() and time!() arrays.
OPEN file$ FOR INPUT AS #1
divisor% = 24
IF LOF(1) / divisor% = INT(LOF(1) / divisor%) THEN
 filength% = LOF(1) / divisor% - 1
ELSE
 filength% = INT(LOF(1) / divisor%)
END IF
REDIM cur!(2 TO filength%), time!(2 TO filength%)
 INPUT #1, dummy$
 FOR k% = 2 TO filength%
   INPUT #1, cur!(k%), time!(k%)
   'Once the loop is finished, maxcur! will contain the value of the
   'maximum current point in the data file.
   IF cur!(k%) > maxcur! THEN maxcur! = cur!(k%)
 NEXT k%
CLOSE #1

'The value of the fitting paraneter, fit!, is generated from the first
'guess values of the nine parameters of the nucleation model.
fit1! = 100000! / (filength% * (maxcur! ^ 2))
total! = diff(p!())
fit! = total! * fit1!
```

```
'The values of the nine parameters and the fitting parameter are printed to
'the screen in scientific format.
PRINT , USING "+#.####^^^^ "; p!(1); p!(2); p!(3); p!(4); p!(5)
PRINT , USING "+#.####^^^^ "; p!(6); p!(7); p!(8); p!(9)
PRINT "Initial diff ="; fit!

'The user types the value which corresponds to the fraction by which each
'parameter will be initially incremented. If count% = 10, for example, the
'the fraction is one tenth.
INPUT "Initial value of count% ", count%

REDIM n!(1 TO 9), in!(1 TO 9)
FOR i% = 1 TO 9
 n!(i%) = p!(i%)
 in!(i%) = p!(i%) / count%
NEXT i%

jump% = 0: cycle% = 0

WHILE count% < 10000

WHILE jump% < 5

jump% = 0
cycle% = cycle% + 1
PRINT "cycle% = "; cycle%

FOR i% = 1 TO 9

PRINT "Now optimising parameter"; i%

IF (p!(i%) + in!(i%)) > ph!(i%) THEN
 jump% = jump% + 1
 GOTO skip1
 ELSE
 n!(i%) = p!(i%) + in!(i%)
 d! = diff(n!())
 IF d! < total! THEN
  total! = d!
  CALL iterate("plus", n!(), i%, in!(i%), total!)
 ELSEIF d! >= total! THEN
skip1:
  IF (p!(i%) - in!(i%)) < pl!(i%) THEN
   jump% = jump% + 1
   GOTO skipthis
   ELSE
   n!(i%) = p!(i%) - in!(i%)
   d! = diff(n!())
   IF d! < total! THEN
    total! = d!
    CALL iterate("minus", n!(), i%, in!(i%), total!)
   ELSEIF d! >= total! THEN
    n!(i%) = p!(i%)
```

```
    jump% = jump% + 1
   END IF
  END IF
 END IF
END IF

'The current optimised values of the parameters are saved in a data file
OPEN "c:\temp\pvalues5.dat" FOR OUTPUT AS #1
FOR l% = 1 TO 9
 PRINT #1, USING "+#.####^^^^"; n!(l%)
NEXT l%
CLOSE #1

skipthis:
PRINT , USING "+#.####^^^^ "; n!(1); n!(2); n!(3); n!(4); n!(5)
PRINT , USING "+#.####^^^^ "; n!(6); n!(7); n!(8); n!(9)
fit! = total! * fit1!
PRINT fit!

NEXT i%

count% = count% + 5
FOR i% = 1 TO 9
 p!(i%) = n!(i%)
 in!(i%) = p!(i%) / count%
NEXT i%

PRINT "count% ="; count%

WEND

count% = count% + 50
PRINT "count% ="; count%
FOR i% = 1 TO 9
 p!(i%) = n!(i%)
 in!(i%) = p!(i%) / count%
NEXT i%

jump% = 0

WEND

PRINT "Finished"

FOR i% = 1 TO 9
 p!(i%) = n!(i%)
NEXT i%
PRINT , USING "+#.####^^^^ "; p!(1); p!(2); p!(3); p!(4); p!(5)
PRINT , USING "+#.####^^^^ "; p!(6); p!(7); p!(8); p!(9)
PRINT total!


'-----------------------------------------------------------------------
```

```
'This function calculates, for a no. of time points equal to the number and
'value of experimental data time points, a theoretical current value
'(cf section 8.2).The sum of the square of the differences between the
'theoretical and experimental current points is also calculated.

FUNCTION diff (m!())

REDIM theory!(2 TO filength%): tot! = 0
FOR i% = 2 TO filength%
 IF time!(i%) < m!(7) THEN
  exp2! = EXP(-m!(2) * (time!(i%)) ^ 2)
  theory!(i%) = m!(9) / (time!(i%) ^ .5) + m!(1) * (1 - exp2!)
 ELSEIF time!(i%) >= m!(7) AND time!(i%) < (m!(7) + m!(8)) THEN
  exp1! = EXP(-(m!(2) / m!(5)) * (time!(i%) - m!(7)) ^ 2)
  exp2! = EXP(-m!(2) * (time!(i%)) ^ 2)
  exp3! = EXP(-m!(4) * (time!(i%) - m!(7)) ^ 2)
  rot! = 1 / (time!(i%) ^ .5)
  theory!(i%) = m!(9) / (time!(i%) ^ .5) + m!(1) * (exp1! - exp2!) +
                m!(3) * rot! * (1 - exp3!)
 ELSEIF time!(i%) >= (m!(7) + m!(8)) THEN
  exp1! = EXP(-(m!(2) / m!(5)) * (time!(i%) - m!(7)) ^ 2)
  exp2! = EXP(-m!(2) * (time!(i%)) ^ 2)
  exp3! = EXP(-m!(4) * (time!(i%) - m!(7)) ^ 2)
  exp4! = EXP(-(m!(4) / m!(6)) * (time!(i%) - m!(7) - m!(8)) ^ 2)
  rot! = 1 / (time!(i%) ^ .5)
  theory!(i%) = m!(9) / (time!(i%) ^ .5) + m!(1) * (exp1! - exp2!) +
                m!(3) * rot! * (exp4! - exp3!)
 END IF
 tot! = tot! + (ABS((cur!(i%) - theory!(i%)))) ^ 2
NEXT i%
ERASE theory!

diff = tot!

END FUNCTION


'-----------------------------------------------------------------------
```

```
'This subprocedure is responsible for continuosly adding (or subtracting) a
'fraction of a parameter (of the nucleation model) to itself until a value
'for the parameter is generated which increases the fitting parameter. The
'previous value for the nucleation model parameter is then retained and
'passed back to the main module.

SUB iterate (sign$, b!(), k%, inc!, dd!)

IF b!(k%) < .01 THEN
 IF sign$ = "minus" THEN
  newinc! = -b!(k%) / 5
 ELSEIF sign$ = "plus" THEN
  newinc! = b!(k%) / 5
 END IF
ELSE
 IF sign$ = "minus" THEN
  newinc! = -inc!
 ELSEIF sign$ = "plus" THEN
  newinc! = inc!
 END IF
END IF

oldb! = b!(k%)

skip$ = "n"
WHILE skip$ = "n"
 b!(k%) = b!(k%) + newinc!
 IF b!(k%) < pl!(k%) OR b!(k%) > ph!(k%) THEN
  b!(k%) = oldb!
  skip$ = "y"
  ELSE
   ddd! = diff(b!())
   IF ddd! < dd! THEN
    dd! = ddd!
    oldb! = b!(k%)
   ELSEIF ddd! >= dd! THEN
    b!(k%) = oldb!
    skip$ = "y"
   END IF
 END IF
WEND


END SUB


'--------------------------------------------------------------------------


********************** END OF NUCMODEL.BAS ******************************
```